frontiers | Research Topics

Individual's mechanics, movement and kinematics post-stroke

Edited by
Yih-Kuen Jan and Veronica Cimolin

Published in
Frontiers in Bioengineering and Biotechnology
Frontiers in Neurology

FRONTIERS EBOOK COPYRIGHT STATEMENT

The copyright in the text of individual articles in this ebook is the property of their respective authors or their respective institutions or funders. The copyright in graphics and images within each article may be subject to copyright of other parties. In both cases this is subject to a license granted to Frontiers.

The compilation of articles constituting this ebook is the property of Frontiers.

Each article within this ebook, and the ebook itself, are published under the most recent version of the Creative Commons CC-BY licence. The version current at the date of publication of this ebook is CC-BY 4.0. If the CC-BY licence is updated, the licence granted by Frontiers is automatically updated to the new version.

When exercising any right under the CC-BY licence, Frontiers must be attributed as the original publisher of the article or ebook, as applicable.

Authors have the responsibility of ensuring that any graphics or other materials which are the property of others may be included in the CC-BY licence, but this should be checked before relying on the CC-BY licence to reproduce those materials. Any copyright notices relating to those materials must be complied with.

Copyright and source acknowledgement notices may not be removed and must be displayed in any copy, derivative work or partial copy which includes the elements in question.

All copyright, and all rights therein, are protected by national and international copyright laws. The above represents a summary only. For further information please read Frontiers' Conditions for Website Use and Copyright Statement, and the applicable CC-BY licence.

ISSN 1664-8714
ISBN 978-2-8325-5027-4
DOI 10.3389/978-2-8325-5027-4

About Frontiers

Frontiers is more than just an open access publisher of scholarly articles: it is a pioneering approach to the world of academia, radically improving the way scholarly research is managed. The grand vision of Frontiers is a world where all people have an equal opportunity to seek, share and generate knowledge. Frontiers provides immediate and permanent online open access to all its publications, but this alone is not enough to realize our grand goals.

Frontiers journal series

The Frontiers journal series is a multi-tier and interdisciplinary set of open-access, online journals, promising a paradigm shift from the current review, selection and dissemination processes in academic publishing. All Frontiers journals are driven by researchers for researchers; therefore, they constitute a service to the scholarly community. At the same time, the *Frontiers journal series* operates on a revolutionary invention, the tiered publishing system, initially addressing specific communities of scholars, and gradually climbing up to broader public understanding, thus serving the interests of the lay society, too.

Dedication to quality

Each Frontiers article is a landmark of the highest quality, thanks to genuinely collaborative interactions between authors and review editors, who include some of the world's best academicians. Research must be certified by peers before entering a stream of knowledge that may eventually reach the public - and shape society; therefore, Frontiers only applies the most rigorous and unbiased reviews. Frontiers revolutionizes research publishing by freely delivering the most outstanding research, evaluated with no bias from both the academic and social point of view. By applying the most advanced information technologies, Frontiers is catapulting scholarly publishing into a new generation.

What are Frontiers Research Topics?

Frontiers Research Topics are very popular trademarks of the *Frontiers journals series*: they are collections of at least ten articles, all centered on a particular subject. With their unique mix of varied contributions from Original Research to Review Articles, Frontiers Research Topics unify the most influential researchers, the latest key findings and historical advances in a hot research area.

Find out more on how to host your own Frontiers Research Topic or contribute to one as an author by contacting the Frontiers editorial office: frontiersin.org/about/contact

Individual's mechanics, movement and kinematics post-stroke

Topic editors
Yih-Kuen Jan — University of Illinois at Urbana-Champaign, United States
Veronica Cimolin — Polytechnic University of Milan, Italy

Citation
Jan, Y.-K., Cimolin, V., eds. (2024). *Individual's mechanics, movement and kinematics post-stroke*. Lausanne: Frontiers Media SA.
doi: 10.3389/978-2-8325-5027-4

Table of contents

04 Editorial: Individual's mechanics, movement and kinematics post-stroke
Veronica Cimolin and Yih-Kuen Jan

06 How Well Do Commonly Used Co-contraction Indices Approximate Lower Limb Joint Stiffness Trends During Gait for Individuals Post-stroke?
Geng Li, Mohammad S. Shourijeh, Di Ao, Carolynn Patten and Benjamin J. Fregly

20 Measures of Interjoint Coordination Post-stroke Across Different Upper Limb Movement Tasks
Anne Schwarz, Janne M. Veerbeek, Jeremia P. O. Held, Jaap H. Buurke and Andreas R. Luft

37 Association Between Finger-to-Nose Kinematics and Upper Extremity Motor Function in Subacute Stroke: A Principal Component Analysis
Ze-Jian Chen, Chang He, Nan Xia, Ming-Hui Gu, Yang-An Li, Cai-Hua Xiong, Jiang Xu and Xiao-Lin Huang

46 Functional Brain Controllability Alterations in Stroke
Xuhong Li, Feng Fang, Rihui Li and Yingchun Zhang

57 A Systematic Review of Fall Risk Factors in Stroke Survivors: Towards Improved Assessment Platforms and Protocols
Masoud Abdollahi, Natalie Whitton, Ramin Zand, Mary Dombovy, Mohamad Parnianpour, Kinda Khalaf and Ehsan Rashedi

71 Baseline robot-measured kinematic metrics predict discharge rehabilitation outcomes in individuals with subacute stroke
Michela Goffredo, Stefania Proietti, Sanaz Pournajaf, Daniele Galafate, Matteo Cioeta, Domenica Le Pera, Federico Posteraro and Marco Franceschini

81 A novel balance training approach: Biomechanical study of virtual reality-based skateboarding
Phunsuk Kantha, Wei-Li Hsu, Po-Jung Chen, Yi-Ching Tsai and Jiu-Jenq Lin

92 Gait characteristics related to fall risk in patients with cerebral small vessel disease
Yajing Wang, Yanna Li, Shoufeng Liu, Peipei Liu, Zhizhong Zhu and Jialing Wu

100 Differences in kinetic factors affecting gait speed between lesion sides in patients with stroke
Yusuke Sekiguchi, Dai Owaki, Keita Honda, Shin-Ichi Izumi and Satoru Ebihara

frontiers | Frontiers in Bioengineering and Biotechnology

TYPE Editorial
PUBLISHED 04 June 2024
DOI 10.3389/fbioe.2024.1430588

Check for updates

OPEN ACCESS

EDITED AND REVIEWED BY
Markus O. Heller,
University of Southampton, United Kingdom

*CORRESPONDENCE
Veronica Cimolin,
veronica.cimolin@polimi.it

RECEIVED 10 May 2024
ACCEPTED 21 May 2024
PUBLISHED 04 June 2024

CITATION
Cimolin V and Jan Y-K (2024), Editorial: Individual's mechanics, movement and kinematics post-stroke.
Front. Bioeng. Biotechnol. 12:1430588.
doi: 10.3389/fbioe.2024.1430588

COPYRIGHT
© 2024 Cimolin and Jan. This is an open-access article distributed under the terms of the Creative Commons Attribution License (CC BY). The use, distribution or reproduction in other forums is permitted, provided the original author(s) and the copyright owner(s) are credited and that the original publication in this journal is cited, in accordance with accepted academic practice. No use, distribution or reproduction is permitted which does not comply with these terms.

Editorial: Individual's mechanics, movement and kinematics post-stroke

Veronica Cimolin[1,2]* and Yih-Kuen Jan[3]

[1]Department of Electronics, Information and Bioengineering, Politecnico di Milano, Milano, Italy, [2]IRCCS Istituto Auxologico Italiano, Piancavallo, Italy, [3]Rehabilitation Engineering Lab, Department of Health and Kinesiology, University of Illinois at Urbana-Champaign, Urbana, IL, United States

KEYWORDS

stroke, rehabilitation, movement, kinematics, biomechanics

Editorial on the Research Topic
Individual's mechanics, movement and kinematics post-stroke

Disability after stroke is a major burden on society, due to its high incidence and prevalence. Among the priorities of rehabilitation programs, stroke rehabilitation aims to restore independence and improve patients' quality of life. Dynamic balance, fall prevention and upper limb recovery are essential features for the clinical management of hemiparetic patients. In this context, the assessment of movement by means of quantitative movement analysis in hemiparetic post-stroke patients is key to planning rehabilitative interventions. Kinematic analysis facilitates the interpretation of the extent and mechanisms of motor recovery, and it has been increasingly applied in neurological research.

Although quantitative biomechanical approaches are objective, sensitive and quantitative, their associations with clinical measures have not been fully studied. Thus, the goal of the Research Topic was to provide a quantitative evaluation of the relationship between lower or upper extremity biomechanics and clinical scores to investigate in depth the motor dysfunction associated with stroke-related movement disabilities, which is critical to improving our understanding and expanding interventional strategies to minimize long-term consequences due to stroke.

We invited authors to submit their latest results in the field, in the form of original papers, reviews, or clinical cases, focusing mainly on biomechanics and movement analysis in stroke patients, rehabilitation programs for stroke patients and their quantitative outcomes and innovative data analysis and models to study the mechanisms of motor recovery; 9 papers were accepted for publication in this Research Topic and they are summarized in the following paragraphs.

The papers could be divided into two main categories: assessment of gait performance and upper limb during specific movements.

In terms of the assessment of gait performance, Li et al. studied the feasibility of muscle co-contraction using two EMG-based Co-Contraction Indices to approximate lower limb joint stiffness trends during gait in two individuals post-stroke patients. Abdollahi et al. conducted a systematic review of fall risk factors in the stroke community in order to identify their similarities and trends. Kantha et al. compared virtual reality (VR)-based skateboarding with walking at a comfortable walking speed on a treadmill in 20 young participants, in terms of kinematics and electromyographic activity of the trunk and legs; the authors demonstrated that the effect of VR skateboarding is particularly manifest when

focusing on the supporting leg. Wang et al. investigated gait characteristics and fall risk in patients with cerebral small vessel disease (CSVD) and demonstrated that CSVD patients with seemingly normal gait and independent ambulation still have a high risk of falling. In particular, gait spatio-temporal kinematic parameters, gait symmetry, and gait variability were found to be important indicators for assessing high-fall risk. Sekiguchi et al. explored the differences in kinetic parameters of slow gait speed in patients with stroke across brain lesion sides. Lastly, with respect to the upper limb assessment category, Schwarz et al. examined inter-joint coordination in post-stroke patients during various upper limb movement tasks using parameters obtained from a wearable sensor, demonstrating that the kinematic parameters of the upper limb after stroke are largely influenced by the task. Cheng et al. investigated the kinematic components of the finger-to-nose test obtained from principal component analysis and the associations with upper extremity motor function in subacute stroke survivors. Li et al. provided an accurate interpretation and assessment of the underlying "motor control" deficits caused by stroke, using functional brain controllability analysis, based on electroencephalography and functional near-infrared spectroscopy, simultaneously recorded during a hand-clenching task. Goffredo et al. developed a predictive model for rehabilitation outcome at discharge assessed by the Motricity Index of the affected upper limb, based on multidirectional 2D robot-measured kinematics in individuals with subacute stroke.

It is evident from the articles in this Research Topic that improved performance in gait and upper limb motor skills leads to reduced risk of falls and better functioning in stroke patients. The articles in this Research Topic provide a foundation for the development of effective rehabilitation interventions to minimize the long-term consequences of stroke.

Author contributions

VC: Writing–review and editing, Writing–original draft. Y-KJ: Writing–review and editing, Writing–original draft.

Funding

The author(s) declare that no financial support was received for the research, authorship, and/or publication of this article. The authors declare that no financial support was received for the research, authorship, and/or publication of this article.

Conflict of interest

The authors declare that the research was conducted in the absence of any commercial or financial relationships that could be construed as a potential conflict of interest.

The author(s) declared that they were an editorial board member of Frontiers, at the time of submission. This had no impact on the peer review process and the final decision.

Publisher's note

All claims expressed in this article are solely those of the authors and do not necessarily represent those of their affiliated organizations, or those of the publisher, the editors and the reviewers. Any product that may be evaluated in this article, or claim that may be made by its manufacturer, is not guaranteed or endorsed by the publisher.

frontiers in Bioengineering and Biotechnology

ORIGINAL RESEARCH
published: 07 January 2021
doi: 10.3389/fbioe.2020.588908

How Well Do Commonly Used Co-contraction Indices Approximate Lower Limb Joint Stiffness Trends During Gait for Individuals Post-stroke?

Geng Li[1], Mohammad S. Shourijeh[1], Di Ao[1], Carolynn Patten[2] and Benjamin J. Fregly[1]*

[1] Rice Computational Neuromechanics Laboratory, Department of Mechanical Engineering, Rice University, Houston, TX, United States, [2] Biomechanics, Rehabilitation, and Integrative Neuroscience Lab, Department of Physical Medicine and Rehabilitation, School of Medicine, University of California, Davis, Davis, CA, United States

OPEN ACCESS

Edited by:
Yih-Kuen Jan,
University of Illinois
at Urbana-Champaign, United States

Reviewed by:
Alessandro Navacchia,
Smith and Nephew, United Kingdom
Jennifer Hicks,
Stanford University, United States

***Correspondence:**
Benjamin J. Fregly
fregly@rice.edu

Specialty section:
This article was submitted to
Biomechanics,
a section of the journal
Frontiers in Bioengineering and
Biotechnology

Received: 18 August 2020
Accepted: 09 December 2020
Published: 07 January 2021

Citation:
Li G, Shourijeh MS, Ao D,
Patten C and Fregly BJ (2021) How
Well Do Commonly Used
Co-contraction Indices Approximate
Lower Limb Joint Stiffness Trends
During Gait for Individuals
Post-stroke?
Front. Bioeng. Biotechnol. 8:588908.
doi: 10.3389/fbioe.2020.588908

Muscle co-contraction generates joint stiffness to improve stability and accuracy during limb movement but at the expense of higher energetic cost. However, quantification of joint stiffness is difficult using either experimental or computational means. In contrast, quantification of muscle co-contraction using an EMG-based Co-Contraction Index (CCI) is easier and may offer an alternative for estimating joint stiffness. This study investigated the feasibility of using two common CCIs to approximate lower limb joint stiffness trends during gait. Calibrated EMG-driven lower extremity musculoskeletal models constructed for two individuals post-stroke were used to generate the quantities required for CCI calculations and model-based estimation of joint stiffness. CCIs were calculated for various combinations of antagonist muscle pairs based on two common CCI formulations: Rudolph et al. (2000) (CCI_1) and Falconer and Winter (1985) (CCI_2). CCI_1 measures antagonist muscle activation relative to not only total activation of agonist plus antagonist muscles but also agonist muscle activation, while CCI_2 measures antagonist muscle activation relative to only total muscle activation. We computed the correlation between these two CCIs and model-based estimates of sagittal plane joint stiffness for the hip, knee, and ankle of both legs. Although we observed moderate to strong correlations between some CCI formulations and corresponding joint stiffness, these associations were highly dependent on the methodological choices made for CCI computation. Specifically, we found that: (1) CCI_1 was generally more correlated with joint stiffness than was CCI_2, (2) CCI calculation using EMG signals with calibrated electromechanical delay generally yielded the best correlations with joint stiffness, and (3) choice of antagonist muscle pairs significantly influenced CCI correlation with joint stiffness. By providing guidance on how methodological choices influence CCI correlation with joint stiffness trends, this study may facilitate a simpler alternate approach for studying joint stiffness during human movement.

Keywords: muscle co-contraction, co-contraction index, joint stiffness, electromyography (EMG), EMG-driven modeling

INTRODUCTION

Muscle co-contraction refers to the simultaneous activation of muscles on opposite sides of a joint. It is an important mechanism used by the central nervous system to regulate joint stability (Hirokawa et al., 1991; McGill et al., 2003) and provide movement accuracy (Gribble et al., 2003; Missenard et al., 2008). Individuals who suffer from orthopedic injuries or neuromuscular disorders use elevated levels of muscle co-contraction (Lamontagne et al., 2000; Rudolph et al., 2000; Higginson et al., 2006; McGinnis et al., 2013) to generate additional joint stiffness so as to compensate for the lack of joint stability (Gollhofer et al., 1984; Kuitunen et al., 2002; Mohr et al., 2018), although evidence in support of this premise is equivocal (Banks et al., 2017). While co-contraction increases joint stiffness which in turn may improve the stability (Latash and Huang, 2015) and accuracy (Wong et al., 2009) of limb movement, it does so at the expense of increased energetic cost (Moore et al., 2014). Quantification of joint stiffness is therefore critical for understanding how this quantity adds both benefit and cost to dynamic movements such as gait.

Stroke is a common clinical condition that often impairs movement through an increase in joint stiffness (Thilmann et al., 1991; Rydahl and Brouwer, 2004; Galiana et al., 2005; Mirbagheri et al., 2008; Gao et al., 2009) and spasticity (Galiana et al., 2005; Mirbagheri et al., 2008) along with a decrease in joint range of motion (Gao et al., 2009). Some clinicians have developed rehabilitation regimens that use stretching and relaxation to help reduce joint stiffness (Bressel and McNair, 2002; Selles et al., 2005; Gao et al., 2011). Other clinicians have used assistive devices with stiffness-informed designs to help improve movement function in stroke survivors. These devices include rehabilitation robots (Vallery et al., 2008), exoskeletons (Liu et al., 2018), and ankle-foot orthoses (Singer et al., 2014). A common theme in these studies is the need for reliable quantification of joint stiffness for the design and evaluation of new treatments. However, joint stiffness is difficult to measure experimentally (Pfeifer et al., 2012) or calculate computationally, and determining it requires musculoskeletal modeling informed by appropriate muscle recruitment strategies (Sartori et al., 2015). Consequently, development of easy-to-use methods for estimating joint stiffness in a clinical setting could be valuable for improving the treatment of individuals post-stroke.

Quantification of muscle co-contraction may offer an alternative for estimating joint stiffness. Although previous studies have reported that muscle co-contraction and joint stiffness are related (Kuitunen et al., 2002; McGinnis et al., 2013; Collins et al., 2014), the relationship between these two quantities remains poorly understood, as initially noted by Hortobágyi and Devita (2000). One issue is that previous studies have quantified joint stiffness primarily in the form of quasi-stiffness. Joint quasi-stiffness is described as the gradient of the torque-angle curve rather than the true characterization of joint stiffness (Rouse et al., 2013). Since joint quasi-stiffness does not change for different levels of muscle co-contraction, it is not an accurate representation of joint stiffness generated by muscle co-contraction. From another perspective, quasi-stiffness represents the joint moment response to changes in not only joint position but also muscle activation and joint velocity (Sartori et al., 2015). To address these issues, the present study defines joint stiffness as the elastic response of a joint moment to changes in only joint position. This definition follows the recommendation of Latash and Zatsiorsky (1993) and provides a reasonable basis for the evaluation of the relationship between muscle co-contraction and joint stiffness.

The Co-Contraction Index (CCI) is a commonly used method for quantifying muscle co-contraction during human movement. Computation of a CCI involves choosing from a wide selection of methods, and previous studies have examined how differences in method affect CCI results (Knarr et al., 2012; Banks et al., 2017; Souissi et al., 2017). Two common CCI formulations (Falconer and Winter, 1985; Rudolph et al., 2000) allow clinical researchers to make a fast and easy assessment of muscle co-contraction using surface electromyographic (EMG) data, and these two formulations have been used in several studies to quantify muscle co-contraction (Kellis, 1998; Di Nardo et al., 2015; Banks et al., 2017). The selected CCI formulation with associated methodological choices could affect the extent to which the CCI is a reasonable surrogate for joint stiffness. Consequently, it would be valuable to evaluate how different methodological choices for calculating a CCI affect the CCI's ability to approximate joint stiffness trends during activities of daily living such as gait.

This study provides a quantitative evaluation of the relationship between lower extremity muscle co-contraction indices and corresponding joint stiffnesses during gait. We calculated CCIs and lower body joint stiffnesses using EMG data collected from the lower extremity muscles of two individuals post-stroke walking at their self-selected speed. CCIs were calculated for the two common CCI formulations noted above using four different methods for EMG data post-processing. Lower body joint stiffnesses were calculated using EMG-driven musculoskeletal models calibrated using the EMG, motion capture, and ground reaction data collected from each subject. Correlations between CCIs and joint stiffnesses for each subject were calculated, and CCI calculation methods that helped improve the correlations were identified. These findings could help clinicians formulate CCIs that yield results more strongly aligned with joint stiffness trends.

MATERIALS AND METHODS

Experimental Data

Walking data collected from two hemiparetic male subjects post-stroke were used for this study. The first subject (male, height 1.70 m, mass 80.5 kg, age 79 years, right-sided hemiparesis, lower extremity Fugl-Meyer Motor Assessment score of 32 out of a maximum 34), herein referred to as subject S1, walked at a self-selected speed of 0.5 m/s. The second subject (male, height 1.83 m, mass 88.5 kg, age 62 years, right-sided

hemiparesis, lower extremity Fugl-Meyer Motor Assessment score of 25 points), herein referred to as subject S2, walked at a self-selected speed of 0.45 m/s. Both subjects walked for multiple cycles on a split-belt instrumented treadmill (Bertec Corp., Columbus, OH, United States) while motion capture (Vicon Corp., Oxford, United Kingdom), ground reaction (Bertec Corp., Columbus, OH, United States), and EMG (Motion Lab Systems, Baton Rouge, LA, United States) data were collected. EMG signals were measured at 1,000 Hz from 16 muscles in each leg (**Table 1**) using a combination of surface and fine-wire electrodes. For more details about the data collection and the experimental protocol, see Meyer et al. (2017). Data from ten gait cycles for each subject were selected for analysis.

EMG Data Processing and EMG-Driven Model Calibration

Raw EMG data were processed using a standard methodology. The data were high-pass filtered at 40 Hz, demeaned, rectified, and low-pass filtered at a variable cutoff frequency of 3.5/period of the gait cycle (Lloyd and Besier, 2003) while using a 4th order

TABLE 1 | Muscles analyzed in this study.

Muscle name (abbreviation)	EMG source	Direction of moment generation			EMG scale in S1		EMG scale in S2	
		Hip	Knee	Ankle	L	R	L	R
Adductor brevis (addbrev)	Adductor longus	FLEX			0.14	0.05	0.05	0.23
Adductor longus (addlong)		FLEX			0.33	0.07	0.05	0.27
Adductor magnus distal (addmag1)		EXT			0.07	0.05	0.05	0.09
Adductor magnus ischial (addmag2)		EXT			0.05	0.05	0.05	0.31
Adductor magnus middle (addmag3)					0.07	0.05	0.05	0.25
Adductor magnus proximal (addmag4)		FLEX			0.13	0.05	0.05	0.66
Gluteus maximus superior (glmax1)	Gluteus maximus	EXT			0.32	0.20	0.43	0.09
Gluteus maximus middle (glmax2)		EXT			0.33	0.20	0.39	0.09
Gluteus maximus inferior (glmax3)		EXT			0.32	0.20	0.51	0.09
Gluteus medius anterior (glmed1)	Gluteus medius	EXT			0.71	0.62	0.06	0.92
Gluteus medius middle (glmed2)		EXT			0.69	0.63	0.06	0.92
Gluteus medius posterior (glmed3)		EXT			0.69	0.62	0.06	0.93
Gluteus minimus anterior (glmin1)					0.32	0.14	0.99	0.16
Gluteus minimus middle (glmin2)					0.30	0.15	0.99	0.16
Gluteus minimus posterior (glmin3)		EXT			0.30	0.15	0.99	0.16
Iliacus (iliacus)	Iliopsoas*	FLEX			0.05	0.05	0.05	0.05
Psoas (psoas)		FLEX			0.99	0.82	0.21	0.06
Semimembranosus (semimem)	Semimem	EXT	FLEX		0.35	0.40	0.26	0.15
Semitendinosus (semiten)		EXT	FLEX		0.30	0.40	0.26	0.15
Biceps femoris long head (bflh)	Bflh	EXT	FLEX		0.76	0.38	0.57	0.14
Biceps femoris short head (bfsh)			FLEX		0.76	0.39	0.57	0.14
Rectus femoris (recfem)	Rectus femoris	FLEX	EXT		0.48	0.27	0.65	0.05
Vastus medialis (vasmed)	Vastus medialis		EXT		0.27	0.50	0.18	0.29
Vastus intermedius (vasint)			EXT		0.31	0.44	0.16	0.28
Vastus lateralis (vaslat)	Vastus lateralis		EXT		0.32	0.11	0.16	0.27
Lateral gastronemius (gaslat)	Gasmed		FLEX	PF	0.05	0.12	0.19	0.30
Medial gastronemius (gasmed)			FLEX	PF	0.14	0.14	0.26	0.44
Tibialis anterior (tibant)	Tbialis anterior			DF	0.61	1.00	1.00	1.00
Tibialis posterior (tibpost)	Tibialis posterior*			PF	0.05	0.05	0.05	0.40
Peroneus brevis (perbrev)	Peroneus longus			PF	0.05	0.98	0.77	0.26
Peroneus longus (perlong)				PF	0.05	0.99	0.76	0.26
Peroneus tertius (pertert)				DF	0.05	0.99	0.77	0.26
Soleus (soleus)	Soleus			PF	0.65	0.96	1.00	0.08
Extensor digitorum longus† (edl)	Edl*			DF	1.00	0.26		
Flexor digitorum longus† (fdl)	Fdl*			PF	1.00	0.05		
Tensor fasciae latae‡ (tfl)	Tfl						0.52	1.00

*Direction of moment generation of each muscle is indicated as FLEX – in the direction of joint flexion, EXT –in the direction of joint extension, DF – in the direction of ankle dorsiflexion, PF – in the direction of ankle plantarflexion. EMG scale is the scale factor applied to the basic EMG signal of a muscle to account for the difference between the physiological maximum and maximum observed during gait trials. S1, Post-stroke subject S1; S2, Post-stroke subject S2. *measured using fine-wire EMG. †measured from only the 1st post-stroke subject (S1). ‡measured from only the 2nd post-stroke subject (S2).*

zero phase-lag Butterworth filter (Meyer et al., 2017). Filtered EMG data were subsequently normalized to the maximum value over all cycles and resampled to 101 normalized time points for each gait cycle. Normalized EMG data for each gait cycle were offset by the minimum value so that the minimum EMG value for each gait cycle was zero. These processing procedures represent the basic approach for EMG processing adopted by other studies for the quantification of muscle co-contraction (Rosa et al., 2014). The EMG signals processed using the aforementioned procedures were defined as the basic EMG signals, EMG_{basic}.

An EMG-driven modeling process was used to calibrate relevant parameters of the lower body musculoskeletal model used to represent each subject (Meyer et al., 2017). The calibrated model parameters included those defining the conversion of basic EMG into muscle excitation, muscle excitation into muscle activation via activation dynamics, and muscle activation into muscle force via a Hill-type muscle tendon model with rigid tendon. The calibration process utilized numerical optimization to adjust model parameter values so as to achieve the closest match between joint moments produced by the EMG-driven musculoskeletal model and those calculated from inverse dynamics. Conversion of basic EMG into muscle excitation involved adding an electromechanical delay and applying a muscle-specific EMG scale factor to EMG_{basic}. Electromechanical delay is defined as the duration from the instant an electrical signal is received to the instant a force response is generated by the muscle. Electromechanical delay was assumed to be the same for all muscles in each leg (Meyer et al., 2017). The delays for subject S1 were 82 ms (left leg) and 93 ms (right leg, paretic side) while for subject S2 they were 100 ms (left leg) and 114 ms (right leg, paretic side). A muscle-specific scale factor (**Table 1**) was used to account for the difference between the estimated maximum EMG value and the maximum value over all experimental trials. The processed EMG signals resulting from calibration of both electromechanical delays and scale factors were defined as fully calibrated EMG signals, $EMG_{calibrated}$.

To isolate the underlying effect of the two EMG parameters on quantification of co-contraction, we introduced two additional types of EMG signals: (1) scaled EMG signals EMG_{scaled}, which are EMG signals normalized to the optimized maximum EMG value but without electromechanical delay, and (2) delayed EMG signals $EMG_{delayed}$, which are electromechanically delayed EMG signals that are not normalized to the optimized maximum value. These signals were obtained as shown below:

$$\mathrm{EMG_{scaled}} = \mathrm{EMG_{basic}} \times \text{scale factor} \tag{1}$$

$$\mathrm{EMG_{delayed}} = \frac{\mathrm{EMG_{calibrated}}}{\text{scale factor}} \tag{2}$$

CCI Computation

CCI values were computed from processed EMG data using the two most common formulations. CCI_1 was based on the formulation reported by Rudolph et al. (2000),

$$\mathrm{CCI_1}\,(t) = \frac{\mathrm{Input}_L\,(t)}{\mathrm{Input}_H\,(t)}\left(\mathrm{Input}_L\,(t) + \mathrm{Input}_H\,(t)\right) \tag{3}$$

while CCI_2 was based on the formulation reported by Falconer and Winter (1985):

$$\mathrm{CCI_2}\,(t) = \frac{2 \times \mathrm{Input}_L\,(t)}{\left(\mathrm{Input}_L\,(t) + \mathrm{Input}_H\,(t)\right)} \tag{4}$$

For both formulations, $Input_L$ and $Input_H$ represent EMG signals from an antagonist muscle pair, where both signals were resampled to 101 normalized time points (0 – 100% of gait cycle at 1% increment). $Input_L$ is the EMG signal with the lower absolute magnitude at time t while $Input_H$ is the EMG signal with the higher absolute magnitude. For both CCI formulations, the input quantities include the four types of EMG signals (EMG_{basic}, EMG_{scaled}, $EMG_{delayed}$, and $EMG_{calibrated}$) described above. Each CCI calculation method used in this study is described by a combination of the selected CCI formulation and the selected EMG type. For example, $EMG_{delayed}$ CCI_1 means the CCI values are calculated using delayed EMG signals based on the Rudolph et al. (2000) CCI formulation.

In addition to varying the types of EMG signals used to compute CCI, this study also investigated how the difference in constituent muscles for an antagonist muscle pair could affect the relationship between CCI and joint stiffness. CCI was computed for three lower limb degrees of freedom (DOFs) in the sagittal plane: hip, knee, and ankle flexion and extension for both non-paretic side and paretic side. Lower extremity muscles were classified by their functional roles during gait (**Table 1**), and one muscle was selected from each of the agonist group and the antagonist group to form various combinations of antagonistic pairs. Antagonistic muscle pairs consisting of small muscles that were not major contributors to overall joint stiffness (less than 2% on average) were not included for the subsequent analyses. The majority of the EMG-based CCIs in previous studies were computed using EMG signals measured from surface muscles (Rosa et al., 2014) because the alternative fine-wire EMG method is invasive and not universally available. Therefore, despite the availability of fine-wire EMG data of deep muscles (iliacus, psoas, tibialis posterior, extensor, and flexor digitorum longus), the analyses in this study focused on CCI computed from surface EMG signals of muscles for the findings to be more applicable in clinical settings. Antagonistic muscle pairs consisting of the aforementioned deep muscles were omitted in the subsequent analyses.

Estimation of Joint Stiffness

Sagittal plane stiffness of the lower extremity joints (hip, knee, and ankle) in each leg was estimated using a model-based formulation (Shourijeh and Fregly, 2020). The derivation starts with expressing joint stiffness as the partial derivative of joint moment M_j with respect to generalized coordinate θ_j corresponding to degree of freedom (DOF) j:

$$K_{\mathrm{joint}} = -\frac{\partial M_j}{\partial \theta_j} \tag{5}$$

The net joint moment M_j can be expressed as the sum of the product of muscle moment arm and tendon force for each muscle spanning the joint:

$$M_j = \sum_{i=1}^{n} r_{ij} F_i^T \tag{6}$$

where r_{ij} represents the moment arm of the ith muscle about DOF j, F_i^T represents the tendon force of the ith muscle, and n is the total number of muscles. By substituting the expression of joint moment M_j into Eq. (5) and performing partial differentiation via product rule, one obtains

$$K_{\text{joint}} = -\frac{\partial M_j}{\partial \theta_j} = -\sum_{i=1}^{n}\left(\frac{\partial r_{ij}}{\partial \theta_j} F_i^T + r_{ij}\frac{\partial F_i^T}{\partial \theta_j}\right) \tag{7}$$

Re-expressing $\frac{\partial F_i^T}{\partial \theta_j}$ as $\frac{\partial F_i^T}{\partial l_i^{MT}}\frac{\partial l_i^{MT}}{\partial \theta_j}$ via the chain rule and taking advantage of the fact that $r_{ij} = -\frac{\partial l_i^{MT}}{\partial \theta_j}$, where $l^{MT}{}_i$ represents the muscle-tendon length of the ith muscle, K_{joint} can be expressed as the sum of the stiffness contributed by each individual muscle K_{mus} as shown below:

$$K_{\text{joint}} = \sum_{i=1}^{n} K_{mus\ i} = -\sum_{i=1}^{n}\left(\frac{\partial r_{ij}}{\partial \theta_j} F_i^T + r_{ij}^2 \frac{\partial F_i^T}{\partial l_i^{MT}}\right) \tag{8}$$

This model-based stiffness formulation assumes that the muscle model possesses a rigid tendon. As moment arms and muscle-tendon lengths of the musculoskeletal model (Meyer et al., 2017) were represented by surrogate models in the form of polynomials of joint kinematics, muscle stiffness around a joint could be computed analytically. Identical to CCI calculations, joint stiffness was calculated at 101 normalized time points within each gait cycle.

Statistical Analyses

The strength of association between CCI (CCI_1 or CCI_2) and joint stiffness K_{joint} was quantified by the Pearson correlation coefficient using the *corrcoef* function in MATLAB (MathWorks, Natick, United States). Correlation was calculated between the two time series for each of the 10 gait cycles analyzed:

$$r_{1_j} = \text{corrcoef}\left(CCI_{1_j}, K_j\right) \tag{9}$$

$$r_{2_j} = \text{corrcoef}\left(CCI_{2_j}, K_j\right) \tag{10}$$

The Wilcoxon rank sum test was performed in MATLAB using the *ranksum* function to compare the mean correlation coefficient between the two classes of data (10 pairs of correlation coefficients for 10 gait cycles). The analysis tested the null hypothesis that the two classes of data came from samples with continuous distributions possessing equal medians. The level of statistical significance was set at $p = 0.05$.

RESULTS

Joint stiffness trends were mostly symmetrical between the non-paretic and paretic side for subject S1 (**Figures 1A,B**, 1st row). For the hip joint on each side, joint stiffness increased steadily in the early stance phase (0 – 15% gait cycle), then were largely maintained at a constant level slightly above 100 N-m/rad for the remainder of the stance phase (15 – 55% gait cycle), then decreased during late stance and swing phases (55 – 100% gait cycle). For the knee joint on each side, joint stiffness increased steadily early in the stance phase (0 – 20% gait cycle) and then gradually decreased from the peak value. For the ankle joint, however, joint stiffness on the paretic side peaked at a magnitude much higher than that on the non-paretic side at approximately 30% gait cycle. The decline in joint stiffness was more gradual on the non-paretic side during swing phase than what was more sudden on the paretic side.

In contrast, joint stiffness trends were asymmetrical between the non-paretic and paretic side for subject S2 (**Figures 2A,B**, 1st row). Joint stiffness for hip, knee, and ankle on the non-paretic side was sustained at a high level to a much later point in the gait cycle before declining than that on the paretic side. The joint stiffness trends coincided with the subject's gait pattern which had both longer than normal stance phase on the non-paretic side (0 – ∼75% gait cycle) and shorter than normal stance phase on the paretic side (0 – ∼50% gait cycle). Also observed from joint stiffness trends of subject S2 was that joint stiffness for the hip on the paretic side reached a peak magnitude much higher than that on the non-paretic side at 35% gait cycle and was followed by a sharp decline which was not seen on the paretic side.

For subject S1, we observed correlation ranged from moderate to strong between CCI_1 and joint stiffness (**Figure 3A**) and from weak to moderate between CCI_2 and joint stiffness (**Figure 3B**). Correlation between CCI_1 and K_{joint}, r_1 was moderate ($0.5 < \bar{r}_1 < 0.7$) for the hip joint, strong ($\bar{r}_1 > 0.7$) for the knee joint, and moderate ($0.5 < \bar{r}_1 < 0.7$) for the ankle joint on both sides. Correlation strength was assessed based on Moore et al. (2015). Correlation between CCI_2 and K_{joint}, r_2 were moderate ($0.5 < \bar{r}_2 < 0.7$) for the hip joint on both sides, moderate ($0.5 < \bar{r}_2 < 0.7$) for the knee joint on both sides, weak ($0.3 < \bar{r}_2 < 0.5$) for the ankle joint on the non-paretic side and moderate ($0.5 < \bar{r}_2 < 0.7$) on the paretic side.

For subject S2, we observed correlation ranged from weak to strong between CCI_1 and joint stiffness (**Figure 4A**) and from weak to strong between CCI_2 and joint stiffness (**Figure 4B**). Correlation between CCI_1 and K_{joint}, r_1 was strong ($\bar{r}_1 > 0.7$) for the hip joint on the non-paretic side and moderate ($0.5 < \bar{r}_1 < 0.7$) on the paretic side, moderate ($0.5 < \bar{r}_1 < 0.7$) for the knee joint on the non-paretic side and strong ($\bar{r}_1 > 0.7$) on the paretic side, weak ($0.3 < \bar{r}_1 < 0.5$) for the ankle joint on the non-paretic side and moderate ($0.5 < \bar{r}_1 < 0.7$) on the paretic side. Correlation r_2 between CCI_2 and K_{joint} were moderate ($0.5 < \bar{r}_2 < 0.7$) for the hip joint on both sides, strong ($\bar{r}_2 > 0.7$) for the knee joint on both sides, weak ($0.3 < \bar{r}_2 < 0.5$) for the ankle joint on the non-paretic side and moderate ($0.5 < \bar{r}_2 < 0.7$) on the paretic side.

The highest mean values for r_1 were generally higher than those for r_2 for both subjects with a few exceptions (**Figures 5A,B**). Correlations r_1 and r_2 were evaluated at six joints for both subjects, which yielded a total of 12 cases for comparing r_1 and r_2. In 7 of the 12 cases, r_1 was larger than r_2 (**Figures 5A,B**):

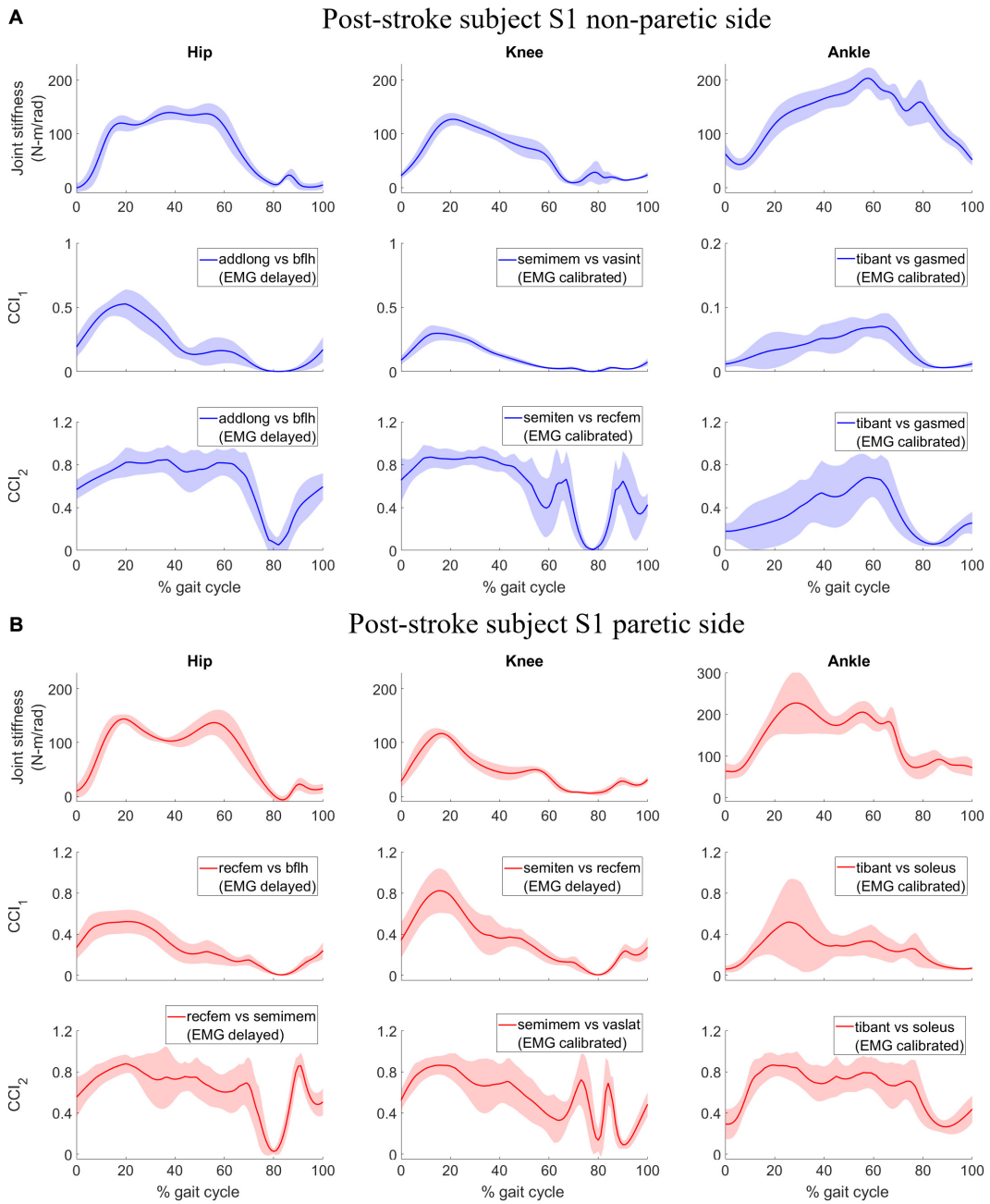

FIGURE 1 | Post-stroke subject S1, lower extremity joint stiffness and sample EMG-based CCI_1 and CCI_2 values (mean ± 1 standard deviation) for **(A)** non-paretic side, and **(B)** paretic side. The sample EMG-based CCIs were selected for display because of their highest correlation with corresponding joint stiffness. The antagonistic pair of muscles selected for CCI computation are identified and EMG signal type is displayed in parenthesis.

S1 Knee (NP) Ankle (NP) Knee (P) Ankle (P), S2 Hip (NP), Ankle (NP), and Knee (P), where NP refers to the non-paretic side and P refers to the paretic side. In only 3 of the 12 cases was r_2 clearly higher than r_1 (**Figures 5A,B**): S1 Hip (NP), S2 Hip (P), Ankle (P). In the other two case, S1 Hip (P) and S2 Knee (NP), neither r_1 nor r_2 was clearly higher than the other.

We also identified the EMG processing methods and antagonistic muscle pairings that would likely yield the highest correlations between the CCIs and joint stiffness. The CCI with highest correlation to joint stiffness at each joint for both subjects was calculated based on either $EMG_{delayed}$ or $EMG_{calibrated}$ (**Figures 3A,B**, **4A,B**). CCIs calculated using EMG_{scaled} did not always yield higher correlations with joint stiffness than did those calculated using EMG_{basic}. The antagonist muscle pairs that yielded that highest correlation between CCIs and joint stiffness (**Figures 3A,B**, **4A,B**) were: 1. Adductors-hamstrings

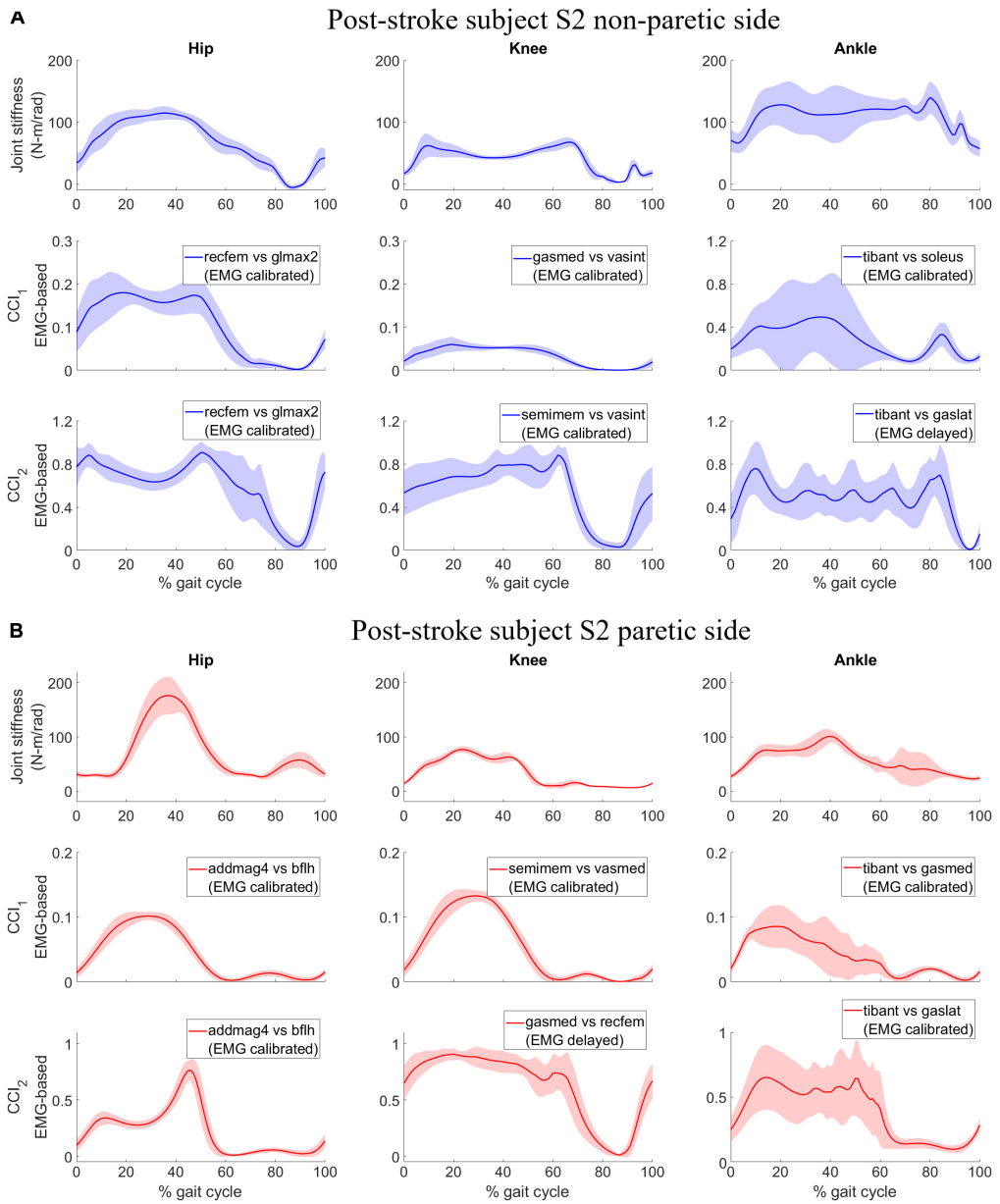

FIGURE 2 | Post-stroke subject S2, lower extremity joint stiffness and sample EMG-based CCI_1 and CCI_2 values (mean ± 1 standard deviation) for both **(A)** non-paretic side, and **(B)** paretic side. The sample EMG-based CCIs were selected for display because of the highest correlation with corresponding joint stiffness. The antagonistic pair of muscles selected for CCI computation are identified and EMG processing method is displayed in parenthesis.

or quadriceps-hamstrings combinations for the hip joints; 2. Quadriceps-hamstrings combinations for the knee joints; 3. Tibialis anterior-gasctronemii or tibialis anterior-soleus combinations for the ankle joints.

DISCUSSION

This study evaluated how well different CCI formulations approximate lower extremity joint stiffness trends during gait for individuals post-stroke. Joint stiffness trends may help reveal gait pathologies in these individuals as demonstrated in this study. In addition, joint stiffness may potentially be used to improve the design of rehabilitation treatments and assistive devices for individuals post-stroke. However, the difficulty of measuring or computing joint stiffness is well documented. It would therefore be beneficial to the clinical community if commonly used co-contraction indices correlated well with joint stiffness, thereby providing easy-to-calculate surrogate measures of joint stiffness. Although moderate to strong correlation was observed between some CCI formulations and corresponding joint stiffness, this correlation was highly dependent on the methodological choices

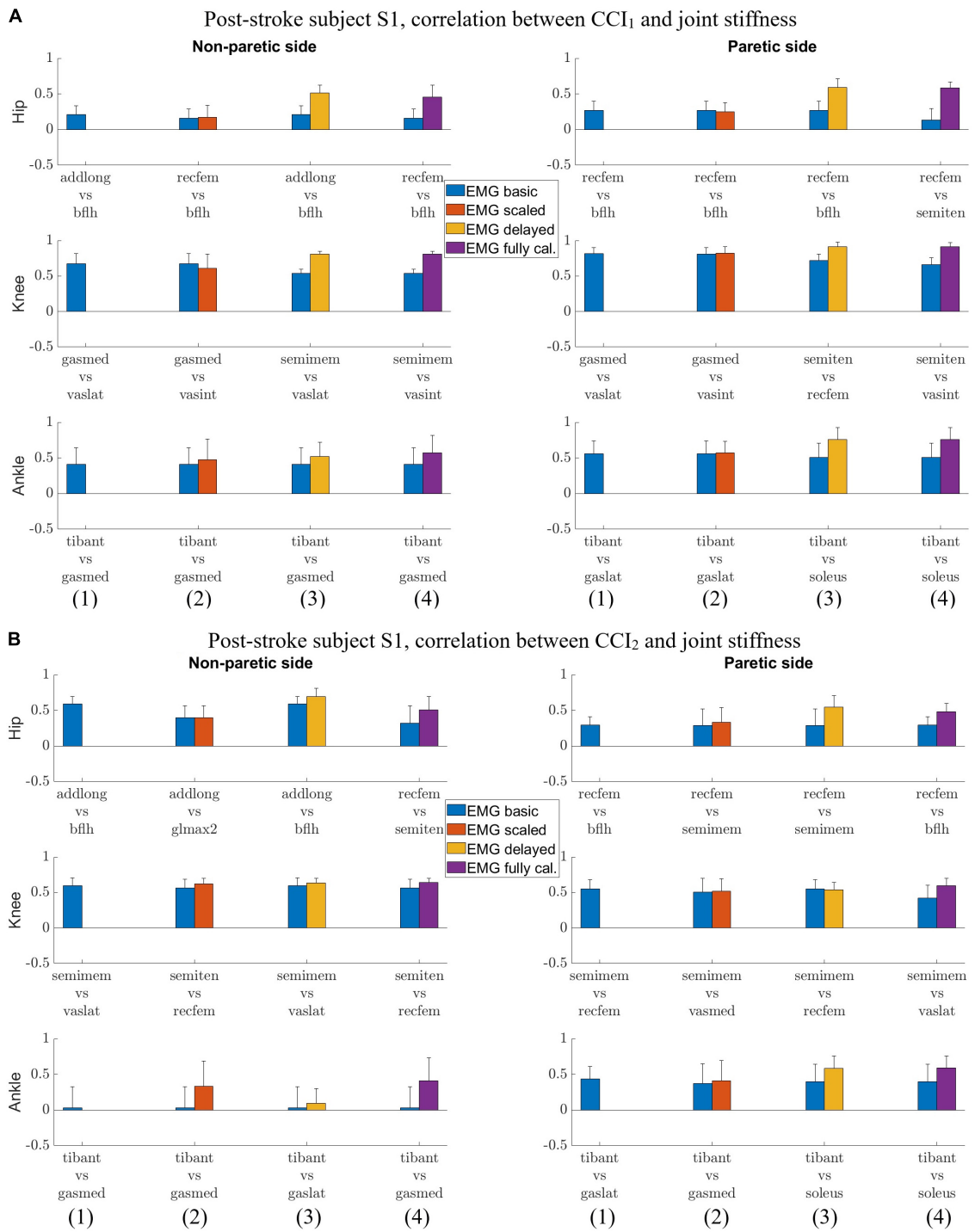

FIGURE 3 | (A) Post-stroke subject S1, correlation between CCI_1 and joint stiffness K_{joint}. Bars are at the mean value of the Pearson correlation coefficient, and error bars are at one standard deviation (+/– depending on the sign of mean value). Each muscle combination for antagonistic pairing displayed in the figure represents the best correlation between K_{joint} and CCI_1 computed using a specific type of EMG signals: (1) EMG_{basic} (blue); (2) EMG_{scaled} (red); (3) $EMG_{delayed}$ (yellow); and (4) $EMG_{calibrated}$ (purple). **(B)** Post-stroke subject S1, correlation between CCI_2 and joint stiffness K_{joint}. Bars are at the mean value of the Pearson correlation coefficient and error bars are at one standard deviation (+/– depending on the sign of mean value). Each muscle combination for antagonistic pairing displayed in the figure represents the best-in-class correlation between K_{joint} and CCI_2 computed using a specific type of EMG signals: (1) EMG_{basic} (blue); (2) EMG_{scaled} (red); (3) $EMG_{delayed}$ (yellow); and (4) $EMG_{calibrated}$ (purple).

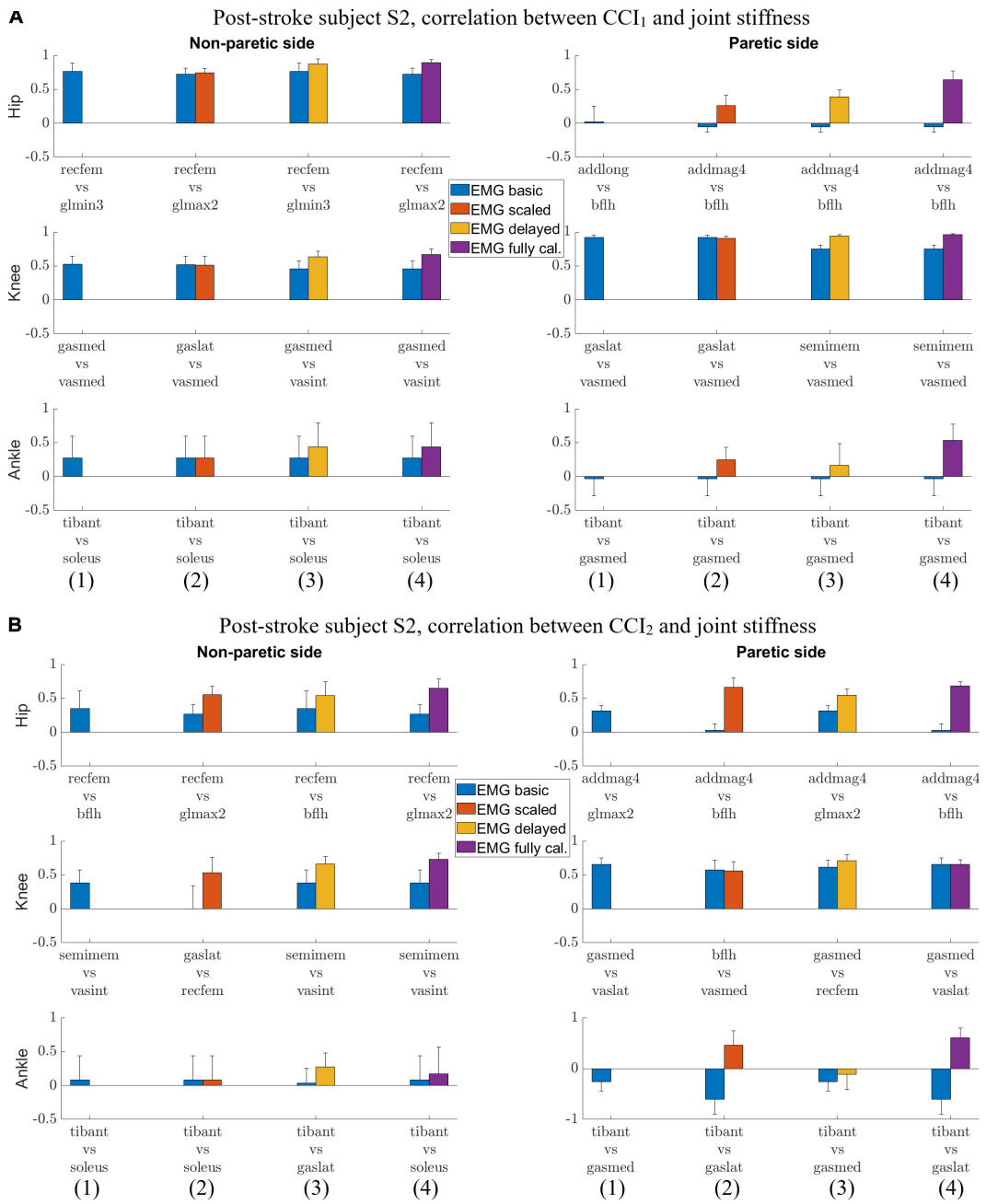

FIGURE 4 | (A) Post-stroke subject S2, correlation between CCI_1 and joint stiffness K_{joint}. Bars are at the mean value of the Pearson correlation coefficient, and error bars are at one standard deviation (+/– depending on the sign of mean value). Each muscle combination for antagonistic pairing displayed in the figure represents the best correlation between K_{joint} and CCI_1 computed using a specific type of EMG signal: (1) EMG_{basic} (blue); (2) EMG_{scaled} (red); (3) $EMG_{delayed}$ (yellow); and (4) $EMG_{calibrated}$ (purple). **(B)** Post-stroke subject S2, correlation between CCI_2 and joint stiffness K_{joint}. Bars are at the mean value of the Pearson correlation coefficient, and error bars are at 1 standard deviation (+/– depending on the sign of mean value). Each muscle combination for antagonistic pairing displayed in the figure represents the best correlation between K_{joint} and CCI_2 computed using a specific type of EMG signal: (1) EMG_{basic} (blue); (2) EMG_{scaled} (red); (3) $EMG_{delayed}$ (yellow); and (4) $EMG_{calibrated}$ (purple).

made for CCI computation. The conditions under which we observed the highest CCI correlations with joint stiffness were obtained can be summarized as follows: (1) CCI_1 formulation (Rudolph et al., 2000) was better than CCI_2 formulation (Falconer and Winter, 1985); (2) EMG signals with calibrated electromechanical delay ($EMG_{delayed}$ and $EMG_{calibrated}$) worked better than did EMG_{basic} or EMG_{scaled} when calculating CCI_1, (3) Some antagonist muscle pairs worked better than did other antagonist muscle pairs when calculating CCI_1. These findings could be used as a preliminary foundation for predicting joint

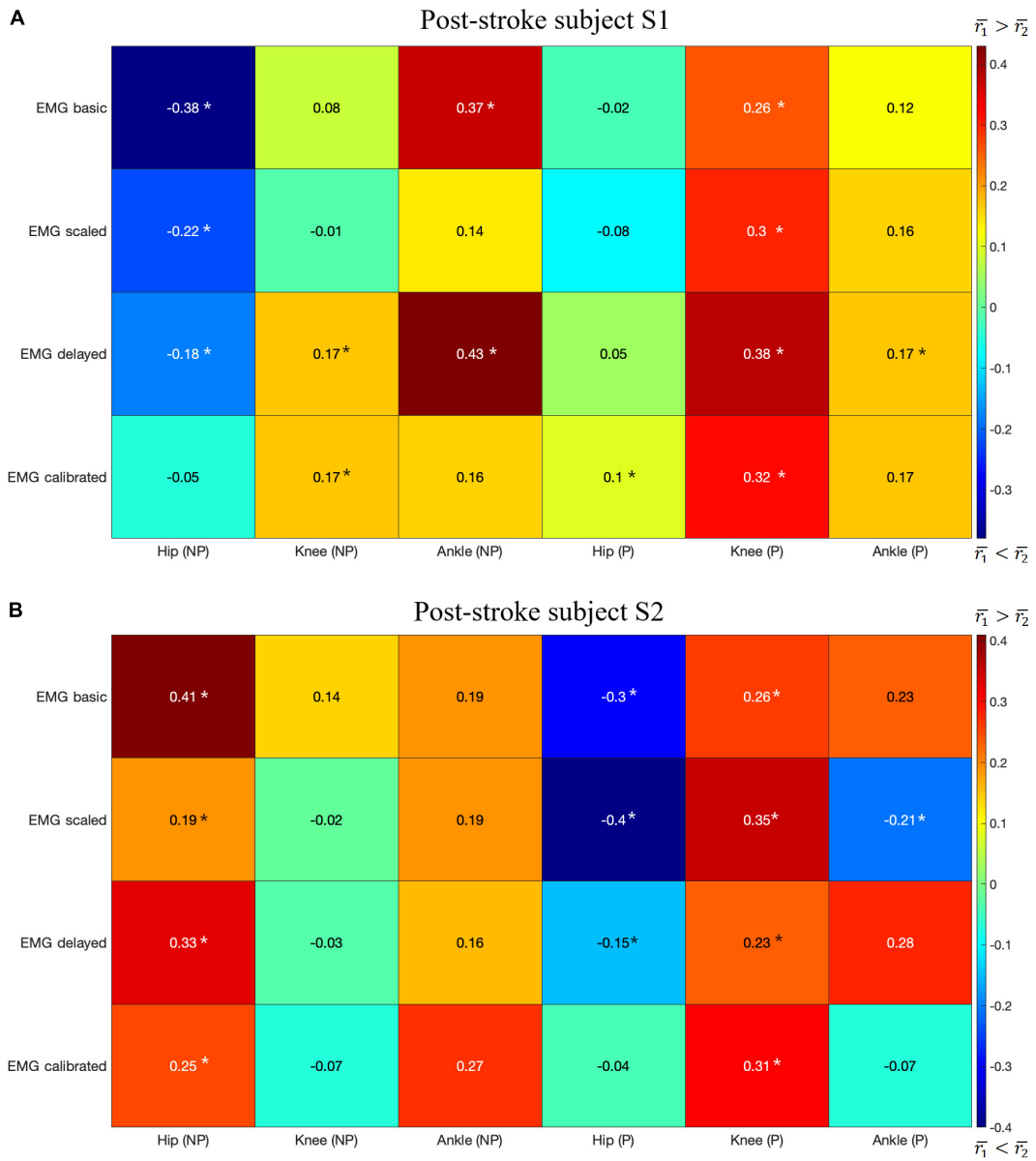

FIGURE 5 | The difference in the highest mean correlation between CCI_1 and K_{joint} ($\overline{r_1}$) and between CCI_2 and K_{joint} ($\overline{r_2}$) for each type of EMG signal. Positive difference (red) indicates CCI_1 has a higher correlation with K_{joint} than does CCI_2, while negative difference (blue) indicates the opposite. NP, non-paretic side, P, paretic side. The results are for: **(A)** Post-stroke subject S1, and **(B)** Post-stroke subject S2. A star (*) indicates a statistically significant Wilcoxon rank sum test result ($p < 0.05$).

stiffness trends from EMG-based measurement of muscle co-contraction.

Joint stiffness trends can help reveal gait pathologies as demonstrated in this study. On the surface, the joint stiffness trends confirmed clinical observations about the post-stroke subjects studied. Subject S1 has relatively high motor functioning post-stroke (Fugl-Meyer Motor Assessment score: 32 points), and joint stiffness trends between both non-paretic and paretic sides were symmetrical to a certain extent just as the gait patterns were. Subject S2 has relatively low motor functioning (Fugl-Meyer Motor Assessment score: 25 points) and gait asymmetry is a direct consequence. This was observed as longer than normal stance phase on the non-paretic side and shorter than normal stance phase on the paretic side, indicating possibly a compensation from the non-paretic side for weakness on the paretic side. The gait asymmetry observed was well supported by the trends of joint stiffness we estimated. Delving deeper into the gait pathologies, both subjects experienced a sudden spike in joint stiffness at joints on the paretic side: S1 (ankle) and S2 (hip). The former incidence was due to the abnormally high activation of the soleus muscle, which was not observed on the non-paretic side. The latter incidence was due to

the abnormal activation of hip flexors in iliacus and psoas, compounded by the unexpectedly large stiffness generation by adductors, which are not conventionally considered as major hip flexors. The model-based estimation of joint stiffness, and calculated CCIs to some extent, may offer a way to probe into the root cause of these pathologies, providing valuable knowledge to both diagnostics and treatment of gait pathologies for stroke survivors.

Co-Contraction Index would be a suitable candidate to consider for addressing the aforementioned clinical needs because of its common adoption in the clinical community and simplicity in usage. Various methodological choices in CCI calculation were explored in this study. One key decision was to not include moment-based CCI and instead focus on EMG-based CCI. Even though moment-based CCI explored in previous studies (Knarr et al., 2012; Souissi et al., 2017) may achieve a stronger correlation with joint stiffness, as a product from advanced neuromusculoskeletal modeling and simulation, the moment-based CCI is considered to be unfit to the aim of this study, which is to build the preliminary knowledge of using some tools that can be readily deployed in the clinical setting to approximate joint stiffness. EMG-based CCI would on the other hand represent a more viable option because of its simplicity and common adoption. As this study focused on EMG-based CCI, key methodological choices in CCI calculation that would help improve correlation with joint stiffness would be identified in the following discussion.

We compared the correlation between CCIs and joint stiffness for each of the six lower extremity joints in both legs of two subjects. The comparison shows that correlation between CCI_1 and joint stiffness K_{joint} (r_1) was generally higher than for CCI_2 (r_2) in more cases if each comparison at a joint on one of the subjects was considered one case (**Figures 5A,B**). r_1 was higher than r_2 in 7 out of the 12 total cases, but lower in 3 other cases: S1 Hip (NP), S2 Hip (P), and Ankle (P). K_{joint} is a sum of the stiffness generated by all the individual muscles K_{mus}. The sum term in the CCI_1 formulation, $Inupt_L$+$Input_H$, was more effective at characterizing this summation than any term in the CCI_2 formulation. This effectiveness became more pronounced when the quantities used for CCI computation from each muscle were accurate proxies for the corresponding K_{mus}. On the other hand, the CCI_2 formulation was more suitable for quantifying the ratio of antagonist muscle activities. This is demonstrated by the observation that the correlation between CCI_2 and K_{joint} was comparable to the correlation between the $Input_L$ / $Input_H$ term of CCI_1 and K_{joint}. Close examination also showed that CCI_2 values for subject S1 reached a peak in magnitude in the swing phase (∼60 to 100% gait cycle) comparable to that during the stance phase (0 to ∼60% gait cycle) at several joints (**Figures 1A,B**). This phenomenon was deemed unlikely to be physiological. This exposes the limitation of the CCI_2 formulation that when the two quantities from antagonist muscles become close in magnitude, CCI_2 would report a high level of co-contraction regardless of how small both quantities might be, as CCI_2 focuses on quantifying the ratio between the two quantities. Since the CCI_1 formulation was a better choice than CCI_2 for approximating joint stiffness trends, the subsequent discussion will focus on the methodological choices involved in calculating CCI_1.

Electromyography processing methods would affect the correlation between EMG-based CCIs and joint stiffness. From the EMG_{basic} signals, two modifications were applied to obtain the other types of processed EMG signals. One modification was adding electromechanical delay from EMG_{basic} to $EMG_{delayed}$. This modification increased the correlation between CCI_1 and K_{joint}. EMG signals are able to convey partial information about joint stiffness because of the relationship between EMG amplitude and F_{mus}. Introducing electro-mechanical delay improves the synchronization between an EMG signal the resulting muscle force. Consequently, the correlation between the EMG signal and K_{mus} increases, resulting in an increased correlation between the $EMG_{delayed}$-based CCI_1 and K_{joint}. The second modification was applying a muscle-specific scale factor (**Table 1**), i.e., from EMG_{basic} to EMG_{scaled} and from $EMG_{delayed}$ to $EMG_{calibrated}$. This modification did not produce a clear improvement in the correlation between resultant CCI_1 and K_{joint}. Applying the scale factor did not change the ability of the EMG signals to represent K_{mus}, and the correlation between scaled EMG signal and K_{mus} remained the same as before scaling. However, the muscle-specific scale factor did change the relative contribution of muscle EMG amplitudes to the sum term in the CCI_1 formulation, $Input_L$+ $Input_H$. In some cases, a change in the sum term caused a decrease in the correlation between resultant CCI_1 and K_{joint}. Although applying muscle-specific scale factors changed muscle force estimates during the calibration of the EMG-driven musculoskeletal model, these scale factors did not consistently increase the correlation between CCI_1 and K_{joint}. Because of a definite improvement in correlation with K_{joint} from having the electromechanical delay, $EMG_{delayed}$-based and $EMG_{calibrated}$-based CCIs both yield higher correlation with K_{joint} than the other EMG-based CCIs. Despite yielding comparable level of correlation with K_{joint}, $EMG_{delayed}$-based CCI_1 is more aligned with our goal than $EMG_{calibrated}$-based for approximating joint stiffness trends using tools readily available in clinical settings, because while the electromechanical delay for both EMGs can be measured experimentally, $EMG_{delayed}$ does not require model-based calibration of the scale factors but $EMG_{calibrated}$ does require that.

This study explored various combinations of antagonistic muscle pairing for computing CCIs. We identified that CCIs computed from the following combinations would likely have higher correlation with the joint stiffness than the others: adductors-hamstrings or quadriceps-hamstrings for the hip joints; quadriceps-hamstrings for the knee joints; tibialis anterior-gasctronemii or tibialis anterior-soleus for the ankle joints. We compared these combinations with the ones in the literature to see if we have identified ones that are less commonly used. For the hip joint, we could only find one study in which CCI was computed (Hoang et al., 2019), which was moment-based and used a formulation different than the two equations examined in this study. Our study found that EMG from conventional hip flexor-extensor

combination, e.g., rectus femoris-biceps femoris long head or rectus femoris-semitendinosus could yield a moderate correlation with hip flexion-extension joint stiffness. We also found the more unconventional adductor-biceps femoris long head combination could present another option to yield a moderate correlation between EMG-based CCI and joint stiffness. For the knee joint, there are two commonly used combinations in the literature: quadriceps-hamstrings (Kellis et al., 2003; McGinnis et al., 2013; Mohr et al., 2018), and quadriceps-gastrocnemii (Rudolph et al., 2000; Lewek et al., 2006; Mohr et al., 2018). Our study found that antagonistic pairs formed from the quadriceps-hamstrings combination is better than the quadriceps-gastrocnemii combination for achieving high correlation between CCI and knee joint stiffness. For the ankle joint, our study found that tibialis anterior-gastrocnemii or tibialis anterior-soleus combinations could yield a moderate correlation between CCI and ankle joint stiffness. The combinations were consistent with the commonly used in the literature (Böhm and Hösl, 2010; Di Nardo et al., 2015). Our study identified the antagonistic muscle pairings used in literature that would yield a correlation between CCI and joint stiffness, and also discovered some alternative options that were less conventional.

Contrary to the general trend noted above that the correlation between CCI_1 and joint stiffness K_{joint} was generally higher than for CCI_2, some discrepancies existed: (1) at the hip joint on the non-paretic side of subject S1; (2) at the hip joint on the paretic side of subject S2; and (3) at the ankle joint on the paretic side of subject S2, where CCI_2 was better correlated with K_{joint}. These discrepancies are possibly because this study presented CCI data of only the muscles from which EMG data could be obtained by surface measurement. Although fine-wire EMG data for some muscles were also collected from the subjects studied to be used for EMG-driven model calibration and estimation of joint stiffness, these muscles were excluded from the CCI analysis, since EMG data would not be available from them in a clinical setting. Among the muscles omitted were iliacus and psoas, two primary hip flexors; and extensor digitorum longus and tibialis posterior, one primary dorsiflexor, and one primary plantarflexor, respectively. These discrepancies could be rectified if the EMG data from the omitted muscles were made available for CCI calculation. Even though invasive, the fine-wire EMG measurement technique could still provide valuable information for the estimation of muscle co-contraction and joint stiffness when such measurements were allowed.

This study also found that the correlation between CCIs and joint stiffness is generally lower at the ankle joints than at other lower body joints for both subjects. It is possibly because a complex joint in the likes of ankle is actuated by a relatively small number of muscles in the musculoskeletal models (Subject S1: 3 dorsiflexors and 7 plantarflexors; Subject S2: 2 and 6, respectively). These muscles actuate motion in the subtalar inversion-eversion DOF in addition to the dorsi or plantar flexion. It is difficult to allocate the precise amount of muscle activation to the actuation of ankle joint in the sagittal plane. Therefore, the comparison between muscle co-contraction and joint stiffness is skewed. Moreover, we chose to omit muscle activities from extensor digitorum longus and tibilais posterior because they were obtained through fine-wire EMG and thus were not suitable for the goals of this study. This decision limited the number of muscles available for representing co-contraction around ankle joint, limiting our options to identifying muscle activities in synchronization with the generation of joint stiffness, hence resulting in a relatively lower correlation between CCIs and joint stiffness at the ankle joints than at the other joints.

One limitation of this study was that the joint stiffness used for comparison with different CCI methods was obtained from a neuromusculoskeletal model instead of experimentally using a joint perturbation technique. A model-based approach was used since the perturbation approach is difficult to implement experimentally, especially for dynamic tasks such as gait (Pfeifer et al., 2012). Consequently, there are very few reports of experimental measurements, especially during dynamic tasks, and they are only preliminary (Kobayashi et al., 2010; Shorter et al., 2019). The model-based approach has been reported to generate joint stiffness estimates that compare well with experimental joint stiffness measurements for isometric conditions (Pfeifer et al., 2012; Sartori et al., 2015). A published model for estimating joint stiffness (Shourijeh and Fregly, 2020) was used in the present study, and the model parameters were calibrated using a validated EMG-driven modeling process (Meyer et al., 2017). Thus, the model closely reproduced the subject's experimental joint moments when the subjects' experimental EMG and kinematic data were used as input, suggesting that the estimated muscle forces and thus joint stiffness values are likely to be at least reasonable. Our model-predictions of joint stiffness are generally consistent with the limited published results (Pfeifer et al., 2012; Sartori et al., 2015). The trends in the model estimates of joint stiffness were also supported by clinical observation as previously discussed. Ideally, if a system that can easily measure joint stiffness in vivo during different activities is developed in the future, it can provide great benefits to the clinical and research community, including direct data to evaluate the models used to estimate joint stiffness.

Another limitation of this study was that it analyzed gait data collected from only two hemiparetic subjects. Although the collection of sixteen channels (including six fine-wire) of EMG from each leg of the subject during walking was time-consuming and not a common practice, it facilitated the calibration of our musculoskeletal model. Although analyzing two subjects limits our ability to draw more general conclusions that could be applied to the stroke population, at the same time, this dataset provided a unique opportunity to build a musculoskeletal model of the subjects and calibrate the model parameters using an EMG-driven framework that did not require prediction of any missing EMG signals as in Sartori et al. (2014). Despite the relatively small number of subjects, the subjects of this study covered a wide spectrum in the post-stroke population, as one maintained relatively high motor functioning abilities while the other was more impaired in motor functioning abilities. The two subjects also exhibited different pathologies during gait.

One had abnormal activation in soleus muscle while the other had abnormal activation in hip flexors. These different pathologies provide unique opportunities and testing cases to evaluate the premise of this study. Future work of the current study would repeat the analysis with data from more subjects post-stroke to be able to make more generalizable conclusions and possible recommendations to the clinicians.

In conclusion, this study demonstrated the feasibility of using EMG-based CCIs to approximate lower limb joint stiffness trends during gait for individuals post-stroke. A number of methodological choices for CCI computation were examined. Key methodological choices to achieve the highest possible correlation between CCI and joint stiffness should include the use of CCI_1 formulation and adding calibrated electromechanical delay to the EMG signals for computing EMG-based CCI_1. Antagonistic muscle pairings that yielded the highest correlations between CCI and joint stiffness were also identified. These findings provide the preliminary knowledge to help clinicians formulate CCI that may yield results more aligned with joint stiffness trends during gait for individuals post-stroke. By using CCI to approximate joint stiffness trends, this study may open an alternative approach to estimate joint stiffness, which is difficult to obtain through either computational modeling or experimental measurement.

DATA AVAILABILITY STATEMENT

The experimental data, OpenSim models, and Matlab code used to perform this study are available at https://simtk.org/projects/ccivsjointstiff.

ETHICS STATEMENT

All experimental procedures were approved by the University of Florida Health Science Center Institutional Review Board (IRB-01) and the subjects provided written informed consent prior to participation.

AUTHOR CONTRIBUTIONS

GL, DA, MS, and BF: conceptualization, investigation, methodology, and formal analysis. BF: funding acquisition. BF and CP: data collection. MS and BF: supervision. GL, MS, BF, and CP: drafting the manuscript. GL, DA, MS, BF, and CP: revising the manuscript. All authors contributed to the article and approved the submitted version.

FUNDING

This work was conducted with support from the Cancer Prevention and Research Institute of Texas (grant RR170026 to BF) and the United States Department of Veterans Affairs (Research Career Scientist Award – Rehabilitation R&D #N9274S to CP).

ACKNOWLEDGMENTS

The authors would like to thank Marleny Arones for her assistance in analyzing the data.

REFERENCES

Banks, C. L., Huang, H. J., Little, V. L., and Patten, C. (2017). Electromyography exposes heterogeneity in muscle co-contraction following stroke. *Front. Neurol.* 8:699. doi: 10.3389/fneur.2017.00699

Böhm, H., and Hösl, M. (2010). Effect of boot shaft stiffness on stability joint energy and muscular co-contraction during walking on uneven surface. *J. Biomech* 43, 2467–2472. doi: 10.1016/j.jbiomech.2010.05.029

Bressel, E., and McNair, P. J. (2002). The effect of prolonged static and cyclic stretching on ankle joint stiffness, torque relaxation, and gait in people with stroke. *Phys. Ther.* 82, 880–887. doi: 10.1093/ptj/82.9.880

Collins, A. T., Richardson, R. T., and Higginson, J. S. (2014). Interlimb symmetry of dynamic knee joint stiffness and co-contraction is maintained in early stage knee osteoarthritis. *J. Electromyogr. Kinesiol.* 24, 497–501. doi: 10.1016/j.jelekin.2014.03.010

Di Nardo, F., Mengarelli, A., Maranesi, E., Burattini, L., and Fioretti, S. (2015). Assessment of the ankle muscle co-contraction during normal gait: a surface electromyography study. *J. Electromyogr. Kinesiol.* 25, 347–354. doi: 10.1016/j.jelekin.2014.10.016

Falconer, K., and Winter, D. A. (1985). Quantitative assessment of co-contraction at the ankle joint in walking. *Electromyogr. Clin. Neurophysiol.* 25, 135–149.

Galiana, L., Fung, J., and Kearney, R. (2005). Identification of intrinsic and reflex ankle stiffness components in stroke patients. *Exp. Brain Res.* 165, 422–434. doi: 10.1007/s00221-005-2320-z

Gao, F., Grant, T. H., Roth, E. J., and Zhang, L. Q. (2009). Changes in passive mechanical properties of the gastrocnemius muscle at the muscle fascicle and joint levels in stroke survivors. *Arch. Phys. Med. Rehabil.* 90, 819–826. doi: 10.1016/j.apmr.2008.11.004

Gao, F., Ren, Y., Roth, E. J., Harvey, R., and Zhang, L. Q. (2011). Effects of repeated ankle stretching on calf muscle-tendon and ankle biomechanical properties in stroke survivors. *Clin. Biomech.* 26, 516–522. doi: 10.1016/j.clinbiomech.2010.12.003

Gollhofer, A., Schmidtbleicher, D., and Dietz, V. (1984). Regulation of muscle stiffness in human locomotion. *Int. J. Sports Med.* 5, 19–22. doi: 10.1055/s-2008-1025874

Gribble, P. L., Mullin, L. I., Cothros, N., and Mattar, A. (2003). Role of cocontraction in arm movement accuracy. *J. Neurophysiol.* 89, 2396–2405. doi: 10.1152/jn.01020.2002

Higginson, J. S., Zajac, F. E., Neptune, R. R., Kautz, S. A., and Delp, S. L. (2006). Muscle contributions to support during gait in an individual with post-stroke hemiparesis. *J. Biomech.* 39, 1769–1777. doi: 10.1016/j.jbiomech.2005.05.032

Hirokawa, S., Solomonow, M., Luo, Z., Lu, Y., and D'Ambrosia, R. (1991). Muscular co-contraction and control of knee stability. *J. Electromyogr. Kinesiol.* 1, 199–208. doi: 10.1016/1050-6411(91)90035-4

Hoang, H. X., Diamond, L. E., Lloyd, D. G., and Pizzolato, C. (2019). A calibrated EMG-informed neuromusculoskeletal model can appropriately account for muscle co-contraction in the estimation of hip joint contact forces in people with hip osteoarthritis. *J. Biomech.* 83, 134–142. doi: 10.1016/j.jbiomech.2018.11.042

Hortobágyi, T., and Devita, P. (2000). Muscle pre- and coactivity during downward stepping are associated with leg stiffness in aging. *J. Electromyogr. Kinesiol.* 10, 117–126. doi: 10.1016/S1050-6411(99)00026-7

Kellis, E. (1998). Quantification of quadriceps and hamstring antagonist activity. *Sports Med.* 25, 37–62. doi: 10.2165/00007256-199825010-00004

Kellis, E., Arabatzi, F., and Papadopoulos, C. (2003). Muscle co-activation around the knee in drop jumping using the co-contraction index. *J. Electromyogr. Kinesiol.* 13, 229–238. doi: 10.1016/S1050-6411(03)00020-8

Knarr, B. A., Zeni, J. A., and Higginson, J. S. (2012). Comparison of electromyography and joint moment as indicators of co-contraction. *J. Electromyogr. Kinesiol.* 22, 607–611. doi: 10.1016/j.jelekin.2012.02.001

Kobayashi, T., Leung, A. K. L., Akazawa, Y., Tanaka, M., and Hutchins, S. W. (2010). Quantitative measurement of spastic ankle joint stiffness using a manual device: a preliminary study. *J. Biomech.* 43, 1831–1834. doi: 10.1016/j.jbiomech.2010.02.024

Kuitunen, S., Komi, P. V., and Kyrolainen, H. (2002). Knee and ankle joint stiffness in sprint running. *Med. Sci. Sports Exerc.* 34, 166–173.

Lamontagne, A., Richards, C. L., and Malouin, F. (2000). Coactivation during gait as an adaptive behavior after stroke. *J. Electromyogr. Kinesiol.* 10, 407–415. doi: 10.1016/S1050-6411(00)00028-6

Latash, M. L., and Huang, X. (2015). Neural control of movement stability: lessons from studies of neurological patients. *Neuroscience* 301, 39–48. doi: 10.1016/j.neuroscience.2015.05.075

Latash, M. L., and Zatsiorsky, V. M. (1993). Joint stiffness: myth or reality? *Hum. Mov. Sci.* 12, 653–692. doi: 10.1016/0167-9457(93)90010-M

Lewek, M. D., Scholz, J., Rudolph, K. S., and Snyder-Mackler, L. (2006). Stride-to-stride variability of knee motion in patients with knee osteoarthritis. *Gait Posture* 23, 505–511. doi: 10.1016/j.gaitpost.2005.06.003

Liu, Y., Guo, S., Hirata, H., Ishihara, H., and Tamiya, T. (2018). Development of a powered variable-stiffness exoskeleton device for elbow rehabilitation. *Biomed. Microdevices* 20:64. doi: 10.1007/s10544-018-0312-6

Lloyd, D. G., and Besier, T. F. (2003). An EMG-driven musculoskeletal model to estimate muscle forces and knee joint moments in vivo. *J. Biomech.* 36, 765–776. doi: 10.1016/S0021-9290(03)00010-1

McGill, S. M., Grenier, S., Kavcic, N., and Cholewicki, J. (2003). Coordination of muscle activity to assure stability of the lumbar spine. *J. Electromyogr. Kinesiol.* 13, 353–359. doi: 10.1016/S1050-6411(03)00043-9

McGinnis, K., Snyder-Mackler, L., Flowers, P., and Zeni, J. (2013). Dynamic joint stiffness and co-contraction in subjects after total knee arthroplasty. *Clin. Biomech.* 28, 205–210. doi: 10.1016/j.clinbiomech.2012.11.008

Meyer, A. J., Patten, C., and Fregly, B. J. (2017). Lower extremity EMG-driven modeling of walking with automated adjustment of musculoskeletal geometry. *PLoS One* 12:e0179698. doi: 10.1371/journal.pone.0179698

Mirbagheri, M. M., Alibiglou, L., Thajchayapong, M., and Rymer, W. Z. (2008). Muscle and reflex changes with varying joint angle in hemiparetic stroke. *J. Neuroeng. Rehabil.* 5:6. doi: 10.1186/1743-0003-5-6

Missenard, O., Mottet, D., and Perrey, S. (2008). The role of cocontraction in the impairment of movement accuracy with fatigue. *Exp. Brain Res.* 185, 151–156.

Mohr, M., Lorenzen, K., Palacios-Derflingher, L., Emery, C., and Nigg, B. M. (2018). Reliability of the knee muscle co-contraction index during gait in young adults with and without knee injury history. *J. Electromyogr. Kinesiol.* 38, 17–27. doi: 10.1016/j.jelekin.2017.10.014

Moore, D. S., Notz, W. I., and Fligner, M. A. (2015). *The Basic Practice of Statistics*. London: Macmillan Higher Education.

Moore, I. S., Jones, A. M., and Dixon, S. J. (2014). Relationship between metabolic cost and muscular coactivation across running speeds. *J. Sci. Med. Sport* 17, 671–676. doi: 10.1016/j.jsams.2013.09.014

Pfeifer, S., Vallery, H., Hardegger, M., Riener, R., and Perreault, E. J. (2012). Model-based estimation of knee stiffness. *IEEE Trans. Biomed. Eng.* 59, 2604–2612. doi: 10.1109/TBME.2012.2207895

Rosa, M. C. N., Marques, A., Demain, S., Metcalf, C. D., and Rodrigues, J. (2014). Methodologies to assess muscle co-contraction during gait in people with neurological impairment – a systematic literature review. *J. Electromyogr. Kinesiol.* 24, 179–191. doi: 10.1016/j.jelekin.2013.11.003

Rouse, E. J., Gregg, R. D., Hargrove, L. J., and Sensinger, J. W. (2013). The difference between stiffness and quasi-stiffness in the context of biomechanical modeling. *IEEE Trans. Biomed. Eng.* 60, 562–568. doi: 10.1109/TBME.2012.2230261

Rudolph, K. S., Axe, M. J., and Snyder-Mackler, L. (2000). Dynamic stability after ACL injury: who can hop? *Knee Surg. Sports Traumatol. Arthrosc.* 8, 262–269. doi: 10.1007/s001670000130

Rydahl, S. J., and Brouwer, B. J. (2004). Ankle stiffness and tissue compliance in stroke survivors: a validation of Myotonometer measurements. *Arch. Phys. Med. Rehabil.* 85, 1631–1637. doi: 10.1016/j.apmr.2004.01.026

Sartori, M., Farina, D., and Lloyd, D. G. (2014). Hybrid neuromusculoskeletal modeling to best track joint moments using a balance between muscle excitations derived from electromyograms and optimization. *J. Biomech.* 47, 3613–3621. doi: 10.1016/j.jbiomech.2014.10.009

Sartori, M., Maculan, M., Pizzolato, C., Reggiani, M., and Farina, D. (2015). Modeling and simulating the neuromuscular mechanisms regulating ankle and knee joint stiffness during human locomotion. *J. Neurophysiol.* 114, 2509–2527. doi: 10.1152/jn.00989.2014

Selles, R. W., Li, X., Lin, F., Chung, S. G., Roth, E. J., and Zhang, L. Q. (2005). Feedback-controlled and programmed stretching of the ankle plantarflexors and dorsiflexors in stroke: effects of a 4-week intervention program. *Arch. Phys. Med. Rehabil.* 86, 2330–2336. doi: 10.1016/j.apmr.2005.07.305

Shorter, A. L., Finucane, S., and Rouse, E. J. (2019). Ankle mechanical impedance during waling in chronic stroke: preliminary results. *IEEE Int. Conf. Rehabil. Robot.* 2019, 246–251. doi: 10.1109/ICORR.2019.8779436

Shourijeh, M. S., and Fregly, B. J. (2020). Muscle synergies modify optimization estimates of joint stiffness during walking. *J. Biomech. Eng.* 142:011011. doi: 10.1115/1.4044310

Singer, M. L., Kobayashi, T., Lincoln, L. S., Orendurff, M. S., and Foreman, K. B. (2014). The effect of ankle-foot orthosis plantarflexion stiffness on ankle and knee joint kinematics and kinetics during first and second rockers of gait in individuals with stroke. *Clin. Biomech.* 29, 1077–1080. doi: 10.1016/j.clinbiomech.2014.09.001

Souissi, H., Zory, R., Bredin, J., and Gerus, P. (2017). Comparison of methodologies to assess muscle co-contraction during gait. *J. Biomech.* 57, 141–145. doi: 10.1016/j.jbiomech.2017.03.029

Thilmann, A. F., Fellows, S. J., and Ross, H. F. (1991). Biomechanical changes at the ankle joint after stroke. *J. Neurol. Neurosurg. Psychiatry* 54, 134–139. doi: 10.1136/jnnp.54.2.134

Vallery, H., Veneman, J., van Asseldonk, E., Ekkelenkamp, R., Buss, M., and van Der Kooij, H. (2008). Compliant actuation of rehabilitation robots. *IEEE Robot. Autom. Mag.* 15, 60–69. doi: 10.1109/MRA.2008.927689

Wong, J., Wilson, E. T., Malfait, N., and Gribble, P. L. (2009). Limb stiffness is modulated with spatial accuracy requirements during movement in the absence of destabilizing forces. *J. Neurophysiol.* 101, 1542–1549. doi: 10.1152/jn.91188.2008

Conflict of Interest: The authors declare that the research was conducted in the absence of any commercial or financial relationships that could be construed as a potential conflict of interest.

Copyright © 2021 Li, Shourijeh, Ao, Patten and Fregly. This is an open-access article distributed under the terms of the Creative Commons Attribution License (CC BY). The use, distribution or reproduction in other forums is permitted, provided the original author(s) and the copyright owner(s) are credited and that the original publication in this journal is cited, in accordance with accepted academic practice. No use, distribution or reproduction is permitted which does not comply with these terms.

frontiers in Bioengineering and Biotechnology

ORIGINAL RESEARCH
published: 28 January 2021
doi: 10.3389/fbioe.2020.620805

Measures of Interjoint Coordination Post-stroke Across Different Upper Limb Movement Tasks

Anne Schwarz[1,2], Janne M. Veerbeek[1], Jeremia P. O. Held[1], Jaap H. Buurke[2,3] and Andreas R. Luft[1,4]*

[1] Vascular Neurology and Neurorehabilitation, Department of Neurology, University Hospital Zurich, University of Zurich, Zurich, Switzerland, [2] Biomedical Signals and Systems (BSS), University of Twente, Enschede, Netherlands, [3] Roessingh Research and Development B.V., Enschede, Netherlands, [4] Cereneo, Center for Neurology and Rehabilitation, Vitznau, Switzerland

Background: Deficits in interjoint coordination, such as the inability to move out of synergy, are frequent symptoms in stroke subjects with upper limb impairments that hinder them from regaining normal motor function. Kinematic measurements allow a fine-grained assessment of movement pathologies, thereby complementing clinical scales, like the Fugl–Meyer Motor Assessment of the Upper Extremity (FMMA-UE). The study goal was to investigate the effects of the performed task, the tested arm, the dominant affected hand, upper limb function, and age on spatiotemporal parameters of the elbow, shoulder, and trunk. The construct validity of the metrics was examined by relating them with each other, the FMMA-UE, and its arm section.

Methods: This is a cross-sectional observational study including chronic stroke patients with mild to moderate upper limb motor impairment. Kinematic measurements were taken using a wearable sensor suit while performing four movements with both upper limbs: (1) isolated shoulder flexion, (2) pointing, (3) reach-to-grasp a glass, and (4) key insertion. The kinematic parameters included the joint ranges of shoulder abduction/adduction, shoulder flexion/extension, and elbow flexion/extension; trunk displacement; shoulder–elbow correlation coefficient; median slope; and curve efficiency. The effects of the task and tested arm on the metrics were investigated using a mixed-model analysis. The validity of metrics compared to clinically measured interjoint coordination (FMMA-UE) was done by correlation analysis.

Results: Twenty-six subjects were included in the analysis. The movement task and tested arm showed significant effects ($p < 0.05$) on all kinematic parameters. Hand dominance resulted in significant effects on shoulder flexion/extension and curve efficiency. The level of upper limb function showed influences on curve efficiency and the factor age on median slope. Relations with the FMMA-UE revealed the strongest and significant correlation for curve efficiency ($r = 0.75$), followed by shoulder flexion/extension ($r = 0.68$), elbow flexion/extension ($r = 0.53$), and shoulder abduction/adduction ($r = 0.49$). Curve efficiency additionally correlated significantly with the arm subsection, focusing on synergistic control ($r = 0.59$).

OPEN ACCESS

Edited by:
Veronica Cimolin,
Politecnico di Milano, Italy

Reviewed by:
Néstor José Jarque-Bou,
University of Jaume I, Spain
Sandeep K. Subramanian,
The University of Texas Health Science Center at San Antonio, United States
Thiago Luiz Russo,
Federal University of São Carlos, Brazil

***Correspondence:**
Anne Schwarz
anne.schwarz@usz.ch

Specialty section:
This article was submitted to Biomechanics, a section of the journal Frontiers in Bioengineering and Biotechnology

Received: 23 October 2020
Accepted: 18 December 2020
Published: 28 January 2021

Citation:
Schwarz A, Veerbeek JM, Held JPO, Buurke JH and Luft AR (2021) Measures of Interjoint Coordination Post-stroke Across Different Upper Limb Movement Tasks. Front. Bioeng. Biotechnol. 8:620805. doi: 10.3389/fbioe.2020.620805

Conclusion: The kinematic parameters of the upper limb after stroke were influenced largely by the task. These results underpin the necessity to assess different relevant functional movements close to real-world conditions rather than relying solely on clinical measures.

Study Registration: clinicaltrials.gov, identifier NCT03135093 and BASEC-ID 2016-02075.

Keywords: upper extremity, stroke, biomechanical phenomena, kinematics, interjoint coordination

INTRODUCTION

Incidences of upper limb impairments after stroke have been reported in 48 to 85% of acute stroke patients (Jørgensen et al., 1999; Persson et al., 2012). Acute deficits might include paresis, ataxia, and loss of sensory function (Yew and Cheng, 2009). The course of recovery from these impairments varies from complete restoration to different degrees of compensatory adaptation (Levin et al., 2009; Bernhardt et al., 2017). Throughout the course, deficits in interjoint coordination have been described as a key feature in stroke-related dysfunctions that is characterized by the reappearance of primitive movement synergies and the presence of joint coupling (Krakauer and Carmichael, 2017). Interjoint coordination has been defined as the process to spatially and temporally arrange the degrees of freedom (DOF) needed to achieve the movement goal (Tomita et al., 2017) and is closely linked to the concept of synergies (Roh et al., 2013; McMorland et al., 2015; Santello and Lang, 2015). Based on two principal synergies, the flexor and the extensor synergy, pathological stereotypical coupling between two or more DOF has been observed as a phenotype of the loss of interjoint coordination after stroke. A loss of interjoint coordination is associated with weakness (Sukal et al., 2007) and spasticity (Allison et al., 2016) along the time course after stroke (Levin, 1996; Cirstea et al., 2003), leading to learned bad or non-use in daily life (Taub et al., 2006; Raghavan, 2015). Determining the level of interjoint coordination and associated motor dysfunction of stroke-related movement disabilities is critical to improve our understanding and expand interventional strategies to minimize long-term consequences due to stroke.

Interjoint coordination after stroke is often assessed by the Fugl–Meyer Motor Assessment of the Upper Extremity (FMMA-UE). This clinical assessment evaluates volitional movement control of the upper limb in a hierarchical manner from proximal to distal segments (Fugl-Meyer et al., 1975) and by taking into account the within-synergy, mixed-synergy, and out-of-synergy movement patterns as proposed by Twitchell (1951) and Brunnstrom (1966, 1970). Although the FMMA-UE has been attested to be of high quality in clinimetric properties (Gladstone et al., 2002), some limitations need to be considered in terms of the measurement construct being used. First, items of the FMMA-UE are assessed on a three-point ordinal scale ("not," "partial," and "fully"), and the "partial" category is very broad. An evaluation of "partial" movement achievement includes limitations in active range of motion or movement deviations, such as shoulder abduction or elbow flexion during shoulder flexion, that can range from small to exaggerated differences and cannot be differentiated further. This level of evaluation of movement quality does not allow to differentiate between physiological and pathological movement behavior (Kwakkel et al., 2017). Second, a full score in FMMA-UE cannot be directly related to complete restitution since deviations in movement kinematics and limitations in daily life might still be present (Thrane et al., 2019). Third, the FMMA-UE assesses mostly abstract movements and limb postures based on empirically derived stroke recovery stages that have little to no relevance to the subject's movements in daily life. Considering the widespread and recommended usage of the FMMA-UE as a primary outcome measure in stroke research trials (Santisteban et al., 2016; Burridge et al., 2019; Kwakkel et al., 2019; Subramanian et al., 2020) and the overall neutral results of most stroke rehabilitation trials (Corbetta et al., 2015; Eraifej et al., 2017; Veerbeek et al., 2017), the question on how far this outcome can sensitively capture changes on the body function level when performing daily life tasks cannot be omitted.

The introduction of modern technology opened new avenues for assessments of motor function. Upper limb kinematic motion analysis in the stroke population has been performed with 2D and 3D set-up conditions for assessing a large number of different kinematic outcome parameters in predominantly pointing or reach-to grasp tasks (Schwarz et al., 2019b). Kinematic parameters measure body functions and thereby characterize aspects of movement control, such as interjoint coordination. Outcome measures to quantify upper limb interjoint coordination include spatial measures of active range of motion in shoulder and elbow and of trunk displacement (van Kordelaar et al., 2012) that have been attested to be of sufficient validity and reliability in 3D pointing tasks (Subramanian et al., 2010; Massie et al., 2011, 2014; Wu et al., 2014). Measures of interjoint coordination, relating at least two DOF, ranged from angle–angle plots (Beer et al., 2007; Woodbury et al., 2009; Alt Murphy et al., 2011), correlation analysis (Yang et al., 2017), slope statistics (Baniña et al., 2017), and ratio or index measures (Cirstea and Levin, 2007; Levin et al., 2016) to mathematically more complex parameters, such as functional Principal Component Analysis (van Kordelaar et al., 2013) or approximate entropy metrics (Sethi et al., 2017). Parallel to this, movement timing or workspace measures, such as circle size area (Sukal et al., 2007; Krabben et al., 2011; Ellis et al., 2016), provide indirect measures as a result of pathological synergies. Taken together, the variety of metrics identified for evaluating interjoint coordination illustrate the wide context and aspects

of this movement construct and tight connection between the movement characteristics and the chosen metric as, for example, the circle size area in a circle drawing task (Houwink et al., 2013). Considering this state-of-the-art in upper limb kinematic assessments, it could be proposed that research on interjoint coordination would profit from task-independent metrics that could be evaluated in various tasks and settings, thereby allowing for comparability, especially for pooling in meta-analysis.

In this study, first, it was questioned whether kinematic parameters representing aspects of interjoint coordination in the shoulder–elbow–trunk complex are different with respect to different movement tasks and the arm being tested by considering the dominant affected side, the upper limb function, and age as covariates. Second, it was examined whether statistically significant correlations can be found between each of the kinematic parameters of the affected side, the FMMA-UE full score, and the FMMA-UE arm subscale that evaluates the shoulder–elbow–trunk complex according to the synergy concept. The findings will provide new insights into the characteristic interjoint coordination in different functional and non-functional upper limb movements after stroke, propose kinematic parameters to quantify spatiotemporal aspects of interjoint coordination, and, as a long-term goal, support the establishment of feasible and repeatable qualitative kinematic assessments in close relation to real-world functional activities.

MATERIALS AND METHODS

A prospective cross-sectional study was performed at the rehabilitation clinic Cereneo, Vitznau, Switzerland, to explore the relationship between upper limb function and activity as measured by clinical assessments and by a wearable motion capture system. The study protocol was approved by the Cantonal Ethics Committee Northwest and Central Switzerland (BASEC-ID: 2016-02075) and prospectively registered in ClinicalTrials.gov (NCT03135093). Between July 2017 and October 2019, 523 patients from the stroke research register of the Department of Neurology, University Hospital Zurich (Zurich, Switzerland) were screened by telephone and onsite screening.

Study Participants

The subjects were deemed eligible when they met the following inclusion criteria: (1) >6 months post-unilateral stroke (hemorrhage or ischemic), (2) at least 18 years of age, and (3) upper limb motor impairment, but at least partially able to lift the arm against gravity (>30° of shoulder flexion) and to flex and extend the fingers for basic grasping. The exclusion criteria were (1) an increased upper limb muscle tone with limitations in range of motion [modified Ashworth Scale (MAS) ≥3], (2) severe sensory deficits in the upper limb [Erasmus modifications to the revised Nottingham Sensory Assessment (EmNSA) of 0 in one of the test regions], (3) a preexisting orthopedic or neurological disease affecting movements of the upper limb, (4) contraindications on ethical grounds, e.g., persons who are decisionally impaired, (5) known or suspected non-compliance, or (6) severe communication or cognitive deficits that cause an inability to follow the study procedures as determined by the Montreal Cognitive Assessment (MoCA) ≤20 points (Dong et al., 2013). The MAS (Bohannon and Smith, 1987) and the EmNSA (Stolk-Hornsveld et al., 2006) were performed with the participant in supine position. The EmNSA was evaluated for the surface, pinprick, sharp-blunt, and proprioceptive discrimination in both arms. Each participant gave a written informed consent according to the Declaration of Helsinki and the Swiss regulatory authorities.

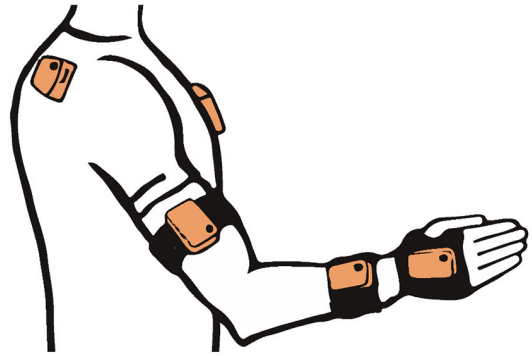

FIGURE 1 | Measurement system set-up.

Study Experiments

An experienced research therapist performed all the study experiments during a single-day measurement at the rehabilitation clinic Cereneo (Vitznau, Switzerland). The study experiments started after onsite screening and informed consent with setting up the wearable kinematic measurement system. When being acquired with the system, the participant performs the FMMA-UE and a set of daily living activities with both upper limbs. The less-affected side was assessed to determine the close-to-physiological-movement behavior on the best available level in delineation to pathological movement behavior of the affected upper limb during functional and non-functional activities.

Measurement System

A portable and wireless sensor-based motion capture system was used to capture upper limb kinematics (Xsens MVN Awinda, Xsens Technologies, the Netherlands). The system consists of 17 inertial measurement units (IMU), a receiver station, and attachment equipment (MVN Manual, 2018). The nine IMUs of the upper body used in this analysis were fixated on a T-shirt above both scapulae with the sensors' x-axes parallel to the spina scapulae and above the sternum, with the sensor aligned with the x-axis, as illustrated in **Figure 1**. The upper extremity IMUs were mounted with elastic Velcro straps on the upper arm above the lateromedial part of the humerus bone, around the distal radioulnar joint, three fingers above the wrist, and on the dorsal palm of the hand by the use of a palm glove or medical tape in case the glove was not fitting. Each IMU contains 3D linear accelerometers, 3D rate gyroscopes, 3D magnetometers, and a battery. Combined with information of the

TABLE 1 | Upper limb movement task characteristics.

Task number	**(1)**	**(2)**	**(3)**	**(4)**
Task name	Shoulder flexion	Pointing ahead	Reach-to-grasp a glass	Key insertion
Set-up Start position End position	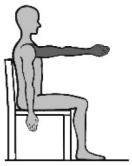	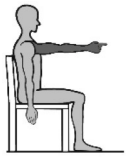		
Task purpose	Non-functional	Functional	Functional	Functional
Description	According to FMMA-UE, item shoulder flexion from 0° to 90°, elbow in 0° extension and neutral forearm	Gesture of pointing in the air at shoulder height, to look ahead/ indicate to a visual scene in the distance	Reach to a non-filled glass placed in 90% arm's length, move it to the mouth, take a sip, and place it back	Pick up a key placed at the medial side of the subjects' hand, take it up, and insert the key into a lock on a top shelf (28.5cm) in 90% arm's length
Upper body effector	Proximal (shoulder, elbow)	Distal (index finger)	Distal (hand, finger)	Distal (MCP, thumb)
Movement focus	Internal	External	External	External
Contact type	No contact	No contact	Grasp contact at end	Grasp contact from start to end
Grasp type	Not applicable	Not applicable	Cylindrical grasp	Palm opposition
Functional motion primitive	Not applicable	Reposition or reach-to-point	Reach-to-grasp	Transport and stabilize
Movement phase for analysis	From movement start to maximum shoulder flexion (90°)	From movement start to maximum shoulder flexion	From movement start to grasp the glass	From key pick-up to insertion into lock

FMMA-UE, Fugl–Meyer Motor Assessment of the Upper Extremity; MCP, metacarpo-phalangeal joint.

subjects' body measures into a biomechanical model, the data of 3D angular velocity, 3D acceleration, 3D earth magnetic field, and atmospheric pressure allow as **Table 3D** orientation for human kinematic motion analysis (MVN software, 2018). The kinematic data are sampled at 60 Hz. The accuracy of the system to measure each body segments' position has been reported as ∼5 mm and the orientation with a measurement error of 3° (Roetenberg et al., 2007a,b). The system was previously validated with a camera-based system (Optotrak) demonstrating comparable results (Robert-Lachaine et al., 2017) and additionally investigated for intra- and interrater reliability with fair to excellent results, even when being used by clinicians with no experience in applying motion capture technologies (Al-Amri et al., 2018).

Setting up the system for each participant included taking body measures, such as body height, shoulder height (distance from the ground to the top of the acromion), and shoulder width (distance between the right and the left lateral border of the acromion), the sensor attachment, and a calibration procedure that consisted of standing in neutral position at the calibration spot, walking 3 m, and returning to the start. The whole procedure took about 15 to 20 min and was completed when the subject returned back to neutral pose standing at the calibration spot. The measurements of all subjects were performed in an upright sitting position on an armless chair in the same examination room of the rehabilitation clinic, as well as the position and orientation of the subject. This allowed to control for possible external inferences that could affect the sensor data of the IMUs, such as electric leads.

Movement Tasks

The selected movements consisted of four different discrete movement tasks: (1) isolated shoulder flexion, (2) pointing ahead, (3) reach-to-grasp a glass, and (4) key insertion into a lock. The selection was based on the shared upper limb workspace along the sagittal plane and discrete reaching movement while discriminating variations in non-functional and functional movements with and without grasp contact in alliance with existing upper limb movement (Schambra et al., 2019) and grasp taxonomies (Feix et al., 2016). An overview of the movement tasks including characteristics such as contact and the underlying motion primitives is provided in **Table 1**. Each movement task was demonstrated and instructed verbally, including demo-trials if necessary. The movement start was defined by a flick on one of the sensors. After task completion, the subjects were asked to return to the start position. For the analysis, the maximum shoulder flexion angle and/or the maximum distance of the hand IMU positional data along the x-axis defined the movement end. The chair had a standard seat height of 46 cm, with a back support 51 cm in height and with a backward inclination that was counterbalanced by fixing a tight pillow at the back of the chair. The table was height-adjustable to allow a subject-specific set up of 0° in all axis of the shoulder, 90° of elbow flexion, and with the hand pronated on the table. The subjects were instructed to perform the task at a comfortable speed while keeping contact with the back of the chair. This instruction was given once at the beginning to not interfere profoundly with the natural movement behavior. Three to six repetitions were performed with each

upper limb to include at least three successful trials in the data analysis (Alt Murphy et al., 2018), starting with the less-affected side and followed by the affected side.

Outcome Measures

The recorded kinematic measures were segmented by movement trial based on the flip signal and the maximal target angle and stored in mvnx files for data transferring and processing in MATLAB (The MathWorks Inc., Natick, MA, USA). For each movement task, participant, and tested upper limb, the shoulder and elbow angles and the positional data of the trunk sensor of all repetitions were extracted for analysis. The kinematic parameters of interest consisted of spatial and spatiotemporal measures.

Spatial Parameters

Spatial measures included joint angle ranges in degrees around one rotation axis and trunk displacement in millimeter. Each joint can be expressed in six DOF around the orthogonally arranged rotation axis, where one joint angle is defined by a joint rotation as the orientation of a distal segment with respect to a proximal segment. Joint rotations are calculated using the Euler sequences ZXY and XZY by the MVN software (MVN Manual, 2018) based on the coordinate system agreed by the International Society of Biomechanics (ISB) (Wu et al., 2005). All angles follow the ISB Euler angle extractions of Z (flexion/extension), X (abduction/adduction), and Y (internal/external rotation), except for the shoulder joint where the Euler sequence XZY is used. The definitions of the origins of the segments are somewhat different from marker-based recommendations since MVN uses a motion tracker placed on the segment rather than markers placed on bony landmarks close to the joint origin (MVN Manual, 2018).

The range of motion was defined by calculating the minimum and maximum angle for all data points from movement onset to end (van Meulen et al., 2015). The standard deviations of the minimum and maximum joint angle were calculated as a measure of variability. For the purpose of this study to evaluate interjoint coordination in the shoulder–elbow complex, shoulder flexion/ extension, shoulder abduction/adduction, and elbow flexion/extension were captured and analyzed. Even though shoulder rotational movements are an important component of the upper limb, they were not considered in this study since the measurement accuracy of rotations around the transversal plane were associated with the largest measurement error ranging from 16° to 34° (Walmsley et al., 2018). The challenge to measure rotational movements on the transversal plane might be related to the larger differences between soft tissue and bone motions during rotation. Elbow flexion/extension was determined by rotation around the z-axes, where elbow extension was represented by 0° and positive values indicating flexion of the elbow. Shoulder flexion–extension was defined as an elevation parallel to the sagittal plane and angles that rotate around the z-axis. Shoulder abduction–adduction was defined as an elevation on the frontal plane and rotates around the x-axes of the shoulder joint. Positive values indicate shoulder flexion or abduction, and negative values indicate shoulder extension or adduction.

In contrast to ISB descriptions of the shoulder with the thorax, clavicle, scapula, and humerus, the MVN model does not define the thorax segment nor the clavicle. The MVN model splits the thorax region into spine segments (MVN Manual, 2018). In alliance with other studies in the field, trunk motions were simplified to trunk displacement as defined by changes in position and orientation of the sternum sensor between movement onset and end (Subramanian et al., 2010). The change in trunk displacement was calculated by subtracting the mean of the first 10 data points from the other position values in the x-, y-, and z-direction and were summarized by:

$$\textbf{Trunk displacement} = \sqrt{\left(Tx^2+Ty^2+Tz^2\right)}$$

where $\boldsymbol{Tx}$ includes frontal displacement, $\boldsymbol{Ty}$ includes sideway displacement, and $\boldsymbol{Tz}$ includes displacement in rotation.

Spatiotemporal Parameters of Shoulder–Elbow Coordination

Angle–angle plots of the shoulder and the elbow flexion angle for each timeframe of the movement were derived to qualitatively analyze interjoint coordination and coupling between shoulder and elbow flexion/extension in reaching, as illustrated in **Figure 2**. For each movement repetition per participant, the elbow and shoulder angles were set to 0° or 90° according to the related starting position and time normalized with respect to the mean trial length to enable comparability.

A shoulder–elbow correlation coefficient was calculated to quantify the relationship between shoulder flexion/extension (SF) and elbow flexion/extension (EF) in the following equation:

$$\mathbf{r}=\frac{\sum_{\mathbf{m}}\sum_{\mathbf{n}}(\mathbf{SF_{mn}}-\mathbf{SF_{mean}})(\mathbf{EF_{mn}}-\mathbf{EF_{mean}})}{\sqrt{\left(\sum_{\mathbf{m}}\sum_{\mathbf{n}}(\mathbf{SF_{mn}}-\mathbf{SF_{mean}})\text{^}2\sum_{\mathbf{m}}\sum_{\mathbf{n}}(\mathbf{EF_{mn}}-\mathbf{EF_{mean}})\text{^}2\right)}}$$

where $SF_{mean} = mean(SF)$ and $EF_{mean} = mean(EF)$.

In the case of isolated joint movements, a low correlation coefficient highlights the ability to uncouple joint movements, whereas a coupling relationship was detected if the change in movement direction of two segments occurred at the same time. In isolated joint motions of task (1), a well-coordinated movement with a constantly extended elbow would result in a correlation coefficient close to 0, whereas pathologically coupled movements would result in a higher correlation coefficient, according to the hypothesis of voluntary joint control. Reaching out for an object on a table is likely to start from an elbow flexed position and then requires the elbow to extend while the shoulder is being elevated so that a negative correlation would be expected for physiological movement and conversely a low correlation in case of pathological coupling with remaining elbow flexion while reaching out.

Shoulder–elbow median slope was defined by the slopes connecting the data points of elbow–shoulder angle–angle plots as depicted in **Figure 2**. The mean slope between elbow flexion/extension and shoulder flexion/extension was used to assess interjoint coordination by Baniña et al. (2017). In this present study, the median slope was selected instead of the mean slope to account for the non-linearity of angle–angle curves, especially in task (2), (3), and (4). The slope changes between

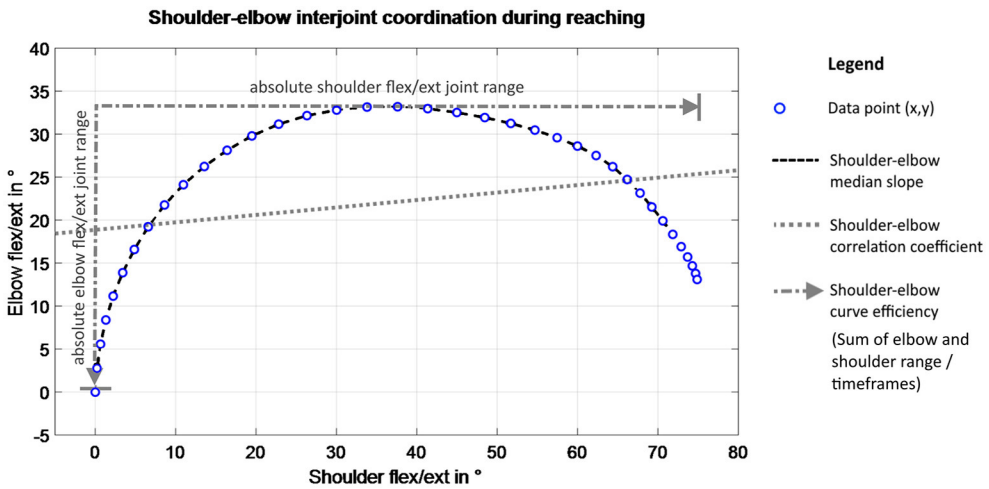

FIGURE 2 | Schematic of shoulder–elbow coordination measures.

the shoulder and elbow per timeframe ranges from positive to negative infinite values, representing the gradient of the curve.

Shoulder–elbow curve efficiency is included to quantify the maximum movement execution in the target DOF for the movement. It was defined by the sum of absolute joint range in shoulder flexion/extension and elbow flexion/extension, as visualized in **Figure 2**, divided by the number of data points of the movement to quantify the amount of both joint ranges in reaching. The sum of absolute joint ranges was normalized with respect to the number of frames to include the temporal efficiency of the movement. For isolated joint movements, such as in task (1), the absolute range in elbow flexion/extension is subtracted from the absolute range in shoulder flexion/extension, divided by the number of timeframes. For the other movement tasks, the absolute ranges in elbow and shoulder flexion/extension were summed up to quantify the upper limb movement magnitude during reaching. Values are given in degrees per frame, with higher values representing more efficient movement activation to reach the movement goal.

Clinical Measurements

The FMMA-UE was collected as a clinical stroke-specific measurement to evaluate upper limb motor impairment (Fugl-Meyer et al., 1975). The FMMA-UE is hierarchically composed, starting with assessing reflex appearance and primitive synergy patterns followed by within- to out-of-synergy movements in the arm subscale, based on the assumption that recovery "follows a definable stepwise course." The FMMA-UE is partitioned into four sections, "upper extremity," "wrist," "hand," and "coordination and speed," as differences in recovery in each subscale could be independent from each other. Each test item is rated based on the best performance with the full FMMA-UE score ranging from zero to 66. For the purpose of this study, upper limb functionality subgroups were considered based on (Hoonhorst et al., 2015). who stratified FMMA-UE scores according to upper limb capacity measures that include grasping and displacement movements. With this subgroup selection, it was intended to investigate differences with respect to the subjects' capacity in grasping performance.

The information on hand dominance was obtained by asking the individual which hand he or she preferred to use for writing and throwing a ball prior to the stroke.

Statistical Analysis

The statistical analysis was performed using Matlab (MATLAB version 2016b, The Mathwork, Natick, MA) and SPSS (SPSS version 26.0, IBM Corp., Armonk, NY, USA). Spatial measures of joint ranges in elbow flexion/extension, shoulder flexion/extension, and shoulder abduction/adduction were presented in absolute range of motion from minima to maxima with the corresponding standard deviations. Trunk displacement was given by absolute displacement from minima to maxima in millimeters. Spatiotemporal measures of shoulder–elbow coordination included the correlation coefficients r, the median slope, and the curve efficiency. All kinematic outcome parameters were explored for determining normal distribution in histograms and QQ plots. The descriptive statistics of the kinematic measures were summarized for all subjects and for each task and tested limb separately.

A linear mixed-model analysis was performed for each kinematic parameter to account for mixed effects in a repeated-measurement design. Each kinematic metric was treated as a dependent variable with respect to the independent fixed factors movement task (shoulder flexion, pointing, reach-to-grasp a glass, key insertion), the tested arm (affected, less-affected side), dominant hand is the affected hand (yes, no), the upper limb functionality group, as assessed with the FMMA-UE (32–47 points, "limited"; 48–52 points, "notable"; 53–66 points "full") (Hoonhorst et al., 2015) and age ($\leq$55 years and $\geq$56 years) (Kwakkel et al., 2017).

The relationship between clinically measured impairment and kinematic measures was examined by Spearman rank

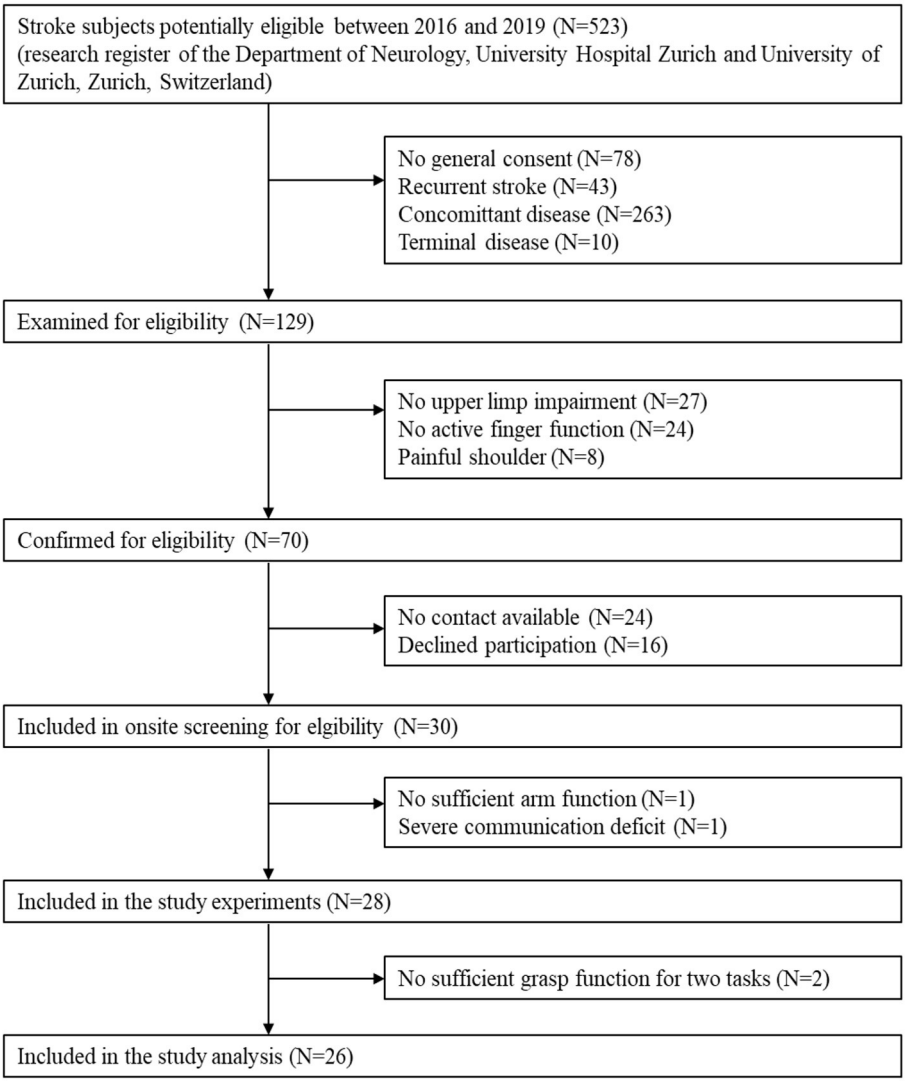

FIGURE 3 | Study flow of the participants.

correlations. To evaluate the relationship between shoulder–elbow coordination, as measured in the FMMA-UE arm subsection when compared to spatiotemporal measures, Spearman rank correlation was used. According to the COSMIN guidelines, correlations between two measures of the same construct should be $r \geq 0.5$, correlations of related measures $r = 0.3–0.5$, and correlations of unrelated constructs $r < 0.3$ (Prinsen et al., 2018). All statistical tests were performed at a significance level of 5%.

RESULTS

A total of 28 stroke subjects were included in the study, of which 26 were included in the data analysis. The study flow of participant inclusion is shown in **Figure 3**. The participant characteristics are summarized in **Table 2**. The study sample represents 26 mild to moderately impaired chronic stroke subjects, of whom 14 subjects were affected in their dominant upper limb. Seventeen subjects of the 26 included showed some resistance against passive movement in at least one of the tested muscles, as defined by a MAS score between 1 and 2. Sensory function was somewhat impaired in 21 subjects as determined by the EmNSA ranging from 29 to 40 points in the affected upper limb.

Kinematic Characteristics per Movement Task of the Affected and Less-Affected Side

Overall, 468 kinematic datasets per arm were included in the analysis, representing 26 stroke subjects, when performing four upper limb movement tasks. The observed QQ plots for the kinematic parameters did not lead to rejecting the assumption

TABLE 2 | Study participant characteristics.

Characteristic	Total (*N* = 26)
Gender, female/male	9/17
Mean age (SD), years	62.19 (12.10)
Mean body height (SD), cm	173.81 (10.94)
Mean BMI (SD), kg/m^2	26.97 (4.23)
Paretic body side, left/right	13/13
Months since stroke[a]	20.50 (12–34)
Initial stroke severity NIHSS[a]	8 (6–11)
MoCA (0–30)[a]	27 (24–28)
MAS sum of the upper extremity (0–14)[ab]	1.75 (0.25–3)
Shoulder internal rotator muscles (%)[b]	42.3
Biceps brachii muscle (%)[b]	69.2
Triceps brachii muscle (%)[b]	11.5
Wrist flexor muscles (%)[b]	23.1
Wrist extensor muscles (%)[b]	15.4
Finger flexor muscles (%)[b]	15.4
Finger extensor muscles (%)[b]	19.2
EmNSA-UE (0–40)[a]	38 (36–39)
FMMA-UE (0–66)[a]	47.50 (40.25–55.00)
FMMA-UE arm subsection (0–36)[a]	26 (22.00–29.75)
FMMA-UE wrist subsection (0–10)[a]	6 (6.00–7.75)
FMMA-UE hand subsection (0–14)[a]	11 (9.00–14.00)
FMMA-UE coordination subsection (0–6)[a]	4 (3.25–5.00)

BMI, body mass index; EmNSA, Erasmus modified version of the Nottingham Sensory Assessment; FMMA-UE, Fugl–Meyer Motor Assessment of the Upper Extremity; MAS, modified Ashworth Scale; MoCA, Montreal Cognitive Assessment; NIHSS, National Institutes of Health Stroke Scale; L, left; SD, standard deviation.
[a]*Values are presented in median (interquartile range).*
[b]*MAS scores between 1 and 2 for the tested muscle.*

of normal distribution in the analyzed data. The spatial measures of joint ranges in elbow flexion/extension, shoulder flexion/extension, shoulder abduction/adduction, and trunk displacement are summarized for all subjects, each movement task, and affected (red-colored) and less-affected upper limb (blue-colored) in **Figures 4A–D**. Each boxplot illustrates the median, the upper and lower quartile, the minimum, and the maximum, as well as outliers shown as a red plus for each of the spatial measures. Different ranges across the spatial measures can be seen between the tasks. While increased trunk motions are shown in **Figures 4C,D** when compared to **Figures 4A,B**, shoulder flexion/extension shows larger ranges in **Figures 4A,B** when compared to **Figures 4C,D**.

The spatiotemporal kinematics are illustrated in terms of shoulder–elbow angle plots for each movement task in **Figures 5A–D**. Each scatter curve represents the normalized mean curve per subject arm and task. Visual exploration of the shoulder–elbow angle plots depicts that deviations in terms of an increase of elbow flexion during shoulder flexion task (1) can be observed in all subjects and both arms while being increased in the affected upper limb in **Figure 5A**. Shoulder–elbow angle plots of the pointing ahead movement in task (2) revealed different movement strategies to emphasize the direction to look at between subjects in both the affected and less-affected upper limb. **Figure 5B** illustrates that subjects tended to either move through wide ranges of elbow flexion–extension, emphasize elbow extension at the end of the movement, or keep the elbow relatively extended throughout the movement. The shoulder–elbow angle plots of task (3) in **Figure 5C** illustrate comparable curve shapes during reaching in the affected and unaffected upper limbs. Similarly, curve shapes during task (4) in **Figure 5D** are comparable in both the affected and the unaffected upper limb. Besides the inter- and intra-individual movement variability, a preservation of the shoulder–elbow coordination can be described across the functional movement tasks when comparing the mean curve shape per subject of the shoulder–elbow plots between the affected side and the less-affected side.

Effects of the Factors on the Spatial and Spatiotemporal Kinematic Measures

The mean estimates and standard deviation of the investigated kinematic parameter are presented for each fixed factor in **Table 3**. The results of the fixed-effects analysis per independent factor (task, tested arm, affected is dominant side, upper limb function, age) on each dependent kinematic measure are shown in **Table 4**. The results of *post hoc* pairwise testing between the four movement tasks and the three upper limb function levels are shown in terms of *p*-values per kinematic parameter and factor in **Table 4**.

Statistically significant differences were found for all movement tasks and all investigated kinematic parameters as displayed in **Table 4**. Trunk displacement ranged from 1.7 to 2.9 cm between tasks and was only statistically significantly different between isolated shoulder flexion and the key insertion task [$F_{(3,\ 58.036)} = 6.119$, $p = < 0.001$]. Effects of the factor of the tested arm were found for all kinematic parameters except of the shoulder–elbow correlation. The factor of affected dominant hand or affected non-dominant resulted in statistically significant effects on shoulder flexion/extension [$F_{(1,\ 39.832)} = 7.058$, $p = 0.011$] and shoulder–elbow curve efficiency [$F_{(1,\ 61.565)} = 6.323$, $p = 0.015$]. Differences with respect to upper limb function were detected for shoulder–elbow curve efficiency [$F_{(2,\ 61.565)} = 7.285$, $p = 0.001$], with significant differences between the limited ($N = 13$) and full function ($N = 10$) and between notable ($N = 3$) and full function in *post hoc* testing. The factor of age revealed significant effects on the dependent variable of shoulder–elbow median slope, with a mean of −0.784 compared to −0.705 in the less-affected side [$F_{(1,\ 34.432)} = 4.344$, $p = 0.045$].

Relationship Between Clinically Measured Impairment and Spatiotemporal Kinematics

For the comparison between spatial and spatiotemporal kinematic measures across tasks per subject and the FMA-UE, correlation coefficients were calculated for each combination and presented in the confusion matrix in **Table 5**. The strongest statistically significant correlation with the FMA-UE was found for curve efficiency ($r = 0.75$), followed by shoulder flexion/extension ($r = 0.68$), elbow flexion/extension ($r = 0.53$),

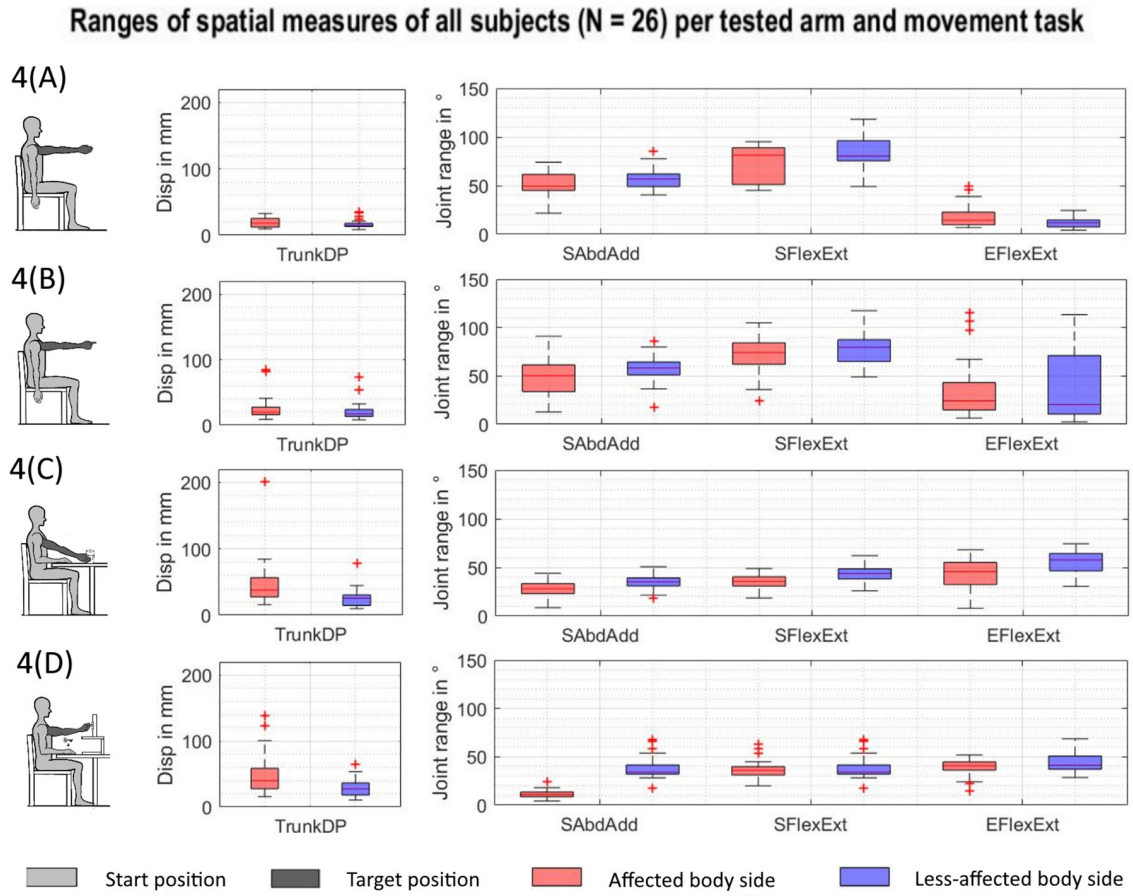

FIGURE 4 | Spatial measures of the affected and less-affected arm per task across subjects ($N = 26$). AS, affected side; EFlexExt, elbow flexion/extension; LAS, less-affected side; SFlexExt, shoulder flexion/extension; SAbdAdd, shoulder abduction/adduction; TrunkDP, trunk displacement. **(A)** Shoulder flexion. **(B)** Pointing ahead. **(C)** reach-to-grasp a glass. **(D)** Key insertion.

and shoulder abduction/adduction ($r = 0.49$). Furthermore, strong correlations were found between elbow flexion/extension and shoulder flexion/extension ($r = 0.53$), between elbow flexion/extension and shoulder abduction/adduction ($r = 0.53$), and between shoulder flexion/extension and shoulder abduction/adduction ($r = 0.57$). For shoulder–elbow curve efficiency, significant correlations were shown with shoulder flexion/extension ($r = 0.85$) and elbow flexion/extension ($r = 0.55$).

The relationship between the FMMA-UE arm subsection and kinematic metrics representing measures of shoulder–elbow coordination was additionally investigated to explore the comparability of kinematic measures and shoulder–elbow coordination as specifically tested in the FMMA-UE arm subsection. In the result, a statistically significant correlation between the clinically measured impaired interjoint coordination and curve efficiency ($r = 0.59$, $p = 0.002$) was found. For the shoulder–elbow correlation coefficient ($r = 0.24$, $p = 0.230$) and shoulder–elbow median slope ($r = 0.09$, $p = 0.653$), no statistically significant correlations were found with the FMMA-UE arm subsection. **Figure 6** illustrates the subjects' mean values of the correlation coefficient, the median slope, and curve efficiency over all tasks and for each task plotted against the FMMA-UE arm subsection.

DISCUSSION

To our knowledge, this was the first study to investigate interjoint coordination during representative upper limb tasks in chronic stroke patients with mild to moderate upper limb motor impairment, aiming to bridge the gap between abstract clinical motor assessments and the kinematic characterization of various upper limb movements performed in daily life. Kinematic metrics reflecting interjoint coordination were investigated and compared across movement tasks by considering the covariates' dominance, age, and upper limb function and related with a recommended standard clinical test, the FMMA-UE (Kwakkel et al., 2017, 2019; Burridge et al., 2019). It was found that the values of kinematic metrics were largely dependent on the movement task and the tested arm, while age and the affected dominant side hardly influenced the metrics. The fact that both spatial and spatiotemporal metrics of the shoulder–elbow

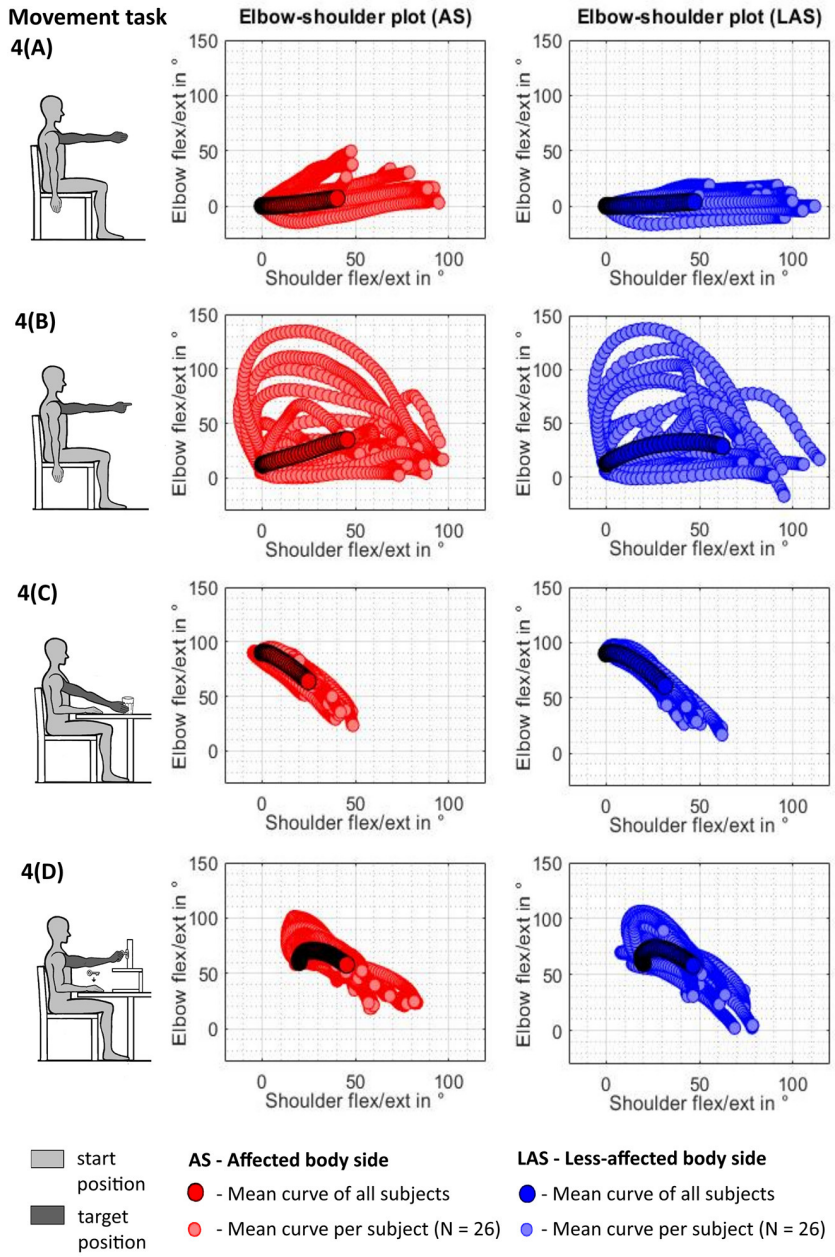

FIGURE 5 | Shoulder–elbow mean curve per tested arm and task across subjects ($N = 26$). **(A)** Shoulder flexion. **(B)** Pointing ahead. **(C)** reach-to-grasp a glass. **(D)** Key insertion.

complex were largely dependent on the movement performed underpins the need to assess upper limb interjoint coordination in different task contexts. Interestingly, the elbow joint ranges were significantly different and less variable during isolated shoulder flexion task (9.4° ± 7.5°), representative for one of the FMMA-UE items, when compared to the pointing task (40.3° ± 26.2°), even though both tasks shared the same person-related workspace and target position, indicating the differences of the FMMA-UE from natural movement behavior. Comparing the results of the clinically measured impairment with the FMMA-UE and the resulting kinematic metrics across all tasks revealed moderate correlations between the FMMA-UE or FMMA-UE arm subsection and metrics on shoulder and elbow joint ranges and shoulder–elbow curve efficiency ($r \geq 0.5$) besides low correlations between trunk metrics and shoulder–elbow correlation coefficient and median slope.

All spatial and spatiotemporal kinematic measures, except the shoulder–elbow correlation coefficient, showed statistically significant discriminability between pathological movement

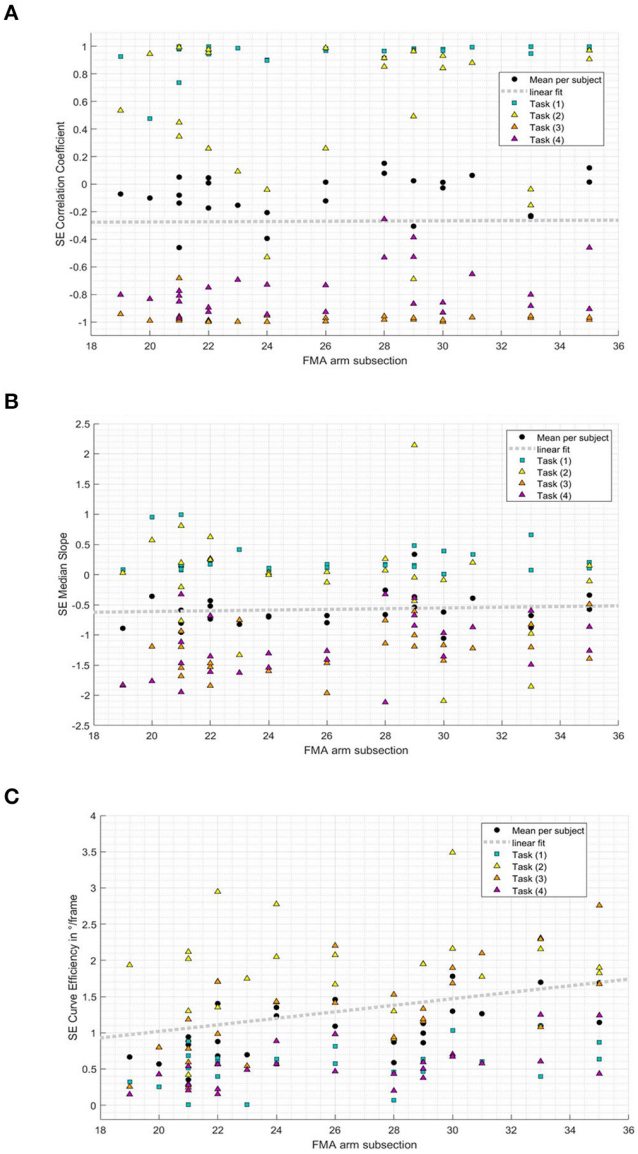

FIGURE 6 | Relation between shoulder–elbow coordination metrics and the Fugl–Meyer Motor Assessment of the Upper Extremity arm subsection (19-35/36) per subject and task. **(A)** Shoulder-elbow correlation coefficient per subject FMMA-UE arm subsection and task. **(B)** Shoulder-elbow median slope per subject FMMA-UE arm subsection and task. **(C)** Shoulder-elbow curve efficiency per subject FMMA-UE arm subsection and task.

behavior of the affected upper limb and physiological movement behavior of the less-affected upper limb.

Trunk motions ranged between a mean of 1.8 and 3.0 cm, tending to increase from the shoulder flexion, pointing ahead, reach-to-grasp a glass, to the key insertion task. This illustrates increased trunk compensation, with an increase in task complexity by requiring distal upper limb interactions with objects (McIsaac et al., 2015). Trunk compensatory movements were shown to be slightly but significantly increased when moving the affected limb (mean of 2.5 cm) when compared to the less-affected upper limb (mean of 2.1 cm). However, these differences were small when compared to previous findings of trunk movements of around 10 cm in stroke subjects during reach-to-point (Cirstea et al., 2003) and reach-to-grasp (Alt Murphy et al., 2018). Hence, the presented results fall within the limits of 2 to 5 cm as a clinically meaningful cutoff score for compensatory trunk movements (Alt Murphy et al., 2013). The differences in the shoulder DOF can be partially explained by differences in target height between tasks, especially between the reach-to-grasp a glass on the table that requires less shoulder flexion when compared to the other movement tasks with targets on shoulder-height level. Shoulder joint ranges in flexion/extension and abduction/adduction were diminished in the affected arm in comparison to the less-affected arm, with joint ranges of 53° vs. 60° and 34° vs. 44°, respectively, suggesting inefficient activation or weakness of the shoulder muscles and the inability to cope with antigravity torques (Roh et al., 2013). Elbow flexion/extension ranged from a mean of 9.4° in isolated shoulder flexion and around 52° during functional task execution. The larger ranges in elbow flexion/extension during functional movements when compared to non-functional isolated shoulder flexion support the idea, that the elbow joint is rather dynamically involved in reaching movements of daily life activities than being involved as a stable or stabilizing component of a movement as predominantly examined in the FMMA-UE.

On the level of spatiotemporal measures of shoulder–elbow coordination, values of the correlation coefficient largely varied between $r = -0.9$ and $r = 0.9$ within and between subjects with a tight connection to the movement tasks as illustrated in **Figure 4**. The correlation coefficient is a measure of the linear relationship between two variables, such as shoulder flexion/extension and elbow flexion/extension. Although the correlation coefficient provides estimates of general trend between two variables, it does not consider non-linearity in rather bell-shaped angle–angle curves. The shoulder–elbow median slope represents estimates of the relationship between two DOF per timeframe (Baniña et al., 2017). Both the correlation coefficient and the median slope are quantifications of the overall trend in the shoulder–elbow curve and depend on both the type of movement as well as whether the shoulder and elbow move inphase or outphase. Consequentially, both metrics are limited to the general relationship between two joints. Shoulder–elbow curve efficiency ranged between a mean of 0.14° and 1.44° per frame with respect to the movement task. Curve efficiency was considerably lower in the shoulder flexion and key insertion task when compared to the other tasks, which could be an indicator of the increased requirements on movement preciseness during key insertion and increased internal attentional focus during isolated shoulder flexion. Curve efficiency was introduced as a novel measure of interjoint coordination that combines the absolute spatial changes in two DOF while considering temporal aspects in terms of timeframes needed to perform the movement. In that sense, curve efficiency accounts for the proposed definition of interjoint coordination by Tomita and coworkers as "a goal-oriented process in which the DOF are organized in both spatial and temporal domains such that the body configuration enables the endpoint to reach to a desired location in a context dependent manner" (Tomita et al., 2017). Herein curve efficiency has proven to be discriminable

TABLE 3 | Descriptive statistics for each kinematic parameter per task and tested arm.

Factor	TrunkDP in mm	SAbAd in°	SFleEx in°	EFlEx in°	SE Corr Coeff	SE median slope	SE curve efficiency in °/frame
Movement							
Task (1)	17.7 ± 6.9	54.0 ± 8.4	77.5 ± 13.5	9.4 ± 7.5	0.94 ± 0.1	0.14 ± 0.1	0.7 ± 0.3
Task (2)	20.1 ± 12.4	53.6 ± 12.2	74.2 ± 14.4	40.3 ± 26.2	0.33 ± 0.4	−0.30 ± 0.7	2.0 ± 0.6
Task (3)	24.6 ± 13.1	32.2 ± 6.1	37.6 ± 8.0	52.2 ± 10.8	−0.96 ± 0.0	−1.38 ± 0.2	1.5 ± 0.5
Task (4)	29.7 ± 15.3	17.7 ± 6.2	36.9 ± 10.3	41.5 ± 8.5	−0.75 ± 0.2	−1.44 ± 0.4	0.6 ± 0.3
Arm teste							
AS	24.8 ± 9.0	34.4 ± 6.1	53.2 ± 8.7	36.9 ± 9.8	0.10 ± 0.1	−0.64 ± 0.3	± 0.3
NA	21.3 ± 12.4	44.4 ± 6.6	59.9 ± 8.9	34.8 ± 11.2	−0.11 ± 0.1	−0.85 ± 0.3	1.4 ± 0.4
Affected is dominant side							
Yes	23.1 ± 10.7	38.8 ± 6.5	53.4 ± 11.6	34.8 ± 11.2	−0.10 ± 0.1	−0.77 ± 0.3	± 0.4
No	22.9 ± 8.6	39.9 ± 5.1	59.7 ± 9.1	36.9 ± 9.8	−0.11 ± 0.1	−0.72 ± 0.2	1.3 ± 0.3
UL function group							
Limited	24.2 ± 9.2	38.7 ± 5.5	57.0 ± 9.8	34.9 ± 10.2	−0.10 ± 0.1	−0.72 ± 0.4	1.2 ± 0.3
Notable	24.7 ± 17.4	40.5 ± 10.8	50.8 ± 19.5	34.3 ± 16.1	−0.09 ± 0.1	−0.83 ± 0.3	± 0.6
Full	20.2 ± 9.4	39.0 ± 5.6	61.9 ± 10.1	38.2 ± 10.4	−0.12 ± 0.1	−0.69 ± 0.4	1.5 ± 0.4
Age group							
≤55 years >56	23.2 ± 12.1	39.3 ± 7.4	57.4 ± 13.3	36.0 ± 12.2	−0.10 ± 0.1	−0.78 ± 0.3	1.2 ± 0.4
years	22.8 ± 8.2	39.5 ± 4.9	55.7 ± 8.6	35.6 ± 9.6	−0.11 ± 0.1	−0.71 ± 0.2	1.2 ± 0.3

Corr Coeff, correlation coefficient; EFlEx, elbow flexion/extension; full, full UL function (FMMA-UE 53-66); limited, limited UL function (FMMA-UE 32-47); notable, notable function (FMMA-UE 48-52); SAbAd, shoulder abduction/adduction; SFlEx, shoulder flexion/extension; TrunkDP, trunk displacement; SE, shoulder–elbow; UL, upper limb.

with respect to the factor whether the affected hand is the dominant hand and with respect to the upper limb motor function group, indicating promising associations with upper limb motor impairment levels.

Taken together, these findings confirm the importance of including different upper limb movement tasks when looking at interjoint coordination in patients after stroke and non-disabled adults as the task strongly affects kinematic metric outcomes (Jeannerod, 1990; Michaelsen et al., 2004; Mesquita et al., 2020). Adding up to these task-related kinematic differences, research on functional brain activation provides evidence that the cerebral control of upper limb movements is arranged in a task-specific action topography by taking the activity as a whole rather than being controlled by separating or combining movement components or specific or fixed brain areas (Handjaras et al., 2015; Leo et al., 2016). The findings of the present study emphasize the importance to consider the effects of the movement purpose, the attentional focus, and the movement complexity on kinematic expressions complementary to clinical assessment evaluations. Unlike the shoulder flexion movement of the FMMA-UE that relies on an internal movement focus and a stable extended elbow position, the three representative functional tasks rely on an external movement focus with mainly inverse kinematics between shoulder flexion and elbow extension and bell-shaped angle–angle profiles. Even though further curve fitting analysis is out of the scope of the present study, a visual inspection of the shoulder–elbow angle plots suggests that motions in the shoulder and elbow were diminished in the affected side when compared to the less-affected side, while the task-associated shapes seem to be largely preserved in the affected limb. These results furthermore underpin the challenge to clearly distinguish pathological from physiological interjoint coordination and movement activation in terms of active range of motion and strength at least in natural surroundings, including the constant influence of gravity.

The relationship between the spatiotemporal kinematic measures and the clinically measured upper limb motor impairment was explored as a part of validity. The herein presented findings on correlation between the FMMA-UE and spatial metrics shoulder flexion/extension and elbow flexion/extension are in line with research on validity (Massie et al., 2011, 2014; Finley et al., 2012; van Kordelaar et al., 2012; de Paiva Silva et al., 2014; Li et al., 2015; Rech et al., 2020). In contrast to existing research (Subramanian et al., 2010; Finley et al., 2012; van Kordelaar et al., 2012; de Paiva Silva et al., 2014; Massie et al., 2014), we did not find a strong correlation between trunk displacement during various tasks and the FMMA-UE total score. The strong correlation between curve efficiency and shoulder flexion/extension and elbow flexion/extension found in this study might be related to the fact that curve efficiency is a derivative of both DOF besides the temporal aspect of this movement parameter. The fact that shoulder–elbow curve efficiency significantly correlated with the FMMA-UE arm subsection supports the idea that it measures the same construct of interjoint coordination in the upper extremity. Future work on upper limb kinematic measurements after stroke should investigate its clinimetric properties, such as reliability, measurement error, and responsiveness.

Limitations

The spatiotemporal kinematic analysis of this study was limited to three out of seven DOF, namely, shoulder flexion/extension,

TABLE 4 | Results of linear mixed model analysis.

Factor	Kinematic metric for interjoint coordination						
	TrunkDP	SAbAd	SFlEx	EFlEx	SE corr coeff	SE median slope	SE curve efficiency
Movement Task	**0.001**	**<0.001**	**<0.001**	**<0.001**	**<0.001**	**<0.001**	**<0.001**
Task (1) vs. Task (2)	1.000	1.000	1.000	**<0.001**	**<0.001**	**0.020**	**<0.001**
Task (1) vs. Task (3)	0.056	**<0.001**	**<0.001**	**<0.001**	**<0.001**	**<0.001**	**<0.001**
Task (1) vs. Task (4)	**0.002**	**<0.001**	**<0.001**	**<0.001**	**<0.001**	**<0.001**	1.000
Task (2) vs. Task (3)	0.861	**<0.001**	**<0.001**	0.129	**<0.001**	**<0.001**	**0.001**
Task (2) vs. Task (4)	0.058	**<0.001**	**<0.001**	1.000	**<0.001**	**<0.001**	**<0.001**
Task (3) vs. Task (4)	0.714	**<0.001**	1.000	**<0.001**	**<0.001**	1.000	**<0.001**
Arm tested AS vs. NA	**0.001**	**<0.001**	**<0.001**	**0.002**	0.395	**<0.001**	**<0.001**
Affected is dominant side (Yes vs. No)	0.935	0.413	**0.011**	0.251	0.089	0.161	**0.015**
UL function group	0.257	0.693	0.051	0.264	0.070	0.069	**0.001**
Limited vs. notable	1.000	1.000	0.325	1.000	0.342	0.122	0.498
Limited vs. full	0.317	1.000	0.244	0.335	0.328	1.000	**0.003**
Notable vs. full	0.791	1.000	0.053	0.755	0.073	0.070	**0.005**
Age group ≤55 years vs. >56 years	0.889	0.888	0.540	0.860	0.125	**0.045**	0.394

Corr Coeff, correlation coefficient; EFlEx, elbow flexion/extension; full, full UL function (FMMA-UE 53-66); limited, limited UL function (FMMA-UE 32-47), notable, notable function (FMMA-UE 48-52); SAbAd, shoulder abduction/adduction; SFlEx, shoulder flexion/extension; TrunkDP, trunk displacement; SE, shoulder-elbow; UL, upper limb. Statistically significant effects ($p < 0.05$) are indicated in bold.

shoulder abduction/adduction, and elbow flexion/extension, even though rotational movements and the forearm and hand component are known to be part of movement quality. We decided to examine interjoint coordination on the basic level of the two joints that contribute most to the movement performance and present characteristic stroke-related movement phenotypes, such as the pathological flexor synergy.

Another limitation relates to the fact that we have considered the less-affected upper limb as the physiological movement comparator, even though we were aware of the evidence on movement limitations in the ipsilesional upper limb (Bustrén et al., 2017). Nevertheless, the less-affected upper limb represents a valuable comparator in the asymmetrical impairment of unilateral stroke and is always available to the patient and the assessor in clinical practice (Lang et al., 2017). For this reason, comparisons between the affected limb and the less-affected upper limb remain the best-available comparator in terms of movement quality measures until a reasonable amount of normative kinematic data from the healthy population is available.

We have not controlled for possible strength limitations and therefore were not able to differentiate between weakness and interjoint coordination in the presented experimental set-up, as gradually studied by by Dewald and colleagues (Sukal et al., 2007; Ellis et al., 2016). This could be induced by including a gradual armload increase during movement task execution. Apart from that, real-world upper limb functions are performed not only in sitting but also in other body positions, such as standing. The fact that the pioneering works on interjoint coordination and synergistic control after stroke emphasized the influence of the postural setting of the subject on synergistic control (Fugl-Meyer et al., 1975) supports further research on this topic and its consideration in upper limb assessments.

In the current study, a wearable inertial sensing suit was used, and this goes against recent recommendations to capture upper limb kinematics by an opto-electronic device (Kwakkel et al., 2019). However, the pros of wearable sensing suits are the wide applicability in flexible environments, the avoidance of problems with marker occlusion during object manipulation, and the comparably less time-consuming system set-up (pre- and post-processing) and costs of the equipment (Walmsley et al., 2018). Based on previous research, the reliability and measurement error has shown to be comparable between inertial sensing and optoelectronic system (Robert-Lachaine et al., 2017), even when the system was used by an unexperienced person (Al-Amri et al., 2018).

Lastly, it needs to be acknowledged that other analytical approaches on the kinematic data, such as dimension–reduction approaches, would have been possible, allowing the presentation of other kinematic outcomes (Schwarz

TABLE 5 | Confusion matrix of the correlation coefficients for each measure combination.

	TrunkDP	SAbAd	SFlEx	EFlEx	SE Corr Coeff	SE median slope	SE curve efficiency
FMA-UE	−0.16 $p = 0.436$ (−0.51–0.24)	**0.49** **p = 0.010** **(0.13–0.73)**	**0.68** **p = 0.000** **(0.40–0.84)**	**0.53** **p = 0.004** **(0.19–0.76)**	0.10 $p = 0.603$ (−0.29–0.47)	0.053 $p = 0.791$ (−0.33–0.42)	**0.75** **p = 0.000** **(0.52–0.88)**
TrunkDP		−0.11 $p = 0.595$ (−0.47–0.28)	−0.12 $p = 0.550$ (−0.48–0.27)	−0.04 $p = 0.831$ (−0.42–0.34)	−0.10 $p = 0.611$ (−0.46–0.29)	−0.08 $p = 0.678$ (−0.45–0.31)	−0.04 $p = 0.846$ (−0.41–0.35)
SAbAd			**0.57** **p = 0.002** **(0.24–0.78)**	**0.53** **p = 0.004** **(0.19–0.76)**	−0.03 $p = 0.880$ (−0.41–0.35)	0.28 $p = 0.154$ (−0.11–0.60)	**0.40** **p = 0.040** **(0.02–0.68)**
SFlEx				**0.53** **p = 0.004** **(0.19–0.76)**	−0.20 $p = 0.318$ (−0.54–0.20)	−0.02 $p = 0.921$ (−0.40–0.36)	**0.85** **p = 0.000** **(0.70–0.93)**
EFlEx					−0.26 $p = 0.198$ (−0.58–0.14)	−0.15 $p = 0.450$ (−0.50–0.24)	**0.55** **p = 0.003** **(0.21–0.77)**
SE Corr Coeff						−0.07 $p = 0.712$ (−0.44–0.31)	−0.18 $p = 0.380$ (−0.52–0.22)
SE slope median							0.01 $p = 0.956$ (−0.37–0.39)

The correlation coefficient, the p-value, and the 95% confidence interval are shown. The italicized measures present statically significant correlations.
EFlexExt, elbow flexion/extension; SFlexExt, shoulder flexion/extension; SAbdAdd, shoulder abduction/adduction; Trunk DP, trunk displacement; SE, shoulder–elbow; Corr Coeff, correlation coefficient; UL, upper limb. The bold measures present statistically significant correlations.

et al., 2019a). Kinematic measures of the movement smoothness domain have been used for quantifying interjoint coordination based on accelerometer or gyroscope signals in the lower limb during gait assessment (Beck et al., 2018) and should be additionally considered in future work of upper limb interjoint coordination besides the herein proposed measures.

Future Research

Future research should expand on an upper limb movement task set (Kwakkel et al., 2019), allowing to assess the widest possible range of the tested subjects' functional capabilities by considering a stepwise increase of movement task complexity, task instruction, and focus (McIsaac et al., 2015). Including a functional planar task on the table level, such as wiping or shape-drawing, besides gesture movements, reach-to-grasp, and manipulating activities should be considered in such a task set and future works to enable kinematic evaluations in stroke subjects with lower levels of upper limb function and reducing load on the shoulder. Dual-task conditions should be included in the highest level of task difficulty to assess the functional capability under real-world conditions, for example, when cooking and talking at the same time, as well as to uncover subliminal deficits that still might impact the person's performance level in daily life. Another important aspect in upper limb assessments reflecting needs of real-world use is the consideration of posture. In this line, it would be interesting to investigate the impact of posture on upper limb kinematics. The resemblance with daily life tasks in such an assessment protocol is likely to ease task understanding and naturalness of the performance even in subjects with difficulties in understanding.

CONCLUSIONS

The presented work on qualitative upper limb movement analysis confirmed that kinematic measures of interjoint coordination in the shoulder–elbow–trunk complex are largely depending on the movement task and the tested arm in chronic stroke patients with mild to moderate upper limb motor impairments. The kinematic metrics during functional movements showed different expressions and variability when compared to those of the non-functional isolated shoulder flexion, supporting the importance to assess different movement tasks in order to get a more complete picture of the patient's quality of movement. The metrics correlate at the best moderately with standard clinical tests, which underlines their benefit. Among the investigated spatiotemporal measures of shoulder–elbow coordination, curve efficiency showed promising discriminability between the affected side and the less-affected side, the factor of affected hand dominance, and upper limb functionality and correlated well with the FMMA-UE and the FMMA-UE arm subsection, respectively. Consequentially, this study contributes to novel approaches in post-stroke upper limb assessment methodologies by combining technological opportunities to

measure aspects of body function during activities that are close to that of the real world and representative for the ICF activities and participation domain.

DATA AVAILABILITY STATEMENT

The raw data supporting the conclusions of this article will be made available by the authors, without undue reservation.

ETHICS STATEMENT

The studies involving human participants were reviewed and approved by Ethikkommission Nordwest- und Zentralschweiz (EKNZ). The patients/participants provided their written informed consent to participate in this study.

AUTHOR CONTRIBUTIONS

AS, JV, and JH contributed to the conception and design of this study. AS organized the database. Data curation was performed by AS, JV, and JH. The methodology and statistical approach was performed by AS and reviewed by JV, JB, and AL. AS wrote the first draft of the manuscript. AL provided the resources. All the authors contributed to manuscript revision and read and approved the submitted version.

FUNDING

This project has received funding from the European Union's Horizon 2020 Research and Innovation Programme under grant agreement number 688857 (SoftPro), from the Swiss State Secretariat for Education, Research and Innovation (contract number 15.0283-1), and from the P&K Pühringer Foundation.

ACKNOWLEDGMENTS

We thank all subjects and their relatives for participating in this study. Thanks to Dr. Bart Klaassen and Saskia Nies for supporting the data access and analysis and to Dr. Robinson Kundert and Dr. Alejandro Mendelez-Calderon for the challenging discussions on interjoint coordination.

REFERENCES

Al-Amri, M., Nicholas, K., Button, K., Sparkes, V., Sheeran, L., and Davies, J. L. (2018). Inertial measurement units for clinical movement analysis: reliability and concurrent validity. *Sensors* 18:719. doi: 10.3390/s18030719

Allison, R., Shenton, L., Bamforth, K., Kilbride, C., and Richards, D. (2016). Incidence, time course and predictors of impairments relating to caring for the profoundly affected arm after stroke: a systematic review. *Physiother. Res. Int*. 21, 210–227. doi: 10.1002/pri.1634

Alt Murphy, M., Murphy, S., Persson, H. C., Bergström, U. B., and Sunnerhagen, K. S. (2018). Kinematic analysis using 3D motion capture of drinking task in people with and without upper-extremity impairments. *J. Vis. Exp*. 133:e57228. doi: 10.3791/57228

Alt Murphy, M., Willen, C., and Sunnerhagen, K. S. (2011). Kinematic variables quantifying upper-extremity performance after stroke during reaching and drinking from a glass. *Neurorehabil. Neural Repair*. 25, 71–80. doi: 10.1177/1545968310370748

Alt Murphy, M., Willén, C., and Sunnerhagen, K. S. (2013). Responsiveness of upper extremity kinematic measures and clinical improvement during the first three months after stroke. *Neurorehabil. Neural Repair*. 27, 844–853. doi: 10.1177/1545968313491008

Baniña, M. C., Mullick, A. A., McFadyen, B. J., and Levin, M. F. (2017). Upper limb obstacle avoidance behavior in individuals with stroke. *Neurorehabil. Neural Repair*. 31, 133–146. doi: 10.1177/1545968316662527

Beck, Y., Herman, T., Brozgol, M., Giladi, N., Mirelman, A., and Hausdorff, J. M. (2018). SPARC: a new approach to quantifying gait smoothness in patients with Parkinson's disease. *J. Neuroeng. Rehabil.* 15:49. doi: 10.1186/s12984-018-0398-3

Beer, R. F., Ellis, M. D., Holubar, B. G., and Dewald, J. P. (2007). Impact of gravity loading on post-stroke reaching and its relationship to weakness. *Muscle Nerve*. 36:242–250. doi: 10.1002/mus.20817

Bernhardt, J., Hayward, K. S., Kwakkel, G., Ward, N. S., Wolf, S. L., Borschmann, K., et al. (2017). Agreed definitions and a shared vision for new standards in stroke recovery research: the stroke recovery and rehabilitation roundtable taskforce. *Int. J. Stroke*. 12, 444–450. doi: 10.1177/1747493017711816

Bohannon, R. W., and Smith, M. B. (1987). Interrater reliability of a modified Ashworth scale of muscle spasticity. *Phys. Ther*. 67, 206–207. doi: 10.1093/ptj/67.2.206

Brunnstrom, S. (1966). Motor testing procedures in hemiplegia: based on sequential recovery stages. *Phys. Ther*. 46, 357–375. doi: 10.1093/ptj/46.4.357

Brunnstrom, S. (1970). *Movement Therapy in Hemiplegia: A Neurophysiological Approach*. New York, NY: Medical Dept, Harper & Row.

Burridge, J., Alt Murphy, M., Buurke, J., Feys, P., Keller, T., Klamroth-Marganska, V., et al. (2019). A systematic review of international clinical guidelines for rehabilitation of people with neurological conditions: what recommendations are made for upper limb assessment? *Front Neurol. Jun* 10:567. doi: 10.3389/fneur.2019.00567

Bustrén, E. L., Sunnerhagen, K. S., and Alt Murphy, M. (2017). Movement kinematics of the ipsilesional upper extremity in persons with moderate or mild stroke. *Neurorehabil. Neural Repair*. 31, 376–386. doi: 10.1177/1545968316688798

Cirstea, M. C., and Levin, M. F. (2007). Improvement of arm movement patterns and endpoint control depends on type of feedback during practice in stroke survivors. *Neurorehabil. Neural Repair*. 21, 398–411. doi: 10.1177/1545968306298414

Cirstea, M. C., Mitnitski, A. B., Feldman, A. G., and Levin, M. F. (2003). Interjoint coordination dynamics during reaching in stroke. *Exp. Brain Res*. 151, 289–300. doi: 10.1007/s00221-003-1438-0

Corbetta, D., Sirtori, V., Castellini, G., Moja, L., and Gatti, R. (2015). Constraint-induced movement therapy for upper extremities in people with stroke. *Cochrane Database Syst. Rev*. 2015:CD004433. doi: 10.1002/14651858.CD004433.pub3

de Paiva Silva, F. P., Freitas, S. M., Silva, P. V., Banjai, R. M., and Alouche, S. R. (2014). Ipsilesional arm motor sequence performance after right and left hemisphere damage. *J Mot Behav*. 46, 407–414. doi: 10.1080/00222895.2014.924473

Dong, Y., Yean Lee, W., Hilal, S., Saini, M., Wong, T. Y., Chen, C. L.-H., et al. (2013). Comparison of the montreal cognitive assessment and the mini-mental state examination in detecting multi-domain mild cognitive impairment in a chinese sub-sample drawn from a population-based study. *Int Psychogeriatr*. 25, 1831–1838. doi: 10.1017/S1041610213001129

Ellis, M. D., Carmona, C., Drogos, J., Traxel, S., and Dewald, J. P. (2016). Progressive abduction loading therapy targeting flexion synergy to regain reaching function in chronic stroke: preliminary results from an rct. *Ann Int Con IEEE Eng Med Biol Soc*. 2016, 5837–5840. doi: 10.1109/EMBC.2016.7592055

Eraifej, J., Clark, W., France, B., Desando, S., and Moore, D. (2017). Effectiveness of upper limb functional electrical stimulation after stroke for the improvement of activities of daily living and motor function: a systematic review and meta-analysis. *Syst Rev*. 6:40. doi: 10.1186/s13643-017-0435-5

Feix, T., Romero, J., Schmiedmayer, H., Dollar, A. M., and Kragic, D. (2016). The GRASP taxonomy of human grasp types," in *IEEE Transactions on Human-Machine Systems*, 46, 66–77. doi: 10.1109/THMS.2015.2470657

Finley, M., Combs, S., Carnahan, K., Peacock, S., and Buskirk, A. V. (2012). Comparison of 'less affected limb' reaching kinematics in individuals with chronic stroke and healthy age-matched controls. *Phys. Occup. Ther. Geriatr*. 30, 245–259. doi: 10.3109/02703181.2012.716506

Fugl-Meyer, A. R., Jääsk,ö L., Leyman, I., Olsson, S., and Steglind, S. (1975). The post-stroke hemiplegic patient. 1. a method for evaluation of physical performance. *Scand. J. Rehabil. Med*. 7:13

Gladstone, D. J., Danells, C. J., and Black, S. E. (2002). The fugl-meyer assessment of motor recovery after stroke: a critical review of its measurement properties. *Neurorehabil. Neural. Repair*. 16, 232–240. doi: 10.1177/154596802401105171

Handjaras, G., Bernardi, G., Benuzzi, F., Nichelli, P. F., Pietrini, P., and Ricciardi, E. (2015). A topographical organization for action representation in the human brain. *Hum. Brain Mapp*. 36, 3832–3844. doi: 10.1002/hbm.22881

Hoonhorst, M. H., Nijland, R. H., van den Berg, J. S., Emmelot, C. H., Kollen, B. J., and Kwakkel, G. (2015). How do fugl-meyer arm motor scores relate to dexterity according to the action research arm test at 6 months poststroke?. *Arch. Phys. Med. Rehabil*. 96, 1845–1849. doi: 10.1016/j.apmr.2015.06.009

Houwink, A., Steenbergen, B., Prange, G. B., Buurke, J. H., and Geurts, A. C. (2013). Upper-limb motor control in patients after stroke: attentional demands and the potential beneficial effects of arm support. *Hum. Mov. Sci*. 32, 377–387. doi: 10.1016/j.humov.2012.01.007

Jeannerod, M. (1990). *The Neural and Behavioral Organization of Goal-Directed Movements*. Oxford: Clarendon Press.

Jørgensen, H. S., Nakayama, H., Raaschou, H. O., and Olsen, T. S., Stroke. (1999). Neurologic and functional recovery the copenhagen stroke study. *Phys. Med. Rehabil. Clin. N. Am*. 10, 887–906. doi: 10.1016/S1047-9651(18)30169-4

Krabben, T., Molier, B. I., Houwink, A., Rietman, J. S., Buurke, J. H., and Prange, G. B. (2011). Circle drawing as evaluative movement task in stroke rehabilitation: an explorative study. *J. Neuroeng. Rehabil*. 8:15. doi: 10.1186/1743-0003-8-15

Krakauer, J. W., and Carmichael, S. T. (2017). *Broken Movement. Neurobiology of Motor Recovery after Stroke*. Cambridge, MA: MIT Press.

Kwakkel, G., Lannin, N. A., Borschmann, K., English, C., Ali, M., Churilov, L., et al. (2017). Standardized measurement of sensorimotor recovery in stroke trials: consensus-based core recommendations from the Stroke Recovery and Rehabilitation Roundtable. *Int. J. Stroke*. 12, 451–461. doi: 10.1177/1747493017711813

Kwakkel, G., van Wegen, E. E. H., Burridge, J. H., Winstein, C. J., van Dokkum, L., Alt Murphy, M., et al. (2019). Standardized measurement of quality of upper limb movement after stroke: consensus-based core recommendations from the second stroke recovery and rehabilitation roundtable. *Neurorehabil. Neural Repair*. 33, 951–958. doi: 10.1177/1545968319886477

Lang, C. E., Waddell, K. J., Klaesner, J. W., and Bland, M. D. (2017). A method for quantifying upper limb performance in daily life using accelerometers. *J. Visualized Exp*. 122:55673. doi: 10.3791/55673

Leo, A., Handjaras, G., Bianchi, M., Marino, H., Gabiccini, M., Guidi, A., et al. (2016). A synergy-based hand control is encoded in human motor cortical areas. *Elife* 5:e13420. doi: 10.7554/eLife.13420

Levin, M. F. (1996). Interjoint coordination during pointing movements is disrupted in spastic hemiparesis. *Brain* 119, 281–293. doi: 10.1093/brain/119.1.281

Levin, M. F., Kleim, J. A., and Wolf, S. L. (2009). What do motor "recovery" and "compensation" mean in patients following stroke? *Neurorehabil. Neural Repair*. 23, 313–319. doi: 10.1177/1545968308328727

Levin, M. F., Liebermann, D. G., Parmet, Y., and Berman, S. (2016). Compensatory versus noncompensatory shoulder movements used for reaching in stroke. *Neurorehabil. Neural Repair*. 30, 635–646. doi: 10.1177/1545968315613863

Li, K. Y., Lin, K. C., Chen, C. K., Liing, R. J., Wu, C. Y., and Chang, W. Y. (2015). Concurrent and predictive validity of arm kinematics with and without a trunk restraint during a reaching task in individuals with stroke. *Arch. Phys. Med. Rehabil*. 96, 1666–1675. doi: 10.1016/j.apmr.2015.04.013

Massie, C., Malcolm, M., Greene, D., and Browning, R. (2014). Biomechanical contributions of the trunk and upper extremity in discrete versus cyclic reaching in survivors of stroke. *Top Stroke Rehabil*. 21, 23–32. doi: 10.1310/tsr2101-23

Massie, C. L., Fritz, S., and Malcolm, M. P. (2011). Elbow extension predicts motor impairment and performance after stroke. *Rehabil. Res. Pract*. 2011:381978. doi: 10.1155/2011/381978

McIsaac, T. L., Lamberg, E. M., and Muratori, L. M. (2015). Building a framework for a dual task taxonomy. *BioMed. Res. Int*. 2015:591475. doi: 10.1155/2015/591475

McMorland, A. J., Runnalls, K. D., and Byblow, W. D. (2015). A neuroanatomical framework for upper limb synergies after stroke. *Front. Hum. Neurosci*. 9:82. doi: 10.3389/fnhum.2015.00082

Mesquita, I. A., Fonseca, P. F. P. D., Borgonovo-Santos, M., Ribeiro, E., Pinheiro, A. R. V., Correia, M. V., et al. (2020). Comparison of upper limb kinematics in two activities of daily living with different handling requirements. *Hum. Mov. Sci*. 72:102632. doi: 10.1016/j.humov.2020.102632

Michaelsen, S. M., Jacobs, S., Roby-Brami, A., and Levin, M. F. (2004). Compensation for distal impairments of grasping in adults with hemiparesis. *Exp. Brain Res*. 157, 162–173. doi: 10.1007/s00221-004-1829-x

MVN Manual (2018). *Xsene MVN User Manual, User Guide Xsens MVN, MVN Link, MVN Awinda, Document MV0319P, Revision X, Oct 2018*. Enschede, NL: Xsens.

Persson, H. C., Parziali, M., Danielsson, A., and Sunnerhagen, K. S. (2012). Outcome and upper extremity function within 72 hours after first occasion of stroke in an unselected population at a stroke unit. A part of the SALGOT study. *BMC Neurol*. 12:162. doi: 10.1186/1471-2377-12-162

Prinsen, C. A. C., Mokkink, L. B., Bouter, L. M., Alonso, J., Patrick, D. L., de Vet, H. C. W., et al. (2018). COSMIN guideline for systematic reviews of patient-reported outcome measures. *Qual. Life Res*. 27, 1147–1157. doi: 10.1007/s11136-018-1798-3

Raghavan, P. (2015). Upper limb motor impairment after stroke. *Phys. Med. Rehabil. Clin. N. Am*. 26, 599–610. doi: 10.1016/j.pmr.2015.06.008

Rech, K. D., Salazar, A. P., Marchese, R. R., Schifino, G., Cimolin, V., and Pagnussat, A. S. (2020). Fugl-meyer assessment scores are related with kinematic measures in people with chronic hemiparesis after stroke. *J. Stroke Cerebrovasc. Dis*. 29:104463. doi: 10.1016/j.jstrokecerebrovasdis.2019.104463

Robert-Lachaine, X., Mecheri, H., Larue, C., and Plamondon, A. (2017). Validation of inertial measurement units with an optoelectronic system for whole-body motion analysis. *Med. Biol. Eng. Comput*. 55, 609–619. doi: 10.1007/s11517-016-1537-2

Roetenberg, D., Baten, C. T., and Veltink, P. H. (2007a). Estimating body segment orientation by applying inertial and magnetic sensing near ferromagnetic materials. *IEEE Trans. Neural. Syst. Rehabil. Eng*. 15, 469–471. doi: 10.1109/TNSRE.2007.903946

Roetenberg, D., Slycke, P. J., and Veltink, P. H. (2007b). Ambulatory position and orientation tracking fusing magnetic and inertial sensing. *IEEE Trans. Biomed. Eng*. 54, 883–890. doi: 10.1109/TBME.2006.889184

Roh, J., Rymer, W. Z., Perreault, E. J., Yoo, S. B., and Beer, R. F. (2013). Alterations in upper limb muscle synergy structure in chronic stroke survivors. *J. Neurophysiol*. 109, 768–781. doi: 10.1152/jn.00670.2012

Santello, M., and Lang, C. E. (2015). Are movement disorders and sensorimotor injuries pathologic synergies? When normal multi-joint movement synergies become pathologic. *Front. Hum. Neurosci*. 8:1050. doi: 10.3389/fnhum.2014.01050

Santisteban, L., Térémetz, M., Bleton, J. P., Baron, J. C., Maier, M. A., and Lindberg, P. G. (2016). Upper limb outcome measures used in stroke rehabilitation studies: a systematic literature review. *PLoS ONE* 11:e0154792. doi: 10.1371/journal.pone.0154792

Schambra, H. M., Parnandi, A., Pandit, N. G., Uddin, J., Wirtanen, A., and Nilsen, D. M. (2019). A taxonomy of functional upper extremity motion. *Front. Neurol*. 10:857. doi: 10.3389/fneur.2019.00857

Schwarz, A., Averta, G., Veerbeek, J. M., Luft, A. R., Held, J. P. O., Valenza, G., et al. (2019a). A functional analysis-based approach to quantify upper limb impairment level in chronic stroke patients: a pilot study. *Annu. Int. Conf. IEEE Eng. Med. Biol. Soc*. 2019, 4198–4204. doi: 10.1109/EMBC.2019.8857732

Schwarz, A., Kanzler, C. M., Lambercy, O., Luft, A. R., and Veerbeek, J. M. (2019b). Systematic review on kinematic assessments of upper limb movements after stroke. *Stroke* 50, 718–727. doi: 10.1161/STROKEAHA.118.023531

Sethi, A., Stergiou, N., Patterson, T. S., Patten, C., and Richards, L. G. (2017). Speed and rhythm affect temporal structure of variability in reaching poststroke: a pilot study. *J. Mot. Behav*. 49, 35–45. doi: 10.1080/00222895.2016.1219304

Stolk-Hornsveld, F., Crow, J. L., Hendriks, E. P., van der Baan, R., and Harmeling-van der Wel, B. C. (2006). The erasmus MC modifications to the (revised) Nottingham Sensory Assessment: a reliable somatosensory assessment measure for patients with intracranial disorders. *Clin. Rehabil*. 20, 160–172. doi: 10.1191/0269215506cr932oa,

Subramanian, S. K., Cross, M. K., and Hirschhauser, C. S. (2020). Virtual reality interventions to enhance upper limb motor improvement after a stroke: commonly used types of platform and outcomes. *Disabil. Rehabil. Assist. Technol.* 23;1–9. doi: 10.1080/17483107.2020.1765422

Subramanian, S. K., Yamanaka, J., Chilingaryan, G., and Levin, M. F. (2010). Validity of movement pattern kinematics as measures of arm motor impairment poststroke. *Stroke* 41, 2303–2308. doi: 10.1161/STROKEAHA.110.593368

Sukal, T. M., Ellis, M. D., and Dewald, J. P. (2007). Shoulder abduction-induced reductions in reaching work area following hemiparetic stroke: neuroscientific implications. *Exp. Brain Res*. 183, 215–223. doi: 10.1007/s00221-007-1029-6

Taub, E., Uswatte, G., Mark, V. W., and Morris, D. M. (2006). The learned nonuse phenomenon: implications for rehabilitation. *Eura. Medicophys*. 42, 241–256.

Thrane, G., Sunnerhagen, K. S., Persson, H. C., Opheim, A., and Alt Murphy, M. (2019). Kinematic upper extremity performance in people with near or fully recovered sensorimotor function after stroke. *Physiother. Theory Pract*. 35, 822–832. doi: 10.1080/09593985.2018.1458929

Tomita, Y., Rodrigues, M. R. M., and Levin, M. F. (2017). Upper limb coordination in individuals with stroke: poorly defined and poorly quantified. *Neurorehabil. Neural Repair*. 31, 885–897. doi: 10.1177/1545968317739998

Twitchell, T. E. (1951). The restoration of motor function following hemiplegia in man. *Brain* 74, 443–480. doi: 10.1093/brain/74.4.443

van Kordelaar, J., van Wegen, E. E., and Kwakkel, G. (2012). Unraveling the interaction between pathological upper limb synergies and compensatory trunk movements during reach-to-grasp after stroke: a cross-sectional study. *Exp. Brain Res*. 221, 251–262. doi: 10.1007/s00221-012-3169-6

van Kordelaar, J., van Wegen, E. E., Nijland, R. H., Daffertshofer, A., and Kwakkel, G. (2013). Understanding adaptive motor control of the paretic upper limb early poststroke: the explicit-stroke program. *Neurorehabil. Neural Repair*. 27, 854–863. doi: 10.1177/1545968313496327

van Meulen, F. B., Reenalda, J., Buurke, J. H., and Veltink, P. H. (2015). Assessment of daily-life reaching performance after stroke. *Ann. Biomed. Eng*. 43, 478–486. doi: 10.1007/s10439-014-1198-y

Veerbeek, J. M., Langbroek-Amersfoort, A. C., van Wegen, E. E., Meskers, C. G., and Kwakkel, G. (2017). Effects of robot-assisted therapy for the upper limb after stroke. *Neurorehabil. Neural Repair*. 31, 107–121. doi: 10.1177/1545968316666957

Walmsley, C. P., Williams, S. A., Grisbrook, T., Elliott, C., Imms, C., and Campbell, A. (2018). Measurement of upper limb range of motion using wearable sensors: a systematic review. *Sports Med. Open*. 4:53. doi: 10.1186/s40798-018-0167-7

Woodbury, M. L., Howland, D. R., McGuirk, T. E., Davis, S. B., Senesac, C. R., Kautz, S., et al. (2009). Effects of trunk restraint combined with intensive task practice on poststroke upper extremity reach and function: a pilot study. *Neurorehabil. Neural Repair*. 23, 78–91. doi: 10.1177/1545968308318836

Wu, C.-Y., Liing, R.-J., Chen, H.-C., Chen, C.-L., and Lin, K.-C. (2014). Arm and trunk movement kinematics during seated reaching within and beyond arm's length in people with stroke: a validity study. *Phys. Ther*. 94, 845–856. doi: 10.2522/ptj.20130101

Wu, G., van der Helm, F. C., Veeger, H. E., Makhsous, M., Van Roy, P., Anglin, C., et al. (2005). ISB recommendation on definitions of joint coordinate systems of various joints for the reporting of human joint motion–Part II: shoulder, elbow, wrist and hand. *J. Biomech*. 38, 981–992. doi: 10.1016/j.jbiomech.2004.05.042

Yang, Q., Yang, Y., Luo, J., Li, L., Yan, T., and Song, R. (2017). Kinematic outcome measures using target-reaching arm movement in stroke. *Ann. Biomed. Eng*. 45, 2794–2803. doi: 10.1007/s10439-017-1912-7

Yew, K. S., and Cheng, E. (2009). Acute stroke diagnosis. *Am. Fam. Physician*. 80, 33–40.

Conflict of Interest: The authors declare that the research was conducted in the absence of any commercial or financial relationships that could be construed as a potential conflict of interest.

Copyright © 2021 Schwarz, Veerbeek, Held, Buurke and Luft. This is an open-access article distributed under the terms of the Creative Commons Attribution License (CC BY). The use, distribution or reproduction in other forums is permitted, provided the original author(s) and the copyright owner(s) are credited and that the original publication in this journal is cited, in accordance with accepted academic practice. No use, distribution or reproduction is permitted which does not comply with these terms.

frontiers in Bioengineering and Biotechnology

ORIGINAL RESEARCH
published: 12 April 2021
doi: 10.3389/fbioe.2021.660015

Association Between Finger-to-Nose Kinematics and Upper Extremity Motor Function in Subacute Stroke: A Principal Component Analysis

Ze-Jian Chen[1,2], Chang He[3], Nan Xia[1,2], Ming-Hui Gu[1,2], Yang-An Li[1,2], Cai-Hua Xiong[3], Jiang Xu[1,2] and Xiao-Lin Huang[1,2]**

[1] Department of Rehabilitation Medicine, Tongji Hospital, Tongji Medical College, Huazhong University of Science and Technology, Wuhan, China, [2] World Health Organization Cooperative Training and Research Center in Rehabilitation, Wuhan, China, [3] State Key Lab of Digital Manufacturing Equipment and Technology, Institute of Rehabilitation and Medical Robotics, Huazhong University of Science and Technology, Wuhan, China

OPEN ACCESS

Edited by:
Veronica Cimolin,
Politecnico di Milano, Italy

Reviewed by:
Qinyin Qiu,
Rutgers University, Newark,
United States
Chi-Wen Lung,
Asia University, Taiwan

***Correspondence:**
Jiang Xu
xujiang@hust.edu.cn
Xiao-Lin Huang
xiaolinh2006@tjh.tjmu.edu.cn

Specialty section:
This article was submitted to Biomechanics, a section of the journal Frontiers in Bioengineering and Biotechnology

Received: 28 January 2021
Accepted: 24 March 2021
Published: 12 April 2021

Citation:
Chen Z-J, He C, Xia N, Gu M-H, Li Y-A, Xiong C-H, Xu J and Huang X-L (2021) Association Between Finger-to-Nose Kinematics and Upper Extremity Motor Function in Subacute Stroke: A Principal Component Analysis. Front. Bioeng. Biotechnol. 9:660015. doi: 10.3389/fbioe.2021.660015

Background: Kinematic analysis facilitates interpreting the extent and mechanisms of motor restoration after stroke. This study was aimed to explore the kinematic components of finger-to-nose test obtained from principal component analysis (PCA) and the associations with upper extremity (UE) motor function in subacute stroke survivors.

Methods: Thirty-seven individuals with subacute stroke and twenty healthy adults participated in the study. Six kinematic metrics during finger-to-nose task (FNT) were utilized to perform PCA. Clinical assessments for stroke participants included the Fugl-Meyer Assessment for Upper Extremity (FMA-UE), Action Research Arm Test (ARAT), and Modified Barthel Index (MBI).

Results: Three principal components (PC) accounting for 91.3% variance were included in multivariable regression models. PC1 (48.8%) was dominated by mean velocity, peak velocity, number of movement units (NMU) and normalized integrated jerk (NIJ). PC2 (31.1%) described percentage of time to peak velocity and movement time. PC3 (11.4%) profiled percentage of time to peak velocity. The variance explained by principal component regression in FMA-UE (R^2 = 0.71) were higher than ARAT (R^2 = 0.59) and MBI (R^2 = 0.29) for stroke individuals.

Conclusion: Kinematic components during finger-to-nose test identified by PCA are associated with UE motor function in subacute stroke. PCA reveals the intrinsic association among kinematic metrics, which may add value to UE assessment and future intervention targeted for kinematic components for stroke individuals.

Clinical Trial Registration: Chinese Clinical Trial Registry (http://www.chictr.org.cn/) on 17 October 2019, identifier: ChiCTR1900026656.

Keywords: stroke, upper extremity, kinematics, motor function, principal component analysis

INTRODUCTION

Stroke is the leading cause of disability worldwide, and upper extremity (UE) motor impairment is one of the most relevant functions affected in stroke (Langhorne et al., 2009; GBD, 2019). The impairment results in poor motor control and exerts a negative impact on UE functional capacity and activities of daily living (ADL). To optimize UE recovery after stroke, it is essential to select multilevel outcome measure for interpretation of motor recovery and clinical decision-making (Winstein et al., 2016; Villepinte et al., 2020). According to the International Classification of Functioning, Disability and Health (ICF) (WHO, 2001), there have been extensive validated UE scales on body function and activity, among which the Fugl-Meyer Assessment of Upper Extremity (FMA-UE), Action Research Arm Test (ARAT), and Modified Barthel Index (MBI) are commonly utilized in clinical practice (Santisteban et al., 2016). However, these ordinal rating scales may carry the potential for examiner bias and lack sensitivity to quantify small but potentially impacting change over time (Lang et al., 2013).

Kinematic analysis facilitates interpreting the extent and mechanisms of motor restoration, and it has been increasingly applied in neurological research (Balasubramanian et al., 2012). Although kinematic approaches are objective, sensitive and quantitative, their associations with clinical measures have not been fully studied (Schwarz et al., 2019). In previous studies of kinematic metrics, multivariable regression models are often employed to explain clinical outcomes. Due to the prerequisites of statistical models, such approaches were unable to include high collinear but potentially useful variables. In the case of collinearity, kinematic metrics of lower correlation with dependent variables were removed from the models (Alt Murphy et al., 2012; van Dokkum et al., 2014; Hussain et al., 2019). However, variables in the models measured only limited aspect of UE motor function, hardly to explain heterogeneity in clinical presentations and the intrinsic correlations among kinematic variables during motor recovery (Tran et al., 2018; Schwarz et al., 2019).

Principal component analysis (PCA) is a dimensionality reduction technique to retain the most variance of dataset without the need to exclude highly correlated variables (Zhang and Castelló, 2017). Since principal components (PCs) are the linear combinations of original variables, dataset can be represented as several statistically independent PCs (Ringnér, 2008). To our knowledge, kinematics studies using PCA regression models have focused on the distal hand. In a recent study, representative features of manual dexterity were extracted by a PCA-based logistic regression method (Lin et al., 2019). The model had shown to increase performance in identifying the severity of hand dysfunction in stroke participants. In another study of participants with mild stroke, three PCs in combination, including grip force scaling, motor coordination and speed of movement could predict manipulation skills measured by Jebsen Taylor Hand Function Test (Allgöwer and Hermsdörfer, 2017). PCA is also widely implemented in other clinical researches such as identification of patient phenotypes and prognosis prediction, but is rarely used in UE kinematics (Ibrahim et al., 2014; Badhiwala et al., 2018).

The aim of this study was to explore the kinematic components of finger-to-nose task (FNT) obtained from PCA and the associations with upper extremity motor function in subacute stroke survivors. Furthermore, we hypothesized that kinematic metrics reflected movement strategy, smoothness and velocity during the FNT; hence, the models were considered to measure aspects of motor impairment (FMA-UE), and explain more variance than activity assessments (ARAT and MBI).

MATERIALS AND METHODS

Participants

A total of 37 individuals with subacute stroke (28 men, aged 49.78 ± 10.26 years) and 20 healthy adults (12 men, aged 52.62 ± 10.23 years) were recruited in the study. The inclusion criteria for subacute stroke individuals were: (1) Clinical diagnosis of unilateral, first-ever subacute stroke verified by brain imaging (MRI or CT). (2) Aged between 18 and 80 years. (3) Showing motor impairment (FMA-UE < 66). (4) Mini-Mental State Examination score ≥ 22 and compliance with the assessments. (5) No complicating medical history such as visual, cardiac or pulmonary disorders. Exclusion criteria were other musculoskeletal or neurological conditions that affect arm function. Control participants were 18–80 years old, and had no neurological or orthopedic disorders (Johansson et al., 2017). All participants in this study were right-handed as determined by the Edinburgh Handedness Inventory (Verdino and Dingman, 1998). Data were extracted from the cohort of a clinical study in the Department of Rehabilitation Medicine. We followed the Strengthening the Reporting of Observational Studies in Epidemiology (STROBE) checklist for cross-sectional studies (Vandenbroucke et al., 2007).

Clinical Assessments

Clinical assessments for stroke participants included the FMA-UE, ARAT, and MBI. The FMA-UE is a reliable and validated measure of motor impairment after stroke. The FMA-UE consists of 33 items (scores ranging from 0 to 66) and higher scores indicate less upper limb impairment (See et al., 2013). The ARAT was used to evaluate functional ability and dexterity of the paretic upper limb. It consists of 19 items (scores ranging from 0 to 57) and higher scores indicate greater arm functional capacity (Yozbatiran et al., 2008). The level of independence in basic activities of living was assessed with the translated version of MBI. The MBI consists of 10 items (scores ranging from 0 to 100), and higher scores indicate greater ADL independence (Leung et al., 2007).

Kinematic Testing Protocol

The kinematic test was accomplished by a portable Inertial Measurement Unit system (IMU, Noraxon USA Inc.). Each IMU sensor contained a coordinate system to measure accelerations and three-dimensional orientations at a sampling frequency of 100 Hz. The IMU system showed

excellent reliability, accuracy and precision in quantifying kinematic testing protocol (Öhberg and Bäcklund, 2019; Park and Lee, 2020). According to a rigid upper body model, four sensors were placed on body segments (head, upper arm, forearm and hand). The system was calibrated before the kinematic testing protocol was implemented. To improve the measurement quality, the device automatically filtered raw data using Kalman filter algorithm.

Participants sat in a height-adjustable chair with their hips and knees flexed to 90°. Positions were not restrained, and compensatory movements were allowed when necessary (Li et al., 2015). Upper extremity maintained in the neutral position, with elbow extension and palm downward initially. The standardized procedure for the finger-to-nose test was introduced by the same researcher, and then was imitated by the participants for three times before the test. On a verbal command, the participants performed FNT as quickly and as accurately as possible, and then returned to the initial posture. Stroke individuals performed the test with the affected arm and the healthy adults performed with the non-dominant arm. The tests were recorded for five times, but a mean of three middle trials was used in statistical calculations (Alt Murphy et al., 2012; Schiefelbein et al., 2019).

Kinematic Analysis

Kinematic analysis focused on UE end-point performance during the going phase of finger-to-nose test. Data recorded in the IMU software were exported to single.csv files, then were imported to and extracted through a semi-automated custom written program in MATLAB (The MathWorks, Natick, Massachusetts, United States) for kinematic analysis. Onset and end of movements were defined using a velocity threshold of 50 mm/s (Menegoni et al., 2009; Schiefelbein et al., 2019). UE kinematic metrics were calculated through the anatomical coordinate system and joint rotation recommended by the International Society Biomechanical (ISB) (Wu et al., 2005). In this study, six kinematic metrics were utilized: movement time (MT), mean velocity (VM), peak velocity (VP), percentage of time to peak velocity (TVP%), number of movement units (NMU) and normalized integrated jerk (NIJ) (Nordin et al., 2014).

MT is an objective and quantitative variable frequently used to reflect movement performance, which was defined as the time taken during the going phase of the test. To define VP, the maximum tangential velocity of the index finger was calculated during each movement segment; and VM was defined as the average tangential velocity. TVP% is the proportion of time spent during the start of the movement until the peak velocity. The number of velocity peaks characterize NMU over a cut-off value corresponding to the 10% of VP. When multiple velocity peaks occur, the movement is composed of several smaller, corrective sub movements. NIJ was utilized to assess movement smoothness, which was calculated using the jerk normalized by MT and length of the task (Johansson et al., 2017; Rodrigues et al., 2017),

$$\mathbf{N}IJ = \sqrt{\frac{\mathbf{M}T^5}{\mathbf{2} \times \mathbf{l}ength^2} \times \sum \mathbf{j}erk(\mathbf{t})^2}$$

where jerk is the third derivate of the endpoint displacement and length is the shortest distance between the start and end positions of the index finger.

Statistical Analysis

Statistical analyses were performed on SPSS version 22.0 and R statistical software. A two-sided p-value of less than 0.05 was set as statistical significance. Categorical variables were compared through Chi squared test, and quantitative variables were compared through one-way ANOVA. The Shapiro-Wilk test was employed to evaluate the normal distribution of quantitative data. The Pearson's correlation coefficients were conducted between the kinematic variables and clinical assessments. The limit for multicollinearity between independent variables was set at 0.7 for Correlation Coefficients.

Data were scaled into a matrix at first because the mean and variance may differ greatly across the variables. Data matrix was calculated using the PCA function of R software. Then the matrix underwent eigenvalue decomposition to obtain its eigenvectors with corresponding eigenvalues. Eigenvector represented the contribution of each kinematic variable to the principal component, and was visualized by the Correlation Circle. Eigenvalue represented the amount of variance explained by the PCs. The model utilized the least number of PCs to achieve ≥90% of the total variance explained. Finally, the original data set was transformed via the eigenvectors as weighting coefficients to obtain principal component scores (Kassambara, 2017). Wilcoxon rank-sum tests were conducted to detect subgroup differences in principal component loadings in age (<50 vs. ≥50), paretic side, type of stroke for stroke participants, and between the groups. Kruskal-Wallis tests were performed to assess the differences in stroke severity (FMA-UE scores 0–22, 23–47, 48–64). The obtained PCs were included as independent variables in multivariable regression to investigate the association between kinematic metrics and clinical assessments. Probability for entry in backward regression was set at 0.05 and removal at 0.10. Adjusted R^2 values with *p*-values, unstandardized coefficient (β), and unique partial correlation coefficients were used to estimate the contribution of each PC to the model.

RESULTS

Demographics and Clinical Characteristics

Demographics and clinical characteristics of the participants were presented in **Table 1**. In this study, individuals with subacute stroke had a moderate UE impairment, with an average FMA scores of 36.22 ± 17.69 and ARAT scores of 23.97 ± 17.38. No statistical difference was observed in age, gender, Body Mass Index and TVP% between healthy participants and stroke individuals. The healthy participants performed the task with higher speed (VP, VM), less time (MT), and better smooth profiles (NMU and NIJ) than the stroke individuals ($P < 0.001$). Multicollinearity was found between MT and NIJ, as well as among VM, VP and NMU. Significant correlations were found between FMA-UE and VP ($r = 0.81$), VM ($r = 0.85$), and NMU

TABLE 1 | Demographics and Clinical Characteristics.

Characteristics	Stroke group (n = 37)	Control group (n = 20)	P-value
Age (years)	49.78 ± 10.26	52.62 ± 10.23	0.318
Gender (M/F)	28/9	12/8	0.319
Body mass index (kg/m^2)	24.43 ± 2.60	23.48 ± 2.64	0.195
MT (s)	1.09 ± 0.31	0.62 ± 0.12	$P < 0.001$*
VP(m/s)	1.61 ± 0.92	4.04 ± 0.67	$P < 0.001$*
VM (m/s)	0.78 ± 0.44	2.19 ± 0.39	$P < 0.001$*
TVP% (%)	42.23 ± 11.30	46.74 ± 5.16	0.156
NMU	2.56 ± 1.25	1.14 ± 0.28	$P < 0.001$*
NIJ	2.86 ± 1.98	0.54 ± 0.18	$P < 0.001$*
Days between onset and enrollment	106.30 ± 65.46	–	–
Type of stroke (ischemic/hemorrhagic)	26/11	–	–
Paretic side (left/right)	22/15	–	–
MMSE (range 0–30)	27.16 ± 2.41	–	–
FMA-UE (range 0–66)	36.22 ± 17.69	–	–
ARAT (range 0–57)	23.97 ± 17.38	–	–
MBI (range 0–100)	72.30 ± 22.20	–	–

Values are presented as means ± standard deviation or as otherwise indicated. MT, movement time; VP, peak velocity; VM, mean velocity; TVP%, percentage of time to peak velocity; NMU, number of movement units; NIJ, normalized integrated jerk; MMSE, Mini-Mental State Examination; FMA-UE, Fugl-Meyer Assessment for Upper Extremity; ARAT, Action Research Arm Test; MBI, Modified Barthel Index.
**P < 0.05.*

($r = -0.65$). ARAT showed significant correlation with VP ($r = 0.76$), VM ($r = 0.8$), and NMU ($r = -0.59$). MBI showed significant correlation with VP ($r = 0.55$), VM ($r = 0.58$), and NMU ($r = -0.45$). MT, TVP% and NIJ were not significantly associated with the clinical assessments (**Figure 1**).

Principal Component Analysis

As shown in the Scree Plot (**Figure 2A**), based on eigenvalue decomposition of the kinematic metrics, the principal components for stroke participants were arranged in the descending order. The first three PCs explained 91.3% variance of the dataset. The quality or proportion of representation of the kinematic variables to the PCs were presented in the squared coordinates (**Figure 2B**). PC1 accounting for 48.8% of the variance was characterized by velocity profiles (VM, VP) and smoothness profiles (NMU, NIJ). PC2 accounting for 31.1% of the variance reflected movement planning (TVP%) and movement time (MT) of stroke survivors. PC3 accounting for 11.4% of the variance mainly described movement planning (TVP%).

The z-scores of each kinematic metric in accounting for the variance of the principal components for the stroke group and control group were demonstrated in the principal component loadings (**Supplementary Figures 1–7** and **Supplementary Tables 1**, **2**). No subgroup differences were found in principal component loadings concerning age, paretic side and type of stroke for stroke participants (**Supplementary Figures 8–10**). Stroke severity measured by the FMA-UE was found to be associated with the principal component loadings (**Supplementary Figure 11** and **Supplementary Tables 3–5**). Besides, correlation circles demonstrated the similarity in loading weights among correlated kinematic variables in the respective PCs (**Figures 2C,D**). Positively correlated kinematic variables were grouped together and negatively correlated variables were positioned on opposite quadrants of the plot. PC1 was positively associated with the velocity variables (VM, VP) and negatively associated with the smoothness variables (NMU, NIJ). PC2 was positively associated with the TVP% and negatively associated with the MT. PC3 was positively associated with all the kinematic variables.

Association With Clinical Assessments

The first three PCs were included in the multivariable regression models with clinical assessments as the dependent variables, including the FMA-UE, ARAT, and MBI. The results and equations of principal component regressions were presented in **Table 2** ($P < 0.001$). PC1 was positively correlated with the clinical assessments and PC2 was negatively correlated. PC3 was positively correlated with the FMA-UE. The backward multiple regression indicated that principal components could explain the most variance in the assessment of motor impairment measured by the FMA-UE. The principal components together explained 71% of the total variance, which demonstrated a unique contribution of 55, 9, and 7%, respectively. In the model of ARAT, the PC1 and PC2 showed significant contribution to the model and explained 59% of the variance, accounting for 51 and 8%, respectively. In the model of MBI, PC1 and PC2 showed significant contribution to the model and explained 29% of the variance, accounting for 22 and 7%, respectively.

DISCUSSION

Conventional multivariable analyses of kinematic data have to meet the criteria of statistical approaches. Potential meaningful variables may be excluded due to high-mathematical collinearity. In this study, the associations between six FNT kinematic variables and UE motor function were explored through PCA for individuals after subacute stroke. Our results showed that the first three principal components explaining 91.3% variance were significantly associated with the clinical assessments for the stroke individuals. The variance explained by principal component regression in FMA-UE ($R^2 = 0.71$) were higher than ARAT ($R^2 = 0.59$) and MBI ($R^2 = 0.29$).

PC1—Movement Speed and Smoothness

PC1 accounting for 48.8% variance of the data, was largely dominated by variables that described the movement speed and smoothness. Speed indexes reflect one's efficiency and ease of movement. Similarly, mean and peak speed have been reported to correlate with upper limb motor impairment in a previous study (Bosecker et al., 2010). Movement speed depends on individual's voluntary effort, ability to control interaction torques of agonist/antagonist muscles and maintain normal inter-joint coordination during timed tasks (Nordin et al., 2014).

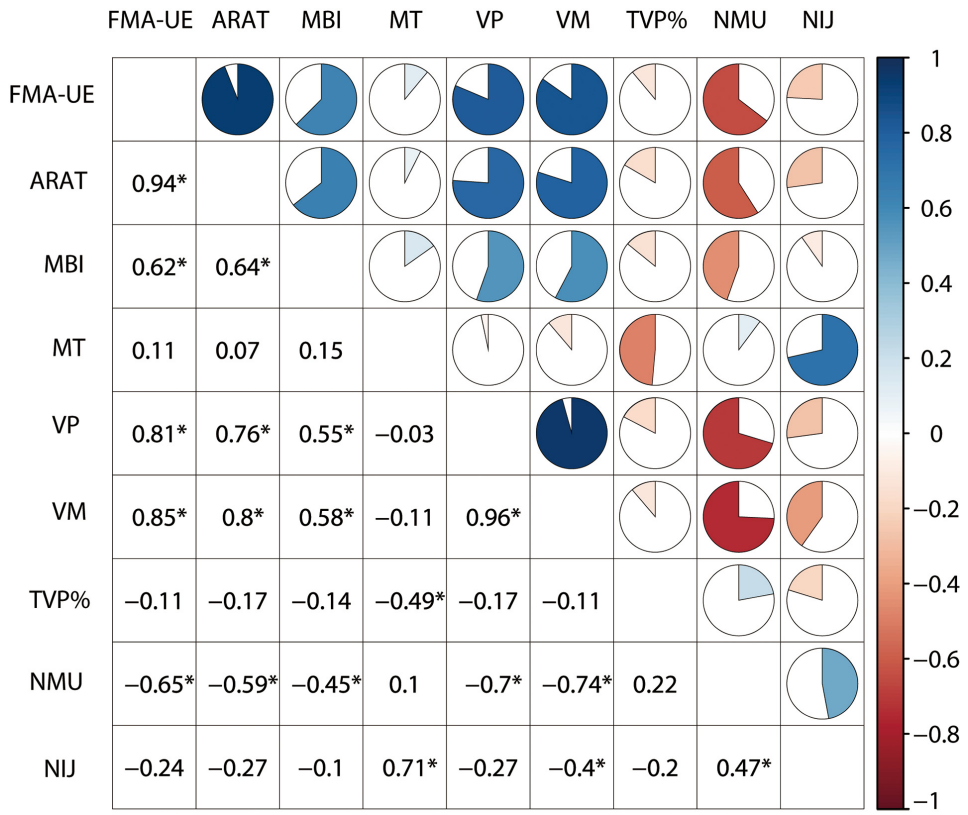

FIGURE 1 | Correlations between clinical assessments and kinematic metrics.

Besides, smoothness is related to the temporal organization or coordination of upper-limb segments since post-stroke individuals typically present excessive discrete movements (Balasubramanian et al., 2015).

Correlation analysis showed that movement speed was negatively associated with NMU ($r = -0.70$ and -0.74) in stroke survivors. However, the correlation analysis was inconsistent with the final equations shown in **Table 2** because there may be intrinsic interactions among variables. A possible explanation may be the case that movement smoothness was sacrificed for increased speed in some participants (Swaine and Sullivan, 1993). However, lower speed cannot ensure increased performance in smoothness as measured by NIJ. It should be noted that NIJ showed not significant association with peak velocity. In addition, measurement of smoothness should be taken with caution because a single smoothness parameter cannot reflect the entire recovery process of stroke survivors (Rohrer et al., 2002). Therefore, smoothness and speed indexes should be in combination as a major kinematic component (PC1) to depict only part of UE performance.

PC2 and PC3—Movement Planning and Time

PC2 accounting for 31.1% variance, was largely dominated by movement planning and movement time; PC3 accounting for 11.4% of the variance mainly described movement planning. TVP% reflects movement planning and is defined as the proportion of time spent from the onset to the peak velocity (Nordin et al., 2014). MT refers to temporal efficiency to perform a certain activity or movement, and is expected to decrease with patient's recovery (Zollo et al., 2011). Compared with healthy adults, post-stroke individuals had prolonged movement duration while the left-shifted velocity peaks were not statistically significant. In the current study, the clinical scales showed weak correlations with TVP% and MT, which were not included in the conventional regression models. However, PC2 and PC3 increased the performance of regression models by 7–9%. This is consistent with a study of robot-based kinematic assessment that movement duration can add value to estimate FMA-UE (Bosecker et al., 2010). The results therefore indicated that PC2 and PC3 may contain a considerable proportion of kinematic information, which should be taken into account when interpreting and estimating UE motor function.

In line with our study, these kinematic variables, especially velocity profiles, have been previously reported to affect UE motor function after stroke (van Dokkum et al., 2014; Schwarz et al., 2019). However, the associations between kinematics and some clinical scales are often weak to moderate and even controversial (Tran et al., 2018), e.g., NIJ and jerk (Rohrer et al., 2002; Gulde and Hermsdörfer, 2018), NMU (Rohrer et al., 2002;

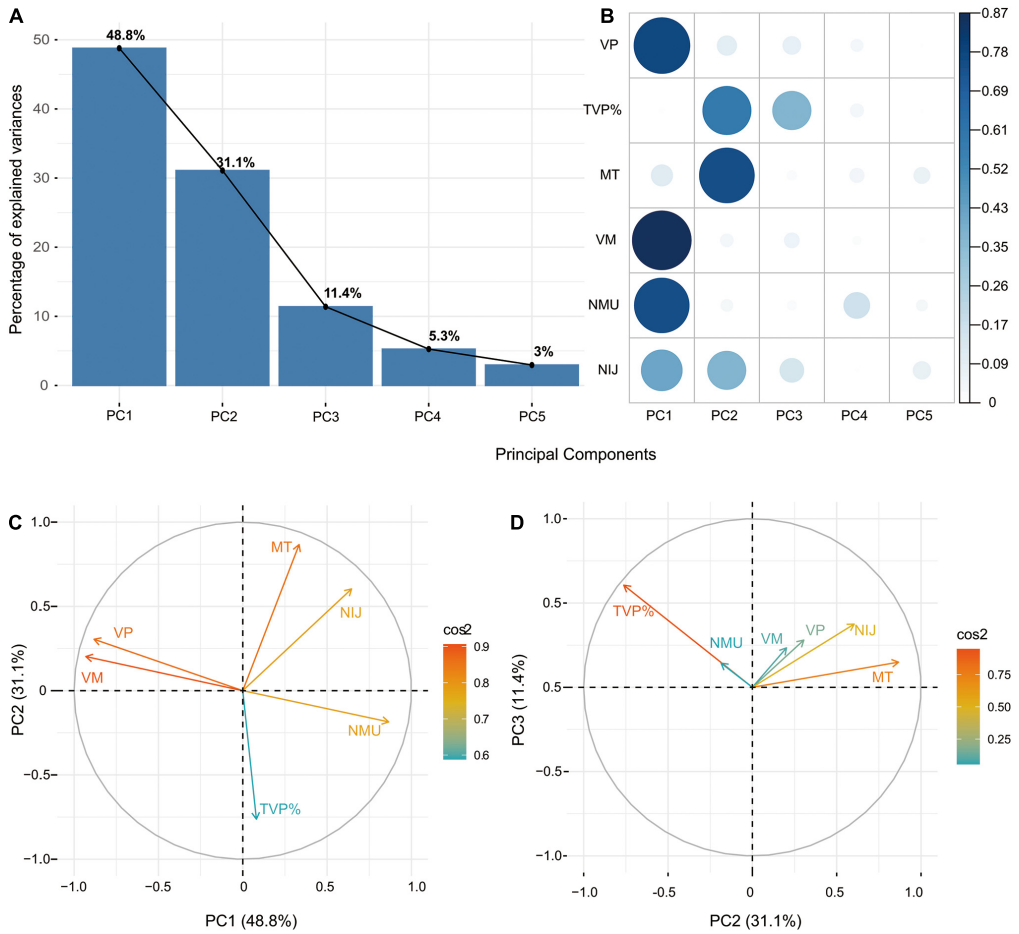

FIGURE 2 | (A) Scree Plot demonstrating the principal components accounting for variances. **(B)** Squared coordinates demonstrating the proportion of representation of the kinematic variables to the PCs. **(C)** Correlation circles demonstrating the similarity in loading weights among correlated kinematic variables in PC1 and PC2. **(D)** Correlation circles demonstrating the similarity in loading weights among correlated kinematic variables in PC2 and PC3.

Otaka et al., 2015), and VP (Gilliaux et al., 2014). Collinearity among these variables, like VM, VP, and NMU, makes it difficult for conventional multivariate statistical models to explain heterogeneous population. Our results indicated that the UE motor function may be associated with multiple variables contained in the kinematic patterns named principal components, instead of separate parameters. In addition, multiple kinematic metrics were weighted and considered as part of the PCs to estimate clinical scales. The same kinematic variables contributed differently to each principal components, suggesting that the intrinsic correlations among variables could exert influence on UE motor function. Equations acquired from PCA-based regression are important for understanding UE motor control during FNT that is often ignored in conventional statistical models. Moreover, the MBI is a questionnaire for ADL instead of an observational measure toward UE motor function. Hence, individuals could have used compensatory behaviors or actually the less affected arm to improve the score, which may be hardly illustrated by the present kinematic assessment (Hsieh et al., 2007).

Our results showed that FNT kinematics could explain more variances in aspects of motor impairment as measured by FMA-UE, than activity assessments as measured by ARAT and MBI. According to our best knowledge, there was no previous report on principal component regression for end-point kinematics of gross movement obtained in subacute stroke survivors. In studies using multivariable linear regression, various task settings were implemented to investigate the variances of clinical scores explained by kinematics. Similarly, the FMA-UE was well explained by trunk displacement and shoulder flexion (51%) for the pointing task, and by trunk displacement alone (52%) for the reach-to-grasp task (Subramanian et al., 2010). In a drinking task, movement smoothness and trunk displacement together explain 67% of the total variance in functional assessment (ARAT), while trunk displacement alone explained 20% of the variance in motor impairment (FMA-UE) (Alt Murphy et al., 2012). The associations between kinematic variables and the capacity activity were relatively low in our study, suggesting that the kinematic testing protocols may be task-specific to measure different aspects of ICF domains after

TABLE 2 | Multivariable regression analysis of the principle components against the clinical assessments.

Independent variables	Unstandardized coefficient β	Standard error	Partial unique contributions	*P*-value of the variable	Adjusted R^2 (model *P*-value)
Dependent variable: z-score of FMA-UE					0.71 (<0.001*)
PC1	0.44	0.05	55%	< 0.001*	
PC2	−0.23	0.07	9%	0.002*	
PC3	0.34	0.11	7%	0.004*	
Equation via inverse transformation:					
FMA-UE = 7.24VP + 16.14TVP% + 6.79MT + 14.69VM − 2.74NMU + 0.79NIJ + 3.50					
Dependent variable: z-score of ARTA					0.59 (<0.001*)
PC1	0.42	0.06	51%	< 0.001*	
PC2	−0.21	0.08	8%	0.012*	
Equation via inverse transformation:					
ARAT = 4.76VP - 20.87TVP% + 2.86MT + 10.11VM − 3.33NMU − 0.57NIJ + 23.75					
Dependent variable: z-score of MBI					0.29 (0.001*)
PC1	0.29	0.08	22%	0.001*	
PC2	−0.22	0.10	7%	0.044*	
Equation via inverse transformation:					
MBI = 4.54VP − 26.21TVP% + 5.80MT + 9.39VM − 3.09NMU − 0.14NIJ + 70.62					

FMA-UE, Fugl-Meyer Assessment for Upper Extremity; ARAT, Action Research Arm Test; MBI, Modified Barthel Index; PC, principal component; MT, movement time; VP, peak velocity; VM, mean velocity; TVP%, percentage of time to peak velocity; NMU, number of movement units; NIJ, normalized integrated jerk.
$^*P < 0.05$.

stroke. In addition, FMA-UE and ARAT were only explained 20 and 13% of the variance in a manual dexterity task with relatively small workspace (Hussain et al., 2019). The varying correlations between kinematics and clinical scales indicate that kinematic tests may likewise measure different ICF domains, which should be taken into consideration the task selection and clinical interpretation of kinematic analysis.

LIMITATIONS

One of the limitations of this study is the relatively limited sample size. Although no subgroup differences were found in principal component loadings concerning age, paretic side and type of stroke for stroke participants, the results must be interpreted with caution when generalizing to a wider range of populations. Moreover, there are currently no guidelines for selecting standardized kinematic assessments and the optimal kinematic metrics. Our results are limited to the similar end-point movement performance of kinematic test and comparable variables utilized during the FNT. Future studies should therefore include much variables (such as the limit of arm movement), comprehensive tasks at different UE segments as well as trunk movement and ICF levels (WHO, 2001; Tran et al., 2018).

CONCLUSION

This study showed that kinematic components during finger-to-nose test identified through PCA are associated with upper extremity motor function. PCA-based regression model indicates that finger-to-nose kinematics reflecting movement strategy, smoothness and velocity, measure much aspects of motor impairment than activity assessments. Such machine-learning method reveals the intrinsic association among kinematic metrics including velocity, smoothness and movement strategy. Our findings provide a new perspective on UE clinical assessment and future rehabilitation targeted for principal components of kinematic metrics.

DATA AVAILABILITY STATEMENT

The data files are available from the corresponding author upon reasonable request.

ETHICS STATEMENT

The studies involving human participants were reviewed and approved by the Ethical Committee of the Tongji Medical College, Huazhong University of Science and Technology. The patients/participants provided their written informed consent to participate in this study.

AUTHOR CONTRIBUTIONS

ZJC, CH, JX, and XL-H conceived the study design. ZJC, CH, NX, MHG, and YAL performed the clinical trials. ZJC and CH analyzed the results, and involved in the interpretation of the results. CH and CHX provided the technical advice for the analyses. ZJC, JX, and XLH drafted the manuscript. All authors contributed to manuscript revision, read, and approved the submission of the manuscript.

FUNDING

This work received financial support for the research and publication of this article from the National Natural Science Foundation of China (U 1913601 and No. 91648203).

SUPPLEMENTARY MATERIAL

The Supplementary Material for this article can be found online at: https://www.frontiersin.org/articles/10.3389/fbioe.2021.660015/full#supplementary-material

REFERENCES

Allgöwer, K., and Hermsdörfer, J. (2017). Fine motor skills predict performance in the Jebsen Taylor Hand Function Test after stroke. *Clin. Neurophysiol.* 128, 1858–1871. doi: 10.1016/j.clinph.2017.07.408

Alt Murphy, M., Willen, C., and Sunnerhagen, K. S. (2012). Movement kinematics during a drinking task are associated with the activity capacity level after stroke. *Neurorehabil. Neural Repair* 26, 1106–1115. doi: 10.1177/1545968312448234

Badhiwala, J. H., Witiw, C. D., Nassiri, F., Jaja, B. N. R., Akbar, M. A., Mansouri, A., et al. (2018). Patient phenotypes associated with outcome following surgery for mild degenerative cervical myelopathy: a principal component regression analysis. *Spine J.* 18, 2220–2231. doi: 10.1016/j.spinee.2018.05.009

Balasubramanian, S., Colombo, R., Sterpi, I., Sanguineti, V., and Burdet, E. (2012). Robotic assessment of upper limb motor function after stroke. *Am. J. Phys. Med. Rehabil.* 91(11 Suppl 3), S255–S269. doi: 10.1097/PHM.0b013e31826bcdc1

Balasubramanian, S., Melendez-Calderon, A., Roby-Brami, A., and Burdet, E. (2015). On the analysis of movement smoothness. *J. Neuroeng. Rehabil.* 12:112. doi: 10.1186/s12984-015-0090-9

Bosecker, C., Dipietro, L., Volpe, B., and Krebs, H. I. (2010). Kinematic robot-based evaluation scales and clinical counterparts to measure upper limb motor performance in patients with chronic stroke. *Neurorehabil. Neural Repair* 24, 62–69. doi: 10.1177/1545968309343214

GBD (2019). Global, regional, and national burden of stroke, 1990-2016: a systematic analysis for the Global Burden of Disease Study 2016. *Lancet Neurol.* 18, 439–458. doi: 10.1016/s1474-4422(19)30034-1

Gilliaux, M., Lejeune, T. M., Detrembleur, C., Sapin, J., Dehez, B., Selves, C., et al. (2014). Using the robotic device REAplan as a valid, reliable, and sensitive tool to quantify upper limb impairments in stroke patients. *J. Rehabil. Med.* 46, 117–125. doi: 10.2340/16501977-1245

Gulde, P., and Hermsdörfer, J. (2018). Smoothness metrics in complex movement tasks. *Front. Neurol.* 9:615. doi: 10.3389/fneur.2018.00615

Hsieh, Y. W., Wang, C. H., Wu, S. C., Chen, P. C., Sheu, C. F., and Hsieh, C. L. (2007). Establishing the minimal clinically important difference of the Barthel Index in stroke patients. *Neurorehabil. Neural Repair* 21, 233–238. doi: 10.1177/1545968306294729

Hussain, N., Sunnerhagen, K. S., and Alt Murphy, M. (2019). End-point kinematics using virtual reality explaining upper limb impairment and activity capacity in stroke. *J. Neuroeng. Rehabil.* 16:82. doi: 10.1186/s12984-019-0551-7

Ibrahim, G. M., Morgan, B. R., and Macdonald, R. L. (2014). Patient phenotypes associated with outcomes after aneurysmal subarachnoid hemorrhage: a principal component analysis. *Stroke* 45, 670–676. doi: 10.1161/strokeaha.113.003078

Johansson, G. M., Grip, H., Levin, M. F., and Häger, C. K. (2017). The added value of kinematic evaluation of the timed finger-to-nose test in persons post-stroke. *J. Neuroeng. Rehabil.* 14:11. doi: 10.1186/s12984-017-0220-7

Kassambara, A. (2017). *Multivariate Analysis II Practical Guide to Principal Component Methods in R*. Scotts Valley, CA: CreateSpace Independent Publishing Platform.

Lang, C. E., Bland, M. D., Bailey, R. R., Schaefer, S. Y., and Birkenmeier, R. L. (2013). Assessment of upper extremity impairment, function, and activity after stroke: foundations for clinical decision making. *J. Hand Ther.* 26, 104–114;quiz115. doi: 10.1016/j.jht.2012.06.005

Langhorne, P., Coupar, F., and Pollock, A. (2009). Motor recovery after stroke: a systematic review. *Lancet Neurol.* 8, 741–754. doi: 10.1016/s1474-4422(09)70150-4

Leung, S. O., Chan, C. C., and Shah, S. (2007). Development of a Chinese version of the Modified Barthel Index– validity and reliability. *Clin. Rehabil.* 21, 912–922. doi: 10.1177/0269215507077286

Li, K. Y., Lin, K. C., Chen, C. K., Liing, R. J., Wu, C. Y., and Chang, W. Y. (2015). Concurrent and predictive validity of arm kinematics with and without a trunk restraint during a reaching task in individuals with stroke. *Arch. Phys. Med. Rehabil.* 96, 1666–1675. doi: 10.1016/j.apmr.2015.04.013

Lin, B. S., Lee, I. J., Hsiao, P. C., and Hwang, Y. T. (2019). An assessment system for post-stroke manual dexterity using principal component analysis and logistic regression. *IEEE Trans. Neural Syst. Rehabil. Eng.* 27, 1626–1634. doi: 10.1109/tnsre.2019.2928719

Menegoni, F., Milano, E., Trotti, C., Galli, M., Bigoni, M., Baudo, S., et al. (2009). Quantitative evaluation of functional limitation of upper limb movements in subjects affected by ataxia. *Eur. J. Neurol.* 16, 232–239. doi: 10.1111/j.1468-1331.2008.02396.x

Nordin, N., Xie, S. Q., and Wünsche, B. (2014). Assessment of movement quality in robot- assisted upper limb rehabilitation after stroke: a review. *J. Neuroeng. Rehabil.* 11:137. doi: 10.1186/1743-0003-11-137

Öhberg, F., and Bäcklund, T. (2019). Portable sensors add reliable kinematic measures to the assessment of upper extremity function. *Sensors (Basel Switzerland)* 19:1241. doi: 10.3390/s19051241

Otaka, E., Otaka, Y., Kasuga, S., Nishimoto, A., Yamazaki, K., Kawakami, M., et al. (2015). Clinical usefulness and validity of robotic measures of reaching movement in hemiparetic stroke patients. *J. Neuroeng. Rehabil.* 12:66. doi: 10.1186/s12984-015-0059-8

Park, E., and Lee, K. (2020). Automatic grading of stroke symptoms for rapid assessment using optimized machine learning and 4-limb kinematics: clinical validation study. *J. Med. Internet Res.* 22:e20641. doi: 10.2196/20641

Ringnér, M. (2008). What is principal component analysis? *Nat. Biotechnol.* 26, 303–304. doi: 10.1038/nbt0308-303

Rodrigues, M. R., Slimovitch, M., Chilingaryan, G., and Levin, M. F. (2017). Does the Finger-to-Nose Test measure upper limb coordination in chronic stroke? *J. Neuroeng. Rehabil.* 14:6. doi: 10.1186/s12984-016-0213-y

Rohrer, B., Fasoli, S., Krebs, H. I., Hughes, R., Volpe, B., Frontera, W. R., et al. (2002). Movement smoothness changes during stroke recovery. *J. Neurosci.* 22, 8297–8304. doi: 10.1523/jneurosci.22-18-08297.2002

Santisteban, L., Térémetz, M., Bleton, J. P., Baron, J. C., Maier, M. A., and Lindberg, P. G. (2016). Upper limb outcome measures used in stroke rehabilitation studies: a systematic literature review. *PLoS One* 11:e0154792. doi: 10.1371/journal.pone.0154792

Schiefelbein, M. L., Salazar, A. P., Marchese, R. R., Rech, K. D., Schifino, G. P., Figueiredo, C. S., et al. (2019). Upper-limb movement smoothness after stroke and its relationship with measures of body function/structure and activity–a cross-sectional study. *J. Neurol. Sci.* 401, 75–78. doi: 10.1016/j.jns.2019.04.017

Schwarz, A., Kanzler, C. M., Lambercy, O., Luft, A. R., and Veerbeek, J. M. (2019). systematic review on kinematic assessments of upper limb movements after stroke. *Stroke* 50, 718–727. doi: 10.1161/strokeaha.118.023531

See, J., Dodakian, L., Chou, C., Chan, V., McKenzie, A., Reinkensmeyer, D. J., et al. (2013). A standardized approach to the Fugl-Meyer assessment and its implications for clinical trials. *Neurorehabil. Neural. Repair.* 27, 732–741. doi: 10.1177/1545968313491000

Subramanian, S. K., Yamanaka, J., Chilingaryan, G., and Levin, M. F. (2010). Validity of movement pattern kinematics as measures of arm motor impairment poststroke. *Stroke* 41, 2303–2308. doi: 10.1161/strokeaha.110.593368

Swaine, B. R., and Sullivan, S. J. (1993). Reliability of the scores for the finger-to-nose test in adults with traumatic brain injury. *Phys. Ther.* 73, 71–78. doi: 10.1093/ptj/73.2.71

Tran, V. D., Dario, P., and Mazzoleni, S. (2018). Kinematic measures for upper limb robot-assisted therapy following stroke and correlations with clinical outcome measures: a review. *Med. Eng. Phys.* 53, 13–31. doi: 10.1016/j.medengphy.2017.12.005

van Dokkum, L., Hauret, I., Mottet, D., Froger, J., Metrot, J., and Laffont, I. (2014). The contribution of kinematics in the assessment of upper limb motor recovery early after stroke. *Neurorehabil. Neural Repair* 28, 4–12. doi: 10.1177/1545968313498514

Vandenbroucke, J. P., von Elm, E., Altman, D. G., Gøtzsche, P. C., Mulrow, C. D., Pocock, S. J., et al. (2007). Strengthening the reporting of observational studies in epidemiology (STROBE): explanation and elaboration. *PLoS Med.* 4:e297. doi: 10.1371/journal.pmed.0040297

Verdino, M., and Dingman, S. (1998). Two measures of laterality in handedness: the Edinburgh Handedness Inventory and the Purdue Pegboard test of manual dexterity. *Percept. Mot. Skills* 86, 476–478. doi: 10.2466/pms.1998.86.2.476

Villepinte, C., Verma, A., Dimeglio, C., De Boissezon, X., and Gasq, D. (2020). Responsiveness of kinematic and clinical measures of upper-limb motor function after stroke: a systematic review and meta-analysis. *Ann. Phys. Rehabil. Med.* 64:101366. doi: 10.1016/j.rehab.2020.02.005

WHO (2001). *ICF, International Classification of Functioning, Disability and Health*. Geneva: World Health Organization.

Winstein, C. J., Stein, J., Arena, R., Bates, B., Cherney, L. R., Cramer, S. C., et al. (2016). Guidelines for adult stroke rehabilitation and recovery: a guideline for healthcare professionals from the American Heart Association/American Stroke Association. *Stroke* 47, e98–e169. doi: 10.1161/str.0000000000000098

Wu, G., van der Helm, F. C., Veeger, H. E., Makhsous, M., Van Roy, P., Anglin, C., et al. (2005). ISB recommendation on definitions of joint coordinate systems of various joints for the reporting of human joint motion–Part II: shoulder, elbow, wrist and hand. *J. Biomech.* 38, 981–992. doi: 10.1016/j.jbiomech.2004.05.042

Yozbatiran, N., Der-Yeghiaian, L., and Cramer, S. C. (2008). A standardized approach to performing the action research arm test. *Neurorehabil. Neural Repair* 22, 78–90. doi: 10.1177/1545968307305353

Zhang, Z., and Castelló, A. (2017). Principal components analysis in clinical studies. *Ann. Transl. Med.* 5:351. doi: 10.21037/atm.2017.07.12

Zollo, L., Rossini, L., Bravi, M., Magrone, G., Sterzi, S., and Guglielmelli, E. (2011). Quantitative evaluation of upper-limb motor control in robot-aided rehabilitation. *Med. Biol. Eng. Comput.* 49, 1131–1144. doi: 10.1007/s11517-011-0808-1

Conflict of Interest: The authors declare that the research was conducted in the absence of any commercial or financial relationships that could be construed as a potential conflict of interest.

Copyright © 2021 Chen, He, Xia, Gu, Li, Xiong, Xu and Huang. This is an open-access article distributed under the terms of the Creative Commons Attribution License (CC BY). The use, distribution or reproduction in other forums is permitted, provided the original author(s) and the copyright owner(s) are credited and that the original publication in this journal is cited, in accordance with accepted academic practice. No use, distribution or reproduction is permitted which does not comply with these terms.

frontiers | Frontiers in Bioengineering and Biotechnology

ORIGINAL RESEARCH
published: 27 June 2022
doi: 10.3389/fbioe.2022.925970

Functional Brain Controllability Alterations in Stroke

Xuhong Li[1], Feng Fang[2], Rihui Li[2,3] and Yingchun Zhang[2]**

[1]Department of Rehabilitation Medicine, The Third Xiangya Hospital, Central South University, Changsha, China, [2]Department of Biomedical Engineering, University of Houston, Houston, TX, United States, [3]Center for Interdisciplinary Brain Sciences Research, Department of Psychiatry and Behavioral Sciences, Stanford University School of Medicine, Stanford, CA, United States

Motor control deficits are very common in stroke survivors and often lead to disability. Current clinical measures for profiling motor control impairments are largely subjective and lack precise interpretation in a "control" perspective. This study aims to provide an accurate interpretation and assessment of the underlying "motor control" deficits caused by stroke, using a recently developed novel technique, i.e., the functional brain controllability analysis. The electroencephalography (EEG) and functional near-infrared spectroscopy (fNIRS) were simultaneously recorded from 16 stroke patients and 11 healthy subjects during a hand-clenching task. A high spatiotemporal resolution fNIRS-informed EEG source imaging approach was then employed to estimate the cortical activity and construct the functional brain network. Subsequently, network control theory was applied to evaluate the modal controllability of some key motor regions, including primary motor cortex (M1), premotor cortex (PMC), and supplementary motor cortex (SMA), and also the executive control network (ECN). Results indicated that the modal controllability of ECN in stroke patients was significantly lower than healthy subjects (p = 0.03). Besides, the modal controllability of SMA in stroke patients was also significant smaller than healthy subjects (p = 0.02). Finally, the baseline modal controllability of M1 was found to be significantly correlated with the baseline FM-UL clinical scores (r = 0.58, p = 0.01). In conclusion, our results provide a new perspective to better understand the motor control deficits caused by stroke. We expect such an analytical methodology can be extended to investigate the other neurological or psychiatric diseases caused by cognitive control or motor control impairment.

Keywords: stroke, brain controllability, motor control, EEG, fNIRS (functional near infrared spectroscopy)

OPEN ACCESS

Edited by:
Yih-Kuen Jan,
University of Illinois at Urbana-Champaign, United States

Reviewed by:
Xiaosu Hu,
University of Michigan, United States
Soha Saleh,
Kessler Foundation, United States

****Correspondence:***
Feng Fang
ffang3@uh.edu,
Yingchun Zhang
yzhang94@uh.edu

Specialty section:
This article was submitted to Biomechanics, a section of the journal Frontiers in Bioengineering and Biotechnology

Received: *22 April 2022*
Accepted: *01 June 2022*
Published: *27 June 2022*

Citation:
Li X, Fang F, Li R and Zhang Y (2022) Functional Brain Controllability Alterations in Stroke. Front. Bioeng. Biotechnol. 10:925970. doi: 10.3389/fbioe.2022.925970

INTRODUCTION

Stroke is the major cause of motor impairment, leading to motor control deficits at acute stage (Langhorne et al., 2011). More than 1.1 million people in the United States report difficulty with functional limitations in daily lives following stroke (Inman et al., 2012). Accurate interpretation and identification of motor impairment after stroke are of cardinal importance for the patient, clinician, and healthcare system (Bonkhoff et al., 2020). Over the past decades, effort has been taken to understand the underlying neural control mechanisms related to motor impairment following stroke to enhance the treatment efficacy of stroke rehabilitation interventions (Collin and Wade, 1990; Mani et al., 2013; Vliet et al., 2020). Emerging evidences have shown that various brain regions are specialized for different aspects of motor control (Mani et al., 2013), indicating it is critical to precisely define and evaluate the controllability of different brain regions that contribute to specific

TABLE 1 | Participants demographics and clinical characteristics.

Patients ID	Age (years)	Sex (F/M)	Affective side	Days after stroke	Lesion location	FM-UL	
						Pre	Post
01	55	Male	R	45	Left basal ganglia	12	\
02	66	Female	R	89	Left pons	18	33
03	36	Male	R	75	Left basal ganglia	30	\
04	46	Male	R	40	Left thalamus	53	\
05	37	Male	R	84	Left coronal radiate	32	\
06	55	Female	R	32	Left pons	56	\
07	61	Female	R	42	Left basal ganglia	14	\
08	47	Male	R	72	Left basal ganglia	20	\
09	36	Male	R	99	Left basal ganglia	17	\
10	43	Male	R	101	Left basal ganglia	18	20
11	63	Female	R	52	Left pons	16	\
12	40	Male	R	56	Left basal ganglia	61	\
13	56	Male	L	62	Right basal ganglia	56	60
14	51	Female	L	44	Right basal ganglia	43	49
15	50	Male	L	32	Right basal ganglia	11	13
16	43	Male	L	110	Right basal ganglia	22	27

motor control deficits caused by stroke. Unfortunately, such a precise evaluation of motor control deficits of stroke, in which both high resolution brain imaging strategy and accurate description of "controllability" are needed, is not currently available.

Recently, advanced neuroimaging techniques, including functional magnetic resonance imaging (fMRI), functional near-infrared spectroscopy (fNIRS), and electroencephalography (EEG), have been widely employed to investigate the dynamic alteration of cortical excitability and network connectivity following stroke, and shown great potential to understand the relationship between the dysfunctional brain network and motor control deficits (Grefkes et al., 2008a; Bajaj et al., 2014; Snyder et al., 2021). For example, previous fMRI study illustrated that the motor control deficits of stroke patients were associated with pathological intra- and inter-hemispheric interactions among key motor regions such as primary motor cortex (M1), premotor cortex (PMC), and supplementary motor cortex (SMA), and executive control network (ECN) (Grefkes et al., 2008a; Zhao et al., 2018). A recent study employing EEG to investigate the resting-state networks under different frequency bands in stroke showed that reduced cortical activity and connectivity in alpha and beta bands in stroke patients might explain the motor impairment caused by stroke (Snyder et al., 2021). Similarly, a previous fNIRS study applying the spectral interdependency methods demonstrated the bi- and uni-directional connectivity between motor brain regions were associated with specific movement suppression and motor control execution, and could provide promising biomarkers to characterize motor control impairment in stroke patients (Bajaj et al., 2014).

While unimodal fMRI, fNIRS, and EEG studies have provided critical insight into the brain network alteration associated with stroke, their limitations have prevented in-depth study to simultaneously extract the spatial and temporal information of the brain activity in a good precision. Specifically, EEG offers high temporal accuracy to unveil the dynamics of neural activity but suffers from the volume conduction problem, which may make the estimation of brain connectivity unreliable (Winter et al., 2007). FMRI and fNIRS show higher spatial resolution to locate the brain activity than EEG (spatial resolution: fMRI > fNIRS > EEG), however, these two neuroimaging techniques are incapable of recovering accurate time course of cortical activity and the accuracy of hemodynamic-based connectivity network is questionable (Roebroeck et al., 2011). To overcome these limitations, a recently developed, spatiotemporal specific method, dynamic brain transition network (DBTN), for EEG and fNIRS (or fMRI) integration analysis was applied to reconstruct highly specific patterns of cortical activity, which were then used to recover the general and conditionally-specific brain networks that support stimulus response (Nguyen et al., 2019; Fang et al., 2020). Previous study has utilized the DBTN source imaging approach to identify biomarkers associated with motor function recovery and document the post-stroke motor reorganization (Li et al., 2020). The results showed that the functional brain connectivity of PMC, M1, and SMA were potential biomarkers to assess the motor function recovery of stroke, and the DBTN source imaging strategy was potentially useful for monitoring and predicting post-stroke motor recovery (Li et al., 2020).

Even though previous studies have reported potential biomarkers to assess the motor control deficits of stroke, all these biomarkers themselves are not directly associated with the "control" assessment of the brain. As such, a specific understanding of the "motor control" deficits caused by stroke, which may lead to advanced interpretation of the physiological symptom observed in stroke patients, is remains lacking. Recently, network control theory has been applied to interpret brain state transitions (Gu et al., 2015). Conventional graph-based measures show the local properties of varied brain regions and their important roles in their network architectures (Sporns, 2018). Differently, control theory-based network measures describe one brain region's capability to change the brain behavior from one state

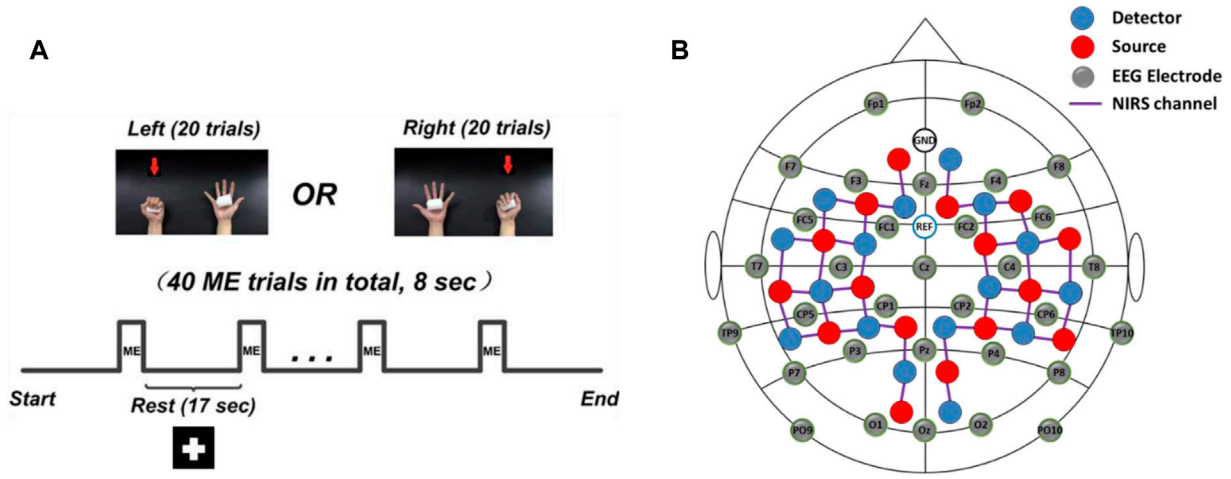

FIGURE 1 | Experimental design. **(A)** The experimental motor executive task used in the study. The "ME" represents motor execution. **(B)** The EEG and fNIRS channel locations.

to another state (Gu et al., 2015). For example, modal controllability diagnostic describes the ability of one brain region to steer the brain networked system into difficult-to-reach state (Gu et al., 2015). Previous study has employed the brain controllability analysis to assess the cognitive control deficit in neurological and psychiatric diseases such as depression and dementia (Fang et al., 2021). However, no study has ever utilized brain controllability measure to assess the motor control deficit of stroke, to specifically describe the "motor control" deficit with a specific "controllability" measurement.

In this study, we integrated our recently developed DBTN-based fNIRS-informed EEG source imaging approach, and functional brain controllability analysis to assess "motor control" deficits caused by stroke. We hypothesized that the modal controllability of the key motor brain regions (M1, PMC, and SMA) and the ECN would decrease among stroke patients compared to healthy subjects. To the best of our knowledge, this study represents the first effort to employ the brain network "controllability" diagnostic to specifically interpret the "motor control" deficits caused by stroke. Additionally, this study is also the first study to apply the brain controllability analysis based on the non-invasive, portal, and costless neuroimaging tools with a high spatiotemporal fNIRS-informed EEG source imaging approach.

MATERIALS AND METHODS

Study Design

Sixteen stroke patients with hemiparesis (5 females and 11 males; age 49.1 ± 9.4 years) were recruited from Guangdong Provincial Work Injury Rehabilitation Center, and 11 age-matched, healthy subjects (3 females and 8 males; age 41.2 ± 15.8 years) were recruited as the control group. All participants are right-handed. The experimental protocol was approved by the ethics committee of the Guangdong Provincial Work Injury Rehabilitation Center (AF/SC-07/2016.30). Participants gave written informed consent according to the Declaration of Helsinki.

The inclusion criteria for stroke patients were as follows: 1) stroke that occurred 1–6 months prior to the first assessment, 2) age between 18 and 70 years, and 3) able to follow instructions and to consent (Mini Mental State Examination score >27). The exclusion criteria were as follows: 1) deficits in communication or attention that would interfere with the experiment participation, 2) contraindication to MRI scanning, and 3) other diseases that would substantially affect the function of upper extremity.

All patients underwent a 4-weeks conventional rehabilitation intervention in the hospital. The intervention included standard physical training (walking, sitting, standing balance, and movement switching), occupational therapy (eating, drinking, swallowing, dressing, bathing, cooking, reading and writing, and using the restroom), and massage for 6 h per day, 5 days per week. Prior to the beginning of intervention, all patients underwent a baseline assessment of upper extremity function by Fugl-Meyer Assessment rating scale (FM-UL, normal = 66) and participated in a concurrent EEG-fNIRS recording (pre-intervention) (Gladstone et al., 2002). Ten patients were not able to complete the entire rehabilitation intervention and thus, were ineligible to participate in the post-intervention EEG-fNIRS recording and clinical assessment. Therefore, only six patients participated in the concurrent EEG-fNIRS recording and clinical assessment of motor function in the post-intervention session. All motor function assessments were performed by an experienced therapist from the Department of Rehabilitation Medicine in the hospital.

Experimental Paradigm

During the experiment, participants received visual instruction through a monitor placed in front of them. A motor executive (ME) paradigm consisted of 40 randomized trials of left- and right-hand clench tasks (20 trials for each hand) was employed.

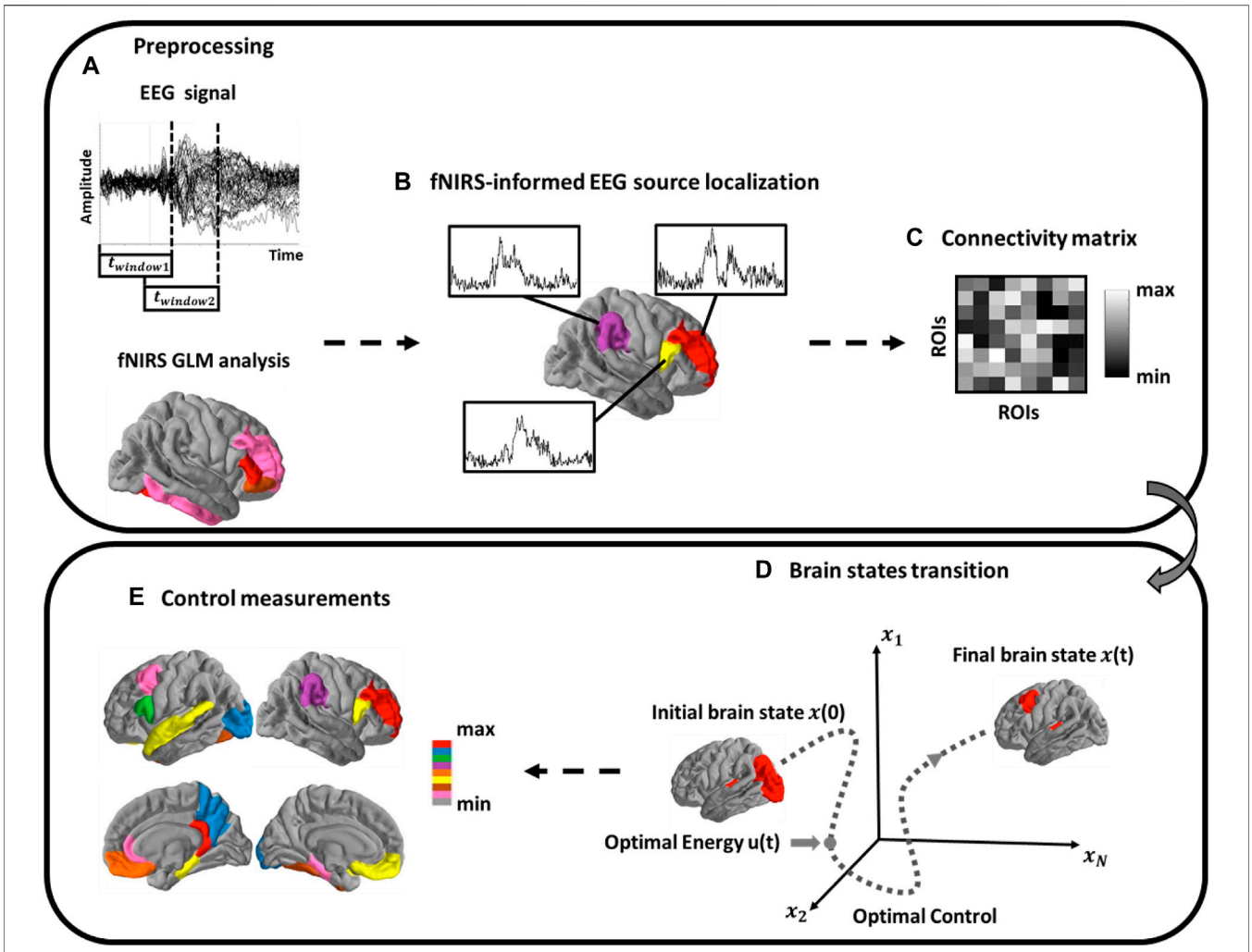

FIGURE 2 | Schematic of Methods. **(A)** EEG analysis using a sliding window scheme. FNIRS activation map is then extracted to form spatial priors; **(B)** Source localization analysis of cortical source activity; **(C)** Functional brain network construction; **(D)** Estimation of brain network dynamic process and the brain controllability analysis; **(E)** Calculate the modal controllability of each single brain region.

Each trial started with an 8-s ME task, indicated by a "+" symbol in a black background (**Figure 1A**). During the ME period, subjects were asked to naturally squeeze a sponge ball with the corresponding hand shown on the monitor. Patients were required to try their best to squeeze the sponge ball using their affected hands without causing any shaking of their bodies. In this study, the whole-hand clenching task was applied since previous studies reported that the whole-hand clenching evoked stronger brain cortical activations than classic motor task such as finger tapping (Grefkes et al., 2008b). Meanwhile, the whole-hand clenching task is relatively easier to be executed by stroke patients who have motor deficits.

Data Acquisition

A concurrent EEG and fNIRS recording paradigm was employed to collect the EEG signal and hemodynamic response signal (**Figure 1B**). Specifically, 32 active EEG electrodes were placed on the scalp, and the EEG signals were measured using an EEG recording system (Brain Products GmbH, Germany) with 500 Hz sampling rate. Meanwhile, a total of 40 fNIRS channels were positioned over the main brain regions, including the motor cortex, frontal cortex, temporal cortex, and occipital cortex. FNIRS signals were recorded simultaneously using a continuous-wave NIRS imaging system (NIRScout, NIRx Medizintechnik GmbH) with 3.91 Hz sampling rate.

EEG fNIRS Preprocessing

The analytical pipeline is shown in **Figure 2**. The raw EEG signals were first filtered by a notch filter at 50 Hz to remove powerline noise and then a fourth-order Butterworth bandpass filter (0.5–45 Hz). Eye movement artifact was then removed using independent component analysis (ICA) strategy. The common average method was utilized to re-reference the EEG signals (Ludwig et al., 2009). After that, EEG signals were segmented into multiple trails that began 2000 ms before the task onset and

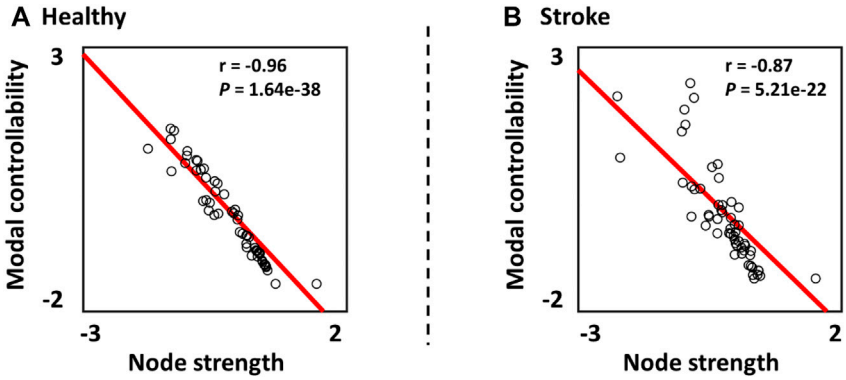

FIGURE 3 | Relationship between the z-scored modal controllability and the z-scored node strength in **(A)** Healthy subjects and **(B)** Stroke patients.

ended 8000 ms after the task onset, and baseline correction was performed for each trial. Finally, we manually inspected and excluded any trial with large artifact.

For the fNIRS signals, a fourth-order Butterworth band pass filter (0.01–0.5 Hz) was applied first to eliminate artifacts such as cardiac interference (0.8 Hz). Following this, motion artifacts were removed from the fNIRS signals using a wavelet-based method (Molavi and Dumont, 2012). The concentration changes of the HbO and HbR were then computed utilizing the modified Beer-Lambert Law (Ferrari and Quaresima, 2012). The obtained signals were manually inspected for every channel, wherein trials with apparent spikes and discontinuous segments were deemed as noisy trials and excluded from further analysis (usually signal changes with amplitude >0.4 au and exceeding a threshold of 100 in change of standard deviation within 0.3 s) (Delgado Reyes et al., 2018). Finally, the general linear model (GLM) was employed to obtain the activated channels that significantly induced by each hand movement, which would be used as spatial priors for the EEG source imaging.

fNIRS-Informed EEG Source Localization

Forward Calculation

In this study, the MNI 305 template was used as common brain model for all subjects (Fonov et al., 2011). The high-density cortical layer and the brain-skull-scalp layers were generated on the brain model using the Freesurfer analysis suite (Fischl, 2012). The boundary element method (BEM) was then employed to construct the 3-layer brain model (Fuchs et al., 2002). A lead-field matrix G was then computed based on the cortical source space, the 3-layer brain model, and the 32 EEG channels *via* forward calculation (Hallez et al., 2007).

Inverse Calculation

Our recently developed high spatiotemporal fNIRS-constrained EEG source imaging approach, DBTN, was employed to perform source analysis (Nguyen et al., 2016; Nguyen et al., 2018; Li et al., 2020). Following this method, electrical activity within the source space is reconstructed based on multimodal, sliding-window calculations, which makes the algorithm spatially precise and resilient to depth bias and noise from volume conduction (Nguyen et al., 2016; Nguyen et al., 2018; Li et al., 2020). Briefly, the calculation of the current density J can be formulated as:

$$J = RG^T\left(GRG^T + \lambda^C\right)^{-1}Y \tag{1}$$

where Y represents the EEG signals and J indicates the unknown source activity. C and R represent the noise and source covariance matrices, respectively. The regularization parameter λ represents a trade-off between the model accuracy and complexity that is traditionally determined through the L-curve method. Within this construction, the source covariance matrix, R, represents prior knowledge about the distribution of J. Under the framework of the high spatiotemporal fNIRS-constrained EEG source imaging (DBTN), however, R is constructed as a weighted sum of the active spatial priors, where each individual prior is a sub-map of the fNIRS activation pattern, as mentioned above:

$$R = \sum_{i=1}^{N} \lambda_i^R Q_i \tag{2}$$

Following this equation, R is defined by the sum of N covariance components $Q = (Q_1, \ldots, Q_N)$, weighted by an unknown hyperparameter λ^R. Each individual covariance component, Q_i, is formed from a subset of the fNIRS map. The hyperparameters λ^R were estimated for each EEG window using a Restricted Maximum Likelihood algorithm (Nguyen et al., 2016), and the corresponding current densities were calculated. The DKT40 atlas was then employed to form 62 regions of interest (ROIs) (Klein and Tourville, 2012). More details about the DBTN methodology can refer to (Nguyen et al., 2016; Nguyen et al., 2018; Li et al., 2020).

Functional Brain Network Controllability Analysis

Functional Network Construction

DBTN-based source localization formed a basis multivariate time-series for subsequent functional connectivity analysis using a measure of weighted phase lag index (wPLI) (Vinck et al., 2011). The wPLI method is a data-driven technique based on the weighted phase differences between two time-series signals. The functional

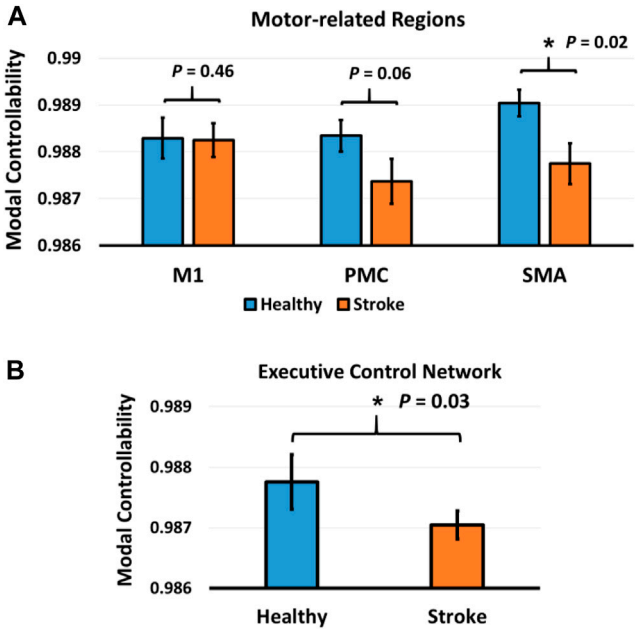

FIGURE 4 | (A) Comparison of modal controllability in M1, PMC, and SMA between stroke patients and healthy subjects. **(B)** Comparison of modal controllability in executive control network (ECN) between stroke patients and healthy subjects. Asterisk represents significant difference ($p < 0.05$) after multiple comparison correction.

brain network was then constructed by the wPLI values and utilized for the following brain network controllability analysis.

Brain Controllability Analysis

One of the critical steps in applying network control theory to the human brain is to define a model for the dynamics of neural processes (Gu et al., 2015; Karrer et al., 2020). In this study, a simplified, noise-free, linear, and time-invariant model was employed to build the brain network dynamic model (Gu et al., 2015). The model equation can be formulated as follows:

$$x(t+1) = Ax(t) + Bu(t) \tag{3}$$

where x describes the state (that is, the magnitude of neurophysiological activity) of brain regions over time, and A is the functional connectivity matrix constructed by the wPLI method. The input matrix B specifies the control nodes and the input u denotes the external stimulation. In this study, the external stimulation of u can be considered as the experimental paradigm shown on the screen that elicited the preceding of motor behaviors in the brain.

The modal controllability was then utilized to evaluate the control capability of various regions in steering the network system into different ease level of states (Medaglia et al., 2017).The modal controllability reflects the ease of a node to push the brain network system into many different difficult-to-reach states (Medaglia et al., 2017). Mathematically, it was defined as:

$$\phi_i = \sum_{j=1}^{N} \left(1 - \lambda_j^2(A)\right) v_{ij}^2 \tag{4}$$

vij is the element of the eigenvectors matrix of A and λj is the jth eigenvalue.

From a cognitive perspective, the brain areas with high modal controllability may be important in switching the brain between many cognitive functions that require significant cognitive effort (Gu et al., 2015). If control energy can be likened to cognitive effort and if brain states can be likened to cognitive functions, then the difficult-to-reach state refers to the brain state that requires significant cognitive effort to reach from the initial brain cognitive state such as from a resting brain state to a motor performance state that is cognitively demanding. In this study, we calculated the modal controllability of the three main motor brain regions, M1, PMC, and SMA, from the contralateral sides, and also the psychological brain system of ECN for both stroke patients and healthy subjects. In this study, the ECN was extracted from the ROIs located in the prefrontal cortex including the ventromedial prefrontal cortex and dorsolateral prefrontal cortex, parietal cortex, and anterior cingulate cortex (Callejas et al., 2005; Duncan, 2013; Dong et al., 2015).

Statistical Analysis

Linear regression analysis was first performed to investigate the relationship between the modal controllability and the node strength (Montgomery et al., 2021). The modal controllability of three different motor brain regions, M1, PMC, and SMA, were computed and compared, respectively, between stroke patients and healthy controls using non-parametric statistical test, Mann Whitney U test (Nachar, 2008). The modal controllability of ECN was also compared between stroke patients and healthy controls using Mann Whitney U test. The baseline modal controllability of M1, PMC, SMA, and ECN were correlated with the baseline clinical scores, FM-UL, using linear regression model. Meanwhile, the changes of modal controllability of the three motor-related regions and the ECN were also correlated with the changes of baseline clinical scores from pre- and post-intervention using linear regression model. False discovery rate (FDR) method was employed for correction of multiple comparisons (Genovese et al., 2002).

RESULTS

Demographic and Clinical Behavior Data

Table 1 summarizes the demographic information of the stroke patients including age, gender, site of the lesion, time of stroke, and clinical assessment scores. Statistical analysis showed that there were no significant differences between stroke patients and healthy subjects in terms of age ($p > 0.05$, t test) and gender ($p > 0.05$, chi-square test) (Satorra and Bentler, 2001; De Winter, 2013).

Controllability of Psychological Brain Network and Motor Brain Regions

In **Figure 3**, the relationship between the modal controllability and the node strength was investigated. The results showed that the z-scored modal controllability was significantly correlated with the z-scored node strength in both healthy subjects ($r = -0.96$, $p = 1.62e\text{-}38$) and

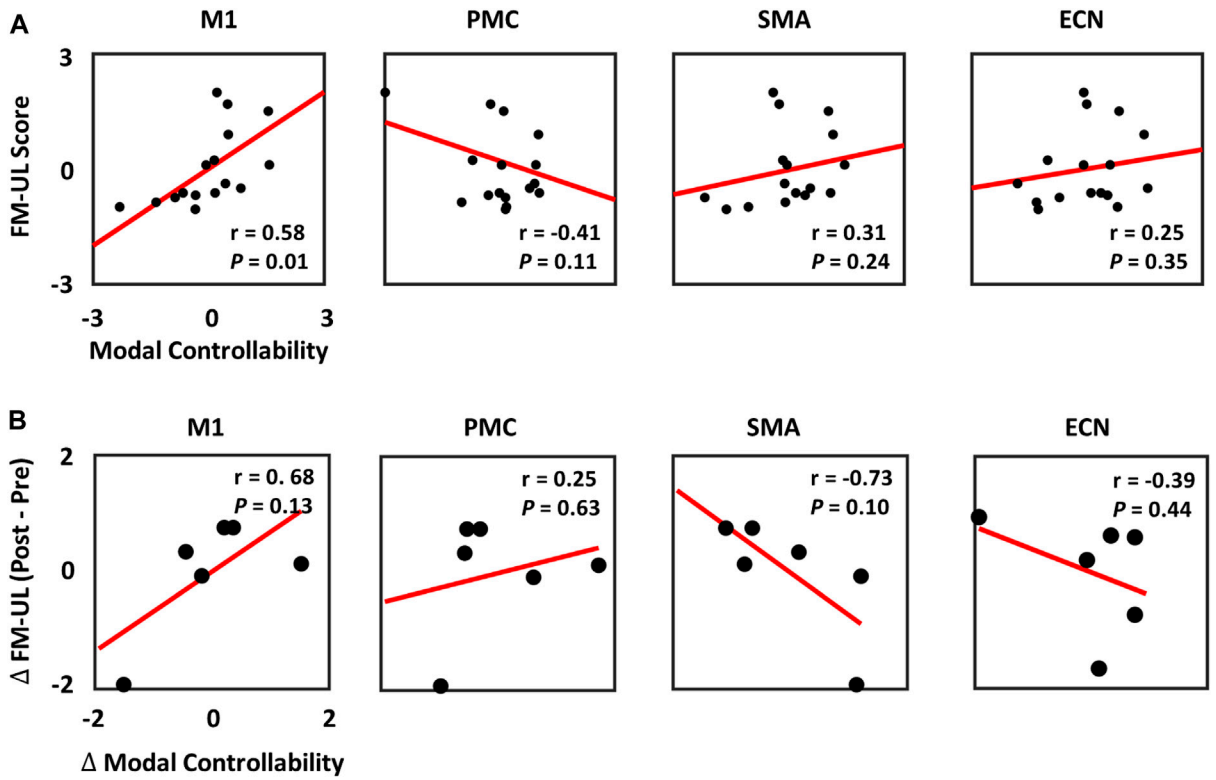

FIGURE 5 | (A) Relationship between the baseline FM-UL scores and the baseline modal controllability in M1, PMC, SMA, and ECN. **(B)** Relationship between the changes of FM-UL scores and the changes of modal controllability at pre- and post-intervention among the 6 stroke patients.

stroke patients (r = −0.87, p = 5.21e-22). The negative correlation between the modal controllability and the node strength are consistent with previous studies (Gu et al., 2015; Wiles et al., 2017).

Then, the modal controllability of ECN was computed and statistically compared between the two groups. As shown in **Figure 4B**, the modal controllability of ECN in healthy subjects was significantly larger than the modal controllability of ECN in stroke patients (p = 0.03). Following this, the modal controllability of three key motor regions, M1, PMC, and SMA, were calculated and statistically compared. In **Figure 4A**, the modal controllability of SMA in healthy subjects was significantly higher than the modal controllability of SMA in stroke patients (p = 0.02, FDR-corrected). The modal controllability of PMC was significantly larger in healthy subjects than stroke patients before multiple correction (p < 0.05, uncorrected), but insignificant after multiple correction (p = 0.06, FDR-corrected). No significant difference of modal controllability in M1 was observed between stroke patients and healthy subjects (p = 0.46, FDR-corrected).

Correlation Between Baseline Controllability and Clinical Scores

The relationship between the baseline modal controllability and the baseline clinical scores (FM-UL) was then explored in stroke patients. The z-scored baseline modal controllability and FM-UL scores were computed and correlated using linear regression model. As shown in **Figure 5A**, the baseline modal controllability of M1 was significantly correlated with the baseline FM-UL scores (r = 0.58, p = 0.01). No significant correlation was observed between the FM-UL scores and the modal controllability of PMC, SMA, and ECN.

In order to identify biomarkers to predict the recovery rate of stroke patients, the changes of modal controllability and the changes of FM-UL scores at pre- and post-intervention recordings were calculated and correlated by the linear regression modal. In **Figure 5B**, the results showed that no significant correlation was observed between the changes of modal controllability and the changes of FM-UL scores based on six stroke patients' data, even though very high correlation existed.

DISCUSSION

While current neuroimaging studies have proposed potential network-level biomarkers to assess the motor control impairment and better understand the underlying neural mechanisms on stroke patients (Grefkes et al., 2008a; Bajaj et al., 2014; Snyder et al., 2021), none of the biomarkers could provide a "control" concept to specifically describe the "motor control" deficits. Therefore, the primary goal of this study is to

assess the "motor control" deficits of stroke patients by performing a high spatiotemporal resolution source imaging analysis, and employing a specific "control" diagnostic, which is the modal controllability (Gu et al., 2015). The main findings in this study are that the modal controllability of SMA and ECN are significantly lower in stroke patients than healthy subjects. In addition, the baseline modal controllability of M1 is found to be significantly correlated with the baseline clinical scores of stroke patients. To the best of our knowledge, this study represents the first attempt to apply the measure of "controllability" to specifically assess the "motor control" deficits caused by stroke. Besides, this is also the first study to employ the brain network controllability analysis based on the non-invasive, portable, and costless neuroimaging modalities associated with a high spatiotemporal fNIRS-informed EEG source localization approach (Nguyen et al., 2018). The methodologies utilized in this study may provide a new perspective to better understand the cognitive control or motor control impairment of different neurological or psychiatric diseases, and promote the development of neuromodulation strategies in an experimentally friendly manner.

In general, most stroke patients suffer from various degrees of motor deficits, which has been associated with the functional impairment across different motor control areas such as M1, PMC, and SMA (Zhao et al., 2018). The PMC and SMA brain regions are appear to be higher level areas that encode complex patterns of motor output and select appropriate motor plans to achieve desired end results, while M1 appears to be relatively lower hierarchy and decomposes movement into simple components in a body map, and these simple movement components are then communicated to the spinal cord for execution (Graziano, 2006). Previous study has employed brain connectivity analysis to assess the relationship between cortical disconnection and motor performance, demonstrating that the cortical disconnection of M1 and SMA are associated with the upper/lower extremity motor control performance of stroke patients (Peters et al., 2018). The results further show that the SMA is important in the temporal organization of movement and becomes more significant in the control of simple motor tasks if the M1 is injured (Peters et al., 2018), indicating that the SMA is more involved in performing difficult tasks than M1. However, the "dis/connection" itself does not have any implication of the "control" capability, to precisely describe the motor control deficits and the ability of various brain regions in guiding the brain into easy or difficult states in response to the tasks. Therefore, in this study, we employed a novel "controllability" measure to specifically describe the "control" ability loss of the above motor regions in stroke patients.

Network control theory is an innovative and leading subfield of dynamic network theory that offers powerful engineering-based concepts to examine functional signaling in the networked systems (Gu et al., 2015). Traditional graph-based measurements such as node degree, betweenness centrality, and clustering coefficient, describe the local properties of the network architecture (Bullmore and Sporns, 2009). However, these locally static graph measures themselves do not have any implication to describe the "control" ability of the regions in controlling the brain state transition (Fang et al., 2021). Differently, controllability diagnostics are systematic-level measures that describe the capability of different brain regions in affecting the network dynamics and steering the brain into various easy or difficult to reach states (Betzel et al., 2016). For example, the modal controllability indicates the capability of a specific brain region in controlling the brain network system into difficult-to-reach states (Gu et al., 2015). In a control perspective, our results demonstrated that the modal controllability of SMA in stroke patients was significantly lower than healthy controls (**Figure 4A**), indicating the SMA showed less control ability to guide the brain network system into hard-to-reach states in stroke patients. Physiologically, as mentioned above, the SMA is more involved in performing cognitively demanding tasks and the disconnection of SMA is associated with motor control deficits of stroke patients (Peters et al., 2018). Instead of interpreting the lost capability of motor control performance based on the static graph measures (dis/connection), our results interpreted the specific "motor control" deficits of stroke patients with a particular systematic measure, "controllability", to precisely describe the "motor control" ability loss in stroke patients. Specifically, our results indicated that the motor control deficits caused by stroke may due to the lost capability of SMA in steering the brain network system into cognitively demanding states. Prior study reported that a subject's cognitive processing and set-shifting speed appears to be coded, to some degree, in the connectivity strength of bilateral intraparietal sulcus nodes of the ECN (Seeley et al., 2007). From a control point of view, our results showed that the capability of ECN to control the brain to enter some difficult states was lost in stroke patients (**Figure 4B**). This may explain the motor impairment of stroke patients in performing some control-demanding tasks that require higher level cognitive processing provided by ECN to complete the difficult tasks.

In this study, we also correlated the controllability values with the clinical scores (FM-UL). In our results, the baseline modal controllability of M1 showed significantly positive correlation with the baseline FM-UL scores (**Figure 5A**). Even though most studies hypothesized the M1 controlled movement at a simple level, some researches also demonstrated that the M1 may serve some complex function than originally hypothesized (Graziano, 2006). Our results further illustrated that the capability of M1 to steer the brain network system into some complex brain states that require a lot of cognitive effort may account for the motor reservation of stroke, and be utilized as biomarkers to predict the reservation of motor performance in stroke patients at baseline. Unfortunately, due to the limited sample size of patients who have both pre- and post-intervention EEG-fNIRS recordings, the changes of modal controllability could not significantly predict the changes of clinical scores, although high correlations were observed (**Figure 5B**). This will be improved as the immediate next step once we have more patients with the post-intervention.

In this study, we quantified the contribution of topological factor (node strength) to the variability in controllability in stroke patients and healthy subjects, respectively. As reported in previous study (Jeganathan et al., 2018), lower correlation between the node strength and the controllability measure indicated that other network features or factors may influence the nodes' controllability. In our results, we showed that the correlation between node strength and controllability in stroke patients was lower than that of health subjects (**Figure 3**). This may indicate that the network alterations caused by stroke may break the underlying

neural control patterns by increasing the effects of other network features in contributing to the normal control patterns.

While the current investigation provides a new perspective to interpret the specific motor control deficits in stroke patients, some limitations and drawbacks must be acknowledged. First and foremost, the sample size is relatively small in this study. Meanwhile, the clinical characteristics of patients are rather heterogeneous, such as lesion size, location, initial motor impairment (11–61), stroke phase (acute/subacute) and stroke subtype (cortical/subcortical). These variables could have certain effects on characterizing the behavioral and neurological outcomes. Besides, even though a high spatiotemporal resolution brain imaging approach was employed to reconstruct the source activities, the brain model utilized for each subject was from a common brain model, which may induce mild bias when estimating the cortical activities. The immediate next step will be collected the magnetic resonance imaging (MRI) data from those participants to construct the patient-specific brain model, to further increase the fNIRS-informed EEG source localization accuracy. Moreover, in this study, we only considered the EEG sources located in the cortical areas due to the shallow penetration depth of fNIRS (around 1–3 cm) in the cortex (Liu et al., 2015), but will be improved with the development of advanced neuroimaging techniques and algorithms. Additionally, the current study employed a simple linear network dynamic model, which remains to be improved to account for the nonlinear effect in future. Finally, as our experimental paradigm asked the subjects to perform motor control behaviors from a resting state, we assumed this is a difficult-to-reach process (compared to the brain states transition between resting to sleeping or resting to resting) that requires significant cognitive effort from the resting state (especially for stroke patients), which is consistent with the definition of modal controllability. In future studies, we may employ other brain controllability measurements such as average controllability and global controllability to investigate the control properties of the brain in stroke and other diseases.

CONCLUSION

This study represents the first attempt to employ the network "controllability" diagnostic to specifically interpret the "motor control" deficits caused by stroke. In addition, the current study is also the first study to apply the brain controllability analysis based on the non-invasive, portal, and costless neuroimaging tools with a high spatiotemporal fNIRS-informed EEG source imaging strategy. The results demonstrated that the modal controllability of SMA and ECN were significantly decreased in stroke patients compared to healthy subjects, and the baseline modal controllability of M1 could be utilized to predict the clinical scores at baseline for stroke patients. The methodologies proposed in this study may be extended to investigate the cognitive/motor control deficits caused by other neurological or psychiatric diseases, and design neuromodulation strategies by employing the network control theory in an experimentally friendly manner.

DATA AVAILABILITY STATEMENT

The dataset is available upon reasonable request to the corresponding author. Requests to access these datasets should be directed to yzhang94@uh.edu.

ETHICS STATEMENT

The studies involving human participants were reviewed and approved by University of Houston. The patients/participants provided their written informed consent to participate in this study.

AUTHOR CONTRIBUTIONS

XL conducted data analysis, interpreted results, drafted the manuscript and also helped with the data collection. FF supervised data analysis, interpreted results, drafted and revised the manuscript. RL helped with data collection, EEG and fNIRS integration analysis, and result interpretation; YZ designed the study, supervised the data analysis, interpreted the results, and revised the manuscript.

REFERENCES

Bajaj, S., Drake, D., Butler, A. J., and Dhamala, M. (2014). Oscillatory Motor Network Activity during Rest and Movement: An fNIRS Study. *Front. Syst. Neurosci.* 8, 13. doi:10.3389/fnsys.2014.00013

Betzel, R. F., Gu, S., Medaglia, J. D., Pasqualetti, F., and Bassett, D. S. (2016). Optimally Controlling the Human Connectome: The Role of Network Topology. *Sci. Rep.* 6 (1), 30770–30814. doi:10.1038/srep30770

Bonkhoff, A. K., Hope, T., Bzdok, D., Guggisberg, A. G., Hawe, R. L., Dukelow, S. P., et al. (2020). Bringing Proportional Recovery into Proportion: Bayesian Modelling of Post-stroke Motor Impairment. *Brain* 143 (7), 2189–2206. doi:10.1093/brain/awaa146

Bullmore, E., and Sporns, O. (2009). Complex Brain Networks: Graph Theoretical Analysis of Structural and Functional Systems. *Nat. Rev. Neurosci.* 10 (3), 186–198. doi:10.1038/nrn2575

Callejas, A., Lupiàñez, J., Funes, M. J., and Tudela, P. (2005). Modulations Among the Alerting, Orienting and Executive Control Networks. *Exp. Brain Res.* 167 (1), 27–37. doi:10.1007/s00221-005-2365-z

Collin, C., and Wade, D. (1990). Assessing Motor Impairment after Stroke: A Pilot Reliability Study. *J. Neurol. Neurosurg. Psychiatry* 53 (7), 576–579. doi:10.1136/jnnp.53.7.576

De Winter, J. C. (2013). Using the Student's T-Test with Extremely Small Sample Sizes. *Pract. Assess. Res. Eval.* 18 (1), 10. doi:10.7275/e4r6-dj05

Delgado Reyes, L. M., Bohache, K., Wijeakumar, S., and Spencer, J. P. (2018). Evaluating Motion Processing Algorithms for Use with Functional Near-Infrared Spectroscopy Data from Young Children. *Neurophotonics* 5 (2), 025008. doi:10.1117/1.NPh.5.2.025008

Dong, G., Lin, X., and Potenza, M. N. (2015). Decreased Functional Connectivity in an Executive Control Network is Related to Impaired Executive Function in Internet Gaming Disorder. *Prog. Neuro Psychopharmacol. Biol. Psychiatry* 57, 76–85. doi:10.1016/j.pnpbp.2014.10.012

Duncan, J. (2013). The Structure of Cognition: Attentional Episodes in Mind and Brain. *Neuron* 80 (1), 35–50. doi:10.1016/j.neuron.2013.09.015

Fang, F., Potter, T., Nguyen, T., and Zhang, Y. (2020). Dynamic Reorganization of the Cortical Functional Brain Network in Affective Processing and Cognitive Reappraisal. *Int. J. Neur. Syst.* 30 (10), 2050051. doi:10.1142/s0129065720500513

Fang, F., Gao, Y., Schulz, P. E., Selvaraj, S., and Zhang, Y. (2021). Brain Controllability Distinctiveness between Depression and Cognitive Impairment. *J. Affect. Disord.* 294, 847–856. doi:10.1016/j.jad.2021.07.106

Ferrari, M., and Quaresima, V. (2012). A Brief Review on the History of Human Functional Near-Infrared Spectroscopy (fNIRS) Development and Fields of Application. *Neuroimage* 63 (2), 921–935. doi:10.1016/j.neuroimage.2012.03.049

Fischl, B. (2012). FreeSurfer. *Neuroimage* 62(2), 774–781. doi:10.1016/j.neuroimage.2012.01.021

Fonov, V., Evans, A. C., Botteron, K., Almli, C. R., McKinstry, R. C., and Collins, D. L. (2011). Unbiased Average Age-Appropriate Atlases for Pediatric Studies. *Neuroimage* 54(1), 313–327. doi:10.1016/j.neuroimage.2010.07.033

Fuchs, M., Kastner, J., Wagner, M., Hawes, S., and Ebersole, J. S. (2002). A Standardized Boundary Element Method Volume Conductor Model. *Clin. Neurophysiol.* 113(5), 702–712. doi:10.1016/s1388-2457(02)00030-5

Genovese, C. R., Lazar, N. A., and Nichols, T. (2002). Thresholding of Statistical Maps in Functional Neuroimaging Using the False Discovery Rate. *Neuroimage* 15 (4), 870–878. doi:10.1006/nimg.2001.1037

Gladstone, D. J., Danells, C. J., and Black, S. E. (2002). The Fugl-Meyer Assessment of Motor Recovery after Stroke: A Critical Review of its Measurement Properties. *Neurorehabil. Neural Repair* 16 (3), 232–240. doi:10.1177/154596802401105171

Graziano, M. (2006). The Organization of Behavioral Repertoire in Motor Cortex. *Annu. Rev. Neurosci.* 29, 105–134. doi:10.1146/annurev.neuro.29.051605.112924

Grefkes, C., Nowak, D. A., Eickhoff, S. B., Dafotakis, M., Küst, J., Karbe, H., et al. (2008). Cortical Connectivity after Subcortical Stroke Assessed with Functional Magnetic Resonance Imaging. *Ann. Neurol.* 63 (2), 236–246. doi:10.1002/ana.21228

Grefkes, C., Eickhoff, S. B., Nowak, D. A., Dafotakis, M., and Fink, G. R. (2008). Dynamic Intra- and Interhemispheric Interactions during Unilateral and Bilateral Hand Movements Assessed with fMRI and DCM. *Neuroimage* 41 (4), 1382–1394. doi:10.1016/j.neuroimage.2008.03.048

Gu, S., Pasqualetti, F., Cieslak, M., Telesford, Q. K., Yu, A. B., Kahn, A. E., et al. (2015). Controllability of Structural Brain Networks. *Nat. Commun.* 6 (1), 8414–8510. doi:10.1038/ncomms9414

Hallez, H., Vanrumste, B., Grech, R., Muscat, J., De Clercq, W., Vergult, A., et al. (2007). Review on Solving the Forward Problem in EEG Source Analysis. *J. Neuroeng Rehabil.* 4 (1), 46–29. doi:10.1186/1743-0003-4-46

Inman, C. S., James, G. A., Hamann, S., Rajendra, J. K., Pagnoni, G., and Butler, A. J. (2012). Altered Resting-State Effective Connectivity of Fronto-Parietal Motor Control Systems on the Primary Motor Network Following Stroke. *Neuroimage* 59 (1), 227–237. doi:10.1016/j.neuroimage.2011.07.083

Jeganathan, J., Perry, A., Bassett, D. S., Roberts, G., Mitchell, P. B., and Breakspear, M. (2018). Fronto-limbic Dysconnectivity Leads to Impaired Brain Network Controllability in Young People with Bipolar Disorder and Those at High Genetic Risk. *NeuroImage Clin.* 19, 71–81. doi:10.1016/j.nicl.2018.03.032

Karrer, T. M., Kim, J. Z., Stiso, J., Kahn, A. E., Pasqualetti, F., Habel, U., et al. (2020). A Practical Guide to Methodological Considerations in the Controllability of Structural Brain Networks. *J. Neural Eng.* 17 (2), 026031. doi:10.1088/1741-2552/ab6e8b

Klein, A., and Tourville, J. (2012). 101 Labeled Brain Images and a Consistent Human Cortical Labeling Protocol. *Front. Neurosci.* 6, 171. doi:10.3389/fnins.2012.00171

Langhorne, P., Bernhardt, J., and Kwakkel, G. (2011). Stroke Rehabilitation. *Lancet* 377 (9778)), 693–1702. doi:10.1016/s0140-6736(11)60325-5

Li, R., Li, S., Roh, J., Wang, C., and Zhang, Y. (2020). Multimodal Neuroimaging Using Concurrent EEG/fNIRS for Poststroke Recovery Assessment: An Exploratory Study. *Neurorehabil. Neural Repair* 34 (12), 1099–1110. doi:10.1177/1545968320969937

Liu, N., Cui, X., Bryant, D. M., Glover, G. H., and Reiss, A. L. (2015). Inferring Deep-Brain Activity from Cortical Activity Using Functional Near-Infrared Spectroscopy. *Biomed. Opt. Express* 6 (3), 1074–1089. doi:10.1364/boe.6.001074

Ludwig, K. A., Miriani, R. M., Langhals, N. B., Joseph, M. D., Anderson, D. J., and Kipke, D. R. (2009). Using a Common Average Reference to Improve Cortical Neuron Recordings from Microelectrode Arrays. *J. neurophysiology* 101 (3), 1679–1689. doi:10.1152/jn.90989.2008

Mani, S., Mutha, P. K., Przybyla, A., Haaland, K. Y., Good, D. C., and Sainburg, R. L. (2013). Contralesional Motor Deficits after Unilateral Stroke Reflect Hemisphere-specific Control Mechanisms. *Brain* 136 (4), 1288–1303. doi:10.1093/brain/aws283

Medaglia, J. D., Pasqualetti, F., Hamilton, R. H., Thompson-Schill, S. L., and Bassett, D. S. (2017). Brain and Cognitive Reserve: Translation *via* Network Control Theory. *Neurosci. Biobehav. Rev.* 75, 53–64. doi:10.1016/j.neubiorev.2017.01.016

Molavi, B., and Dumont, G. A. (2012). Wavelet-based Motion Artifact Removal for Functional Near-Infrared Spectroscopy. *Physiol. Meas.* 33 (2), 259–270. doi:10.1088/0967-3334/33/2/259

Montgomery, D. C., Peck, E. A., and Vining, G. G. (2021). *Introduction to Linear Regression Analysis*. 6th edn. New Jersey. US: John Wiley & Sons.

Nachar, N. (2008). The Mann-Whitney U: A Test for Assessing whether Two Independent Samples Come from the Same Distribution. *Tutor Quant. Methods Psychol.* 4 (1), 13–20. doi:10.20982/tqmp.04.1.p013

Nguyen, T., Potter, T., Nguyen, T., Karmonik, C., Grossman, R., and Zhang, Y. (2016). EEG Source Imaging Guided by Spatiotemporal Specific fMRI: Toward an Understanding of Dynamic Cognitive Processes. *Neural Plast.* 2016, 1–10. doi:10.1155/2016/4182483

Nguyen, T., Potter, T., Grossman, R., and Zhang, Y. (2018). Characterization of Dynamic Changes of Current Source Localization Based on Spatiotemporal fMRI Constrained EEG Source Imaging. *J. Neural Eng.* 15 (3), 036017. doi:10.1088/1741-2552/aa9fb2

Nguyen, T., Zhou, T., Potter, T., Zou, L., and Zhang, Y. (2019). The Cortical Network of Emotion Regulation: Insights from Advanced EEG-fMRI Integration Analysis. *IEEE Trans. Med. Imaging* 38 (10), 2423–2433. doi:10.1109/tmi.2019.2900978

Peters, D. M., Fridriksson, J., Stewart, J. C., Richardson, J. D., Rorden, C., Bonilha, L., et al. (2018). Cortical Disconnection of the Ipsilesional Primary Motor Cortex is Associated with Gait Speed and Upper Extremity Motor Impairment in Chronic Left Hemispheric Stroke. *Hum. Brain Mapp.* 39 (1), 120–132. doi:10.1002/hbm.23829

Roebroeck, A., Formisano, E., and Goebel, R. (2011). The Identification of Interacting Networks in the Brain Using fMRI: Model Selection, Causality and Deconvolution. *Neuroimage* 58 (2), 296–302. doi:10.1016/j.neuroimage.2009.09.036

Satorra, A., and Bentler, P. M. (2001). A Scaled Difference Chi-Square Test Statistic for Moment Structure Analysis. *Psychometrika* 66 (4), 507–514. doi:10.1007/bf02296192

Seeley, W. W., Menon, V., Schatzberg, A. F., Keller, J., Glover, G. H., Kenna, H., et al. (2007). Dissociable Intrinsic Connectivity Networks for Salience Processing and Executive Control. *J. Neurosci.* 27 (9), 2349–2356. doi:10.1523/jneurosci.5587-06.2007

Snyder, D. B., Schmit, B. D., Hyngstrom, A. S., and Beardsley, S. A. (2021). Electroencephalography Resting-state Networks in People with Stroke. *Brain Behav.*, 2021, e02097. doi:10.1002/brb3.2097

Sporns, O. (2018). Graph Theory Methods: Applications in Brain Networks. *Dialogues Clin. Neurosci.* 20 (2), 111–121. doi:10.31887/dcns.2018.20.2/osporns

Vinck, M., Oostenveld, R., Van Wingerden, M., Battaglia, F., and Pennartz, C. M. A. (2011). An Improved Index of Phase-Synchronization for Electrophysiological Data in the Presence of Volume-Conduction, Noise and Sample-Size Bias. *Neuroimage* 55 (4), 1548–1565. doi:10.1016/j.neuroimage.2011.01.055

Vliet, R., Selles, R. W., Andrinopoulou, E. R., Nijland, R., Ribbers, G. M., Frens, M. A., et al. (2020). Predicting Upper Limb Motor Impairment Recovery after Stroke: A Mixture Model. *Ann. Neurol.* 87 (3), 383–393. doi:10.1002/ana.25679

Wiles, L., Gu, S., Pasqualetti, F., Parvesse, B., Gabrieli, D., Bassett, D. S., et al. (2017). Autaptic Connections Shift Network Excitability and Bursting. *Sci. Rep.* 7 (1), 44006–44015. doi:10.1038/srep44006

Winter, W. R., Nunez, P. L., Ding, J., and Srinivasan, R. (2007). Comparison of the Effect of Volume Conduction on EEG Coherence with the Effect of Field Spread on MEG Coherence. *Stat. Med.* 26 (21), 3946–3957. doi:10.1002/sim.2978

Zhao, Z., Wu, J., Fan, M., Yin, D., Tang, C., Gong, J., et al. (2018). Altered Intra- and Inter-network Functional Coupling of Resting-State Networks Associated with Motor Dysfunction in Stroke. *Hum. Brain. Mapp.* 39 (8), 3388–3397. doi:10.1002/hbm.24183

Conflict of Interest: The authors declare that the research was conducted in the absence of any commercial or financial relationships that could be construed as a potential conflict of interest.

Publisher's Note: All claims expressed in this article are solely those of the authors and do not necessarily represent those of their affiliated organizations, or those of the publisher, the editors and the reviewers. Any product that may be evaluated in this article, or claim that may be made by its manufacturer, is not guaranteed or endorsed by the publisher.

Copyright © 2022 Li, Fang, Li and Zhang. This is an open-access article distributed under the terms of the Creative Commons Attribution License (CC BY). The use, distribution or reproduction in other forums is permitted, provided the original author(s) and the copyright owner(s) are credited and that the original publication in this journal is cited, in accordance with accepted academic practice. No use, distribution or reproduction is permitted which does not comply with these terms.

frontiers | Frontiers in Bioengineering and Biotechnology

SYSTEMATIC REVIEW
published: 08 August 2022
doi: 10.3389/fbioe.2022.910698

A Systematic Review of Fall Risk Factors in Stroke Survivors: Towards Improved Assessment Platforms and Protocols

*Masoud Abdollahi[1], Natalie Whitton[1], Ramin Zand[2], Mary Dombovy[3], Mohamad Parnianpour[4], Kinda Khalaf[5] and Ehsan Rashedi[1]**

[1]Industrial and Systems Engineering Department, Rochester Institute of Technology, Rochester, NY, United States, [2]Department of Neurology, Geisinger Neuroscience Institute, Danville, PA, United States, [3]Department of Rehabilitation and Neurology, Unity Hospital, Rochester, NY, United States, [4]Department of Mechanical Engineering, Sharif University of Technology, Tehran, Iran, [5]Department of Biomedical Engineering, Khalifa University of Science and Technology, and Health Engineering Innovation Center, Abu Dhabi, United Arab Emirates

Background/Purpose: To prevent falling, a common incident with debilitating health consequences among stroke survivors, it is important to identify significant fall risk factors (FRFs) towards developing and implementing predictive and preventive strategies and guidelines. This review provides a systematic approach for identifying the relevant FRFs and shedding light on future directions of research.

Methods: A systematic search was conducted in 5 popular research databases. Studies investigating the FRFs in the stroke community were evaluated to identify the commonality and trend of FRFs in the relevant literature.

Results: twenty-seven relevant articles were reviewed and analyzed spanning the years 1995–2020. The results confirmed that the most common FRFs were age (21/27, i.e., considered in 21 out of 27 studies), gender (21/27), motion-related measures (19/27), motor function/impairment (17/27), balance-related measures (16/27), and cognitive impairment (11/27). Among these factors, motion-related measures had the highest rate of significance (i.e., 84% or 16/19). Due to the high commonality of balance/motion-related measures, we further analyzed these factors. We identified a trend reflecting that subjective tools are increasingly being replaced by simple objective measures (e.g., 10-m walk), and most recently by quantitative measures based on detailed motion analysis.

Conclusion: There remains a gap for a standardized systematic approach for selecting relevant FRFs in stroke fall risk literature. This study provides an evidence-based methodology to identify the relevant risk factors, as well as their commonalities and trends. Three significant areas for future research on post stroke fall risk assessment have been identified: 1) further exploration the efficacy of quantitative detailed motion analysis; 2) implementation of inertial measurement units as a cost-effective and accessible tool in

OPEN ACCESS

Edited by:
Yih-Kuen Jan,
University of Illinois at Urbana-Champaign, United States

Reviewed by:
Rossella Rizzo,
University of Palermo, Italy
Tatiana Dias de Carvalho,
National University of La Matanza, Argentina

***Correspondence:**
Ehsan Rashedi
exreie@rit.edu

Specialty section:
This article was submitted to Biomechanics, a section of the journal Frontiers in Bioengineering and Biotechnology

Received: 01 April 2022
Accepted: 22 June 2022
Published: 08 August 2022

Citation:
Abdollahi M, Whitton N, Zand R, Dombovy M, Parnianpour M, Khalaf K and Rashedi E (2022) A Systematic Review of Fall Risk Factors in Stroke Survivors: Towards Improved Assessment Platforms and Protocols. Front. Bioeng. Biotechnol. 10:910698. doi: 10.3389/fbioe.2022.910698

Abbreviations: 10MWT, 10 Meter Walk Test; ADL, Activity of Daily Living; BBS, Berg Balance Scale; COP, Center of Pressure; FES, Fall Efficacy Scale; FRF, Fall Risk Factor; FSST, Four Square Step Test; IMU, Inertial Measurement Unit; OR, Odds Ratio; RMS, Root Mean Square; TUG, Timed Up and Go.

clinics and beyond; and 3) investigation of the capability of cognitive-motor dual-task paradigms and their association with FRFs.

Keywords: stroke, fall risk factors, fall risk assessment, cost-benefit analysis, dual-task paradigm, performance assesment, detailed motion analysis

1 INTRODUCTION

Stroke is currently considered as the second leading cause of mortality for individuals above the age of 60 years, and the fifth leading cause of death in individuals aged 15–59 years old, worldwide (Thrift et al., 2017). According to the World Health Organization (WHO), every year, 15 million people are diagnosed with stroke, of which, approximately 6 million die and another 5 million are left with permanent disabilities (CDC, 2019) (National library of medicine, 2022) (Thomas et al., 2000). In the United States, more than 795,000 people suffer a stroke every year, leading to an annual financial burden of nearly $46 billion, including the cost of health care services, medications, and missed days of work. Falling is a very common complication consequent to stroke, where both physical (weakness, paralysis, sensory disturbances, and impaired postural control) and mental impairments (mental fatigue, depression and impaired cognitive function) associated with stroke can contribute to regular falls (Larén et al., 2018). Moreover, most stroke patients, especially those who have suffered ischemic strokes, are prescribed antiplatelets or anticoagulants for secondary stroke prevention, which could increase their propensity for post-trauma and bleeding upon falling. Indeed, falls are seven times more prevalent among this population in comparison to healthy individuals and are often more consequential (Langhorne et al., 2000; Weerdesteyn et al., 2008; Melillo et al., 2015; Wei et al., 2017). Research studies have indicated that approximately half of stroke patients experience at least one fall in the first year post-stroke and that falling leads to further morbidity and mortality along with a dramatic increase in the cost of care (Andersson et al., 2006; Mackintosh et al., 2006; Ashburn et al., 2008; Kerse et al., 2008; Baetens et al., 2011; Simpson et al., 2011; Blennerhassett et al., 2012; Tilson et al., 2012; Yoshimoto et al., 2016). Moreover, falling often causes hip fractures and various other motion restrictions, which poses limitations on performing activities of daily living (ADLs) (Pouwels et al., 2009). This, in turn, triggers a viscous cycle in terms of the effect of immobility on the musculoskeletal system, leading to further compromise in musculoskeletal health and mobility of stroke patients and hence an increased risk of falls. It is, therefore, imperative to assess the risk of falling among stroke survivors during their path to partial or full recovery leverage the information towards more effective predictive and rehabilitation strategies.

In the last two decades, several studies have targeted fall risk assessment among stroke survivors (Ashburn et al., 2008; Baetens et al., 2011; Allin et al., 2016; An et al., 2017). More specifically, a growing body of literature has been exploring the association between the different fall risk factors (FRFs) and the frequency of falls. Risk factors are typically categorized into different groups, including demographics, medications, physical capability, cognitive impairments, among others. For example, the outcome of timed up and go (TUG) testing, during which the participant is asked to stand up from a chair, walk for three meters, return, and again sit on the same chair, can be considered as a FRF (Podsiadlo and Richardson, 1991; Jalayondeja et al., 2014; Pinto et al., 2016). Overall, most studies on fall risk assessment of stroke survivors follow a common approach, whereby several risk factors are identified to generate an initial pool of factors to be analyzed. Implementing statistical analysis tools, these factors are then compared between stroke patients who have fallen and those who have not. The published articles in this area indicate that there are more than 100 FRFs which can be included in the initial pool. However, due to the large number and variety of risk factors, it is not feasible to consider all of them in one study, which makes it challenging to select the appropriate initial list of FRFs.

To the best of our knowledge, only three review papers on fall risk assessment within the stroke community were published prior to this study. Walsh et al. (2016) conducted a systematic review on fall risk prediction models for stroke patients. Their results discussed several models to assess fall risk, recommending that future studies need to focus on the validation and improvement of current available models. In another study, Tan and Tan. (2016). used a narrative review to explore the epidemiology of falls within the stroke community. They categorized the risk factors for the elderly stroke population into several groups, including motor deficits, cognitive function, medication, and psychological risk factors, concluding with suggestions for fall prevention and management strategies for stroke survivors. Xu et al. (2018) conducted a meta-analysis of common FRFs to identify the most significant ones leading to falls. Their findings indicated that impaired mobility, reduced balance, use of sedative/psychotropic medications, disability in self-care, depression, cognitive impairment, and history of prior falls all had strong associations with falls among stroke survivors. One of the main limitations of this meta-analysis, on the other hand, was the insufficient number of observational studies meeting the requirement to be involved in the analysis of each risk factor. Their findings indicated that impaired mobility and reduced balance, with odds ratios (OR) of 4.36 and 3.87, respectively, proved to be the most impactful factors for falls among stroke survivors (Xu et al., 2018). It must be noted, however, that the reported OR data were calculated from only three studies, since the authors excluded a significant portion of studies due to the high heterogeneity, as well as lack of providing OR data in their results. The characteristics of this study, therefore, cast some uncertainty as to the conclusions regarding the most significant fall risk factors despite shedding light on this relevant issue.

Hence, although numerous studies were conducted to identify FRFs for stroke survivors, further work incorporating less heterogeneity and proper outcome assessment (e.g., involving OR) is still needed to validate the association of common FRFs with fall occurrence for the stroke community.

To bridge the aforementioned knowledge gap in literature, researchers need to establish a standard reference point for identifying the appropriate FRFs to generate an initial pool of risk factors. To this end, this review will provide a commonality analysis on the FRFs and their significance ratio among the articles considering each factor. Furthermore, the articles will be explored to categorize their considered FRFs into subjective and objective classes. Finally, the articles will be reviewed to identify the trend of implementing motion analysis to identify the risk of fall in stroke community. Briefly, the results of this study will help: 1) to provide evidence-based data by which researchers can determine which FRFs to include in the initial pool of factors; 2) to explore changes over time regarding the most salient FRFs as described by researchers; and 3) to identify the potential opportunities such as conducting detailed motion analysis employing IMU sensors while performing cognitive-motor dual-task to improve the quality of fall risk assessment among stroke survivors. The outcome of this study may facilitate the development of a more efficient and accurate approach/model to conduct future fall risk assessment studies.

2 METHODS

2.1 Search Strategy

In order to conduct the review, the guidelines for Preferred Reporting Items for Systematic review and Meta-analyses (PRISMA) were implemented (Page et al., 2021). A systematic review approach was developed to identify the relevant articles for the review. We identified the potentially eligible studies by systematically searching the databases: MEDLINE, EMBASE, Web of Science, and PubMed. The search queries were primarily conducted from 1995 until 2020, without restriction on study design, document type, or language. Specifically, the title, abstract, and keywords in potentially relevant articles were searched for specific words: ("stroke" OR "cerebrovascular accident" OR "cerebrovascular apoplexy" OR "cerebrovascular disease" OR "cerebrovascular stroke") AND ("falls" OR "falling") AND ("prospective" OR "follow up" OR "cohort" OR "case-control" OR "longitudinal study" OR "cohort study" OR "observational study" OR "case-control study"). The entry terms for each keyword were extracted implementing the Medical Subject Heading (MeSH) tool. The same search terms and Boolean combinations were used to identify the relevant articles while using the advance search in each database. We augmented the search results by manually forward and backward (in Google Scholar) citation tracking. Additional articles were added from the authors' archives or through cross-referencing.

2.2 Study Selection

Studies addressing the prediction of fall risk and/or those identifying significant risk factors among stroke survivors were recorded. Since the focus of this review was to evaluate the factors involved in the FRFs among stroke patients, any prospective study describing a follow-up period of more than one day was included. Two authors independently searched the literature and merged their results, and then the final selected studies were carefully reviewed to ensure that all the articles met the inclusion criteria for the review. The inclusion criteria consisted of: 1) a prospective study on stroke survivors; 2) assessing the risk of fall; 3) published in English. Studies were excluded if participants had other neurological diseases, such as Alzheimer, Parkinson's disease, multiple sclerosis, and spinal cord injury.

2.3 Data Extraction

The results of the comprehensive database search were screened for relevance, and the selected papers were analyzed. The data from each study were extracted using a format developed by the authors. The form included the following information from each article: Authors, Publication date (year), Location of the study, Sample size, Setting, Number of Parameters, Labeling of the Participants, Significant Factors, Non-Significant Factors, Univariate/Bivariate analysis: Output Type, Multivariate Analysis (Model): Method, Age of the participants, and Notes.

2.4 Risk of Bias

Most fall risk assessment studies could be categorized as cohort studies which fall under the umbrella of observational studies. Considering the various available tools to assess the risk of bias in observational studies (Deeks et al., 2003), the Cochrane Tool to Assess Risk of Bias in Cohort Studies was selected (Higgins, 2008). The tool includes eight questions with 4 choices each. One of the questions was not applicable in fall risk assessment studies and consequently removed from the analysis. The remaining questions were related to the selection of the cohorts, comparability, and assessment of outcome. The seven questions were answered for each of the 27 articles by two authors (i.e., MA and ER) independently. The cases of discrepancy in the results in terms of risk of bias assessment for each paper were addressed in a meeting between the two authors. Since there were seven questions with four possible answers reflecting the quality of the study in various aspects (ranging from 0 for high risk of bias to 3 for low risk of bias), the overall score for each study was between 0 and 21. Studies with scores of <14, 14 to 17, and >17 were classified as low, acceptable, and good quality, respectively.

2.5 Fall Risk Factor Commonality and Significance Analysis

As noted earlier, it was not feasible to conduct a thorough meta-analysis on the various FRFs due to the limited number of studies for each FRF required for such an analysis. This impediment stems from discrepancies in the heterogeneity of factors, as well as discrepancies in the format of outcomes—principally involving a variety of preferred statistical measures. To address these issues, we have developed a list of significant risk factors towards affording researchers better insight into the commonality and significance of the factors. Using this risk factor-specific

approach, we have reported the number of studies considering each factor, as well as the number of studies in which that particular factor was determined to be significant. In order to simplify the process of comparing factors, a scale was created for each factor to calculate the ratio of the number of studies which identified a given FRF to be a significant to the number of the studies considering that factor.

$$Significance\ Ratio\,(SR) = \frac{\text{Number of the studies finding the FRF to be significant in fall risk}}{\text{Number of the studies considering the FRF}}$$

Note that if at least one of the items in a particular category had a significant impact on the fall risk, the category was classified as a significant factor. As an example, Mansfield et al. conducted a balance test requiring participants to stand as still as possible on a force plate. They subsequently calculated the mediolateral root mean square (RMS) of the center of pressure (COP), identifying it as a significant risk factor for falls, in contrast, to the anteroposterior RMS of COP which was determined to be non-significant. Therefore, since there was a factor from the category of balance-related measures among the significant FRFs, we considered that category (i.e., balance-related measures) as significant in that study.

2.6 Analysis of the Balance and Mobility-Related Factors in Fall Risk

This study also analyzed changes over time in the methods assessing the balance and mobility of stroke patients and how that information factored into the fall risk assessment process. Accordingly, any articles considering these factors were further analyzed to determine all implemented approaches. Initially, the identified balance and mobility-related factors from literature were categorized as either subjective or objective. We have also classified objective balance and mobility-related factors according to the equipment used for assessment, which provides researchers with a more accurate depiction of the level of motion analysis achieved in the various studies. For example, TUG testing typically measures the time for accomplishing a specific physical task, notably standing from/sitting on a chair, walking, and turning. Since the only equipment measuring the output of this test (i.e., time) is a timer, we can conclude that it does not pay sufficient attention to more detailed motion analysis parameters such as gait characteristics. However, a similarly designed study might utilize a force plate or inertial measurement unit (IMU) sensors which can deliver more detailed gait-analysis data, potentially improving the accuracy of identifying the risk for falls among stroke victims.

3 RESULTS

3.1 Study Identification

A total of 10,746 articles were initially identified through the process of searching the databases and relevant repositories as described above. Due to duplication and not meeting the inclusion criteria, a portion of these articles were removed, resulting in a total of 27 articles considered relevant (**Figure 1**).

3.2 Study Characteristics

The characteristics of interest included publication year, location, sample size, setting, and details of the patient labeling, as shown in **Table 1**.

Assessment of the risk of bias indicated that all the articles in the review had at least acceptable quality based on formula described earlier. The detailed results of this analysis are shown in **Table 2**.

The frequency for the 14 most common FRFs assessed in the articles is shown in **Table 3**. The FRFs were classified into six categories: sociodemographic risk factors, sensorimotor risk factors, cognitive risk factors, psychosocial risk factors, medical risk factors, and balance and mobility risk factors.

Table 4 provides the extracted data from articles that considered stability and motion-based factors, which were then categorized as either subjective or objective. Moreover, the objective factors were subsequently classified into two groups: 1) studies without force/motion sensors; 2) studies with force/motion sensors (i.e., involving detailed motion analysis).

4 DISCUSSION

To the best of our knowledge, up to date, there is no comprehensive literature review on fall risk assessment among stroke survivors. The most recent review presented a relevant meta-analysis on the various FRFs impacting stroke population (Xu et al., 2018), but only included a handful of studies which met the data-analysis requirements. There is a need, therefore, for identifying FRFs and understanding associated commonalities and trends in recent fall risk assessment articles to develop effective interventions. Towards this we reviewed a total of 27 articles spanning almost 3 decades from multiple countries to identify the most frequently cited FRFs and the number of studies categorizing them as significant risk factors. The second objective of this review was to explore changes in how different researchers consider these FRFs and propose specific ones which could potentially provide better outcomes. Such analysis could determine how shifting to a new level of FRF-based research, in conjunction with detailed motion analysis, could assist in developing more accurate fall risk prediction and assessment models.

4.1 Common FRFs and Significance Ratios

According to the commonality table (**Table 3**), the most common FRFs, as described in literature, included age, gender, motion-related measures, balance-related measures, motor function/impairment, and cognitive impairment. The significance ratio for age, cognitive impairment, and gender were 38%, 36%, and 24%, respectively, which demonstrates the lack of consensus among studies regarding the impact of these factors on fall risk assessment. By contrast, the significance ratio for motion-related measures, balance-related measures, and motor function/impairment were 84%, 81%, and 65%, respectively. These percentages imply a consensus that these factors have a significant impact on fall risk among stroke survivors. The

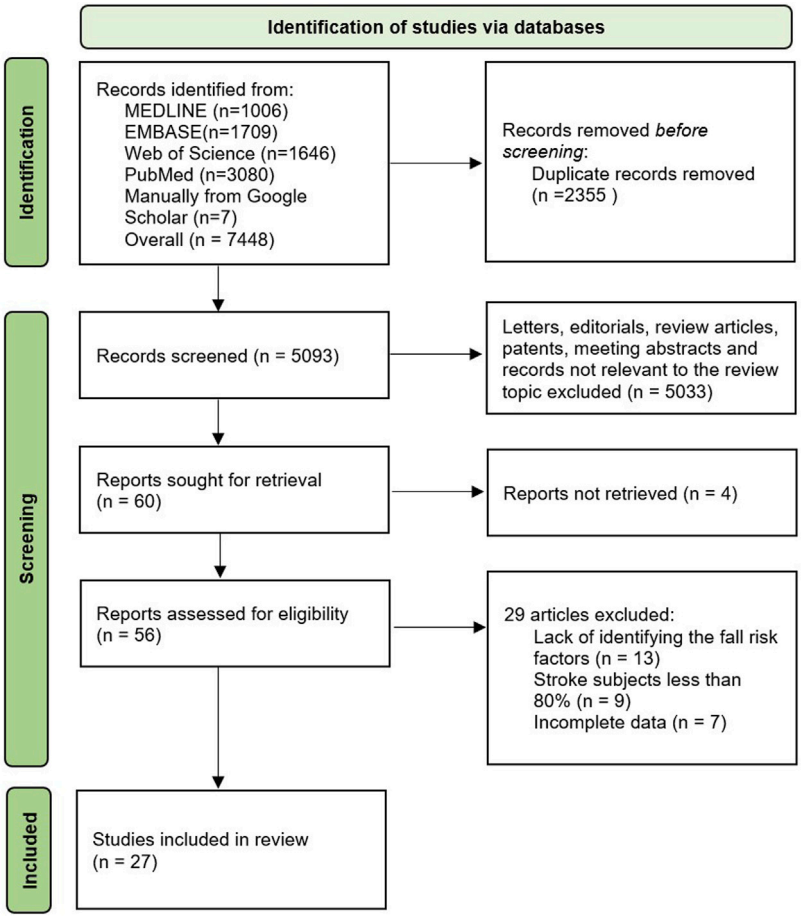

FIGURE 1 | Identification of the eligible studies to be included in the review.

large significance ratio for motion-based measures is compatible with earlier findings (Xu et al., 2018).

Among the less common FRFs, such as history of falls, depression, visual impairment, and fall efficacy scale (FES), FES presented the highest significance ratio. Representing the level of fear of falling among stroke survivor, FES had a significance ratio of 75%, which is the third largest after motion- and balance-related measures with significance ratios of 84% and 81%, respectively. It is noteworthy that visual impairment with a 43% significance ratio was among the important FRFs, which also confirms the importance of factors associated with balance control. In fact, vison, along with proprioception and balance-control mechanisms in the inner ear, are the primary systems for maintaining human balance. Consequently, since visual impairment could affect balance, a stroke victim's vision represents a potentially important factor in fall risk assessment. Moreover, an inclusive assessment of balance measures should represent the combined effects of vision, as well as other sensory systems and proprioception in fall risk. Hence, it is highly recommended that both balance and FES should be considered in the initial pool of FRFs in future studies. Finally, the FRFs with the least significance ratios were urinary incontinence/medications, use of sedative/psychotropic medications, duration of stroke, and stroke type. It is worthy to note, that among the eight articles which considered stroke type, none identified it as a significant fall risk factor (**Table 1**).

As mentioned, the most common significant factors among the pool of reviewed articles were balance and motion-related measures, thus confirming the critical importance of these measures in determining the risk for falls among stroke victims. The list of measures in the various reviewed articles revealed that numerous subjective and objective scales were used to evaluate balance and motion in stroke survivors (**Table 4**). For example, subjective tools such as Katz ADL, Fugl-Meyer, and the Barthel index were routinely implemented in the assessed studies (Nyberg and Gustafson, 1997; Olsson et al., 2005; Jalayondeja et al., 2014). In general, these approaches help to determine self-reported physical status of patients by asking them to report about the quality of their daily physical activities, or by subjectively evaluating their physical capabilities by a clinician using observational gait and balance assessment measures. By contrast, more objective measures such as 10 MWT, 6 MWT, TUG, and FSST must be administered by someone who is skilled in their use (Persson et al., 2011; Simpson et al., 2011;

TABLE 1 | The characteristics of the reviewed articles.

Article	Location	Sample size	Setting	Follow-up details
Nyberg and Gustafson, (1997)	Sweden	135	Hospital stay/2–4 weeks after the stroke/after acute phase/stroke rehabilitation unit	8 weeks
Yates et al. (2002)	United States	280	Data collected in 3–14 days of stroke onset.	1, 3, and 6 months
Lamb et al. (2003)	United States	94	At home	12 months
Olsson et al. (2005)	Sweden	158	Hospital stay/2–4 weeks after the stroke/after acute phase/stroke rehabilitation unit	8 weeks
Mackintosh et al. (2006)	Australia	55	Community	6 months
Wada et al. (2007)	Japan	101	Community	12 months
Ashburn et al. (2008)	United Kingdom	115	Community	12 months
Kerse et al. (2008)	New Zealand	1,104	Community	6 months
Divani et al. (2009)	United States	1,174	Community	24 months
Maeda et al. (2009)	Japan	72	Admitted to rehabilitation center	Variant
Persson et al. (2011)	Norway	96	Rehabilitation hospital and community	12 months
Simpson et al. (2011)	Canada	80	Community	13 months
Nyström and Hellström, (2013)	Sweden	68	Acute stroke unit/newly diagnosed with stroke	6 weeks
Alemdaroğlu et al. (2012)	Turkey	66	Rehabilitation hospital, then home	6 months
Blennerhassett et al. (2012)	Australia	30	Community	6–36 months
Jalayondeja et al. (2014)	Thailand	97	Stroke patients enrolled within 1 month of their stroke/outpatients/fall at home or outside	6 months
Breisinger et al. (2014)	United States	419	Admitted to rehabilitation unit	Variant
Callaly et al. (2015)	Ireland	522	Community	24 months
Mansfield et al. (2015)	Canada	95	Rehabilitation hospital and community	6 months
Goljar et al. (2016)	Slovenia	232	Admitted for the first time to the stroke rehabilitation ward/stroke patients during their first inpatient rehabilitation	12 months
Pinto et al. (2016)	Brazil	131	Outpatients in stroke clinic	2 years
Taylor-Piliae et al. (2016)	United States	10	Mix of outpatients and post-stroke at least 3 months after stroke	2 days
Yoshimoto et al. (2016)	Japan	65	Patients discharged from a rehabilitation ward	12 months
Wei et al. (2017)	Taiwan	112	Hospital or rehabilitation ward and then community	6 months
Lee and Jung, (2017)	South Korea	71	Community	12 months
Foster et al. (2018)	United Kingdom	7,267	Immediate data from hospitalized patients	10 years
Persson et al. (2018)	Sweden	504	Stroke unit at hospital	4 days

Blennerhassett et al., 2012). These tests usually measure the time needed to accomplish a physical task, such as walking for 10 meters (10 MWT).

It is expected that reviewing the utilization of different factors reported in earlier studies could lead to beneficial information in the fall risk assessment and hence inspire more effective management strategies of stroke survivors. For example, exploring the evolution of balance and motion-based tools confirmed that earlier studies focused more on the implementation of subjective versus objective tools. Specifically, articles dating from 1997 to 2014 (12 out 19 articles) used subjective tools to assess the balance and motion of stroke survivors (**Table 4**). Moreover, in some of these studies, subjective measures were combined with standard objective tests such as TUG and 10 MWT, which are designed to measure a single parameter, such as speed or time while the subject performs a specific task. As described earlier, TUG testing requires the patient to stand up from a normal chair, walk for 3 m, return, and sit on the chair again; the output of this test is the time required to complete the task. Clearly, this type of assessment does not provide detailed motion parameters, such as those obtained from instrumented force plates or motion sensors. In 2015, Mansfield et al. was the first research team to conduct a study that considered a detailed analysis of motion during quiet standing (i.e., balance testing) and walking (i.e., gait testing) (Mansfield et al., 2015). Later, Taylor-Pilliae et al. investigated the capability of a single motion sensor in motion-monitoring of stroke survivors over the course of 48 h during usual daily activities (Taylor-Piliae et al., 2016). It should be noted that this study was more of a feasibility analysis designed to assess the capacity of the system in identifying fall risk indicators during posture transition and gait; thus, subjective measures were not considered. To the best of our knowledge, the study by Lee and Jung. (2017) was the only one to integrate both subjective tools along with the balance related-measures from detailed motion analysis The results of this study revealed that postural sway velocity with eyes-closed on a soft surface outperformed other subjective and objective measures such as BBS, Fugle-Meyer Assessment, and weight-bearing asymmetry in fall prediction for post-stroke individuals. Finally, Wei et al. (2017) conducted a study to explore the correlation between gait and balance parameters with respect to falls among stroke survivors.

Overall, among the reviewed articles, there were only four studies involving detailed motion analysis designed to identify the effect of motion in fall risk assessment (Mansfield et al., 2015; Taylor-Piliae et al., 2016; Lee and Jung, 2017; Wei et al., 2017).

TABLE 2 | Risk of bias assessment using Cochrane Tool to Assess Risk of Bias in Cohort Studies.

Article	1 Was selection of exposed and non-exposed cohorts drawn from the same population?	2 Can we be confident in the assessment of exposure?	3 Did the study match exposed and unexposed for all variables that are associated with the outcome of interest or did the statistical analysis adjust for these prognostic variables?	4 Can we be confident in the assessment of the presence or absence of prognostic factors?	5 Can we be confident in the assessment of outcome?	6 Was the follow up of cohorts adequate?	7 Were co-interventions similar between groups?	Sum	Quality
Nyberg and Gustafson, (1997)	3	2	3	2	3	2	2	17	Good
Yates et al. (2002)	3	2	2	2	3	3	2	17	Good
Lamb et al. (2003)	3	2	3	2	1	3	2	16	Acceptable
Olsson et al. (2005)	3	2	3	2	3	2	2	17	Good
Mackintosh et al. (2006)	3	2	3	2	2	3	2	17	Good
Wada et al. (2007)	3	2	3	2	3	3	2	18	Good
Ashburn et al. (2008)	3	2	3	2	3	3	2	18	Good
Kerse et al. (2008)	3	2	3	2	3	3	2	18	Good
Divani et al. (2009)	3	2	3	2	3	3	2	18	Good
Maeda et al. (2009)	3	2	2	2	2	2	2	15	Acceptable
Persson et al. (2011)	3	2	3	2	3	3	2	18	Good
Simpson et al. (2011)	3	2	3	2	3	3	2	18	Good
Anna and Karin (2012)	3	2	2	2	2	2	2	15	Acceptable
Alemdaroglu et al. (2012)	3	2	3	2	3	3	2	18	Good
Blennerhassett et al. (2012)	3	2	2	2	3	3	2	17	Good
Jalayondeja et al. (2014)	3	2	3	2	2	3	2	17	Good
Breisinger et al. (2014)	3	2	3	3	3	2	2	18	Good
Callaly et al. (2015)	3	2	3	2	2	3	2	17	Good
Mansfield et al. (2015)	3	2	3	3	2	3	2	18	Good
Goljar et al. (2016)	3	2	3	2	1	3	2	16	Acceptable
Pinto et al. (2016)	3	2	2	2	3	3	2	17	Good
Taylor-Pilliae et al. (2016)	1	3	2	3	2	1	2	14	Acceptable
Yoshimoto et al. (2016)	3	2	2	2	3	3	2	17	Good
Wei et al. (2017)	3	2	3	3	2	3	2	18	Good
Lee and Jung, (2017)	3	2	3	3	2	3	2	18	Good
Foster et al. (2018)	3	2	3	3	2	2	2	17	Good
Persson et al. (2018)	3	3	3	2	2	2	2	17	Good

These studies were among the seven most-recent reviewed articles, which implies a trend towards clarifying the role of motion in fall risk identification within the stroke community. These four studies are further explored in **Section 4.2** to investigate the potential for improving the accuracy of fall risk assessment models *via* the implementation of a thorough motion analysis protocol of stroke survivors.

4.2 Opportunities to Improve Fall Risk Assessment

Considering the gaps in the existing literature may shed some light on the future directions for this important area of study. The initial pool of FRFs in future studies could be identified according to **Table 3**, coupled with other relevant reviews on the FRFs impacting the stroke community. According to the results of this

TABLE 3 | Commonalities among the 14 most significant FRFs in the articles.

Risk factors	Number of studies considering the factor	Number of studies in which the factor was significant	Significance ratio (%)	References
Age	21	8	38	Nyberg and Gustafson, (1997); Yates et al. (2002); Mackintosh et al. (2006); Wada et al. (2007); Ashburn et al. (2008); Kerse et al. (2008); Divani et al. (2009); Maeda et al. (2009); Persson et al. (2011); Simpson et al. (2011); Alemdaroğlu et al. (2012); Breisinger et al. (2014); Jalayondeja et al. (2014); Callaly et al. (2015); Goljar et al. (2016); Pinto et al. (2016); Yoshimoto et al. (2016); Lee and Jung, (2017); Wei et al. (2017); Foster et al. (2018); Persson et al. (2018)
Gender (female)	21	5	24	Nyberg and Gustafson, (1997); Yates et al. (2002); Olsson et al. (2005); Mackintosh et al. (2006); Wada et al. (2007); Ashburn et al. (2008); Kerse et al. (2008); Divani et al. (2009); Maeda et al. (2009); Persson et al. (2011); Simpson et al. (2011); Breisinger et al. (2014); Jalayondeja et al. (2014); Callaly et al. (2015); Goljar et al. (2016); Pinto et al. (2016); Yoshimoto et al. (2016); Lee and Jung, (2017); Wei et al. (2017); Foster et al. (2018); Persson et al. (2018)
History of fall	9	4	44	Nyberg and Gustafson, (1997); Mackintosh et al. (2006); Ashburn et al. (2008); Kerse et al. (2008); Divani et al. (2009); Alemdaroğlu et al. (2012); Callaly et al. (2015); Pinto et al. (2016); Foster et al. (2018)
Motor function/impairment (lower Extremities)	17	11	65	Nyberg and Gustafson, (1997); Yates et al. (2002); Lamb et al. (2003); Olsson et al. (2005); Wada et al. (2007); Ashburn et al. (2008); Divani et al. (2009); Maeda et al. (2009); Persson et al. (2011); Alemdaroğlu et al. (2012); Nyström and Hellström, (2013); Jalayondeja et al. (2014); Callaly et al. (2015); Goljar et al. (2016); Pinto et al. (2016); Lee and Jung, (2017); Wei et al. (2017)
Cognitive impairment	11	4	36	Nyberg and Gustafson, (1997); Lamb et al. (2003); Wada et al. (2007); Kerse et al. (2008); Maeda et al. (2009); Simpson et al. (2011); Alemdaroğlu et al. (2012); Jalayondeja et al. (2014); Goljar et al. (2016); Wei et al. (2017); Persson et al. (2018)
Depression	8	4	50	Nyberg and Gustafson, (1997); Lamb et al. (2003); Olsson et al. (2005); Mackintosh et al. (2006); Kerse et al. (2008); Alemdaroğlu et al. (2012); Callaly et al. (2015); Wei et al. (2017)
fall Efficacy Scale (FES)	4	3	75	Mackintosh et al. (2006); Blennerhassett et al. (2012); Wei et al. (2017); Persson et al. (2018)
Visual impairment	7	3	43	Nyberg and Gustafson, (1997); Yates et al. (2002); Lamb et al. (2003); Olsson et al. (2005); Mackintosh et al. (2006); Divani et al. (2009); Alemdaroğlu et al. (2012)
Duration of stroke	8	3	38	Lamb et al. (2003); Wada et al. (2007); Ashburn et al. (2008); Divani et al. (2009); Maeda et al. (2009); Alemdaroğlu et al. (2012); Goljar et al. (2016); Pinto et al. (2016)
Stroke type	8	0	0	Yates et al. (2002); Wada et al. (2007); Kerse et al. (2008); Maeda et al. (2009); Breisinger et al. (2014); Jalayondeja et al. (2014); Goljar et al. (2016); Wei et al. (2017)
Urinary incontinence/ medications	8	2	25	Nyberg and Gustafson, (1997); Lamb et al. (2003); Olsson et al. (2005); Divani et al. (2009); Persson et al. (2011); Alemdaroğlu et al. (2012); Callaly et al. (2015); Pinto et al. (2016)
Use of sedative/psychotropic medications	4	1	25	Nyberg and Gustafson, (1997); Olsson et al. (2005); Wada et al. (2007); Alemdaroğlu et al. (2012)
Balance-related measures	16	13	81	Nyberg and Gustafson, (1997); Lamb et al. (2003); Olsson et al. (2005); Mackintosh et al. (2006); Ashburn et al. (2008); Maeda et al. (2009); Persson et al. (2011); Simpson et al. (2011); Alemdaroğlu et al. (2012); Blennerhassett et al. (2012); Jalayondeja et al. (2014); Mansfield et al. (2015); Yoshimoto et al. (2016); Lee and Jung, (2017); Wei et al. (2017); Persson et al. (2018)
Motion-related measures	19	16	84	Nyberg and Gustafson, (1997); Lamb et al. (2003); Olsson et al. (2005); Mackintosh et al. (2006); Ashburn et al. (2008); Kerse et al. (2008); Maeda et al. (2009); Persson et al. (2011); Simpson et al. (2011); Alemdaroğlu et al. (2012); Blennerhassett et al. (2012); Jalayondeja et al. (2014); Mansfield et al. (2015); Pinto et al. (2016); Taylor-Piliae et al. (2016); Yoshimoto et al. (2016); Lee and Jung, (2017); Wei et al. (2017); Persson et al. (2018)

TABLE 4 | The stability and mobility-related risk factors in the articles.

Article	Stability & mobility		
	Subjective	Objective	
		Without force/motion sensors	With force/motion sensors (detailed motion analysis)
Nyberg and Gustafson, (1997)	Katz ADL (activities of daily living), Fugl-meyer		
Lamb et al. (2003)	Balance problems and ADL difficulties while performing various tasks such as walking, dressing, and toileting		
Olsson et al. (2005)	Katz ADL, Fugl-meyer		
Mackintosh et al. (2006)	BBS score	Fast gait speed and step test score	
Ashburn et al. (2008)	BBS score, nottingham extended ADL, Rivermead upper limb, rivermead total score, rivermead leg and trunk,rivermead gross function	Mean functional reach	
Kerse et al. (2008)	Barthel index, FAI score (activity)		
Maeda et al. (2009)	BBS score		
Persson et al. (2011)	BBS score, SwePASS	10 MWT, TUG	
Simpson et al. (2011)	BBS score, ABC: Activity-Specific Balance Confidence Scale	TUG, 6 MWT	
Alemdaroğlu et al. (2012)	Fugl-Meyer		
Blennerhassett et al. (2012)	Environmental analysis of mobility questionnaire (EAMQ)	6 MWT, Four Square Step Test (FSST), Step Test (ST)	
Jalayondeja et al. (2014)	BBS score, Barthel Index	Timed up & Go (s), 10-m walk test (m/s): preferred speed & maximum speed, 2-min walk test	
Mansfield et al. (2015)			Detailed analysis of COP and gait
Pinto et al. (2016)	Quality of life (EQ-5D)	Timed up and Go quartile	
Taylor-Piliae et al. (2016)		postural transition (PT) duration (in seconds), Gait speed (meters per second)	Aborted PT attempts (number per day), Steps (number), Duration of gait (% of total activity)
Yoshimoto et al. (2016)	Barthel Index	10-m walking speed (m/s), One-leg standing time of the affected side (s), One-leg standing time of the unaffected side (s)	
Wei et al. (2017)			Gait and balanced detailed parameters
Lee and Jung, (2017)	Korean modified barthel index, fugl-meyer assessment, BBS, functional ambulation category		Postural sway velocity: eye open/closed firm/soft surface
Persson et al. (2018)	SwePASS, Self-perceived impaired postural control (section 13 BBS), Self-perceived previous physical activity level was assessed using the Saltin-Grimby Physical Activity Scale		

review and (Xu et al., 2018), balance and motion-related measures represent the most common and significant fall risk factors. These measures can be categorized into three classes: 1) subjective, 2) objective without force/motion sensors, and 3) objective with force/motion sensors (detailed motion analysis). Most of the reviewed studies implemented subjective tools for assessing the balance and motion of participants. However, as explained earlier, researchers in this area, have recently started to pay more attention to objective assessment of balance and motion analysis, especially with the rapidly emerging smart wearable tools and technologies, which promise a paradigm shift in gait and balance quantification of various movement pathologies including stroke (Mohan et al., 2021). With respect to objective categories, it remains to be determined which class (i.e., with or without force/motion sensors) could lead to more accurate fall risk assessment among stroke survivors. Hence, conducting fall risk assessment studies which includes measures from all three classes would be of great assistance in guiding researchers and clinicians in determining the most appropriate platform for assessing fall risk.

To augment the numerous available tests for assessing balance and motion in stroke survivors, the effect of the data type (i.e., subjective or objective) of a given system for capturing balance/motion data needs to be explored. **Table 5** lists studies which incorporated a detailed balance and motion analysis and the systems/sensors which they utilized. The results indicate that IMUs, force plates, and pressure mats were typically implemented to investigate balance and gait. Force plates were mostly intended to calculate the location of the center of pressure (COP), as well as to determine balance-related parameters, such as the range of trajectory of the COP in different directions during quiet standing. Due to the fact that force plates typically limit data collection to a laboratory environment, utilizing wearable IMU sensors for motion and balance analysis is preferred since these

TABLE 5 | The articles conducted detailed balance and motion analysis and their implemented sensors.

The study	The analysis	Implemented sensors for data collection
Mansfield et al. (2015)	Detailed analysis of center of pressure and gait	Force plate & Pressure mat
Taylor-Piliae et al. (2016)	Postural transition (PT) duration (in seconds), gait speed (meters per second), aborted PT attempts (number per day), steps (number), duration of gait (% of total activity)	IMU sensor on chest
Wei et al. (2017)	Detailed analysis of center of pressure and gait	IMU sensor (location not clarified) & load sensors in the shoes
Lee and Jung, (2017)	Detailed analysis of center of pressure	Force plate

sensors can be implemented outside a controlled environment; indeed, balance assessment using IMU sensors is a well-established approach (Mancini et al., 2011). The same techniques could be implemented to evaluate balance in stroke survivors using IMU sensors, where many potential locations can be identified for IMU sensor placement while collecting data from a participant in clinical settings and/or during ADLs. Accordingly, a recommended future study would involve identifying the optimal location(s) for IMU senor(s) placement with which the highest accuracy for fall risk assessment could be achieved.

Another area within the scope of improvement of fall risk assessment studies involves the type of tasks during which motion data is collected. Importantly, although the significance ratio for cognitive impairment as an FRF was found to be 36%, cognitive factors may have larger impact on fall risk assessment when physical task performance is also factored in. For instance, dual-task paradigms are often utilized in fall risk assessment of the elderly population and patients suffering from multiple sclerosis (Wajda et al., 2013; Muir-Hunter and Wittwer, 2016; Rydalch et al., 2019; Rizzo et al., 2021). Likewise, there are many studies on the effect of cognitive-motor interference on the performance of stroke survivors (Haggard et al., 2000; Bowen et al., 2001; Cockburn et al., 2003; Hyndman et al., 2006; Kemper et al., 2006; Plummer-D'Amato et al., 2008; Dennis et al., 2009; Plummer-D'Amato et al., 2010; Plummer et al., 2013; Plummer et al., 2014). Specifically, it has been proven that when stroke survivors perform a cognitive task while walking, their gait speed (Bowen et al., 2001; Hyndman et al., 2006; Plummer-D'Amato et al., 2008), stride length (Hyndman et al., 2006; Plummer-D'Amato et al., 2008), cadence (Kemper et al., 2006; Plummer-D'Amato et al., 2008), and stride duration (Haggard et al., 2000; Cockburn et al., 2003; Plummer-D'Amato et al., 2008) all decrease. These findings are significant since most individuals are under some level of cognitive load while they are performing daily life activities. For example, remembering directions, listening to music, or chatting with a friend while walking are common across all communities and age brackets. Thus, in order to determine a more accurate fall risk assessment platform among stroke survivors, it would be best to assess performance using a dual-task paradigm. Cognitive-motor dual-task implementation would provide more realistic information about the functionality of stroke survivors during daily activities. Furthermore, it could transfer the performance quality of stroke survivors to some extreme region of difficulty, whereby discriminating between high fall risk (vs. low fall risk) individuals could be performed more easily. Such an approach could facilitate the development of fall risk assessment models with higher accuracy, especially in comparison to available models in the literature which rely on single-task paradigms for the functional assessment of stroke victims. Hence, future studies should prioritize dual-task paradigms for assessing the risk for falls within the stroke community.

Several methods could be implemented to execute cognitive-motor dual-task paradigm. To this end, there will be a physical task such as walking, TUG test, and balance test tied with a second task which is mainly to put a cognitive load on the stroke survivors. The physical task could be selected according to the objective of the studies. However, to put the cognitive load on the individuals, there are limited number of methods to be utilized. Generally, there are five categories of activities to be considered in dual-task paradigms. The first approach is the n-back tasks in which the subject is presented with a sequence of stimuli, and the task consists of indicating when the current stimulus matches the one from n steps earlier in the sequence (Voelcker-Rehage et al., 2006; Plummer-D'Amato et al., 2008; Coulacoglou and Saklofske, 2017). The load factor n can be adjusted to make the task more or less difficult. This method is basically putting the cognitive load through using working memory. Second method is the auditory clock which is associated with visuospatial cognition (Plummer-D'Amato et al., 2008; Kao and Pierro, 2021; Plummer et al., 2021). In this method, the participant hears a time (e.g., "two-oh-seven") and are asked to say "yes" if both hands are in a particular half of the clock and "no" if they are not. The spontaneous speech, auditory Stroop task, and counting backward are the other classes of activities to perform cognitive-motor dual-task (Brown and Marsden, 1991; Plummer-D'Amato et al., 2008). Among these, the researchers could select one or more of them and conduct the fall risk assessment study in stroke community. Since, it has not been investigated in the field of fall risk assessment in stroke survivors, comparison of the fall risk accuracy while using the mentioned methods and finding the most adequate method of implementing cognitive-motor dual-task paradigm could also be of a great help in the future studies.

There are several limitations in this review and the relevant literature which need to be improved in the future studies. The main drawback in the literature is that the studies did not provide the effect size for their analyses on the FRFs. Due to this gap in the literature, Xu et al., could not perform any analyses on the FRF with more than four articles which is a very few sample size to make a reliable decision based on it (Xu et al., 2018). To address

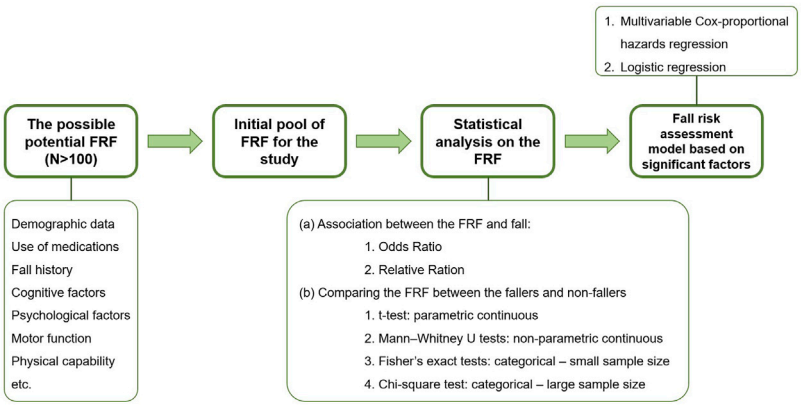

FIGURE 2 | The general path of fall risk assessment studies in stroke survivors with a focus on implemented statistical analysis methods.

this issue, this review focused on the commonality analysis to provide a more inclusive insight considering all the articles including each FRF. However, we did not implement some data from the articles in the pool of review such as sample size, the statistical method, accuracy of the assessment, etc. Hence, having a consistent approach in the future studies on fall risk assessments in stroke survivors and reporting the effect size in a proper format would help the field to get a better and accurate understanding about the impact of various FRFs by providing an inclusive/reliable meta-analysis based on a rich pool of articles in the literature.

There is a significant benefit in providing a review on the statistical methods implemented to analyze the FRFs in the literature. So far, the reviews on the FRFs have been focused on the outcome of the statistical analyses. However, a review of the implemented statistical methods in the studies could help the researchers to compare and select the adequate statistical methods for their analyses. Furthermore, this type of study could investigate the effects of using various statistical approaches/models on the outcome of the fall risk assessment. Such a review study on the methods could be considered as a potential next phase for this systematic review. To this end, a preliminary review was conducted on the articles involved in this review and the statistical methods were summarized in **Figure 2**. The results of this preliminary review showed that in general, there were six statistical methods implemented in the articles to analyze the effects of each FRF on fall risk. Depending on the type of the analysis and the risk factor, researchers have selected their own set of statistical tools/methods to evaluate the impact of the FRFs on fall risk level. In the next step, in some of the studies, a fall risk assessment model was developed based on the significant FRFs utilizing either multivariable Cox (proportional hazards) regression (e.g., (Foster et al., 2018; Persson et al., 2018)) or logistic regression (e.g., (Lamb et al., 2003; Yoshimoto et al., 2016)). Recently, machine learning approaches such as support vector machine (SVM), multi-layer perceptron (MLP), random forest, decision tree, naïve Bayes, and boosted tree are showing promising results in classifying faller and non-fallers in community dwelling older people (Qiu et al., 2018). Hence, it is highly recommended to explore the capability of these tools to develop fall risk assessment models in stroke community.

According to the results of this review, motion analysis demonstrates a high capability for identifying those at risk for falling. However, obtaining accurate and timely patient information (especially from patients with impaired mobility) is a critical issue which needs to be addressed in future studies. Recent advancements in wearable tools and smartphone technologies, as well as in computational platforms, big data mining and artificial intelligence, have certainly improved options for monitoring and evaluating patients, where several literature reports describe the successful implementation of smartphone motion data to categorize physical status attributes, such as balance or fatigue level (Hou et al., 2018; Karvekar et al., 2020). Similarly, if researchers can validate the capability of a single IMU sensor in fall risk assessment with high accuracy, the developed model could be utilized as a smartphone application. Such an application would reduce the need for clinical visits and provide real-time continuous fall risk assessment data during ADL to clinicians, while engaging patients in self-monitoring and rehabilitation.

5 CONCLUSION

This study presented a systematic review of 27 published papers on fall risk factors and fall risk assessment post stroke, with findings indicating that balance and motion-related measures constitute the most common and significant factors for this at-risk population. Further analysis of these studies demonstrated a clear paradigm shift from using traditional subjective tools to more quantitative objective approaches for assessing balance and motion deficits. Due to the relevance of these two factors in fall risk identification, it is recommended that further studies are needed to investigate an optimal combination of balance/motion

assessment tools and protocols for investigating the fall risk for stroke survivors. Considering the accessibility and low cost of high performance IMU sensors, IMU-based analysis, along with other smart sensors, is suggested for capturing motion and balance dynamics. Furthermore, cognitive-motor dual-task studies are highly recommended for future implementation on fall risk assessment of stroke patients for more realistic outcomes. Given the multiple challenges that stroke sufferers face and the critical importance of avoiding additional physical and emotional harm resulting from falls, research targeting the development of advanced fall risk assessment models should be prioritized.

DATA AVAILABILITY STATEMENT

The original contributions presented in the study are included in the article, further inquiries can be directed to the corresponding author.

AUTHOR CONTRIBUTIONS

MA, RZ, MD, MP, KK, and ER conceptualized study. MA and NW collected articles. MA, NW, and ER extracted data. MA performed the analysis and wrote the manuscript. All authors reviewed and revised the manuscript.

REFERENCES

Alemdaroğlu, E., Uçan, H., Topçuoğlu, A. M., and Sivas, F. (2012). In-hospital Predictors of Falls in Community-Dwelling Individuals after Stroke in the First 6 Months after a Baseline Evaluation: a Prospective Cohort Study. *Arch. Phys. Med. Rehabil.* 93 (12), 2244–2250. doi:10.1016/j.apmr.2012.06.014

Allin, L. J., Wu, X., Nussbaum, M. A., and Madigan, M. L. (2016). Falls Resulting from a Laboratory-Induced Slip Occur at a Higher Rate Among Individuals Who Are Obese. *J. Biomechanics* 49 (5), 678–683. doi:10.1016/j.jbiomech.2016.01.018

An, S. H., Jee, Y. J., Shin, H. H., and Lee, G. C. (2017). Validity of the Original and Short Versions of the Dynamic Gait Index in Predicting Falls in Stroke Survivors. *Rehabil. Nurs.* 42 (6), 325–332. doi:10.1002/rnj.280

Andersson, A. G., Kamwendo, K., Seiger, A., and Appelros, P. (2006). How to Identify Potential Fallers in a Stroke Unit: Validity Indexes of Four Test Methods. *J. Rehabil. Med.* 38 (3), 186–191. doi:10.1080/16501970500478023

Anna, N., and Karin, H. (2012). Fall Risk Six Weeks From Onset of Stroke and the Ability of the Prediction of Falls in Rehabilitation Settings Tool and Motor Function to Predict Falls. *Clin. Rehab.* 27 (5). doi:10.1177/2F0269215512464703

Ashburn, A., Hyndman, D., Pickering, R., Yardley, L., and Harris, S. (2008). Predicting People with Stroke at Risk of Falls. *Age ageing* 37 (3), 270–276. doi:10.1093/ageing/afn066

Baetens, T., Kegel, A., Calders, P., Vanderstraeten, G., and Cambier, D. (2011). Prediction of Falling Among Stroke Patients in Rehabilitation. *J. Rehabil. Med.* 43 (10), 876–883. doi:10.2340/16501977-0873

Blennerhassett, J. M., Dite, W., Ramage, E. R., and Richmond, M. E. (2012). Changes in Balance and Walking from Stroke Rehabilitation to the Community: a Follow-Up Observational Study. *Archives Phys. Med. Rehabilitation* 93 (10), 1782–1787. doi:10.1016/j.apmr.2012.04.005

Bowen, A., Wenman, R., Mickelborough, J., Foster, J., Hill, E., and Tallis, R. (2001). Dual-task Effects of Talking while Walking on Velocity and Balance Following a Stroke. *Age ageing* 30 (4), 319–323. doi:10.1093/ageing/30.4.319

Breisinger, T. P., Skidmore, E. R., Niyonkuru, C., Terhorst, L., and Campbell, G. B. (2014). The Stroke Assessment of Fall Risk (SAFR): Predictive Validity in Inpatient Stroke Rehabilitation. *Clin. Rehabil.* 28 (12), 1218–1224. doi:10.1177/0269215514534276

Brown, R. G., and Marsden, C. D. (1991). Dual Task Performance and Processing Resources in Normal Subjects and Patients with Parkinson's Disease. *Brain* 114 (Pt 1A), 215–231. doi:10.1093/brain/114.4.1903

Callaly, E. L., Ni Chroinin, D., Hannon, N., Sheehan, O., Marnane, M., Merwick, A., et al. (2015). Falls and Fractures 2 Years after Acute Stroke: the North Dublin Population Stroke Study. *Age Ageing* 44 (5), 882–886. doi:10.1093/ageing/afv093

CDC (2019) *Stroke Facts Online.* Atlanta, Georgia: Center for Disease Control and Prevention. Available at: https://www.cdc.gov/stroke/facts.htm.

Cockburn, J., Haggard, P., Cock, J., and Fordham, C. (2003). Changing Patterns of Cognitive-Motor Interference (CMI) over Time during Recovery from Stroke. *Clin. Rehabil.* 17 (2), 167–173. doi:10.1191/0269215503cr597oa

Coulacoglou, C., and Saklofske, D. H. (2017). Executive Function, Theory of Mind, and Adaptive Behavior. *Psychomterics Psychol. Assess. Princ. Appl.*, 91–130. doi:10.1016/b978-0-12-802219-1.00005-5

Deeks, J. J., Dinnes, J., D'Amico, R., Sowden, A. J., Sakarovitch, C., Song, F., et al. (2003). Evaluating Non-randomised Intervention Studies. *Health Technol. Assess.* 7 (27), 1–173. doi:10.3310/hta7270

Dennis, A., Dawes, H., Elsworth, C., Collett, J., Howells, K., Wade, D. T., et al. (2009). Fast Walking under Cognitive-Motor Interference Conditions in Chronic Stroke. *Brain Res.* 1287, 104–110. doi:10.1016/j.brainres.2009.06.023

Divani, A. A., Vazquez, G., Barrett, A. M., Asadollahi, M., and Luft, A. R. (2009). Risk Factors Associated with Injury Attributable to Falling Among Elderly Population with History of Stroke. *Stroke* 40 (10), 3286–3292. doi:10.1161/strokeaha.109.559195

Foster, E. J., Barlas, R. S., Bettencourt-Silva, J. H., Clark, A. B., Metcalf, A. K., Bowles, K. M., et al. (2018). Long-Term Factors Associated with Falls and Fractures Poststroke. *Front. Neurol.* 9, 210. doi:10.3389/fneur.2018.00210

Goljar, N., Globokar, D., Puzić, N., Kopitar, N., Vrabič, M., Ivanovski, M., et al. (2016). Effectiveness of a Fall-Risk Reduction Programme for Inpatient Rehabilitation after Stroke. *Disabil. Rehabilitation* 38 (18), 1811–1819. doi:10.3109/09638288.2015.1107771

Haggard, P., Cockburn, J., Cock, J., Fordham, C., and Wade, D. (2000). Interference between Gait and Cognitive Tasks in a Rehabilitating Neurological Population. *J. Neurology, Neurosurg. Psychiatry* 69 (4), 479–486. doi:10.1136/jnnp.69.4.479

Higgins, J. P. (2008). *Cochrane Handbook for Systematic Reviews of Interventions Version 5.0. 1.* London, United Kingdom: The Cochrane Collaboration. Available at: http://www.cochrane-handbook.org.

Hou, Y.-R., Chiu, Y.-L., Chiang, S.-L., Chen, H.-Y., and Sung, W.-H. (2018). Feasibility of a Smartphone-Based Balance Assessment System for Subjects with Chronic Stroke. *Comput. methods programs Biomed.* 161, 191–195. doi:10.1016/j.cmpb.2018.04.027

Hyndman, D., Ashburn, A., Yardley, L., and Stack, E. (2006). Interference between Balance, Gait and Cognitive Task Performance Among People with Stroke Living in the Community. *Disabil. Rehabil.* 28 (13-14), 849–856. doi:10.1080/09638280500534994

Jalayondeja, C., Sullivan, P. E., and Pichaiyongwongdee, S. (2014). Six-month Prospective Study of Fall Risk Factors Identification in Patients Post-stroke. *Geriatrics Gerontology Int.* 14 (4), 778–785. doi:10.1111/ggi.12164

Kao, P.-C., and Pierro, M. A. (2021). Dual-task Treadmill Walking at Self-Paced versus Fixed Speeds. *Gait Posture* 89, 92–101. doi:10.1016/j.gaitpost.2021.07.001

Karvekar, S., Abdollahi, M., and Rashedi, E. (2021). Smartphone-based Human Fatigue Level Detection Using Machine Learning Approaches. *Ergonomics* 64(07), 1–28. doi:10.1080/00140139.2020.1858185

Kemper, S., McDowd, J., Pohl, P., Herman, R., and Jackson, S. (2006). Revealing Language Deficits Following Stroke: the Cost of Doing Two Things at once. *Aging, Neuropsychology, Cognition* 13 (1), 115–139. doi:10.1080/13825580500501496

Kerse, N., Parag, V., Feigin, V. L., McNaughton, H., Hackett, M. L., Bennett, D. A., et al. (2008). Falls after Stroke. *Stroke* 39 (6), 1890–1893. doi:10.1161/strokeaha.107.509885

Lamb, S. E., Ferrucci, L., Volapto, S., Fried, L. P., Guralnik, J. M., and Study, W. s. H. a. A. (2003). Risk Factors for Falling in Home-Dwelling Older Women with Stroke. *Stroke* 34 (2), 494–501. doi:10.1161/01.str.0000053444.00582.b7

Langhorne, P., Stott, D. J., Robertson, L., MacDonald, J., Jones, L., McAlpine, C., et al. (2000). Medical Complications after Stroke. *Stroke* 31 (6), 1223–1229. doi:10.1161/01.str.31.6.1223

Larén, A., Odqvist, A., Hansson, P. O., and Persson, C. U. (2018). Fear of Falling in Acute Stroke: The Fall Study of Gothenburg (FallsGOT). *Top. Stroke Rehabil.* 25 (4), 256–260. doi:10.1080/10749357.2018.1443876

Lee, H. H., and Jung, S. H. (2017). Prediction of Post-stroke Falls by Quantitative Assessment of Balance. *Ann. Rehabil. Med.* 41 (3), 339. doi:10.5535/arm.2017.41.3.339

Mackintosh, S. F., Hill, K. D., Dodd, K. J., Goldie, P. A., and Culham, E. G. (2006). Balance Score and a History of Falls in Hospital Predict Recurrent Falls in the 6 Months Following Stroke Rehabilitation. *Archives Phys. Med. rehabilitation* 87 (12), 1583–1589. doi:10.1016/j.apmr.2006.09.004

Maeda, N., Kato, J., and Shimada, T. (2009). Predicting the Probability for Fall Incidence in Stroke Patients Using the Berg Balance Scale. *J. Int. Med. Res.* 37 (3), 697–704. doi:10.1177/147323000903700313

Mancini, M., King, L., Salarian, A., Holmstrom, L., McNames, J., and Horak, F. B. (2011). Mobility Lab to Assess Balance and Gait with Synchronized Body-Worn Sensors. *J. Bioeng. Biomed. Sci.*, 007. doi:10.4172/2155-9538.S1-007

Mansfield, A., Wong, J. S., McIlroy, W. E., Biasin, L., Brunton, K., Bayley, M., et al. (2015). Do measures of Reactive Balance Control Predict Falls in People with Stroke Returning to the Community? *Physiotherapy* 101 (4), 373–380. doi:10.1016/j.physio.2015.01.009

Melillo, P., Orrico, A., Scala, P., Crispino, F., and Pecchia, L. (2015). Cloud-Based Smart Health Monitoring System for Automatic Cardiovascular and Fall Risk Assessment in Hypertensive Patients. *J. Med. Syst.* 39 (10), 109. doi:10.1007/s10916-015-0294-3

Mohan, D. M., Khandoker, A. H., Wasti, S. A., Ismail Ibrahim Ismail Alali, S., Jelinek, H. F., and Khalaf, K. (2021). Assessment Methods of Post-stroke Gait: A Scoping Review of Technology-Driven Approaches to Gait Characterization and Analysis. *Front. Neurology* 12, 885. doi:10.3389/fneur.2021.650024

Muir-Hunter, S. W., and Wittwer, J. E. (2016). Dual-task Testing to Predict Falls in Community-Dwelling Older Adults: a Systematic Review. *Physiotherapy* 102 (1), 29–40. doi:10.1016/j.physio.2015.04.011

National library of medicine (2022) Available at: https://www.nlm.nih.gov/mesh/meshhome.html

Nyberg, L., and Gustafson, Y. (1997). Fall Prediction Index for Patients in Stroke Rehabilitation. *Stroke* 28 (4), 716–721. doi:10.1161/01.str.28.4.716

Nyström, A., and Hellström, K. (2013). Fall Risk Six Weeks from Onset of Stroke and the Ability of the Prediction of Falls in Rehabilitation Settings Tool and Motor Function to Predict Falls. *Clin. Rehabil.* 27 (5), 473. doi:10.1177/0269215512464703

Olsson, E., Löfgren, B., Gustafson, Y., and Nyberg, L. (2005). Validation of a Fall Risk Index in Stroke Rehabilitation. *J. Stroke Cerebrovasc. Dis.* 14 (1), 23–28. doi:10.1016/j.jstrokecerebrovasdis.2004.11.001

Page, M. J., McKenzie, J. E., Bossuyt, P. M., Boutron, I., Hoffmann, T. C., Mulrow, C. D., et al. (2021). The PRISMA 2020 Statement: an Updated Guideline for Reporting Systematic Reviews. *BMJ* 372, n71. doi:10.1136/bmj.n71

Persson, C., Hansson, P., and Sunnerhagen, K. (2011). Clinical Tests Performed in Acute Stroke Identify the Risk of Falling during the First Year: Postural Stroke Study in Gothenburg (POSTGOT). *J. Rehabil. Med.* 43 (4), 348–353. doi:10.2340/16501977-0677

Persson, C. U., Kjellberg, S., Lernfelt, B., Westerlind, E., Cruce, M., and Hansson, P.-O. (2018). Risk of Falling in a Stroke Unit after Acute Stroke: The Fall Study of Gothenburg (FallsGOT). *Clin. Rehabil.* 32 (3), 398–409. doi:10.1177/0269215517728325

Pinto, E. B., Nascimento, C., Monteiro, M., Castro, M., Maso, I., Campos, A., et al. (2016). Proposal for a New Predictive Scale for Recurrent Risk of Fall in a Cohort of Community-Dwelling Patients with Stroke. *J. Stroke Cerebrovasc. Dis.* 25 (11), 2619–2626. doi:10.1016/j.jstrokecerebrovasdis.2016.06.045

Plummer, P., Eskes, G., Wallace, S., Giuffrida, C., Fraas, M., Campbell, G., et al. (2013). Cognitive-motor Interference during Functional Mobility after Stroke: State of the Science and Implications for Future Research. *Archives Phys. Med. rehabilitation* 94 (12), 2565–2574. doi:10.1016/j.apmr.2013.08.002

Plummer, P., Villalobos, R. M., Vayda, M. S., Moser, M., and Johnson, E. (2014). Feasibility of Dual-Task Gait Training for Community-Dwelling Adults after Stroke: a Case Series. *Stroke Res. Treat.* 2014, 538602. doi:10.1155/2014/538602

Plummer, P., Zukowski, L. A., Feld, J. A., and Najafi, B. (2021). Cognitive-motor Dual-Task Gait Training within 3 Years after Stroke: a Randomized Controlled Trial. *Physiother. Theory Pract.*, 1–16. doi:10.1080/09593985.2021.1872129

Plummer-D'Amato, P., Altmann, L. J., Saracino, D., Fox, E., Behrman, A. L., and Marsiske, M. (2008). Interactions between Cognitive Tasks and Gait after Stroke: a Dual Task Study. *Gait Posture* 27 (4), 683–688. doi:10.1016/j.gaitpost.2007.09.001

Plummer-D'Amato, P., Altmann, L. J. P., Behrman, A. L., and Marsiske, M. (2010). Interference between Cognition, Double-Limb Support, and Swing during Gait in Community-Dwelling Individuals Poststroke. *Neurorehabil Neural Repair* 24 (6), 542–549. doi:10.1177/1545968309357926

Podsiadlo, D., and Richardson, S. (1991). The Timed "Up & Go": a Test of Basic Functional Mobility for Frail Elderly Persons. *J. Am. geriatrics Soc.* 39 (2), 142–148. doi:10.1111/j.1532-5415.1991.tb01616.x

Pouwels, S., Lalmohamed, A., Leufkens, B., de Boer, A., Cooper, C., van Staa, T., et al. (2009). Risk of Hip/Femur Fracture after Stroke. *Stroke* 40 (10), 3281–3285. doi:10.1161/strokeaha.109.554055

Qiu, H., Rehman, R. Z. U., Yu, X., and Xiong, S. (2018). Application of Wearable Inertial Sensors and a New Test Battery for Distinguishing Retrospective Fallers from Non-fallers Among Community-Dwelling Older People. *Sci. Rep.* 8 (1), 16349–16410. doi:10.1038/s41598-018-34671-6

Rizzo, R., Knight, S. P., Davis, J. R. C., Newman, L., Duggan, E., Kenny, R. A., et al. (2021). SART and Individual Trial Mistake Thresholds: Predictive Model for Mobility Decline. *Geriatrics* 6 (3), 85. doi:10.3390/geriatrics6030085

Rydalch, G., Bell, H. B., Ruddy, K. L., and Bolton, D. A. E. (2019). Stop-signal Reaction Time Correlates with a Compensatory Balance Response. *Gait Posture* 71, 273–278. doi:10.1016/j.gaitpost.2019.05.015

Simpson, L. A., Miller, W. C., and Eng, J. J. (2011). Effect of Stroke on Fall Rate, Location and Predictors: a Prospective Comparison of Older Adults with and without Stroke. *PLoS One* 6 (4), e19431. doi:10.1371/journal.pone.0019431

Tan, K., and Tan, M. (2016). Stroke and Falls-Clash of the Two Titans in Geriatrics. *Geriatrics* 1 (4), 31. doi:10.3390/geriatrics1040031

Taylor-Piliae, R. E., Mohler, M. J., Najafi, B., and Coull, B. M. (2016). Objective Fall Risk Detection in Stroke Survivors Using Wearable Sensor Technology: a Feasibility Study. *Top. Stroke Rehabilitation* 23 (6), 393–399. doi:10.1179/1074935715Z.00000000059

Thomas, T., Stephen, B., and Colin, M. (2000). The Global Burden of Cerebrovascular Disease. *Cerebovascular Dis.*

Thrift, A. G., Thayabaranathan, T., Howard, G., Howard, V. J., Rothwell, P. M., Feigin, V. L., et al. (2017). Global Stroke Statistics. *Int. J. stroke* 12 (1), 13–32. doi:10.1177/1747493016676285

Tilson, J. K., Wu, S. S., Cen, S. Y., Feng, Q., Rose, D. R., Behrman, A. L., et al. (2012). Characterizing and Identifying Risk for Falls in the LEAPS Study. *Stroke* 43 (2), 446–452. doi:10.1161/STROKEAHA.111.636258

Voelcker-Rehage, C., Stronge, A. J., and Alberts, J. L. (2006). Age-related Differences in Working Memory and Force Control under Dual-Task Conditions. *Neuropsychol. Dev. Cogn. B Aging Neuropsychol. Cogn.* 13 (3-4), 366–384. doi:10.1080/138255890969339

Wada, N., Sohmiya, M., Shimizu, T., Okamoto, K., and Shirakura, K. (2007). Clinical Analysis of Risk Factors for Falls in Home-Living Stroke Patients Using Functional Evaluation Tools. *Archives Phys. Med. rehabilitation* 88 (12), 1601–1605. doi:10.1016/j.apmr.2007.09.005

Wajda, D. A., Motl, R. W., and Sosnoff, J. J. (2013). Dual Task Cost of Walking Is Related to Fall Risk in Persons with Multiple Sclerosis. *J. Neurol. Sci.* 335 (1-2), 160–163. doi:10.1016/j.jns.2013.09.021

Walsh, M. E., Horgan, N. F., Walsh, C. D., and Galvin, R. (2016). Systematic Review of Risk Prediction Models for Falls after Stroke. *J. Epidemiol. Community Health* 70 (5), 513–519. doi:10.1136/jech-2015-206475

Weerdesteyn, V., Niet, M. d., van Duijnhoven, H. J. R., and Geurts, A. C. H. (2008). Falls in Individuals with Stroke. *Jrrd* 45 (8), 1195–1213. doi:10.1682/jrrd.2007.09.0145

Wei, T.-S., Liu, P.-T., Chang, L.-W., and Liu, S.-Y. (2017). Gait Asymmetry, Ankle Spasticity, and Depression as Independent Predictors of Falls in Ambulatory Stroke Patients. *PLoS One* 12 (5), e0177136. doi:10.1371/journal.pone.0177136

Xu, T., Clemson, L., O'Loughlin, K., Lannin, N. A., Dean, C., and Koh, G. (2018). Risk Factors for Falls in Community Stroke Survivors: a Systematic Review and Meta-Analysis. *Archives Phys. Med. rehabilitation* 99 (3), 563–573. doi:10.1016/j.apmr.2017.06.032

Yates, J. S., Lai, S. M., Duncan, P. W., and Studenski, S. (2002). Falls in Community-Dwelling Stroke Survivors: an Accumulated Impairments Model. *J. Rehabil. Res. Dev.* 39 (3), 385

Yoshimoto, Y., Oyama, Y., Tanaka, M., and Sakamoto, A. (2016). One-leg Standing Time of the Affected Side Moderately Predicts for Postdischarge Falls in Community Stroke Patients. *J. stroke Cerebrovasc. Dis.* 25 (8), 1907–1913. doi:10.1016/j.jstrokecerebrovasdis.2016.03.032

Conflict of Interest: The authors declare that the research was conducted in the absence of any commercial or financial relationships that could be construed as a potential conflict of interest.

Publisher's Note: All claims expressed in this article are solely those of the authors and do not necessarily represent those of their affiliated organizations, or those of the publisher, the editors and the reviewers. Any product that may be evaluated in this article, or claim that may be made by its manufacturer, is not guaranteed or endorsed by the publisher.

Copyright © 2022 Abdollahi, Whitton, Zand, Dombovy, Parnianpour, Khalaf and Rashedi. This is an open-access article distributed under the terms of the Creative Commons Attribution License (CC BY). The use, distribution or reproduction in other forums is permitted, provided the original author(s) and the copyright owner(s) are credited and that the original publication in this journal is cited, in accordance with accepted academic practice. No use, distribution or reproduction is permitted which does not comply with these terms.

frontiers | Frontiers in Bioengineering and Biotechnology

TYPE Original Research
PUBLISHED 06 December 2022
DOI 10.3389/fbioe.2022.1012544

Check for updates

OPEN ACCESS

EDITED BY
Yih-Kuen Jan,
University of Illinois at Urbana-Champaign, United States

REVIEWED BY
Yingchun Zhang,
University of Houston, United States
Anne Schwarz,
University of Zurich and University Hospital Zurich, Switzerland

*CORRESPONDENCE
Sanaz Pournajaf,
s.pournajaf@gmail.com

SPECIALTY SECTION
This article was submitted to Biomechanics,
a section of the journal Frontiers in Bioengineering and Biotechnology

RECEIVED 05 August 2022
ACCEPTED 16 November 2022
PUBLISHED 06 December 2022

CITATION
Goffredo M, Proietti S, Pournajaf S, Galafate D, Cioeta M, Le Pera D, Posteraro F and Franceschini M (2022), Baseline robot-measured kinematic metrics predict discharge rehabilitation outcomes in individuals with subacute stroke.
Front. Bioeng. Biotechnol. 10:1012544.
doi: 10.3389/fbioe.2022.1012544

COPYRIGHT
© 2022 Goffredo, Proietti, Pournajaf, Galafate, Cioeta, Le Pera, Posteraro and Franceschini. This is an open-access article distributed under the terms of the Creative Commons Attribution License (CC BY). The use, distribution or reproduction in other forums is permitted, provided the original author(s) and the copyright owner(s) are credited and that the original publication in this journal is cited, in accordance with accepted academic practice. No use, distribution or reproduction is permitted which does not comply with these terms.

Baseline robot-measured kinematic metrics predict discharge rehabilitation outcomes in individuals with subacute stroke

Michela Goffredo[1], Stefania Proietti[2,3], Sanaz Pournajaf[1]*, Daniele Galafate[1], Matteo Cioeta[1], Domenica Le Pera[1], Federico Posteraro[4] and Marco Franceschini[1,3]

[1]Department of Neurological and Rehabilitation Sciences, IRCCS San Raffaele Roma, Rome, Italy, [2]Unit of Clinical and Molecular Epidemiology, IRCCS San Raffaele Roma, Rome, Italy, [3]Department of Human Sciences and Promotion of the Quality of Life, San Raffaele University, Rome, Italy, [4]Rehabilitation Department, Versilia Hospital, Camaiore, Italy

Background: The literature on upper limb robot-assisted therapy showed that robot-measured metrics can simultaneously predict registered clinical outcomes. However, only a limited number of studies correlated pre-treatment kinematics with discharge motor recovery. Given the importance of predicting rehabilitation outcomes for optimizing physical therapy, a predictive model for motor recovery that incorporates multidirectional indicators of a patient's upper limb abilities is needed.

Objective: The aim of this study was to develop a predictive model for rehabilitation outcome at discharge (i.e., muscle strength assessed by the Motricity Index of the affected upper limb) based on multidirectional 2D robot-measured kinematics.

Methods: Re-analysis of data from 66 subjects with subacute stroke who underwent upper limb robot-assisted therapy with an end-effector robot was performed. Two least squares error multiple linear regression models for outcome prediction were developed and differ in terms of validation procedure: the Split Sample Validation (SSV) model and the Leave-One-Out Cross-Validation (LOOCV) model. In both models, the outputs were the discharge Motricity Index of the affected upper limb and its sub-items assessing elbow flexion and shoulder abduction, while the inputs were the admission robot-measured metrics.

Results: The extracted robot-measured features explained the 54% and 71% of the variance in clinical scores at discharge in the SSV and LOOCV validation procedures respectively. Normalized errors ranged from 22% to 35% in the SSV models and from 20% to 24% in the LOOCV models. In all models, the movement path error of the trajectories characterized by elbow flexion and shoulder extension was the significant predictor, and all correlations were significant.

Conclusion: This study highlights that motor patterns assessed with multidirectional 2D robot-measured metrics are able to predict clinical evalutation of upper limb muscle strength and may be useful for clinicians to assess, manage, and program a more specific and appropriate rehabilitation in subacute stroke patients.

KEYWORDS

robot-assisted therapy, stroke, motor recovery, upper extremity, kinematics, biomarkers, predictors

Introduction

Most stroke survivors experience upper limb motor impairments that negatively influence Activities of Daily Living (ADL) (Nichols-Larsen et al., 2005). Over the past two decades, robotic devices have been shown to provide intensive and highly repeatable therapy, enrich the sensorimotor experience, and offer customizable and repeatable support during treatment (Mehrholz et al., 2018; Morone et al., 2020; Gandolfi et al., 2021). In particular, Mehrholz et al. evidenced the efficacy of upper limb Robot-assisted Therapy (ulRT) in improving ADL, arm function, and arm muscle strength (Mehrholz et al., 2018) in stroke patients.

Recently, robots have been recognised not only as a rehabilitation device but also as a measurement tool, suggesting that they can provide a standardized and objective measure of a patient's motor control and improve research knowledge on treatment effects and stroke recovery (Agrafiotis et al., 2021). In this regard, studies on ulRT have analyzed the Robot-Measured Kinematic (RMK) data to assess ulRT-induced biomechanical changes and patient progress over time (Dipietro et al., 2011; Balasubramanian et al., 2012; Panarese et al., 2012; Mazzoleni et al., 2013; Tran et al., 2018; Goffredo et al., 2019). Furthermore, RMK data have also been shown to be able to capture relevant aspects of goal-directed movements that may reveal pathological motor synergies in stroke survivors (Dipietro et al., 2011; Panarese et al., 2012; Goffredo et al., 2019). RMK metrics were also found to correlate with motor impairment as measured by Fugl-Meyer upper limb assessment (Colombo et al., 2005; Duret et al., 2016) and to be representative of pathological motor synergies when different directions of movement were analyzed (Panarese et al., 2012; Goffredo et al., 2019). The latter is in accordance with the kinematic approach to identify how the central nervous system represents and implements the motor control strategies necessary to obtain the movements in stroke patients (Micera et al., 2005). RMK data were also processed to predict the clinical assessment outcomes (Krebs et al., 2014; Duret et al., 2019; Agrafiotis et al., 2021; Goffredo et al., 2021; Grimm et al., 2021; Moretti et al., 2021), considering the importance of biomarkers of neurorehabilitation outcomes for evidence-based practice (Langhorne et al., 2009; Scott and &Dukelow, 2011; Duret et al., 2015; Franceschini et al., 2018). In this context, the Predict REcovery Potential (PREP2) tool is the predominant predictor of upper limb functional outcomes from clinical assessment, Magnetic Resonance Imaging (MRI) and Transcranial Magnetic Stimulation (TMS) biomarkers, with an impact on rehabilitation planning and realistic treatment goal setting (Stinear et al., 2017). Although PREP2 predicts correctly approximately 70% of patients, the major limitation is that TMS is not readily available in many clinical settings (Connell et al., 2021). Therefore, in rehabilitation hospitals equipped with robots for ulRT, an alternative, ecological robot-based method to predict rehabilitation outcome could be the analysis of RMK data at baseline. However, to the best of our knowledge there is no evidence in literature on the RMK-based predictors of clinical outcomes at discharge that account for motor synergies at baseline.

Considering the importance of quantitative indicators of upper limb function, Krebs *et al.* and Moretti *et al.* found that RMK metrics from a 2D robot can be biomarkers of clinical outcomes registered on the same day (Krebs et al., 2014; Moretti et al., 2021). Their findings were consistent with those of Grimm et al. who analyzed exoskeleton-based kinematics (Grimm et al., 2021). On the other hand, Agrafiotis *et al.*, developed RMK-based models of clinical outcomes with the aim of removing inter- and intra-rater variability and reducing the sample size in stroke clinical trials (Agrafiotis et al., 2021). To our knowledge, only Duret *et al.* predicted upper limb recovery at the end of ulRT (Duret et al., 2019). They found that selected RMK parameters, calculated from the total end-effector trajectory did not predict the upper limb Fugl-Meyer Assessment. In our previous paper (Goffredo et al., 2021), we analyzed RMK metrics calculated from reaching movements with different directions. Specifically, the movement path error, the mean movement speed, and the number of speed peaks of each point-to-point trajectory were analyzed. Then, a generalized linear analysis was applied to estimate the relationships between the RMK measures at baseline and the (clinical and RMK) data at the end of ulRT, considering each direction of movement separately. The analysis revealed that a subset of the RMK metrics was correlated with the probability of rising one class in the Motricity Index at the end of ulRT. Our multidirectional 2D analysis of RMK metrics showed that pre-treatment kinematic data are representative of pathological motor synergies in stroke survivors, i.e., the ability to perform movements of shoulder (ab-adduction, internal and external rotation) and elbow (flexion-extension)

is representative of flexor synergy in stroke patients (Goffredo et al., 2021). However, despite the importance of predicting rehabilitation outcomes for clinician decision-making and treatment optimization, there is a paucity of literature on post-ulRT rehabilitation outcomes based on patients' upper limb abilities and motor synergies at baseline.

The aim of this study is to re-analyze the retrospective data from our previous study to develop a multidirectional 2D RMK-based predictive model for rehabilitation outcome (i.e., muscle strength assessed by the Motricity Index of the affected upper limb) at the end of ulRT. Potential predictors included patient demographics, stroke characteristics, and pre-treatment RMK metrics calculated considering upper limb movements which are representative of the stroke flexor synergy. In order to reliably predict the discharge rehabilitation outcome, we compared two least squares error multiple linear regression models that differ in terms of the output validation procedure.

Materials and methods

This is a re-analysis of data acquired and processed by the IRCCS San Raffaele Roma (Rome, Italy) in an observational retrospective study (Ethical approval no. 06/17; 22/02/2017) on stroke inpatients who underwent ulRT in addition to the conventional therapy (Goffredo et al., 2021).

Patients and treatments

Sixty-six stroke patients who were trained for 20 sessions (5 times/week; 45 min per session) with the In Motion 2 robot (Bionik Laboratories, Watertown, MA, United States), were included in the study. The persons were inpatients admitted to the IRCCS San Raffaele Roma (Rome, Italy) between January 2011 and December 2017 who satisfied the following inclusion criteria: age between 18 and 80 years; first event of unilateral hemiparetic stroke; subacute phase (RT started within 30 ± 7 days post stroke); upper limb Chedoke-McMaster scores between 2 and 5; Motricity Index affected upper limb<100; ulRT for 20 sessions. Subjects were excluded from the study if they had bilateral impairment; chronic phase; ulRT for less than 20 sessions; interruption of the ulRT for more than three consecutive days; presence of other severe medical conditions; incomplete data in the database. More detailed information on the ulRT conducted by the patients is available in the previous papers of the authors (Goffredo et al., 2019; Goffredo et al., 2021).

Data collection and feature extraction

The following demographic and clinical data have been collected at baseline: age, gender, affected side, stroke onset time, and etiology. Moreover, the following clinical outcomes were recorded before (T1) and after (T2) the ulRT: Motricity Index of the affected Upper Limb (MI_{UL}) (Bohannon, 1999), Motricity Index sub-item assessing the elbow flexion (MI_{ELBOW}), and Motricity Index sub-item assessing the shoulder abduction ($MI_{SHOULDER}$). The MI_{UL} is a discrete scale measuring the muscle strength of the paretic upper extremity. Three actions were separately assessed: pinch grasp, elbow flexion, and shoulder abduction. Each action was scored (0–33) with a MI sub-item composed of six classes, as defined by Wade (Wade, 1989). The total upper extremity score (MI_{UL}) was calculated by adding one to the sum of the three sub-items (maximum possible score = 100). The MI sub-item related to the pinch grip was not considered in this study because the InMotion2-based ulRT typically involves the elbow and shoulder joints.

The RMK metrics were calculated from the trajectories (200 Hz) recorded by the robot, considering each movement direction separately (Goffredo et al., 2021). Figure 1 shows the reference system (coinciding with the lesion side) used to calculate the RMK metrics. Considering the results of our previous analysis of kinematic biomarkers for upper-limb motor recovery (Goffredo et al., 2021), we extracted the features that were correlated with muscle strength at discharge, i.e.: Movement Path Error direction A (MPE_A), direction C (MPE_C), and direction D (MPE_D); and mean Movement Speed direction B (MS_B).

The MPE is a measure of accuracy (the value is 0 if the trajectory lies exactly on a straight line connecting the initial and the final target): it is computed as the mean value of the distance between each point of the actual path travelled by the subject from the ideal one (i.e., the straight line connecting the central target and the peripheral one). Since the considered peripheral targets are along the x and y axes, the MPE computation is the following:

$$MPE = \begin{cases} \frac{1}{N}\sum_{k=1}^{N}|y[k]| & direction\ D \\ \frac{1}{N}\sum_{k=1}^{N}|x[k]| & directions\ A\ and\ C \end{cases} \quad (1)$$

where N is the number of samples for each trajectory, identified by the coordinates x[k] and y[k] in the xy plane. The MS has been computed from the discrete-time velocity signals $v_x[k]$ and $v_y[k]$ along the x and y axes, respectively as the mean value of the resultant velocities in the xy plane:

$$MS = \frac{1}{N}\sum_{k=1}^{N}\sqrt{(v_x[k])^2 + \left(v_y[k]\right)^2} \quad (2)$$

All RMK metrics were recorded at T1 and showed good test-retest reliability (Koeppel and Pila, 2020). Prior to modeling, age, stroke onset time, and RMK metrics have been standardized by subtracting the mean and scaling to unit variance. Figure 1 includes the list of features used for model development.

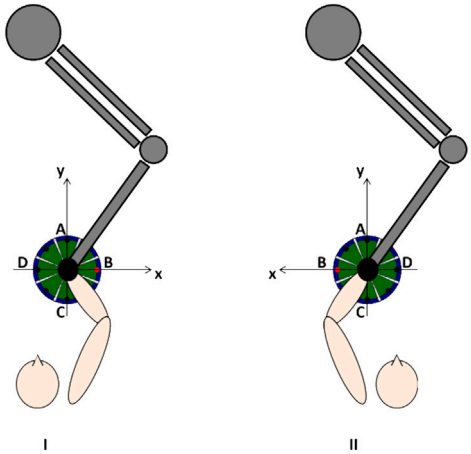

Feature	Description
$MPE_A(T1)$	Movement Path Error direction A before ulRT
$MPE_C(T1)$	Movement Path Error direction C before ulRT
$MPE_D(T1)$	Movement Path Error direction D before ulRT
$MS_B(T1)$	mean Movement Speed direction B before ulRT

FIGURE 1
Experimental setup, reference system in case of right (I) or left (II) affected limb, and description of the features considered for the models' development.

Statistical analysis and predictive models

All statistical analyses were performed using the R statistical package system v. 4.2.0 (R Foundation for Statistical Computing, Austria). A significance level of 5% (p-value ≤ 0.05) was assumed. Demographic and clinical data were reported with frequencies and percentages if they were categorical variables, while continuous variables were expressed with mean and standard deviation, median, and interquartile range.

The study compared two types of outcome prediction models that differed in terms of the validation procedure. The first model was the least squares error multiple linear regression model with the Split Sample Validation procedure (SSV model). The second model was the least squares error multiple linear regression with the Leave-One-Out Cross-Validation procedure (LOOCV model). In both models, the outputs were MI_{ELBOW} (T2), $MI_{SHOULDER}$ (T2), and MI_{UL} (T2) discharge scores (adjusted for age, sex, stroke onset time, and clinical assessment scores admission), whereas the inputs were the RMK metrics at admission.

For the SSV models, 75% of the data were randomly separated for model training, whereas the remaining 25% were set aside for model validation (Bosecker et al., 2010). The Chi-square test for categorical variables, and ANalysis Of VAriance (ANOVA) for continuous variables when normally distributed, and otherwise Mann Whitney test, confirmed that the training and validation data sets were not significantly different. Moreover, the data set was randomly divided into four groups (25% data each), and the Kruskal Wallis test (Bonferroni's correction) confirmed that there was no significant difference (p-value>0.05) between any combination of these groups in training and validation sets.

For the LOOCV models, one of the 66 records was removed, and the remaining were used to build the model. The resulting model was then used to make predictions about the record set aside (Bishop, 1995). This was repeated for each of the 66 cases.

Each prediction model was described by the percentage of variance explained (R^2), the adjusted R^2 (R_{adj}^2), the Mean Absolute Error (MAE), Root Means Squared Error (RMSE), and normalized RMSE ($RMSE_n$). The normalized MAE (MAE_n) was calculated to compare the performance of the model for the different dependent variables.

Results were assessed by correlation between therapist-assigned values and corrected predicted values (Spearman's rank correlation coefficient, r, and associated p values). Since the MI_{UL} is a discrete variable, each predicted value was corrected using a nearest neighbor procedure by assigning the score with the minimum Euclidean distance from the valid scores. Results were assessed by correlation between therapist-assigned scores and corrected predicted scores (Spearman's rank correlation coefficient, r, and associated p-values). The strength of the correlations calculated in the analyses was interpreted as follows; |r|=0–0.3 very weak, |r|=0.31–0.5 weak, |r|=0.51–0.7 moderate, and |r|=0.71–1.0 strong (Moore et al., 2013).

Ethical considerations

Since March 2012, the Italian Data Protection Authority (Garante per la protezione dei dati personali) declared that IRCCS (Istituto di Ricovero e Cura a Carattere Scientifico - Institute for scientific research and healthcare) is authorized to perform retrospective studies without the approval of the local Ethical Committee, and mandatory formal communication is

TABLE 1 Sample characteristics at baseline (T1).

	All data (n = 66)	Training set (n = 50)	Validation set (n = 16)
Age (years)	64.97 ± 12.75	64.84 ± 13.55	65.38 ± 10.26
Sex, male/female	44 (66.7%)/22 (33.3%)	32 (64.0%)/18 (36.0%)	12 (75.0%)/4 (25.0%)
Side, right/left	39 (59.1%)/27 (40.9%)	27 (54.0%)/23 (46.0%)	12 (75.0%)/4 (25.0%)
Stroke onset time (days)	15.27 ± 18.07	12.88 ± 7.97	22.75 ± 33.59
Etiology, ischemic/hemorrhagic	47 (71.2%)/19 (28.8%)	34 (68.0%)/16 (32.0%)	13 (81.3%)/3 (18.8%)
MI_{ELBOW}(T1)	14.0 (9.0–19.0)	14.0 (9.0–19.0)	16.5 (2.25–25.0)
$MI_{SHOULDER}$(T1)	14.0 (9.0–19.0)	14.0 (9.0–19.0)	16.5 (2.25–25.0)
MI_{UL}(T1)	42.0 (19.0–62.0)	40.5 (19.0–58.75)	50.5 (8.25–76.0)

Data are shown as N (%), mean ± SD, or median (IQR). Motricity Index affected elbow flexion (MI_{ELBOW}); Motricity Index affected shoulder abduction ($MI_{SHOULDER}$); Motricity Index affected Upper Limb (MI_{UL}); before ulRT (T1).

sufficient. Such communication relative to this study was registered by the Ethical Committee of the IRCCS San Raffaele Roma (Rome, Italy) on 22/02/2017 (code number: 06/17).

Results

In this study, we compared outcome predictors obtained by two modeling procedures differing from one another by output validation.

Split sample validation models

Table 1 shows the patient's demographics and clinical characteristics at baseline: data are shown for all recruited subjects, training set, and validation set separately. No significant differences (p-value>0.05) were registered between the training and the validation sets.

Predictive models for muscle strength at T2 of each clinical outcome were developed using the least squares error multiple linear regression on the training set. In all models, the movement path errors in the C (MPE_C) and D (MPE_D) directions were significant predictors (p-value<0.05). Specifically, MPE_C provided larger contribution (MI_{ELBOW}: $\beta = -5.16$; $MI_{SHOULDER}$: $\beta = -5.02$; MI_{UL}: $\beta = -13.52$) than MPE_D (MI_{ELBOW}: $\beta = 3.37$; $MI_{SHOULDER}$: $\beta = 3.37$; MI_{UL}: $\beta = 8.26$).

The training and validation results of the SSV models for estimating the MI_{ELBOW} (T2), $MI_{SHOULDER}$ (T2), and MI_{UL} (T2) are shown in Table 2. All correlations were significant at p-value < 0.05. The residual plots had no significant patterns, indicating that no underlying trends in the data were missed and that the model was fit. The MI_{ELBOW} registered a moderate correlation in the training set ($R^2 = 0.683$), but a weak one in the validation set ($R^2 = 0.481$). This decrease is more remarkable in $MI_{SHOULDER}$, which is characterized by an R^2 of 0.640 in the training set and a very weak level of correlation in the validation one ($R^2 = 0.200$). The MI_{UL} showed the highest R^2 value in both datasets. The resulting models explained 64%–76% of the variance in discharge scores, in the training set. For predicting the clinical outcomes of a patient in the validation set, the average error was 6.098 points for the MI_{ELBOW} model (range 0–33), 8.357 points for the $MI_{SHOULDER}$ model (range 0–33), and 17.265 points for the MI_{UL} model (range 1–100).

To illustrate the MI score predictions, the actual score of each patient was plotted together with the predictions generated by the models (Figure 2). The correlation between the therapist-assigned scores and predicted scores was moderate for MI_{ELBOW} (r = 0.794; p-value < 0.001) and $MI_{SHOULDER}$ (r = 0.627; p-value < 0.001), and strong for MI_{UL} (r = 0.839; p-value < 0.001).

Leave-one-out cross-validation models

The following LOOCV predictive models of discharge MI_{ELBOW}, $MI_{SHOULDER}$, and MI_{UL} were obtained:

$$\widehat{MI}_{ELBOW}(T2) = 12.99 - 4.89 \cdot MPE_C(T1) \quad (3)$$

$$\widehat{MI}_{SHOULDER}(T2) = 13.70 - 4.26 \cdot MPE_C(T1) \quad (4)$$

$$\widehat{MI}_{UL}(T2) = 32.50 - 11.99 \cdot MPE_C(T1) \quad (5)$$

The generalizability of each model was evaluated by testing its ability to predict scores of patients who were not involved in the development of the model (Table 3). In all models, the MPE_C (i.e., the error of the trajectory towards the body) was the significant predictor, and all correlations were significant (p-value<0.05). The residual plots did not have any significant correlations. The resulting models explained 46.4%–67.6% of the variance in discharge scores, and the normalized RMSE ranged from 17% to 22%.

Figure 3 depicts the actually measured score with the predicted ones generated by the models. The correlation coefficients between the therapist-assigned scores and the model's output evidences a significant correlation in all

TABLE 2 SSV predictive models for the clinical outcomes (MI_{ELBOW}, $MI_{SHOULDER}$, MI_{UL}) at the end of ulRT (T2). Results of the training and validation sets are depicted separately.

	SSV models							
	Training set (n = 50)				Validation set (n = 16)			
	RMSE	$RMSE_n$ (%)	R^2 (R^2_{adj})	MAE (MAE_n)	RMSE	$RMSE_n$ (%)	R^2 (R^2_{adj})	MAE (MAE_n)
MI_{ELBOW}(T2)	5.547	17	0.683 (0.622)	4.234 (18%)	8.186	25	0.481 (0.35)	6.098 (24%)
$MI_{SHOULDER}$(T2)	5.294	16	0.640 (0.570)	4.372 (19%)	11.588	35	0.200 (0.14)	8.357 (35%)
MI_{UL}(T2)	13.859	14	0.765 (0.719)	10.400 (15%)	21.650	21.8	0.628 (0.54)	17.265 (24%)

Motricity Index affected elbow flexion (MI_{ELBOW}); Motricity Index affected shoulder abduction ($MI_{SHOULDER}$); Motricity Index affected Upper Limb (MI_{UL}); Root Mean Square Error (RMSE); normalized Root Mean Square Error ($RMSE_n$);percentage of variance explained (R^2); adjusted percentage of variance explained (R_{adj}^2); Mean Absolute Error (MAE); normalized Mean Absolute Error (MAE_n); after ulRT (T2).

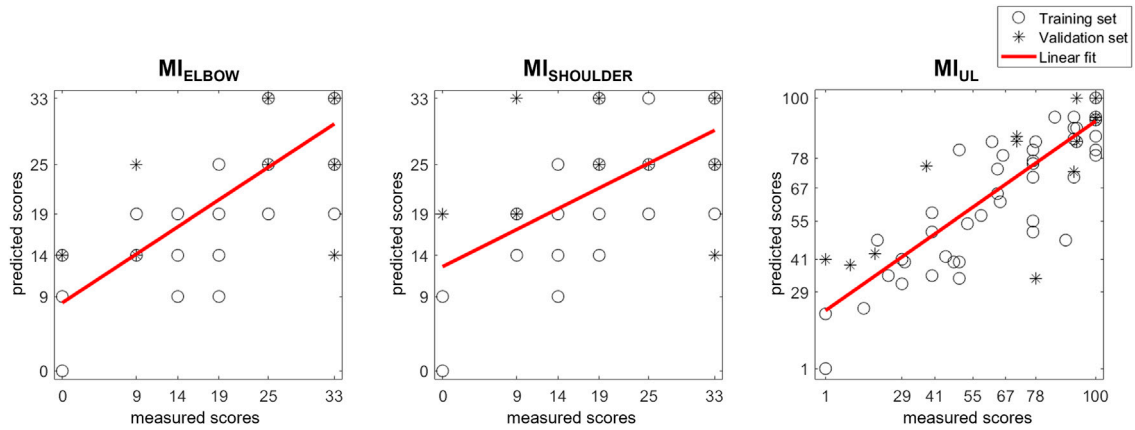

FIGURE 2
Scatter plot of MI scores prediction with SSV models. Each patient's actual score was plotted together with the predictions generated by the models. Training and validation sets are depicted separately. The results of a linear polynomial fitting are also shown.

outcomes: MI_{ELBOW} (r = 0.747; p-value < 0.001), $MI_{SHOULDER}$ (r = 0.653; p-value < 0.001), and MI_{UL} (r = 0.813; p-value < 0.001).

Discussion

Predicting rehabilitation outcomes based on pre-treatment characteristics would be of great benefit to clinicians in setting realistic rehabilitation goals, personalizing treatment activities, and supporting patient discharge in an appropriate setting (Stinear et al., 2017). In the present article, we examined the predictive abilities of two types of multiple linear regression models to reliably predict the rehabilitation outcome at discharge using RMK-based features. Specifically, both SSV and LOOCV validation procedures were considered. Since the ability to perform point-to-point reaching movements in different directions is considered in the literature to be representative of different synergies involved in the performance of reaching tasks (Panarese et al., 2012; Goffredo et al., 2019), pre-treatment RMK metrics were considered as predictive features for rehabilitation outcomes at discharge in the models developed in this study, with each direction of movement assessed separately.

The procedure consisted of a re-analysis of 66 inpatients with subacute stroke who were included in a 4-week ulRT and whose data had been examined in our previous studies with different aims (Goffredo et al., 2019; Goffredo et al., 2021). In particular, in Goffredo et al. (Goffredo et al., 2021), a relationship was found between RMK measures at baseline and (clinical and RMK) data at the end of ulRT, considering each direction of movement separately (Goffredo et al., 2021), and revealing that a subset of kinematic parameters was correlated with the probability of rising one class in the Motricity Indexes (when considered as

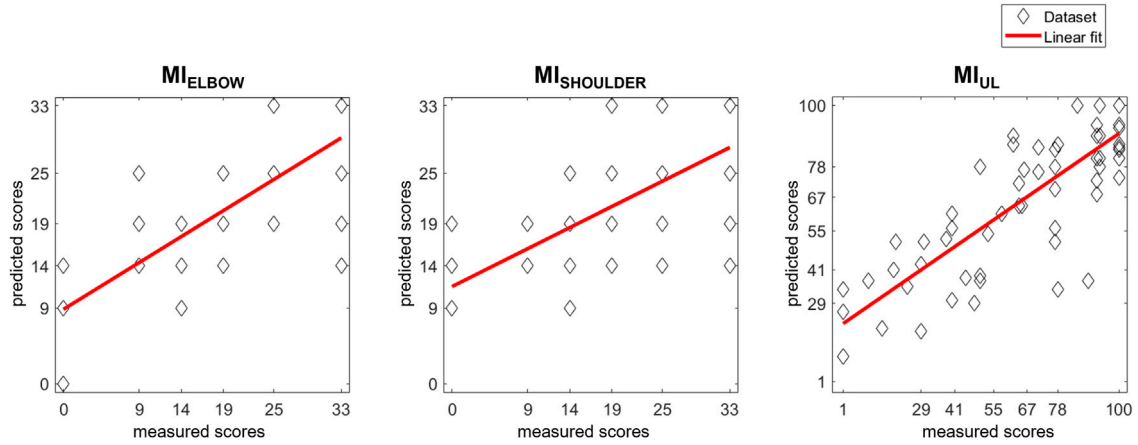

FIGURE 3
Scatter plot of MI scores prediction with LOOCV models. Each patient's actual score was plotted together with the predictions generated by the models. The results of a linear polynomial fitting are also shown.

TABLE 3 Results from the predictive models for the discharge clinical outcomes (MI_{ELBOW}, $MI_{SHOULDER}$, MI_{UL})by applying the Leave-One-Out Cross-Validation (LOOCV) procedure.

	LOOCV models			
	RMSE	$RMSE_n$ (%)	R^2 (R^2_{adj})	MAE (MAE_n)
MI_{ELBOW}(T2)	6.768	20	0.676 (0.631)	5.165 (22%)
$MI_{SHOULDER}$(T2)	7.177	22	0.600 (0.545)	5.680 (24%)
MI_{UL}(T2)	17.103	17	0.753 (0.719)	13.487 (20%)

The "new patients" MAE is the averaged error across all left-out subjects during the LOOCV procedure. Abbreviations:Motricity Index affected elbow flexion (MI_{ELBOW}); Motricity Index affected shoulder abduction ($MI_{SHOULDER}$); Motricity Index affected Upper Limb (MI_{UL}); Root Mean Square Error (RMSE); normalized Root Mean Square Error ($RMSE_n$);percentage of variance explained (R^2); adjusted percentage of variance explained (R_{adj}^2); Mean Absolute Error (MAE); normalized Mean Absolute Error (MAE_n); after ulRT (T2).

categorical variables). In contrast, in the present study, we developed models to predict Motricity Indexes at discharge from selected RMK features and found that the SSV and LOOCV validation procedures explained 54% and 71% of the variance in clinical scores at discharge respectively. Normalized errors ranged from 22% to 35% in the SSV models, and from 20% to 24% in the LOOCV ones.

Our findings are in agreement with the studies of Agrafiotis *et al.* (Agrafiotis et al., 2021) and Moretti *et al.* (Moretti et al., 2021), although they analyzed chronic stroke patients. Both studies found a significant correlation between RMK metrics and clinical outcomes (upper limb Fugl-Meyer Assessment (Agrafiotis et al., 2021; Moretti et al., 2021), Motor Power (Agrafiotis et al., 2021), NIH stroke scale (Agrafiotis et al., 2021), modified Rankin scale (Agrafiotis et al., 2021), Wolf Motor Function Test (Moretti et al., 2021), Barthel Index (Moretti et al., 2021), and Medical Research Council score (Moretti et al., 2021) demonstrating that traditional stroke assessment scales can be accurately reproduced by robotic measurements. The outcomes of these studies pave the way for the use of RMK data to reduce the sample size needed for future clinical trials on chronic stroke patients (Agrafiotis et al., 2021) and to objectively, quantitatively, and rapidly assess impairments in body function (Moretti et al., 2021). However, most published studies on this topic examined the relationships between technology-based metrics and clinical assessment outcomes measured close in time (e.g., concurrently) (Krebs et al., 2014; Grimm et al., 2021; Olesh et al., 2014; Wang et al., 1109). Conversely, our findings showed that baseline data collected from a rehabilitation robotic device are able to predict clinical outcomes at discharge with statistically significant accuracy. Mostafavi *et al.* (Mostafavi et al., 2013) showed results similar to ours although the RMK metrics derived from an exoskeleton robot and the predicted rehabilitation outcome at discharge was an overall measure of disability in ADL (i.e., the Functional Independence Measure).

Data analysis showed that the significant features for predicting the discharge Motricity Indexes were the errors of the trajectories towards the body, which were strongly influenced by the typical postural patterns of the upper extremity after stroke (Raghavan, 2015): the trajectory towards the body is performed by flexing the elbow and extending the shoulder and is representative of upper limb spastic co-contraction (Bensmail et al., 2010) and the typical pathological flexor strategy of stroke survivors (Hefter et al., 2012; McMorland et al., 2015). In our analysis, the error of the trajectory towards the body was a significant predictor in both SSV and LOOCV models, showing that the less accurate and controlled the trajectory towards the pathological patterns is, the smaller muscle strength, assessed with the Motricity Index, is at the end of the ulRT. Our findings agree partly with Gialanella & Santoro (Gialanella and Santoro, 2015), who showed that at the end of rehabilitation, the motor score of the functional independence measure was lower in patients having at admission, the only flexor synergy of the affected limbs. Similarly, the systematic review by Coupar *et al.* (Coupar et al., 2012) found strong evidence that less impairment at baseline is associated with better upper limb recovery. Conversely, the outcomes of our model are not in accordance with Welmer *et al.* (Welmer et al., 2006) who found that stroke patients with typical pathological synergies had significantly better functioning scores.

In our previous analysis of the data (Goffredo et al., 2021), the error of the trajectory towards the body negatively affects the probability of increasing one class in the discharge Motricity Indexes. However, in the re-analysis of data with least squares multiple linear regression, we found that the error of the trajectory towards the body was a significant predictor of Motricity Indexes, which strongly correlate ($r > 0.8$ for the MI_{UL}) with the therapist-assigned ones (Figures 2, 3). The comparison between the SSV and the LOOCV models showed that the error of the trajectory towards the body was a significant predictor in both models, whereas the same metric towards target D appeared in the SSV models.

In the literature, the most widely recognized predictor of upper limb functional outcome is the PREP2 tool (Stinear et al., 2017; Connell et al., 2021), which is based on clinical, MRI, and TMS biomarkers. Despite its high accuracy, the major characteristic of PREP2 is that TMS is not readily available in many clinical settings. Therefore, in rehabilitation hospitals equipped with robots for ulRT, our ecological, quantitative, objective analysis of baseline RMK data could be a valuable alternative to predict the rehabilitation outcome. Furthermore, since RMK metrics are representative of the ability to perform goal-directed movements, RMK biomarkers are able to predict rehabilitation outcomes according to the motor synergies at the baseline.

This study has the following limitations due to its retrospective design: a limited number of subjects; lack of an ICF-based assessment (considering body function, activity, and participation); and lack of RMK data from able-bodied subjects. Considering the SSV models, the training and validation datasets differed with respect to the time of stroke onset: although no statistical significance was found between groups (p-value>0.05), it may have influenced the presence of stereotypic movement synergies. Although the analysis normalized the time of stroke onset before modelling, future studies with a more homogeneous sample of patients would be interesting. The limitation of the study in terms of database size can be partially overcome considering that LOOCV models are more reliable and unbiased than SSV ones (Bishop, 1995) and seem particularly suitable when the dataset is small and an accurate estimation of model performance is required. In addition, the LOOCV models confirmed the outcomes of the SSV procedure with a correlation of up to $R^2 = 0.753$ ($RMSE_n = 17\%$). However, the future research agenda should consider large longitudinal studies including different categories of robots for upper limb rehabilitation (Gandolfi et al., 2021), evaluating the patients with an ICF-based assessment, and comparing the outcomes with a control group composed of able-bodied subjects.

Nevertheless, the study highlights that in stroke ulRT, the motor patterns assessed with RMK metrics strongly relate to discharge rehabilitation outcome and that the accuracy in performing elbow flexion movement is a significant predictor of outcome. The developed models, thus, are able to predict the clinical assessment of upper limb muscle strength and can be useful to clinicians to assess, manage, and program a more specific and appropriate rehabilitation in subacute stroke patients.

Conclusion

Multidirectional 2D RMK-based predictive models were developed and validated for discharge rehabilitation outcomes in sixty-six subacute stroke patients who performed ulRT with a planar end-effector robot. Accuracy in performing elbow flexion and shoulder extension movements was found to be a significant predictor of muscle strength at the end of ulRT: patients with a pathological upper limb flexor strategy were less likely to increase muscle strength at discharge.

Since the potential recovery of motor function depends on the synergies that occur after stroke, quantitative and measurable knowledge of upper limb function before initiation of physical therapy could be useful for an accurate and individualized prognosis, allowing more realistic expectations for recovery and helping to set realistic goals with a personalized rehabilitation program. In this respect, the results of this study suggest that subacute stroke patients with a marked flexor strategy tend to have a worse rehabilitation outcome at discharge: in these cases, physical therapy should focus on developing beneficial health synergies and avoid reinforcing pathological patterns.

Data availability statement

The raw data supporting the conclusions of this article will be made available by the authors, without undue reservation.

Ethics statement

The studies involving human participants were reviewed and approved by Ethical Committee of the IRCCS San Raffaele Roma (Rome, Italy) on 22/02/2017 (code number: 06/17). Written informed consent for participation was not required for this study in accordance with the national legislation and the institutional requirements.

Author contributions

MG has made substantial contributions to conception and design. SaP, DG, and MC participated in the enrolment phase, carried out the treatment, and carried out the clinical and kinematic assessments. MG and StP designed the algorithm for data analysis. MG participated in the study design and coordination and statistical analysis. MF, FP, SaP, StP, and DL participated in the manuscript revisions. MG gave the final approval of the version. All authors contributed to the article and approved the submitted version.

Funding

MG, StP, SaP, DG, MC, DLP, and MF were supported by the Italian Ministry of Health (Ricerca corrente).

Conflict of interest

The authors declare that the research was conducted in the absence of any commercial or financial relationships that could be construed as a potential conflict of interest.

Publisher's note

All claims expressed in this article are solely those of the authors and do not necessarily represent those of their affiliated organizations, or those of the publisher, the editors and the reviewers. Any product that may be evaluated in this article, or claim that may be made by its manufacturer, is not guaranteed or endorsed by the publisher.

References

Agrafiotis, D. K., Yang, E., Littman, G. S., Byttebier, G., Dipietro, L., DiBernardo, A., et al. (2021). Accurate prediction of clinical stroke scales and improved biomarkers of motor impairment from robotic measurements. *Plos one* 16 (1), e0245874. doi:10.1371/journal.pone.0245874

Balasubramanian, S., Colombo, R., Sterpi, I., Sanguineti, V., and Burdet, E. (2012). Robotic assessment of upper limb motor function after stroke. *Am. J. Phys. Med. Rehabilitation* 91 (11), S255–S269. doi:10.1097/phm.0b013e31826bcdc1

Bensmail, D., Robertson, J. V., Fermanian, C., and Roby-Brami, A. (2010). Botulinum toxinto treat upper-limb spasticity in hemiparetic patients: Analysis of functionand kinematics of reaching movements. *Neurorehabil. Neural Repair* 24, 273–281. doi:10.1177/1545968309347682

Bishop, C. M. (1995). *Neural networks for pattern recognition*. Oxford, United Kingdom: Oxford University Press.

Bohannon, R. W. (1999). Motricity index scores are valid indicators of paretic upper extremity strength following stroke. *J. Phys. Ther. Sci.* 11 (2), 59–61. doi:10.1589/jpts.11.59

Bosecker, C., Dipietro, L., Volpe, B., and Igo Krebs, H. (2010). Kinematic robot-based evaluation scales and clinical counterparts to measure upper limb motor performance in patients with chronic stroke. *Neurorehabil. Neural Repair* 24 (1), 62–69. doi:10.1177/1545968309343214

Colombo, R., Pisano, F., Micera, S., Mazzone, A., Delconte, C., Carrozza, M., et al. (2005). Robotic techniques for Upper Limb Evaluation and rehabilitation of stroke patients. *IEEE Trans. Neural Syst. Rehabil. Eng.* 13 (3), 311–324. doi:10.1109/tnsre.2005.848352

Connell, L. A., Chesworth, B., Ackerley, S., Smith, M. C., and Stinear, C. M. (2021). Implementing the PREP2 algorithm to predict upper limb recovery potential after stroke in clinical practice: A qualitative study. *Phys. Ther.* 101 (5), pzab040. doi:10.1093/ptj/pzab040

Coupar, F., Pollock, A., Rowe, P., Weir, C., and Langhorne, P. (2012). Predictors of upper limb recovery after stroke: A systematic review and meta-analysis. *Clin. Rehabil.* 26 (4), 291–313. doi:10.1177/0269215511420305

Dipietro, L., Krebs, H. I., Volpe, B. T., Stein, J., Bever, C., Mernoff, S. T., et al. (2011). Learning, not adaptation, characterizes stroke motor recovery: Evidence from kinematic changes induced by robot-assisted therapy in trained and untrained task in the same workspace. *IEEE Trans. Neural Syst. Rehabil. Eng.* 20 (1), 48–57. doi:10.1109/tnsre.2011.2175008

Duret, C., Hutin, E., Lehenaff, L., and Gracies, J. M. (2015). Do all sub acute stroke patients benefit from robot-assisted therapy? A retrospective study. *Restor. neurology Neurosci.* 33 (1), 57–65. doi:10.3233/rnn-140418

Duret, C., Pila, O., Grosmaire, A. G., and Koeppel, T. (2019). Can robot-based measurements improve prediction of motor performance after robot-assisted upper-limb rehabilitation in patients with moderate-to-severe sub-acute stroke? *Restor. Neurol. Neurosci.* 37 (2), 119–129. doi:10.3233/rnn-180892

Duret, C., Courtial, O., and Grosmaire, A. G. (2016). Kinematic measures for upper limb motor assessment during robot-mediated training in patients with severe sub-acute stroke. *Restor. Neurol. Neurosci.* 34 (2), 237–245. doi:10.3233/rnn-150565

Franceschini, M., Goffredo, M., Pournajaf, S., Paravati, S., Agosti, M., De Pisi, F., et al. (2018). Predictors of activities of daily living outcomes after upper limb robot-assisted therapy in subacute stroke patients. *PloS one* 13 (2), e0193235. doi:10.1371/journal.pone.0193235

Gandolfi, M., Valè, N., Posteraro, F., Morone, G., Dell'orco, A., Botticelli, A., et al. (2021). State of the art and challenges for the classification of studies on electromechanical and robotic devices in neurorehabilitation: A scoping review. *Eur. J. Phys. Rehabil. Med.* 57, 831–840. doi:10.23736/s1973-9087.21.06922-7

Gialanella, B., and Santoro, R. (2015). Prediction of functional outcomes in stroke patients: The role of motor patterns according to limb synergies. *Aging Clin. Exp. Res.* 27 (5), 637–645. doi:10.1007/s40520-015-0322-7

Goffredo, M., Mazzoleni, S., Gison, A., Infarinato, F., Pournajaf, S., Galafate, D., et al. (2019). Kinematic parameters for tracking patient progress during upper limb robot-assisted rehabilitation: An observational study on subacute stroke subjects. *Appl. Bionics Biomech.* 20, 1–12. doi:10.1155/2019/4251089

Goffredo, M., Pournajaf, S., Proietti, S., Gison, A., Posteraro, F., and Franceschini, M. (2021). Retrospective robot-measured upper limb kinematic data from stroke patients are novel biomarkers. *Front. Neurol.* 12, 803901. doi:10.3389/fneur.2021.803901

Grimm, F., Kraugmann, J., Naros, G., and Gharabaghi, A. (2021). Clinical validation of kinematic assessments of post-stroke upper limb movements with a multi-joint arm exoskeleton. *J. Neuroeng. Rehabil.* 18 (1), 92–11. doi:10.1186/s12984-021-00875-7

Hefter, H., Jost, W. H., Reissig, A., Zakine, B., Bakheit, A. M., and Wissel, J. (2012). Classification of posture in poststroke upper limb spasticity: A potential decision tool for botulinum toxin A treatment? *Int. J. Rehabilitation Res.* 35 (3), 227–233. doi:10.1097/mrr.0b013e328353e3d4

Koeppel, T., and Pila, O. (2020). Test-retest reliability of kinematic assessments for upper limb robotic rehabilitation. *IEEE Trans. Neural Syst. Rehabil. Eng.* 28 (9), 2035–2042. doi:10.1109/tnsre.2020.3013705

Krebs, H. I., Krams, M., Agrafiotis, D. K., Di Bernardo, A., Chavez, J. C., Littman, G. S., et al. (2014). Robotic measurement of arm movements after stroke establishes biomarkers of motor recovery. *Stroke* 45 (1), 200–204. doi:10.1161/strokeaha.113.002296

Langhorne, P., Sandercock, P., and Prasad, K. (2009). Evidence-based practice for stroke. *Lancet Neurol.* 8 (4), 308–309. doi:10.1016/s1474-4422(09)70060-2

Mazzoleni, S., Sale, P., Franceschini, M., Bigazzi, S., Carrozza, M. C., Dario, P., et al. (2013). Effects of proximal and distal robot-assisted upper limb rehabilitation on chronic stroke recovery. *NeuroRehabilitation* 33 (1), 33–39. doi:10.3233/nre-130925

McMorland, A. J., Runnalls, K. D., and Byblow, W. D. (2015). A neuroanatomical framework for upper limb synergies after stroke. *Front. Hum. Neurosci.* 9, 82. doi:10.3389/fnhum.2015.00082

Mehrholz, J., Pohl, M., Platz, T., Kugler, J., and Elsner, B. (2018). Electromechanical and robot-assisted arm training for improving activities of daily living, arm function, and arm muscle strength after stroke. *Cochrane Database Syst. Rev.* 9, CD006876. doi:10.1002/14651858.CD006876.pub5

Micera, S., Carpaneto, J., Posteraro, F., Cenciotti, L., Popovic, M., and Dario, P. (2005). Characterization of upper arm synergies during reaching tasks in able-bodied and hemiparetic subjects. *Clin. Biomech.* 20 (9), 939–946. doi:10.1016/j.clinbiomech.2005.06.004

Moore, D. S., Notz, W. I., and Flinger, M. A. (2013). *The basic practice of statistics*. New York: WH Freeman and Company, 138.

Moretti, C. B., Hamilton, T., Edwards, D. J., Peltz, A. R., Chang, J. L., Cortes, M., et al. (2021). Robotic kinematic measures of the arm in chronic stroke: Part 2–strong correlation with clinical outcome measures. *Bioelectron. Med.* 7 (1), 21–13. doi:10.1186/s42234-021-00082-8

Morone, G., Cocchi, I., Paolucci, S., and Iosa, M. (2020). Robot-assisted therapy for arm recovery for stroke patients: State of the art and clinical implication. *Expert Rev. Med. devices* 17 (3), 223–233. doi:10.1080/17434440.2020.1733408

Mostafavi, S. M., Glasgow, J. I., Dukelow, S. P., Scott, S. H., and Mousavi, P. IEEE, 1–6.Prediction of stroke-related diagnostic and prognostic measures using robot-based evaluationProceedings of the 2013 IEEE 13th International Conference on Rehabilitation Robotics (ICORR)24-26 June 2013

Nichols-Larsen, D. S., Clark, P. C., Zeringue, A., Greenspan, A., and Blanton, S. (2005). Factors influencing stroke survivors' quality of life during subacute recovery. *Stroke* 36 (7), 1480–1484. doi:10.1161/01.STR.0000170706.13595.4f

Olesh, E. V., Yakovenko, S., and Gritsenko, V. (2014). Automated assessment of upper extremity movement impairment due to stroke. *PloS one* 9 (8), e104487. doi:10.1371/journal.pone.0104487

Panarese, A., Colombo, R., Sterpi, I., Pisano, F., and Micera, S. (2012). Tracking motor improvement at the subtask level during robot-aided neurorehabilitation of stroke patients. *Neurorehabil. Neural Repair* 26 (7), 822–833. doi:10.1177/1545968311431966

Raghavan, P. (2015). Upper limb motor impairment after stroke. *Phys. Med. Rehabil. Clin. N. Am.* 26, 599–610. doi:10.1016/j.pmr.2015.06.008

Scott, S. H., and Dukelow, S. P. (2011). Potential of robots as next-generation technology for clinical assessment of neurological disorders and upper-limb therapy. *J. Rehabilitation Res. Dev.* 48 (4), 335. doi:10.1682/jrrd.2010.04.0057

Stinear, C. M., Byblow, W. D., Ackerley, S. J., Smith, M. C., Borges, V. M., and Barber, P. A. (2017). PREP2: A biomarker-based algorithm for predicting upper limb function after stroke. *Ann. Clin. Transl. Neurol.* 4 (11), 811–820. doi:10.1002/acn3.488

Tran, V. D., Dario, P., and Mazzoleni, S. (2018). Kinematic measures for upper limb robot-assisted therapy following stroke and correlations with clinical outcome measures: A review. *Med. Eng. Phys.* 53, 13–31. doi:10.1016/j.medengphy.2017.12.005

Wade, D. T. (1989). Measuring arm impairment and disability after stroke. *Int. Disabil. Stud.* 11, 89–92. doi:10.3109/03790798909166398

Wang, J., Yu, L., Wang, J., Guo, L., Gu, X., and Fang, Q. IEEE, 1–4. doi:10.1109/ISBB.2014.6820907Automated Fugl-Meyer assessment using SVR modelProceedings of the 2014 IEEE International Symposium on Bioelectronics and Bioinformatics (IEEE ISBB 2014)11-14 April 2014Chung Li, Taiwan

Welmer, A. K., Holmqvist, L. W., and Sommerfeld, D. K. (2006). Hemiplegic limb synergies in stroke patients. *Am. J. Phys. Med. rehabilitation* 85 (2), 112–119. doi:10.1097/01.phm.0000197587.78140.17

frontiers | Frontiers in Bioengineering and Biotechnology

TYPE Original Research
PUBLISHED 10 February 2023
DOI 10.3389/fbioe.2023.1136368

Check for updates

OPEN ACCESS

EDITED BY
Yih-Kuen Jan,
University of Illinois at Urbana-Champaign,
United States

REVIEWED BY
Ben-Yi Liau,
Feng Chia University, Taiwan
Li-Wei Chou,
National Yang Ming Chiao Tung University,
Taiwan

*CORRESPONDENCE
Wei-Li Hsu,
wlhsu@ntu.edu.tw

SPECIALTY SECTION
This article was submitted to
Biomechanics,
a section of the journal
Frontiers in Bioengineering and
Biotechnology

RECEIVED 03 January 2023
ACCEPTED 26 January 2023
PUBLISHED 10 February 2023

CITATION
Kantha P, Hsu W-L, Chen P-J, Tsai Y-C and Lin J-J (2023), A novel balance training approach: Biomechanical study of virtual reality-based skateboarding.
Front. Bioeng. Biotechnol. 11:1136368.
doi: 10.3389/fbioe.2023.1136368

COPYRIGHT
© 2023 Kantha, Hsu, Chen, Tsai and Lin. This is an open-access article distributed under the terms of the Creative Commons Attribution License (CC BY). The use, distribution or reproduction in other forums is permitted, provided the original author(s) and the copyright owner(s) are credited and that the original publication in this journal is cited, in accordance with accepted academic practice. No use, distribution or reproduction is permitted which does not comply with these terms.

A novel balance training approach: Biomechanical study of virtual reality-based skateboarding

Phunsuk Kantha[1], Wei-Li Hsu[1,2]*, Po-Jung Chen[1], Yi-Ching Tsai[1] and Jiu-Jenq Lin[1,3]

[1]School and Graduate Institute of Physical Therapy, College of Medicine, National Taiwan University, Taipei, Taiwan, [2]Physical Therapy Center, National Taiwan University Hospital, Taipei, Taiwan, [3]Division of Physical Therapy, Department of Physical Medicine and Rehabilitation, National Taiwan University Hospital, Taipei, Taiwan

Introduction: The use of virtual reality (VR) technology in training and rehabilitation gained increasing attention in recent years due to its potential to provide immersive and interactive experiences. We developed a novel VR-based balance training, VR-skateboarding, for improving balance. It is important to investigate the biomechanical aspects of this training, as it would have benefited both health professionals and software engineers.

Aims: This study aimed to compare the biomechanical characteristics of VR-skateboarding with those of walking.

Materials and Methods: Twenty young participants (10 males and 10 females) were recruited. Participants underwent VR-skateboarding and walking at the comfortable walking speed, with the treadmill set at the same speed for both tasks. The motion capture system and electromyography were used to determine joint kinematics and muscle activity of the trunk and legs, respectively. The force platform was also used to collect the ground reaction force.

Results: Participants demonstrated increased trunk flexion angles and muscle activity of trunk extensor during VR-skateboarding than during walking ($p < 0.01$). For the supporting leg, participants' joint angles of hip flexion and ankle dorsiflexion, as well as muscle activity of knee extensor, were higher during VR-skateboarding than during walking ($p < 0.01$). For the moving leg, only hip flexion increased in VR-skateboarding when compared to walking ($p < 0.01$). Furthermore, participants increased weight distribution in the supporting leg during VR-skateboarding ($p < 0.01$).

Conclusion: VR-skateboarding is a novel VR-based balance training that has been found to improve balance through increased trunk and hip flexion, facilitated knee extensor muscles, and increased weight distribution on the supporting leg compared to walking. These differences in biomechanical characteristics have potential clinical implications for both health professionals and software engineers. Health professionals may consider incorporating VR-skateboarding into training protocols to improve balance, while software engineers may use this information to design new features in VR systems. Our study suggests that the impact of VR-skateboarding particularly manifest when focusing on the supporting leg.

KEYWORDS

balance, virtual reality, skateboarding, biomechanics, training

Introduction

Virtual reality (VR) technology allows users to interact with computer-generated environments in a simulated environment (Cipresso et al., 2018). In healthcare, VR has been used as a tool for rehabilitation and training, with the potential to improve motor function, cognitive function, and psychological wellbeing in individuals with various conditions, such as stroke, low back pain, and Parkinson's disease (Lheureux et al., 2020; Liang et al., 2022; Yalfani et al., 2022). The immersive nature of VR can increase adherence and motivation to training programs and lead to improved outcomes (Moon et al., 2021; Recenti et al., 2021). Moreover, VR can be used for sensory integration exercise as it engages multiple senses, including vestibular, vision, and proprioception, simultaneously (Yen et al., 2011). Thus, studies have found that VR-based training can be effective in improving motor function, balance, and mobility in individuals who have had a stroke, as well as cognitive function in those with brain injury and other neurological conditions (Kumar et al., 2018; Chen et al., 2021). VR-based training has also been shown to have positive effects on psychological well-being, such as reducing anxiety and depression in individuals with chronic pain (Rawlins et al., 2021). Therefore, VR-based training has the potential to enhance the effectiveness of various interventions in healthcare.

Exergames, also known as exercise games, are interactive technology-based physical activities that are designed to provide an enjoyable and engaging way to get physically active (Sween et al., 2014). Exergames have gained popularity in recent years, particularly among older adults or individuals with chronic conditions, as a way to promote physical activity and improve physical fitness (Sween et al., 2014; Moret et al., 2022). Exergames can involve a wide range of physical activities, from dancing and jumping to moving arms and using other body movements to control the game (Asín-Prieto et al., 2020; Lopes et al., 2020). Research has shown that regular participation in exergames can improve coordination, balance, and other physical fitness measures, as well as reduce stress and improve mental health outcomes such as mood and cognitive function (Sween et al., 2014; Moret et al., 2022). Exergames can be played on video game consoles, smartphones, and VR head-mounted displays, and are suitable for people of all ages and fitness levels (Asín-Prieto et al., 2020). The evidence on the effects of exergames on health outcomes is mixed, overall, they suggest that exergames can be a useful tool for promoting physical activity and improving physical and mental health.

Unilateral leg training is a type of exercise that focuses on strengthening and conditioning one leg at a time (Liao et al., 2022). This type of training can be useful for a variety of purposes, including improving muscle imbalances, preventing injuries, and rehabilitating after an injury (Manca et al., 2017; Liao et al., 2022). Unilateral leg training can be performed using a variety of exercises, such as lunges, single-leg squats, and single-leg deadlifts, using body weight or added resistance (Baumgart et al., 2017; Manca et al., 2017). This type of training can be especially beneficial for athletes and individuals with a history of lower body injuries, as it can help to improve balance, stability, and overall leg strength (Liao et al., 2022). In addition, research has shown that unilateral leg training can be effective for improving muscle strength and power, as well as increasing muscle activation and coordination (Zhou et al., 2022). Unilateral leg training can be incorporated into a well-rounded fitness routine along with other forms of exercise to improve overall physical fitness and balance performance (Manca et al., 2017; Liao et al., 2022). However, it is important to use proper technique to prevent injury and ensure optimal results.

In order to combine VR-based training, exergames, and unilateral leg training, we developed an exergame called virtual reality skateboarding (VR-skateboarding). Moreover, VR technology was used to simulate a real-world environment in a safe setting, as well as to provide task-specific training for balance in the unilateral leg. However, the biomechanical characteristics of VR-skateboarding have not yet been fully explored. Therefore, we conducted a study to compare the biomechanical characteristics of VR-skateboarding with those of walking. We chose to compare these two activities because they involve similar movement patterns, such as repetitive leg movements. We hypothesized that VR-skateboarding would result in greater joint angles, muscle activity, and weight distribution compared to walking, which could potentially improve balance. The findings of this study could be useful for health professionals in understanding the mechanisms of training effects and designing training protocols, as well as for software engineers in creating new features and implementing multidisciplinary approaches.

Materials and methods

VR-skateboarding

VR-skateboarding is a training approach that combines VR and treadmill technology. It involved using a skateboard that was integrated with a split-belt treadmill (QQ-mill, Motekforce Link, Netherlands), as shown in Figure 1; Supplementary file S1. The skateboard was placed on the stationary belt of the treadmill, while the moving belt was set to a comfortable walking speed for the participant. Comfortable walking speed was measured using a 10-m walk test, which is the most common and reliable test (Bohannon, 1997; Bohannon and Williams Andrews, 2011; Cheng et al., 2020b). The leg that was placed on the skateboard was referred to as the "supporting leg," while the leg that slide on the moving belt was referred to as the "moving leg." For safety purposes, the skateboard wheels were fixed statically on the stationary belt of the treadmill. Handrails were also available at waist level for support during VR-skateboarding, if needed.

A virtual scenario for VR-skateboarding was created using Unity3D software (version 5.3.2, San Francisco, United States) and displayed using virtual reality head-mounted displays (HTC VIVE, HTC Corporation, New Taipei City, Taiwan). The virtual scenario depicted skateboarding on a city road, as shown in Figure 2. Three wireless inertial measurement unit sensors (HTC VIVE trackers, HTC Corporation, New Taipei City, Taiwan) were used in VR-skateboarding as follows: 1) two trackers were placed on the participant's legs to track leg movements. The speed and distance travelled in the virtual scenario were adjusted based on the movement of the tracker on the moving leg; 2) one tracker was attached in front of the skateboard and used to control the left and right direction of skateboarding to avoid obstacles in the virtual scenario. The cumulative distance travelled was provided as real-time virtual feedback and a final score to motivate participants during VR-skateboarding.

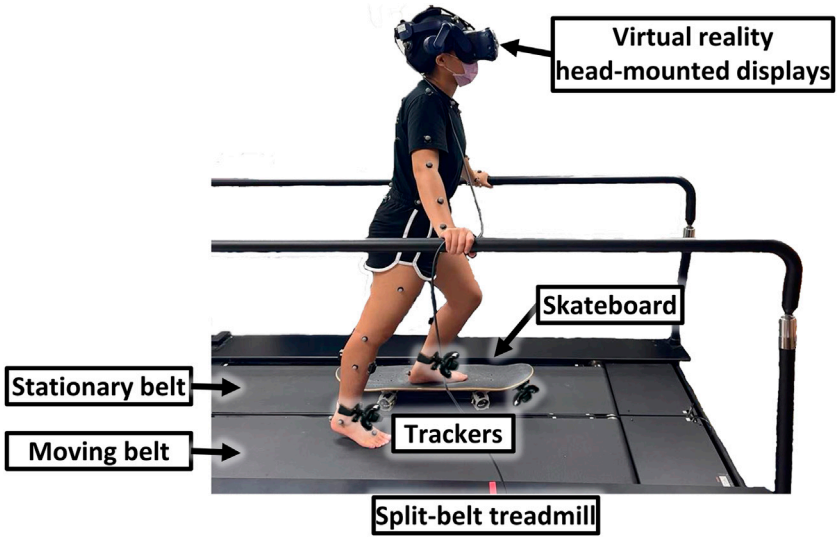

FIGURE 1
An illustration of a virtual reality skateboarding system.

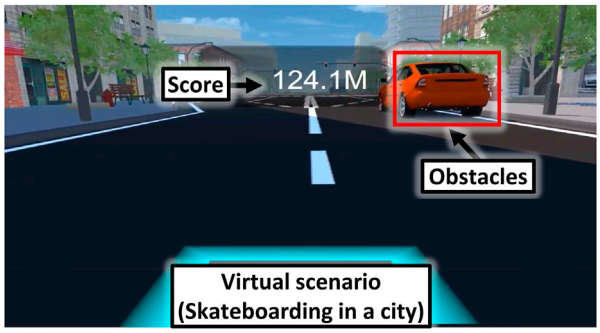

FIGURE 2
An illustration of a virtual scenario.

Participants

The eligibility of participants was assessed based on inclusion and exclusion criteria. The inclusion criteria included being between the ages of 20 and 40 years and not having any symptoms such as leg pain or numbness. The exclusion criteria included having had previous surgery and having neurological disorders such as stroke, lumbar radiculopathy, or spinal cord injury.

Procedure

For walking, participants were asked to walk on the split-belt treadmill at a comfortable walking speed for 1 min × 5 times. Then, participants were asked to perform VR-skateboarding using their non-dominant leg as the supporting leg on the skateboard. Participants were instructed to skate with their dominant leg as the moving leg at a comfortable walking speed for 1 min × 5 times. According to previous studies, treadmill speed has the potential to impact biomechanical characteristics during movement (Möckel et al., 2003; Matjačić et al., 2019). In order to eliminate confounding factors from treadmill speed, the treadmill was set to the same speed (i.e., comfortable walking speed) for both VR-skateboarding and walking.

Evaluation

Joint kinematics measurements

A 3-dimensional motion capture system (VICON ver. 2.5, Oxford Metrics Ltd., Oxford, United Kingdom) with ten infrared cameras (VICON Bonita, Oxford Metrics, United Kingdom) was used to collect joint kinematic data at a sampling rate of 120 Hz. The system used 45 spherical retro-reflective markers (14 mm) placed over anatomical landmarks based on the Plug-In-Gait model (Cheng et al., 202b).

Muscle activity measurements

Surface electromyography (EMG) (TrignoTM, Delsys Inc., Boston, MA, United States) was used to collect muscle activity data (i.e., erector spinae: trunk extensor; gluteus medius: hip abductor; rectus femoris: knee extensor; and tibialis anterior: ankle dorsiflexor) (Wang et al., 2015). The sampling rate of the EMG was 960 Hz.

Ground reaction force measurements

Two force platforms (QQ-mill, Motekforce Link, Amsterdam, Netherlands) were used to collect ground reaction force (GRF) data. The force platforms were able to sample at a frequency of 960 Hz using LabVIEW software (National Instruments, Austin, TX, United States).

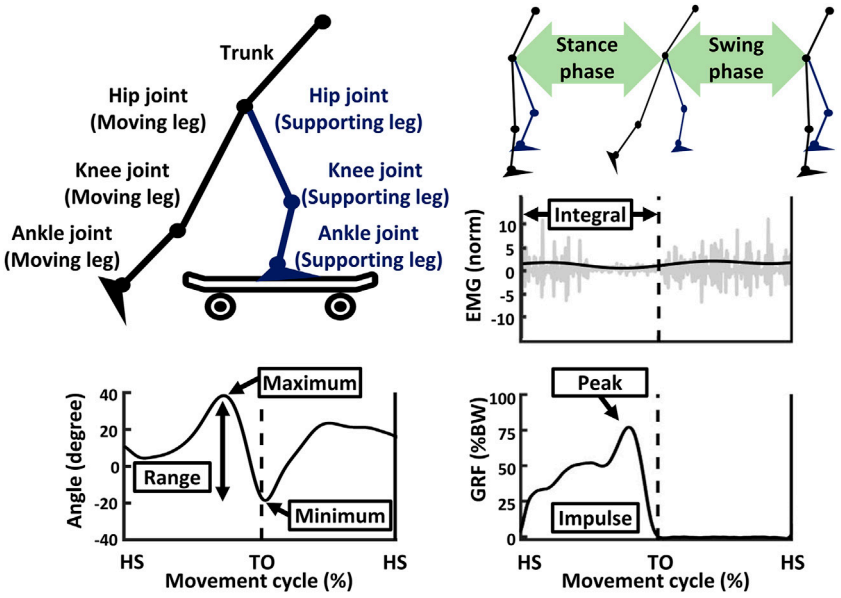

FIGURE 3
An illustration of data processing. EMG, electromyography; GRF, ground reaction force; %BW, percentage of body weight; HS, heel-strike of moving leg; TO, toe-off of moving leg.

Data processing

Data from the motion capture system, EMG, and force platforms were processed using a custom program written in MATLAB R2020a software (MathWorks, Natrick, MA, United States). The GRF of the moving leg was used to identify the movement cycle (i.e., the stance and swing phases) of each stride. A GRF threshold of 10 N was used to identify the movement cycle (Baumgart et al., 2017). A total of 100 stable strides were selected for analysis (Kubinski et al., 2015). The stance phase occurs from heel-strike to toe-off, while the swing phase occurs from toe-off to heel-strike, as shown in Figure 3.

For joint kinematics, the data were filtered using a 2nd-order low-pass Butterworth filter with a cut-off frequency of 3 Hz. The filtered data was smoothed using a moving average (Chien and Hsu, 2018). The minimum, maximum, and range values of the trunk, hip, knee, and ankle joints during entire movement cycle were calculated (Smith et al., 2016).

For muscle activities, the EMG data were filtered using a 2nd-order Butterworth filter with bandpass and notch filters at 30–350 Hz and 60 Hz, respectively (Adewuyi et al., 2016). The filtered data was full-wave rectified (using a root mean square) and smoothed (using a moving average) (Tabard-Fougère et al., 2018). The EMG was normalized using the resting EMG for each muscle (Wang et al., 2015). The EMG data was also time-normalized from 0 to 100 percent for each phase (Androwis et al., 2018). The integrals of normalized EMG (i.e., trunk extensor, hip abductor, knee extensor, and ankle dorsiflexor) were then separately reported for the stance and swing phases, as well as for the entire movement cycle (Vigotsky et al., 2017; Wu et al., 2019).

For GRF, the data were filtered using a 2nd-order low-pass Butterworth filter with a cut-off frequency of 5 Hz. The filtered data was smoothed using a moving average (Cheng et al., 2020a). The peak values of GRF in entire movement cycle were computed, while the impulse values of GRF were separately computed for the stance and swing phases, as well as for the entire movement cycle (Golyski et al., 2018; Lee et al., 2020; Jafarnezhadgero et al., 2021).

Statistical analysis

Statistical analysis was performed in Predictive Analytics Software Statistics 18.0 for Windows (SPSS, Chicago, IL, United States). The normality of all variables was determined using the Shapiro–Wilk test. Nevertheless, the data were not normally distributed. Thus, the non-parametric Wilcoxon signed-rank test was used to compare the variables between VR-skateboarding and walking. The p-value was set at 0.05 as statistically significant.

Results

Twenty young participants (age: 27.4 ± 2.8 years, height: 167.2 ± 10.0 cm, weight: 61.2 ± 11.6 kg, body mass index: 21.7 ± 2.0 kg/m^2) were recruited, with ten of them being female. All participants were right-leg dominant and used the left leg as the supporting leg and the right leg as the moving leg during VR-skateboarding. The average speed for VR-skateboarding and walking was 1.2 ± 0.1 m/s.

Joint kinematics

The joint kinematic results for both VR-skateboarding and walking are illustrated in Figure 4; Table 1.

During VR-skateboarding, participants exhibited greater minimum and maximum trunk angles and a wider range of movement in their trunk compared to walking ($z = -3.92$, $p <$

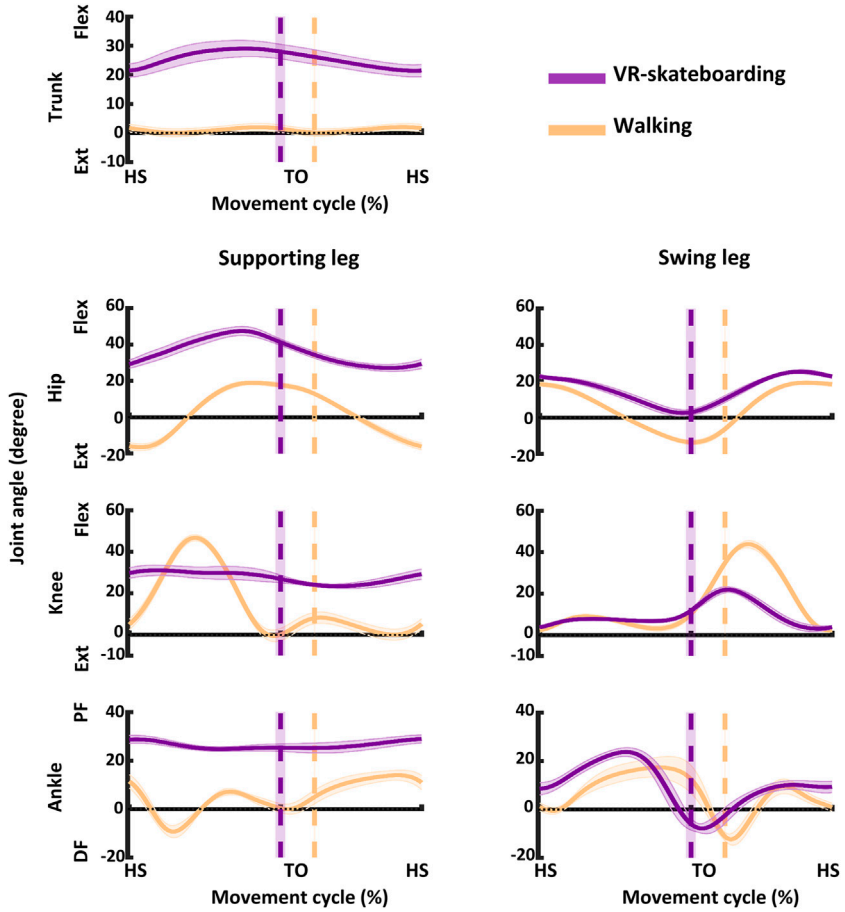

FIGURE 4
An illustration of joint kinematics. The solid line represents the mean and the shaded area represents the standard deviation. Flex, flexion; Ext, extension; PF, plantarflexion; DF, dorsiflexion; HS, heel-strike of moving leg; TO, toe-off of moving leg; VR-skateboarding, virtual reality skateboarding.

TABLE 1 Comparison of the joint kinematics during the entire movement cycle between VR-skateboarding and walking.

Body Segments		Joint Angle (degree)					
		Minimum		Maximum		Range	
		VR-skateboarding	Walking	VR-skateboarding	Walking	VR-skateboarding	Walking
Trunk		20.05 ± 2.14*	−0.45 ± 1.44	30.25 ± 2.60*	2.87 ± 1.25	10.19 ± 2.33*	3.32 ± 1.19
Hip	Supporting Leg	26.02 ± 1.59*	−17.18 ± 2.01	48.32 ± 2.83*	19.30 ± 1.04	22.30 ± 2.23*	36.48 ± 2.24
	Moving Leg	1.80 ± 1.60*	−13.77 ± 1.21	26.16 ± 1.21*	19.85 ± 1.04	24.36 ± 2.22*	33.62 ± 1.39
Knee	Supporting Leg	22.32 ± 1.98*	−1.65 ± 2.39	31.80 ± 3.36*	47.13 ± 1.38	9.48 ± 2.77*	48.78 ± 1.81
	Moving Leg	2.54 ± 1.04*	1.59 ± 1.13	23.28 ± 1.61*	44.99 ± 2.51	20.74 ± 2.00*	43.40 ± 2.24
Ankle	Supporting Leg	24.42 ± 2.79*	−9.03 ± 3.02	30.25 ± 2.12*	15.14 ± 2.53	5.82 ± 2.45*	24.17 ± 2.53
	Moving Leg	−12.09 ± 4.31	−13.08 ± 1.89	27.26 ± 4.84*	18.25 ± 4.50	39.35 ± 7.52*	31.33 ± 4.63

Values are mean ± standard deviation. VR-skateboarding, virtual reality skateboarding. Wilcoxon signed-rank test: *statistically significant values ($p < 0.05$).

0.01; z = −3.92, $p < 0.01$; and z = −3.92, $p < 0.01$, respectively). This indicated that participants bent their trunk forward more and moved in a wider range during VR-skateboarding when compared to walking.

In the supporting leg, participants demonstrated increased minimum and maximum hip (z = −3.92, $p < 0.01$; and z = −3.92, $p < 0.01$, respectively) and ankle (z = −3.92, $p < 0.01$; and z = −3.92, $p < 0.01$, respectively) angles during VR-

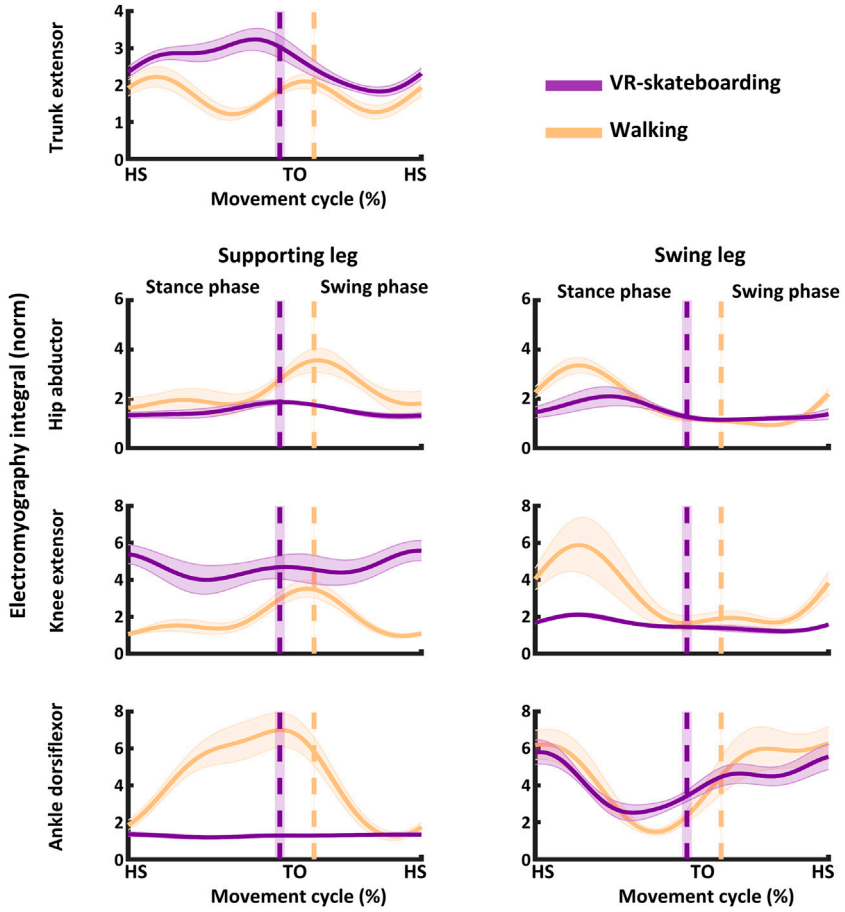

FIGURE 5
An illustration of muscle activity. The solid line represents the mean and the shaded area represents the standard deviation. HS, heel-strike of moving leg; TO, toe-off of moving leg; VR-skateboarding, virtual reality skateboarding.

skateboarding compared to walking. However, participants had reduced range of movement in the hip and ankle joints ($z = -3.92$, $p < 0.01$; and $z = -3.92$, $p < 0.01$, respectively) during VR-skateboarding compared to walking. The knee also showed increased minimum angle ($z = -3.92$, $p < 0.01$) but reduced maximum angle and range of movement ($z = -3.92$, $p < 0.01$; and $z = -3.92$, $p < 0.01$, respectively) during VR-skateboarding. The findings suggest that, in the supporting leg, VR-skateboarding entailed greater flexion in the hip and ankle joints and a smaller range of movement compared to walking. Additionally, during VR-skateboarding, participants demonstrated decreased flexion in the knee joint and a reduced range of movement in this joint.

In the moving leg, the hip joint angles showed a lower range of motion ($z = -3.92$, $p < 0.01$) during VR-skateboarding compared to walking, with both the minimum and maximum angles being higher ($z = -3.92$, $p < 0.01$; and $z = -3.92$, $p < 0.01$, respectively) in VR-skateboarding. The knee joint also showed a lower range of motion during VR-skateboarding ($z = -3.92$, $p < 0.01$), with the minimum angle being higher ($z = -2.72$, $p < 0.01$) and the maximum angle being lower ($z = -3.92$, $p < 0.01$). Whereas, the ankle joint demonstrated a greater range of motion during VR-skateboarding ($z = -3.80$, $p < 0.01$), with the maximum angle being higher ($z = -3.92$, $p < 0.01$) and the minimum angle showing no significant difference ($z = -1.30$, $p = 0.19$) compared to walking. VR-skateboarding involved greater hip flexion and a smaller range of movement in the moving leg compared to walking. However, it also entailed decreased knee flexion and a reduced range of movement, as well as increased ankle dorsiflexion and a greater range of movement.

Muscle activity

The muscle activity results for both VR-skateboarding and walking are illustrated in Figure 5; Table 2.

Muscle activity of the trunk extensor in the stance phase, swing phase, and entire movement cycle was higher during VR skateboarding than during walking ($z = -3.92$, $p < 0.01$; $z = -3.92$, $p < 0.01$; and $z = -3.92$, $p < 0.01$, respectively). This indicated that VR-skateboarding appeared to involve higher muscle activity in the trunk extensor muscles compared to walking.

In the supporting leg, muscle activity of the knee extensor was higher in the stance phase, swing phase, and entire movement cycle ($z = -3.92$, $p < 0.01$; $z = -3.92$, $p < 0.01$; $z = -3.92$, $p < 0.01$; and $z = -3.92$, $p < 0.01$, respectively) during VR-skateboarding than during walking. However, muscle activity in the hip abductor and ankle dorsiflexor was lower in the stance phase ($z = -3.80$, $p < 0.01$; and

TABLE 2 Comparison of the muscle activity between VR-skateboarding and walking.

Muscle groups		Electromyography integral (norm)					
		Stance Phase		Swing Phase		Entire Movement Cycle	
		VR-skateboarding	Walking	VR-skateboarding	Walking	VR-skateboarding	Walking
Trunk Extensors		2.88 ± 0.23*	1.71 ± 0.21	2.20 ± 0.16*	1.58 ± 0.17	2.54 ± 0.18*	1.65 ± 0.17
Hip Abductors	Supporting Leg	1.49 ± 0.13*	2.19 ± 0.31	1.55 ± 0.09*	2.56 ± 0.26	1.52 ± 0.09*	2.38 ± 0.28
	Moving Leg	1.82 ± 0.45*	2.16 ± 0.17	1.42 ± 0.43*	1.33 ± 0.38	1.62 ± 0.32*	1.75 ± 0.21
Knee Extensors	Supporting Leg	4.10 ± 0.77*	2.57 ± 0.25	4.58 ± 0.53*	2.56 ± 0.26	4.34 ± 0.57*	2.56 ± 0.27
	Moving Leg	1.82 ± 0.18*	3.61 ± 0.79	1.40 ± 0.23*	2.33 ± 0.53	1.61 ± 0.20*	2.97 ± 0.55
Ankle Dorsiflexors	Supporting Leg	1.23 ± 0.11*	2.57 ± 0.24	1.31 ± 0.10*	2.54 ± 0.25	1.27 ± 0.10*	2.56 ± 0.24
	Moving Leg	1.44 ± 0.28*	3.69 ± 0.57	1.42 ± 0.29*	5.92 ± 1.18	1.43 ± 0.27*	4.81 ± 0.79

Values are mean ± standard deviation. VR-skateboarding, virtual reality skateboarding. Wilcoxon signed-rank test: *statistically significant values ($p < 0.05$).

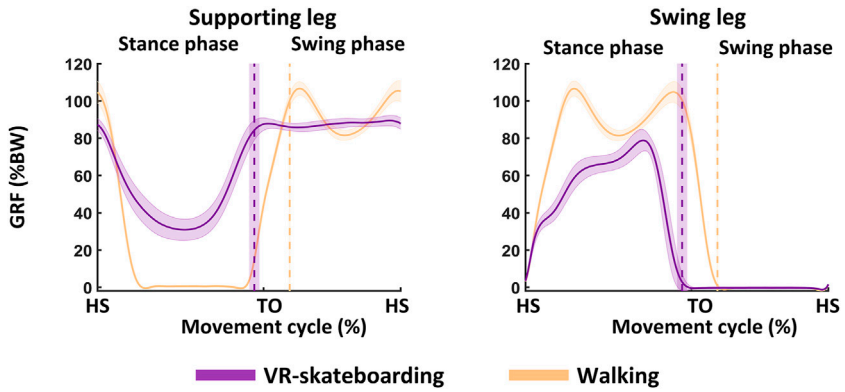

FIGURE 6
An illustration of ground reaction force. The solid line represents the mean and the shaded area represents the standard deviation. GRF, ground reaction force; %BW, percentage of body weight; HS, heel-strike of moving leg; TO, toe-off of moving leg; VR-skateboarding, virtual reality skateboarding.

z = −3.92, $p < 0.01$, respectively), swing phase (z = −3.92, $p < 0.01$; and z = −3.92, $p < 0.01$, respectively), and entire movement cycle (z = −3.92, $p < 0.01$; and z = −3.92, $p < 0.01$, respectively) during VR-skateboarding than during walking. The results suggest that VR-skateboarding entailed distinct muscle activity patterns compared to walking, specifically higher activity in the knee extensor but lower activity in the hip abductor and ankle dorsiflexor.

In the moving leg, VR-skateboarding was associated with lower muscle activity in the hip abductor during the stance phase (z = −3.17, $p < 0.01$) and entire movement cycle (z = −2.68, $p < 0.01$) compared to walking, but no significant difference was observed in the swing phase (z = −0.85, $p = 0.39$). Additionally, VR-skateboarding involved lower muscle activity in the knee extensor and ankle dorsiflexor in the stance phase (z = −3.92, $p < 0.01$; and z = −3.92, $p < 0.01$, respectively), swing phase (z = −3.92, $p < 0.01$; and z = −3.92, $p < 0.01$, respectively), and entire movement cycle (z = −3.92, $p < 0.01$; and z = −3.92, $p < 0.01$, respectively) compared to walking. These findings suggest that muscle activity in the hip abductor, knee extensor, and ankle dorsiflexor of the moving leg was lower during VR-skateboarding compared to walking, except for the hip abductor in the swing phase, which showed no difference.

Ground reaction force

Our results showed that the average stance phase during walking was 63.58% ± 0.24%. During VR-skateboarding, the average stance phase was 51.91% ± 1.74%. Hence, the stance phase was shorter during VR-skateboarding than during walking (z = −3.92, $p < 0.01$). The GRF results for both VR-skateboarding and walking are illustrated in Figure 6; Table 3 and Table 4.

In the supporting leg, the peak GRF during VR-skateboarding was lower than during walking (z = −3.92, $p < 0.01$). However, the impulse GRF during VR skateboarding was higher in the stance phase (z = −3.92, $p < 0.01$) and entire movement cycle (z = −3.92, $p < 0.01$) but lower in the swing phase (z = −3.92, $p < 0.01$) compared to walking. These results indicated that during VR-skateboarding, the force loading on the supporting leg and weight distribution in the swing phase were less compared to walking, but there was a greater distribution of weight during the stance phase and throughout the entire movement cycle.

In the moving leg, the peak and impulse GRF during VR-skateboarding was lower than walking (z = −3.92, $p < 0.01$; and z = −3.92, $p < 0.01$, respectively). The results showed that during VR-

TABLE 3 Comparison of the peak ground reaction force during the entire movement cycle between VR-skateboarding and walking.

Body segments	Peak ground reaction force (% body weight)	
	VR-skateboarding	Walking
Supporting leg	95.64 ± 2.08*	111.76 ± 2.35
Moving leg	83.28 ± 5.39*	111.48 ± 2.71

Values are mean ± standard deviation. VR-skateboarding, virtual reality skateboarding. Wilcoxon signed-rank test: *statistically significant values ($p < 0.05$).

TABLE 4 Comparison of the impulse ground reaction force between VR-skateboarding and walking.

Body Segments	*Impulse Ground Reaction Force (% Body Weight)*					
	Stance phase		Swing phase		Entire movement cycle	
	VR-skateboarding	Walking	VR-skateboarding	Walking	VR-skateboarding	Walking
Supporting leg	48.34 ± 5.84*	24.79 ± 0.85	87.95 ± 2.20*	93.64 ± 3.08	68.15 ± 3.05*	59.21 ± 1.88
Moving leg	53.51 ± 3.88*	76.72 ± 3.22	N/A	N/A	N/A	N/A

Values are mean ± standard deviation. VR-skateboarding, virtual reality skateboarding; N/A, not applicable. Wilcoxon signed-rank test: *statistically significant values ($p < 0.05$).

skateboarding, the force loading on the moving leg and weight distribution in the swing phase were lower compared to walking.

Discussion

Our study found that there were differences in joint kinematics, muscle activity, and weight distribution between VR-skateboarding and walking, particularly in the supporting leg. Previous research on skateboarding had primarily focused on the "ollie" technique, which involves using the skateboard to jump over obstacles, and therefore was not directly comparable to VR-skateboarding in our study (Frederick et al., 2006; Hu et al., 2021). Our results indicated that the supporting leg during VR-skateboarding involved higher trunk, hip, and ankle movements, as well as higher muscle activity of the knee extensor, and a higher weight distribution compared to walking. Based on these findings, we recommended VR-skateboarding as a potential rehabilitation training approach for improving balance.

During VR-skateboarding, participants demonstrated a greater range of trunk movement and flexion compared to walking. Previous research has indicated that trunk bending can help maintain the center of mass within the base of support during activities such as a unilateral squat (Eliassen et al., 2018; van den Tillaar and Larsen, 2020). In our study, VR-skateboarding involved balancing on a skateboard, which may have required participants to lean forward or bend their trunk to maintain balance and control. This may have explained the observed increase in trunk flexion during VR-skateboarding, as such movements may not have been necessary for walking. Our findings were consistent with previous studies that have shown that increases in trunk flexion can enhance muscle activity in the trunk extensor muscles eccentrically during the stance and swing phases (Voglar et al., 2016; Yoder et al., 2019). The flexion position involved in VR-skateboarding may also have increased the demands on the trunk extensor to maintain balance and control. Additionally, it is possible that the use of VR technology in VR-skateboarding may have contributed to the observed differences in trunk angles and movement (Horsak et al., 2021; Meinke et al., 2022). The visual input provided by the VR headset may have influenced the participant's trunk angles and movement in order to maintain balance and control within the virtual environment (Lin et al., 2019a; Benady et al., 2021). As a result, the increased trunk bending during VR-skateboarding may have led to higher muscle activity in the trunk extensor compared to walking. The increased trunk bending during VR-skateboarding leading to higher muscle activity in the trunk extensor may be an effective approach of exercising to improve balance.

In the supporting leg, VR-skateboarding resulted in higher hip and ankle joint kinematics, as well as increased muscle activity of the knee extensor, compared to walking. This could be attributed to the height difference between the skateboard and the treadmill belt, which required participants to constantly flex the joints in the supporting leg to maintain balance. Previous research has shown that the knee extensor and hip abductor in the supporting leg are activated to hold body weight during unilateral squatting (Eliassen et al., 2018; van den Tillaar and Larsen, 2020). Our study also found that the activation of the knee extensor in the supporting leg during VR-skateboarding was higher than during walking, both in the stance and swing phases. However, the activation of the hip abductor was lower during VR-skateboarding, possibly due to the support provided by the handrail (Komisar et al., 2019). In addition, the activation of the ankle dorsiflexor was lower during VR-skateboarding due to the stationary position of the supporting foot. This fixed position of the ankle joint may also have contributed to the decrease in ankle dorsiflexor activation observed in previous studies (Macrum et al., 2012; Guillén-Rogel et al., 2017).

In the moving leg, VR-skateboarding required participants to increase hip flexion and ankle dorsiflexion in order to maintain trunk flexion and clear their feet from the ground. However, participants exhibited lower joint angles of knee flexion during VR-skateboarding compared to walking. This may have been due to the shorter stance phase in VR-skateboarding, which can limit the range of motion at the hip and knee joints. Previous research has shown that a

shorter stance phase can result in reduced knee flexion angles (Yen et al., 2019). Additionally, the muscle activity of the lower extremity in the non-weight-bearing leg tends to decrease when body weight is reduced or shifted to the other leg (Clark et al., 2004; Kristiansen et al., 2019). Our results showed a decrease in muscle activity of the hip abductor and knee extensor in the moving leg, which may have been a result of participants shifting their weight to the supporting leg. However, while the joint kinematics and muscle activation in the moving leg were reduced, the weight shifting to the supporting leg can be beneficial for balance training of the unilateral leg specifically.

The results of this study indicated that VR-skateboarding was associated with a lower force loading but higher weight distribution on the supporting leg when compared to walking. This decrease in force loading was believed to be due to the support provided by holding onto the handrail, while the increase in weight distribution was likely due to weight shifting (Clark et al., 2004; Wu et al., 2018; Kristiansen et al., 2019). Weight shifting has been found to improve balance by strengthening muscles, improving coordination, and enhancing control of the body's center of mass, leading to increased stability during movement (Lin et al., 2019a; Lin et al., 2019b). Additionally, VR-skateboarding was found to have a shorter stance phase for the moving leg compared to walking. Although this study conducted VR-skateboarding at the same speed as walking, there were still differences in movement cycles. One possible explanation for this is that both legs were moving during walking, so participants needed to shift their center of mass to the new base of support provided by the supporting leg (Lin et al., 2019a). This process required time and distance to complete (Lin et al., 2019a). However, in VR-skateboarding, the supporting leg consistently supported the body weight, allowing the moving leg to swing more freely. Previous research has shown that gait training with a shorter stance phase can reorganize walking patterns and improve walking speed (Stolze et al., 2001; Yen et al., 2019). The decreased force loading, increased weight distribution, and reduced duration of movement cycles observed in VR-skateboarding may have the potential to reduce joint loading, enhance weight bearing, and improve walking speed, respectively. These factors may have contributed to the potential benefits of VR-skateboarding as a rehabilitation tool for individuals with balance impairments.

Clinical implications

The clinical significance of this study is the potential use of VR-skateboarding as a rehabilitation training approach to improve balance. When performing VR-skateboarding, participants had greater range of movement and flexion in their trunk compared to when walking, as well as increased muscle activity and weight distribution in the supporting leg. These differences in biomechanics contributed to increase joint and muscle coordination during VR-skateboarding. Additionally, VR-skateboarding might also be considered a type of closed kinetic chain exercise, where the foot is fixed. Our results indicated that participants consistently kept the foot of the supporting leg on the skateboard. Previous studies have revealed that closed kinetic chain exercises can promote muscle co-contraction to stabilize the trunk and legs. This muscle co-contraction also aids in improving proprioception, or the ability to sense the position and movement of one's body in space, subsequently improving balance. Furthermore, the use of VR technology may have influenced the observed differences in joint kinematics, muscle activity, and weight distribution. These findings suggest that VR-skateboarding may be an effective training approach for improving balance in individuals undergoing rehabilitation.

In addition, the consideration of the biomechanical characteristics of VR-skateboarding is important for software engineers creating new features and implementing multidisciplinary approaches. By understanding the biomechanics, software engineers can design features that are ergonomic and user-friendly, ensuring that the products they develop are comfortable, safe, and appropriate for balance training. This is particularly important for products or systems that would be used by a wide range of individuals with different physical abilities and characteristics, as it allows for the creation of solutions that are accessible and inclusive. Incorporating a multidisciplinary approach also enables software engineers to consider the diverse needs and perspectives of different populations, such as those with unilateral leg symptoms, to create well-rounded and effective solutions. Overall, the incorporation of biomechanical characteristics in the development process can lead to the creation of innovative and highly functional products and systems that meet the needs of a diverse range of users.

Study limitations

This study had a few limitations. First, for safety reasons, participants held onto a handrail while VR-skateboarding. This may have partially supported their body weight and potentially affected joint kinematics, muscle activity or weight distribution. However, we believed that handrail use is necessary in patient populations to prevent accidents during training. Second, this study conducted the experiment on the same population and at the same speed (i.e., comfortable walking speed). Moreover, participants were all healthy individuals with no leg abnormalities. Therefore, the results of VR-skateboarding in this study should be interpreted with caution when applied to patient populations or different speeds. Third, participants performed VR-skateboarding and walking with bare feet in this study. According to previous studies, wearing shoes can change biomechanical characteristics, particularly reducing force loading (Zhang et al., 2013; Udofa et al., 2019). Hence, this factor should be taken into consideration when applying our findings to VR-skateboarding while wearing shoes.

Conclusion

VR-skateboarding was a novel VR-based balance training approach. The results of our study demonstrated that VR-skateboarding involved increased movement and muscle activity in the trunk, hips, and ankles, particularly in the supporting leg, compared to walking. The weight distribution was also found to increase when participants stood on the skateboard with their supporting leg. These findings suggested that VR-skateboarding may be a promising rehabilitation tool for improving balance. Additionally, we proposed that future developments and applications of this training should prioritize the strengthening of the supporting leg in order to maximize its therapeutic benefits.

Data availability statement

The raw data supporting the conclusion of this article will be made available by the authors, without undue reservation.

Ethics statement

The studies involving human participants were reviewed and approved by the Human Participants Review Committee of National Taiwan University Hospital. The patients/participants provided their written informed consent to participate in this study.

Author contributions

The research was conceptualized and designed by PK, J-JL, and W-LH. PK and P-JC conducted the experiments, and PK and Y-CT contributed analytical tools. The data was analyzed by PK and P-JC, and the manuscript was written by PK and W-LH. All authors approved the final version of the manuscript.

Funding

This work was supported by grants from the National Health Research Institutes (NHRI-EX112-11019EI) and National Science and Technology Council (MOST 109-2221-E-002-100-MY3) awarded to W-LH.

Acknowledgments

We would like to express our gratitude to National Taiwan University (NTU-112L7807) and all of the individuals who contributed to this research. We would like to thank our study participants for their time and effort in participating in the study.

Conflict of interest

The authors declare that the research was conducted in the absence of any commercial or financial relationships that could be construed as a potential conflict of interest.

Publisher's note

All claims expressed in this article are solely those of the authors and do not necessarily represent those of their affiliated organizations, or those of the publisher, the editors and the reviewers. Any product that may be evaluated in this article, or claim that may be made by its manufacturer, is not guaranteed or endorsed by the publisher.

Supplementary material

The Supplementary Material for this article can be found online at: https://www.frontiersin.org/articles/10.3389/fbioe.2023.1136368/full#supplementary-material

References

Adewuyi, A. A., Hargrove, L. J., and Kuiken, T. A. (2016). Evaluating EMG feature and classifier selection for application to partial-hand prosthesis control. *Front. Neurorobot* 10, 15. doi:10.3389/fnbot.2016.00015

Androwis, G. J., Pilkar, R., Ramanujam, A., and Nolan, K. J. (2018). Electromyography assessment during gait in a robotic exoskeleton for acute stroke. *Front. Neurol.* 9, 630. doi:10.3389/fneur.2018.00630

Asín-Prieto, G., Martínez-Expósito, A., Barroso, F. O., Urendes, E. J., Gonzalez-Vargas, J., Alnajjar, F. S., et al. (2020). Haptic adaptive feedback to promote motor learning with a robotic ankle exoskeleton integrated with a video game. *Front. Bioeng. Biotechnol.* 8, 113. doi:10.3389/fbioe.2020.00113

Baumgart, C., Hoppe, M. W., and Freiwald, J. (2017). Phase-specific ground reaction force analyses of bilateral and unilateral jumps in patients with ACL reconstruction. *Orthop. J. Sports Med.* 5 (6), 232596711771091. doi:10.1177/2325967117710912

Benady, A., Zadik, S., Ben-Gal, O., Cano Porras, D., Wenkert, A., Gilaie-Dotan, S., et al. (2021). Vision affects gait speed but not patterns of muscle activation during inclined walking—a virtual reality study. *Front. Bioeng. Biotechnol.* 9, 632594. doi:10.3389/fbioe.2021.632594

Bohannon, R. W. (1997). Comfortable and maximum walking speed of adults aged 20-79 Years: Reference values and determinants. *Age Ageing* 26 (1), 15–19. doi:10.1093/ageing/26.1.15

Bohannon, R. W., and Williams Andrews, A. (2011). Normal walking speed: A descriptive meta-analysis. *Physiotherapy* 97 (3), 182–189. doi:10.1016/j.physio.2010.12.004

Chen, H.-L., Lin, S.-Y., Yeh, C.-F., Chen, R.-Y., Tang, H.-H., Ruan, S.-J., et al. (2021). Development and feasibility of a kinect-based constraint-induced therapy program in the home setting for children with unilateral cerebral palsy. *Front. Bioeng. Biotechnol.* 9, 755506. doi:10.3389/fbioe.2021.755506

Cheng, C.-H., Lai, D.-M., Lau, P. Y., Wang, S.-F., Chien, A., Wang, J.-L., et al. (2020a). Upright balance control in individuals with cervical myelopathy following cervical decompression surgery: A prospective cohort study. *Sci. Rep.* 10 (1), 10357. doi:10.1038/s41598-020-66057-y

Cheng, Y. S., Chien, A., Lai, D. M., Lee, Y. Y., Cheng, C. H., Wang, S. F., et al. (2020b). Perturbation-based balance training in postoperative individuals with degenerative cervical myelopathy. *Front. Bioeng. Biotechnol.* 8, 108. doi:10.3389/fbioe.2020.00108

Chien, J. E., and Hsu, W. L. (2018). Effects of dynamic perturbation-based training on balance control of community-dwelling older adults. *Sci. Rep.* 8 (1), 17231. doi:10.1038/s41598-018-35644-5

Cipresso, P., Giglioli, I. A. C., Raya, M. A., and Riva, G. (2018). The past, present, and future of virtual and augmented reality research: A network and cluster analysis of the literature. *Front. Psychol.* 9, 2086. doi:10.3389/fpsyg.2018.02086

Clark, B. C., Manini, T. M., Ordway, N. R., and Ploutz-Snyder, L. L. (2004). Leg muscle activity during walking with assistive devices at varying levels of weight bearing11No commercial party having a direct financial interest in the results of the research supporting this article has or will confer a benefit on the authors or on any organization with which the authors are associated. *Arch. Phys. Med. Rehabil.* 85 (9), 1555–1560. doi:10.1016/j.apmr.2003.09.011

Eliassen, W., Saeterbakken, A. H., and van den Tillaar, R. (2018). Comparison of bilateral and unilateral squat exercises on barbell kinematics and muscle activation. *Int. J. Sports Phys. Ther.* 13 (5), 871–881. doi:10.26603/ijspt20180871

Frederick, E. C., Determan, J. J., Whittlesey, S. N., and Hamill, J. (2006). Biomechanics of skateboarding: Kinetics of the ollie. *J. Appl. Biomech.* 22 (1), 33–40. doi:10.1123/jab.22.1.33

Golyski, P. R., Bell, E. M., Husson, E. M., Wolf, E. J., and Hendershot, B. D. (2018). Modulation of vertical ground reaction impulse with real-time biofeedback: A feasibility study. *J. Appl. Biomech.* 34 (2), 134–140. doi:10.1123/jab.2017-0004

Guillén-Rogel, P., San Emeterio, C., and Marín, P. J. (2017). Associations between ankle dorsiflexion range of motion and foot and ankle strength in young adults. *J. Phys. Ther. Sci.* 29 (8), 1363–1367. doi:10.1589/jpts.29.1363

Horsak, B., Simonlehner, M., Schöffer, L., Dumphart, B., Jalaeefar, A., and Husinsky, M. (2021). Overground walking in a fully immersive virtual reality: A comprehensive study on the effects on full-body walking biomechanics. *Front. Bioeng. Biotechnol.* 9, 780314. doi:10.3389/fbioe.2021.780314

Hu, X., Liang, F., Fang, Z., Qu, X., Zhao, Z., Ren, Z., et al. (2021). Automatic temporal event detection of the ollie movement during skateboarding using wearable IMUs. *Sports Biomech.*, 1–15. doi:10.1080/14763141.2021.1990384

Jafarnezhadgero, A. A., Pourrahimghoroghchi, A., Darvishani, M. A., Aali, S., and Dionisio, V. C. (2021). Analysis of ground reaction forces and muscle activity in individuals with anterior cruciate ligament reconstruction during different running strike patterns. *Gait Posture* 90, 204–209. doi:10.1016/j.gaitpost.2021.09.167

Komisar, V., Nirmalanathan, K., King, E. C., Maki, B. E., and Novak, A. C. (2019). Use of handrails for balance and stability: Characterizing loading profiles in younger adults. *Appl. Ergon.* 76, 20–31. doi:10.1016/j.apergo.2018.11.006

Kristiansen, M., Odderskær, N., and Kristensen, D. H. (2019). Effect of body weight support on muscle activation during walking on a lower body positive pressure treadmill. *J. Electromyogr. Kinesiol* 48, 9–16. doi:10.1016/j.jelekin.2019.05.021

Kubinski, S. N., McQueen, C. A., Sittloh, K. A., and Dean, J. C. (2015). Walking with wider steps increases stance phase gluteus medius activity. *Gait Posture* 41 (1), 130–135. doi:10.1016/j.gaitpost.2014.09.013

Kumar, D., González, A., Das, A., Dutta, A., Fraisse, P., Hayashibe, M., et al. (2018). Virtual reality-based center of mass-assisted personalized balance training system. *Front. Bioeng. Biotechnol.* 5, 85. doi:10.3389/fbioe.2017.00085

Lee, D. H., Chang, W. N., and Jeon, H. J. (2020). Comparison of ground reaction force during gait between the nonparetic side in hemiparetic patients and the dominant side in healthy subjects. *J. Exerc Rehabil.* 16 (4), 344–350. doi:10.12965/jer.2040488.244

Lheureux, A., Lebleu, J., Frisque, C., Sion, C., Stoquart, G., Warlop, T., et al. (2020). Immersive virtual reality to restore natural long-range autocorrelations in Parkinson's disease patients' gait during treadmill walking. *Front. Physiol.* 11, 572063. doi:10.3389/fphys.2020.572063

Liang, H.-W., Tai, T.-L., Li, Y.-H., and Chen, Y.-C. (2022). Application of a virtual reality tracker-based system to measure seated postural stability in stroke patients. *J. Neuroeng Rehabil.* 19 (1), 71. doi:10.1186/s12984-022-01052-0

Liao, K. F., Nassis, G. P., Bishop, C., Yang, W., Bian, C., and Li, Y. M. (2022). Effects of unilateral vs. Bilateral resistance training interventions on measures of strength, jump, linear and change of direction speed: A systematic Review and meta-analysis. *Biol. Sport* 39 (3), 485–497. doi:10.5114/biolsport.2022.107024

Lin, I.-S., Lai, D.-M., Ding, J.-J., Chien, A., Cheng, C.-H., Wang, S.-F., et al. (2019a). Reweighting of the sensory inputs for postural control in patients with cervical spondylotic myelopathy after surgery. *J. Neuroeng Rehabil.* 16 (1), 96. doi:10.1186/s12984-019-0564-2

Lin, J. T., Hsu, C. J., Dee, W., Chen, D., Rymer, W. Z., and Wu, M. (2019b). Motor adaptation to weight shifting assistance transfers to overground walking in people with spinal cord injury. *Pm R.* 11 (11), 1200–1209. doi:10.1002/pmrj.12132

Lopes, J. B. P., Miziara, I. M., Galli, M., Cimolin, V., and Oliveira, C. S. (2020). Effect of transcranial direct current stimulation combined with xbox-kinect game experience on upper limb movement in down syndrome: A case report. *Front. Bioeng. Biotechnol.* 8, 514. doi:10.3389/fbioe.2020.00514

Macrum, E., Bell, D. R., Boling, M., Lewek, M., and Padua, D. (2012). Effect of limiting ankle-dorsiflexion range of motion on lower extremity kinematics and muscle-activation patterns during a squat. *J. Sport Rehabil.* 21 (2), 144–150. doi:10.1123/jsr.21.2.144

Manca, A., Dragone, D., Dvir, Z., and Deriu, F. (2017). Cross-education of muscular strength following unilateral resistance training: A meta-analysis. *Eur. J. Appl. Physiol.* 117 (11), 2335–2354. doi:10.1007/s00421-017-3720-z

Matjačić, Z., Zadravec, M., and Olenšek, A. (2019). Influence of treadmill speed and perturbation intensity on selection of balancing strategies during slow walking perturbed in the frontal plane. *Appl. Bionics Biomech.* 2019, 1–14. doi:10.1155/2019/1046459

Meinke, A., Peters, R., Knols, R. H., Swanenburg, J., and Karlen, W. (2022). Feedback on trunk movements from an electronic game to improve postural balance in people with nonspecific low back pain: Pilot randomized controlled trial. *JMIR Serious Games* 10 (2), e31685. doi:10.2196/31685

Möckel, G., Perka, C., Labs, K., and Duda, G. (2003). The influence of walking speed on kinetic and kinematic parameters in patients with osteoarthritis of the hip using a force-instrumented treadmill and standardised gait speeds. *Arch. Orthop. Trauma Surg.* 123 (6), 278–282. doi:10.1007/s00402-003-0513-0

Moon, S., Huang, C.-K., Sadeghi, M., Akinwuntan, A. E., and Devos, H. (2021). Proof-of-Concept of the virtual reality comprehensive balance assessment and training for sensory organization of dynamic postural control. *Front. Bioeng. Biotechnol.* 9, 678006. doi:10.3389/fbioe.2021.678006

Moret, B., Nucci, M., and Campana, G. (2022). Effects of exergames on mood and cognition in healthy older adults: A randomized pilot study. *Front. Psychol.* 13, 1018601. doi:10.3389/fpsyg.2022.1018601

Rawlins, C. R., Veigulis, Z., Hebert, C., Curtin, C., and Osborne, T. F. (2021). Effect of immersive virtual reality on pain and anxiety at a veterans affairs health care facility. *Front. Virtual Real* 2. doi:10.3389/frvir.2021.719681

Recenti, M., Ricciardi, C., Aubonnet, R., Picone, I., Jacob, D., Svansson, H. Á. R., et al. (2021). Toward predicting motion sickness using virtual reality and a moving platform assessing brain, muscles, and heart signals. *Front. Bioeng. Biotechnol.* 9, 635661. doi:10.3389/fbioe.2021.635661

Smith, Y., Louw, Q., and Brink, Y. (2016). The three-dimensional kinematics and spatiotemporal parameters of gait in 6-10 Year old typically developed children in the cape metropole of south Africa - a pilot study. *BMC Pediatr.* 16 (1), 200. doi:10.1186/s12887-016-0736-1

Stolze, H., Kuhtz-Buschbeck, J. P., Drücke, H., Jöhnk, K., Illert, M., and Deuschl, G. (2001). Comparative analysis of the gait disorder of normal pressure hydrocephalus and Parkinson's disease. *J. Neurol. Neurosurg. Psychiatry* 70 (3), 289–297. doi:10.1136/jnnp.70.3.289

Sween, J., Wallington, S. F., Sheppard, V., Taylor, T., Llanos, A. A., and Adams-Campbell, L. L. (2014). The role of exergaming in improving physical activity: A Review. *J. Phys. Act. Health* 11 (4), 864–870. doi:10.1123/jpah.2011-0425

Tabard-Fougère, A., Rose-Dulcina, K., Pittet, V., Dayer, R., Vuillerme, N., and Armand, S. (2018). EMG normalization method based on grade 3 of manual muscle testing: Within- and between-day reliability of normalization tasks and application to gait analysis. *Gait Posture* 60, 6–12. doi:10.1016/j.gaitpost.2017.10.026

Udofa, A. B., Clark, K. P., Ryan, L. J., and Weyand, P. G. (2019). Running ground reaction forces across footwear conditions are predicted from the motion of two body mass components. *J. Appl. Physiol.* 126 (5), 1315–1325. doi:10.1152/japplphysiol.00925.2018

van den Tillaar, R., and Larsen, S. (2020). Kinematic and EMG comparison between variations of unilateral squats under different stabilities. *Sports Med. Int. Open* 4 (2), E59–e66. doi:10.1055/a-1195-1039

Vigotsky, A. D., Halperin, I., Lehman, G. J., Trajano, G. S., and Vieira, T. M. (2017). Interpreting signal amplitudes in surface electromyography studies in sport and rehabilitation sciences. *Front. Physiol.* 8, 985. doi:10.3389/fphys.2017.00985

Voglar, M., Wamerdam, J., Kingma, I., Sarabon, N., and van Dieën, J. H. (2016). Prolonged intermittent trunk flexion increases trunk muscles reflex gains and trunk stiffness. *PLoS One* 11 (10), e0162703. doi:10.1371/journal.pone.0162703

Wang, T. Y., Pao, J. L., Yang, R. S., Jang, J. S., and Hsu, W. L. (2015). The adaptive changes in muscle coordination following lumbar spinal fusion. *Hum. Mov. Sci.* 40, 284–297. doi:10.1016/j.humov.2015.01.002

Wu, C. H., Mao, H. F., Hu, J. S., Wang, T. Y., Tsai, Y. J., and Hsu, W. L. (2018). The effects of gait training using powered lower limb exoskeleton robot on individuals with complete spinal cord injury. *J. Neuroeng Rehabil.* 15 (1), 14. doi:10.1186/s12984-018-0355-1

Wu, M., Hsu, C. J., and Kim, J. (2019). Forced use of paretic leg induced by constraining the non-paretic leg leads to motor learning in individuals post-stroke. *Exp. Brain Res.* 237 (10), 2691–2703. doi:10.1007/s00221-019-05624-w

Yalfani, A., Abedi, M., and Raeisi, Z. (2022). Effects of an 8-week virtual reality training program on pain, fall risk, and quality of life in elderly women with chronic low back pain: Double-blind randomized clinical trial. *Games Health J.* 11 (2), 85–92. doi:10.1089/g4h.2021.0175

Yen, C. L., Chang, K. C., Wu, C. Y., and Hsieh, Y. W. (2019). The relationship between trunk acceleration parameters and kinematic characteristics during walking in patients with stroke. *J. Phys. Ther. Sci.* 31 (8), 638–644. doi:10.1589/jpts.31.638

Yen, C. Y., Lin, K. H., Hu, M. H., Wu, R. M., Lu, T. W., and Lin, C. H. (2011). Effects of virtual reality-augmented balance training on sensory organization and attentional demand for postural control in people with Parkinson disease: A randomized controlled trial. *Phys. Ther.* 91 (6), 862–874. doi:10.2522/ptj.20100050

Yoder, A. J., Silder, A., Farrokhi, S., Dearth, C. L., and Hendershot, B. D. (2019). Lower extremity joint contributions to trunk control during walking in persons with transtibial amputation. *Sci. Rep.* 9 (1), 12267. doi:10.1038/s41598-019-47796-z

Zhang, X., Paquette, M. R., and Zhang, S. (2013). A comparison of gait biomechanics of flip-flops, sandals, barefoot and shoes. *J. Foot Ankle Res.* 6 (1), 45. doi:10.1186/1757-1146-6-45

Zhou, S., Zhang, S. S., and Crowley-McHattan, Z. J. (2022). A scoping Review of the contralateral effects of unilateral peripheral stimulation on neuromuscular function. *PLoS One* 17 (2), e0263662. doi:10.1371/journal.pone.0263662

frontiers | Frontiers in Neurology

TYPE Clinical Trial
PUBLISHED 06 June 2023
DOI 10.3389/fneur.2023.1166151

Check for updates

OPEN ACCESS

EDITED BY
Yih-Kuen Jan,
University of Illinois at Urbana-Champaign,
United States

REVIEWED BY
Chi-Wen Lung,
Asia University, Taiwan
Qinyin Qiu,
Rutgers University, Newark, United States

*CORRESPONDENCE
Jialing Wu
✉ wywjl2009@hotmail.com

†These authors have contributed equally to this work and share first authorship

RECEIVED 14 February 2023
ACCEPTED 15 May 2023
PUBLISHED 06 June 2023

CITATION
Wang Y, Li Y, Liu S, Liu P, Zhu Z and Wu J (2023) Gait characteristics related to fall risk in patients with cerebral small vessel disease.
Front. Neurol. 14:1166151.
doi: 10.3389/fneur.2023.1166151

COPYRIGHT
© 2023 Wang, Li, Liu, Liu, Zhu and Wu. This is an open-access article distributed under the terms of the Creative Commons Attribution License (CC BY). The use, distribution or reproduction in other forums is permitted, provided the original author(s) and the copyright owner(s) are credited and that the original publication in this journal is cited, in accordance with accepted academic practice. No use, distribution or reproduction is permitted which does not comply with these terms.

Gait characteristics related to fall risk in patients with cerebral small vessel disease

Yajing Wang[1,2†], Yanna Li[1,2†], Shoufeng Liu[1,2], Peipei Liu[1,2], Zhizhong Zhu[1,3] and Jialing Wu[1,2*]

[1]Clinical College of Neurology, Neurosurgery and Neurorehabilitation, Tianjin Medical University, Tianjin, China, [2]Department of Neurology, Tianjin Huanhu Hospital, Tianjin Key Laboratory of Cerebral Vascular and Neurodegenerative Diseases, Tianjin Neurosurgical Institute, Tianjin, China, [3]Department of Rehabilitation, Tianjin Huanhu Hospital, Tianjin, China

Background: Falls and gait disturbance are significant clinical manifestations of cerebral small vessel disease (CSVD). However, few relevant studies are reported at present. We aimed to investigate gait characteristics and fall risk in patients with CSVD.

Methods: A total of 119 patients with CSVD admitted to the Department of Neurology at Tianjin Huanhu Hospital between 17 August 2018 and 7 November 2018 were enrolled in this study. All patients underwent cerebral magnetic resonance imaging scanning and a 2-min walking test using an OPAL wearable sensor and Mobility Lab software. Relevant data were collected using the gait analyzer test system to further analyze the time-space and kinematic parameters of gait. All patients were followed up, and univariate and multivariate logistic regression analyses were conducted to analyze the gait characteristics and relevant risk factors in patients with CSVD at an increased risk of falling.

Results: All patients were grouped according to the presence or absence of falling and fear of falling and were divided into a high-fall risk group ($n = 35$) and a low-fall risk group ($n = 72$). Logistic multivariate regression analysis showed that the toe-off angle [odds ratio (OR) = 0.742, 95% confidence interval (CI) 0.584–0.942, $p < 0.05$], toe-off angle coefficient of variation (CV) (OR = 0.717, 95% CI: 0.535–0.962, $p < 0.05$), stride length CV (OR = 1.256, 95% CI: 1.017–1.552, $p < 0.05$), and terminal double support CV (OR = 1.735, 95% CI: 1.271–2.369, $p < 0.05$) were statistically significant ($p < 0.05$) and were independent risk factors for high-fall risk in patients with CSVD.

Conclusion: CSVD patients with seemingly normal gait and ambulation independently still have a high risk of falling, and gait spatiotemporal-kinematic parameters, gait symmetry, and gait variability are important indicators to assess the high-fall risk. The decrease in toe-off angle, in particular, and an increase in related parameters of CV, can increase the fall risk of CSVD patients.

KEYWORDS

cerebral small vessel disease, walking, fall, gait analysis, gait parameters

1. Introduction

Cerebral small vascular disease (CSVD) refers to a series of imaging and clinical manifestations that characterize a syndrome caused by any functional or structural pathological damage to small cerebral vessels, such as terminal arterioles, venules, and capillaries. Gait disorder is one of the main symptoms of CSVD patients (1, 2). Studies

have shown that most falls of stroke patients after discharge occurs during walking, and gait disorder is an independent predictor of patients' fall risk. However, most studies are described by scale, observation, and other methods, with low accuracy, strong subjectivity, and limited dimensions (3). With the development of ergonomics, a large number of gait parameters can be obtained using wearable sensor devices, and gait symmetry and gait variability can be calculated (4). Both reflect the ability to maintain a stable and consistent walking rhythm in the motor control system. However, we found that there were few studies on gait symmetry and variability in patients with CSVD (5, 6). Therefore, we used wearable devices to measure the parameters related to the gait of patients with CSVD. Furthermore, we calculated gait symmetry and variability. We investigated the gait parameters that contributed to the high risk of falls among follow-up patients with a high risk of falling. Through our study, we can provide early rehabilitation treatment for patients with CSVD and reduce the occurrence of falls.

2. Materials and methods

2.1. Patients

In this study, 119 patients with CSVD were hospitalized at the Department of Neurology of Tianjin Huanhu Hospital, Tianjin, China between 17 August 2018 and 7 November 2018. The study was registered with the Chinese Clinical Trial Registry (Clinical Trial Registration No. ChiCTR2100042031) and was approved by the Ethics Committee of Tianjin Huanhu Hospital. All patients underwent head magnetic resonance imaging, including T2, fluid-attenuated inversion recovery, diffusion-weighted imaging, apparent diffusion coefficient, and gradient echo sequences. All patients were able to walk and complete the evaluation independently. All the clinical data were complete.

The inclusion criteria were as follows: (1) age $\geq$18 years; (2) met the diagnostic criteria for mild stroke [National Institutes of Health Stroke Scale (NIHSS) score $\leq$3]; (3) according to the pathogenesis, the selection (Trial of Org 10172 in Acute Stroke Treatment) type was small-artery occlusion; (4) all participants could walk independently and safely for 2 min without help from others or assistive devices; and (5) all participants were fully informed of the research process and signed the informed consent form.

The exclusion criteria were as follows: clinical diagnosis of dementia, mental disorders, severe cerebral hemorrhage, and other systemic diseases affecting gait, such as joint injury, arthritis, cervical spine disease, and lumbar spine disease.

Participants were selected according to inclusion criteria and exclusion criteria (Figure 1).

2.2. Study design

2.2.1. General assessment

General clinical data of all patients, including age, sex, height, weight, and medical history, were collected and analyzed.

2.2.2. Assessment of gait function

All enrolled patients underwent a 2-min walk test under the guidance of a physician, which was conducted in an empty room dedicated to the evaluation. The patients walked freely along a straight line which could be turned back for 2 min. Patients were simulated in advance to ensure that they were familiar with the test. At the start of the experiment, the OPAL wearable sensor (APDM) and Mobility Lab software (https://apdm.com/wearable-sensors/) were used for the 2-min walking test. The instrument had a total of six sensors, which were placed on the patient's body by professionals according to the following positions. The first sensor was worn at the uppermost sternal handle of the sternum, the second sensor was worn at the lowermost fifth lumbar vertebra at the lumbosacral junction, and the third and fourth sensors were worn on the dorsal side of the bilateral wrist joint. The fifth and sixth sensors were worn on the dorsum of both feet.

2.2.3. Assessment of gait parameters

Gait parameter data were collected through the gait analysis and test system and transmitted to a computer terminal. Then, the time-space and kinematic gait parameters were analyzed. Gait symmetry was assessed using the Asymmetry Index (AI). The AI was calculated as follows:

$$\mathrm{AI} = |\mathrm{XL} - \mathrm{XR}|/\max(\mathrm{XL}, \mathrm{XR}) \times 100,$$

with L and R representing the left and right sides of the patient, respectively (5). X represents the corresponding gait parameter used in the analysis. This study mainly included stride length, single-limb support, terminal double support, swing, foot strike angle, and toe-off angle. Gait variability was assessed using the coefficient of variation. First, the coefficient of variation (CV) was calculated using the formula "standard deviation/mean," which represents the gait variability (CVL represents the left variability and CVR represents the right variability). The next step was to integrate the variability of the left and right gait parameters using the formula (7, 8):

$$\sqrt{(CVL + CVR)/2} \times 100.$$

The parameters included were stride length, single limb support, terminal double support, swing, toe-off angle, and foot strike angle.

2.2.4. Main outcomes

All patients were followed up for the presence of falls and the presence of fear of falling (FOF). The assessment of FOF was as follows: According to the FOF scale developed by American scholar Tinetti in 1993 (9), patients were asked, "Are you afraid or worried about falling?" The presence of FOF was determined by answering "not afraid," "slightly afraid,"' "somewhat afraid," and "very afraid." Those who answered "not afraid" were defined as having no FOF, and those who answered with any other option were defined as having a FOF. Based on the presence of FOF or falling, the patients were divided into a high-fall risk (HFR) group and a low-fall risk (LFR) group. If the patient had no history of falls and answered

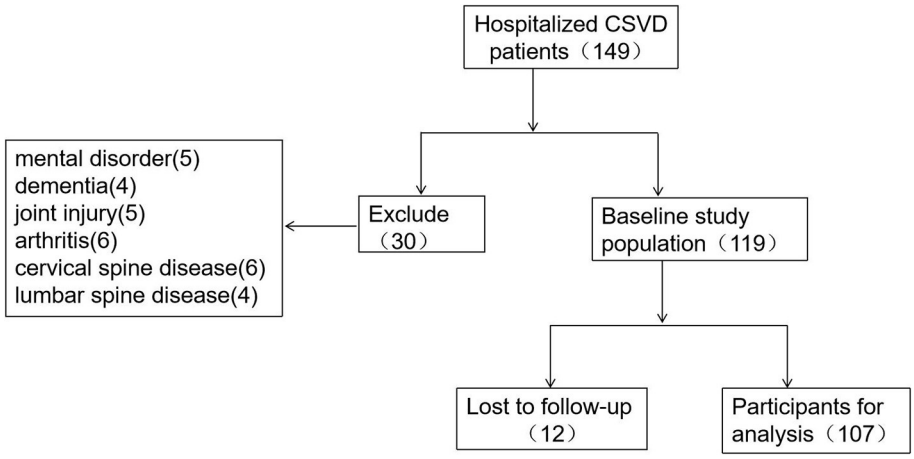

FIGURE 1
Flow chart of the inclusion and exclusion process of included patients.

as "not afraid," they were assigned to the LFR group, and patients who had a history of falls or answered "slightly afraid," "somewhat afraid," or "very afraid," were assigned to the HFR group.

2.3. Statistical analysis

Data processing was performed using SPSS 24.0 software (SPSS Inc., Chicago, IL, USA). Normally distributed numerical data were presented as the mean ± standard deviation (x ± s), and the independent sample *t*-test was used for comparison between the groups. Numerical data that showed a skewed distribution were presented as the median (the first quartile, third quartile) [M (Q1, Q3)], and the Mann–Whitney *U*-test was used for comparison between groups. Count data were expressed in the form of cases (percentage) [*n* (%)], and an X^2 test was used for comparison between groups. Data from both groups were analyzed using multivariate logistic regression, and a *p*-value of <0.05 was considered statistically significant. In this study, logistic regression was used for the multivariate analysis of the two groups of data.

3. Results

3.1. Baseline clinical characteristics

The demographic characteristics of the LFR and HFR groups are summarized in Table 1. A total of 119 patients were included in this study, and the mean (SD) age was 59.55 (9.89) years. In total, 94 cases were male patients, 25 cases were female patients, and 12 cases were lost to follow-up, including the LFR (72 cases) and HFR group (35 cases). Age, sex, height, weight, diabetes mellitus, cardiac disease, and smoking did not differ significantly between the groups; however, the presence of hypertension was higher in the HFR group compared with the LFR group ($p < 0.05$) (Table 1).

3.2. Gait analysis in the LFR group and HFR group

Compared to patients in the LFR group, patients in the HFR group had lower stride frequency, slower stride speed, shorter stride length, and longer gait cycle time ($p < 0.05$). Simultaneously, the proportion of double limb support and terminal double support increased during each gait cycle, while the proportion of single limb support and swing decreased ($p < 0.05$). As shown in Table 2, the patients in the HFR group had smaller foot strike and toe-off angles ($p < 0.05$) (Table 2).

3.3. Comparison of gait symmetry between the two groups

This study compared gait symmetry between the two groups and found that the foot strike angle AI increased in patients in the HFR group ($p < 0.05$), whereas the stride length AI, toe-off angle AI, single-limb support AI, terminal double support AI, and swing AI showed no significant differences between the groups ($p > 0.05$) (Table 3).

3.4. Comparison of gait variability between the two groups

After analyzing gait variability in both groups, we found that the stride length CV, single limb support CV, terminal double support CV, swing CV, foot strike angle CV, and toe-off angle CV were significantly higher in the HFR vs. LFR group ($p < 0.05$) (Table 4).

TABLE 1 Demographic characteristics of participants.

	LFR group ($n = 72$)	HFR group ($n = 35$)	X^2/t-value	P-value
Male [n (%)]	54 (75.00)	28 (80.00)	0.329	0.566
Age (year)	59.28 ± 10.46	61.80 ± 7.54	−1.274	0.206
Height (cm)	168.96 ± 6.54	170.43 ± 7.37	−1.046	0.298
Weight (kg)	74.25 ± 12.94	73.37 ± 10.75	0.347	0.729
Hypertension [n (%)]	48 (67.6)	30 (85.7)	3.995	0.047[a]
Diabetes [n (%)]	26 (36.6)	13 (37.1)	0.003	0.958
cardiac disease [n (%)]	9 (12.7)	7 (20.0)	0.981	0.322
smoke [n (%)]	40 (56.3)	26 (74.3)	3.214	0.073

LFR group, low-fall risk group; HFR group, high-fall risk group.
[a]P < 0.05.

TABLE 2 Comparison of time-space and kinematic parameters between the two groups ($x \pm s$).

	Mean ± SD		t-value	P-value
	LFR group ($n = 72$)	HFR group ($n = 35$)		
Stride frequency (steps/min)	106.4 ± 9.21	100.20 ± 12.52	2.909	0.004[a]
Stride speed (m/s)	0.92 ± 0.21	0.79 ± 0.25	2.832	0.006[a]
Stride length (m)	1.03 ± 0.20	0.93 ± 0.23	2.386	0.019[a]
Gait cycle (s)	1.14 ± 0.10	1.22 ± 0.19	−3.030	0.003[a]
Double limbs support (%GCT)	22.50 ± 5.64	25.32 ± 7.16	−2.220	0.029[a]
Single limb support (%GCT)	38.75 ± 2.81	37.36 ± 3.58	2.199	0.030[a]
Terminal double support (%GCT)	11.24 ± 2.79	12.62 ± 3.57	−2.186	0.031[a]
Swing (%GCT)	38.76 ± 2.80	37.36 ± 3.59	2.202	0.030[a]
Foot strike angle (degrees)	18.48 ± 6.18	14.73 ± 6.64	2.877	0.005[a]
Toe off angle (degrees)	33.17 ± 5.17	29.45 ± 6.37	3.233	0.002[a]

LFR group, low-fall risk group; HFR group, high-fall risk group.
[a]P < 0.05.

TABLE 3 Comparison of gait symmetry between the two groups [%, M (Q1, Q3)].

	LFR group ($n = 72$)	HFR group ($n = 35$)	Z-value	P-value
Stride length AI	0.96 (0.77, 1.69)	1.55 (0.77, 2.99)	−1.755	0.079
Single limb support AI	1.74 (0.77, 3.69)	2.77 (1.13, 5.16)	−1.454	0.146
Terminal double support AI	8.03 (2.94, 16.31)	10.66 (4.41, 19.96)	−1.627	0.104
Swing AI	1.72 (0.83, 3.82)	2.65 (1.15, 4.96)	−1.481	0.139
Foot strike angle AI	10.96 (5.84, 22.55)	19.89 (7.69, 33.91)	−2.105	0.035[a]
Toe off angle AI	4.46 (2.04, 6.57)	6.66 (3.68, 13.49)	−1.939	0.053

LFR group, low-fall risk group; HFR group, high-fall risk group; AI, asymmetry index.
[a]P < 0.05.

3.5. The regression analysis of influencing factors

All statistically significant gait indicators were included in the logistic multivariate regression analysis. The parameters of the toe-off angle, toe-off angle CV, stride length CV, and terminal double support CV were statistically significant ($p < 0.05$). These were identified as independent risk factors for falling in patients with CSVD. However, the remaining time-space and kinematic parameters of gait, gait symmetry parameters, and gait variability parameters were not statistically significant ($p > 0.05$) (Table 5).

4. Discussion

4.1. Fall and fear of falling in patients with CSVD

Falls caused by gait disorders in patients with CSVD seriously affect their quality of life and are closely related to a poor prognosis

TABLE 4 Comparison of gait variability between the two groups [%, *M* (*Q*1, *Q*3)].

	LFR group ($n = 72$)	HFR group ($n = 35$)	*Z*-value	*P*-value
Stride length CV	20.67 (18.43, 25.64)	23.95 (19.93, 26.80)	−2.085	0.037[a]
Single limb support CV	16.10 (14.27, 18.94)	18.75 (16.25, 20.92)	−2.962	0.003[a]
Terminal double support CV	30.46 (28.16, 33.16)	33.22 (29.30, 37.50)	−3.054	0.002[a]
Swing CV	16.08 (14.13, 19.91)	18.67 (16.68, 22.08)	−3.114	0.002[a]
Foot strike angle CV	34.56 (28.75, 42.24)	40.34 (32.69, 53.28)	−2.626	0.009[a]
Toe off angle CV	22.18 (19.06, 25.22)	26.11 (24.06, 29.40)	−3.758	0.000[b]

LFR group, low-fall risk group; HFR group, High-fall risk group; CV, coefficient of variation.
[a] $P < 0.05$.
[b] $P < 0.001$.

TABLE 5 Results of the multivariate logistic regression analysis.

	β value	SE	wald	*P*-value	OR value	95% CI	
						Lower limit	Upper limit
Stride frequency (steps/min)	−0.110	0.395	0.078	0.780	0.896	0.413	1.943
Stride speed (m/s)	0.122	0.179	0.466	0.495	1.130	0.795	1.606
Stride length (m)	−0.052	0.167	0.097	0.756	0.949	0.684	1.318
Gait cycle (s)	0.016	0.267	0.004	0.952	1.016	0.603	1.714
Double limbs support (%GCT)	−0.045	0.556	0.007	0.935	0.956	0.321	2.843
Single limb support (%GCT)	−0.293	1.100	0.071	0.790	0.746	0.086	6.445
Terminal double support (%GCT)	−1.035	1.022	1.024	0.312	0.355	0.048	2.636
Swing (%GCT)	−0.901	1.074	0.703	0.402	0.406	0.049	3.336
Foot strike angle (degrees)	0.084	0.130	0.424	0.515	1.088	0.844	1.403
Toe off angle (degrees)	−0.299	0.122	6.015	0.014[a]	0.742	0.584	0.942
Foot strike angle AI	0.023	0.024	0.864	0.353	1.023	0.975	1.073
Stride length CV	−0.332	0.150	4.911	0.027[a]	0.717	0.535	0.962
Foot strike angle CV	0.113	0.067	2.800	0.094	1.119	0.981	1.277
Toe off angle CV	0.228	0.108	4.496	0.034[a]	1.256	1.017	1.552
Single limb support CV	−0.348	0.367	0.899	0.343	0.706	0.344	1.449
Terminal double support CV	0.551	0.159	12.027	0.001[a]	1.735	1.271	2.369
Swing CV	−0.499	0.402	1.539	0.215	0.607	0.276	1.336
Hypertension	1.080	0.691	2.442	0.118	2.944	0.760	11.408

AI, asymmetry index; CV, coefficient of variation.
[a] $P < 0.05$.

(1, 2). FOF is a precursor to falling in patients with CSVD. FOF refers to the reduction of confidence or fall efficacy to avoid falling while participating in certain activities that the patients are capable of (9). Some studies (10) have shown that FOF not only exists in elderly people who have a history of falling but also in elderly people who have never experienced a fall. FOF reduces the patients' confidence in activities, which is not conducive to the rehabilitation of motor function in patients with stroke and affects the recovery of their neurological function. One study has shown that the incidence of FOF in patients with stroke during hospitalization was 54%, and the incidence of FOF in stroke patients after discharge was 32–66% (11). Our study found that the incidence of FOF in patients with CSVD who could walk independently was 32.71%. The possible reasons are related to the included population in this study and the time from onset to follow-up. The mean age of CSVD patients included in this study was 59.55 ± 9.89 years, NIHSS score ≤3 points, and the time from onset to follow-up was 4 years. Therefore, younger patients, mild stroke, and short follow-up time may lead to a lower risk of falls.

4.2. Time-space parameters and kinematic parameters of gait in patients with CSVD

Spatio-temporal parameters and kinematic parameters are important indicators of gait. Abnormal spatio-temporal and kinematic parameters often lead to gait instability, and patients are more likely to fall (12). In our study, we found that patients with CSVD in the HFR group had a shortened stride length, reduced stride frequency, and decreased stride speed. A reduction in stride length usually means a reduction in forward propulsion force and impairment of balance (13). Stride speed reflects the movement ability of an individual, and a decrease of 0.1 m/s has a significant clinical significance (14). The decline in walking speed reflects a decrease in the propulsion of the gait and is a sign of gait damage, and patients are more likely to fall when they want to increase their walking speed or are not prepared. In our study, the average stride speed in the HFR group decreased by 0.13 m/s compared to the LFR group, i.e., fall risk increased. We found that not only was the gait cycle of patients in the HFR group extended but also the proportion of double limb support and terminal double support in the gait cycle was extended, and the proportion of single limb support was reduced. This was to prevent falls and maintain body balance, which further absorbed shocks and maintained load-bearing stability by extending the time both feet contact the ground during double limb support and shortening the instability of single limb support (15). Stride frequency is negatively correlated with the gait cycle (16). When the gait cycle is prolonged, the gait frequency decreases, which is a compensatory manifestation of gait. Once entering the decompensation stage, the probability of patients falling increases sharply. Swing mainly reflects an individual's floor-clearance ability (17). The proportion of swing-phase patients in the HFR group was significantly shortened, resulting in a reduction in their floor clearance ability.

We included the important parameters of gait kinematics: the foot strike angle and toe-off angle. The foot strike angle reflects shock absorption and maintains forward stability (18), while the toe-off angle reflects the forward gait force, which is an important reflection of the ground clearance ability of the foot (19). In our study, we found that the foot strike and toe-off angles in patients with high-fall risk decreased during walking, indicating that CSVD not only affects the stability of the body moving forward but also affects the driving force for forward movement, resulting in patients with decreased ground clearance ability of the foot, increased instability, and increased fall risk.

4.3. Symmetry and variability of gait in patients with CSVD

In our study, not only the conventional gait parameters were analyzed, but the symmetry and variability of gait were quantified using formulas. The AI of the foot strike angle in the HFR group was significantly higher compared to the LFR group. In related studies (20), human gait symmetry is typically assumed to be consistent with left and right gait functions. The gait symmetry of healthy humans can effectively reduce the energy consumption of walking, reduce the risk of falling, and provide a stable and comfortable walking mode (21). The higher the AI, the greater the asymmetry deviation of the bilateral limbs during walking, and the higher the influence on the stability of walking (22). Therefore, the results of our study indicated that the lower extremities of patients in the HFR group had greater differences in shock absorption and maintenance of progressive stability while walking stability was poor. Compared with the LFR group, the AI of each gait parameter in the HFR group was higher, indicating that the gait asymmetry of the left and right limbs was more prominent in the HFR group during walking. Some studies have found that the increase of gait parameter asymmetry in stroke patients during walking is related to the decrease in progressive stability, impaired balance function, and increased risk of falls. Our further analysis found that there was a significant difference in the AI elevation of the foot strike angle between the two groups, and the foot strike angle reflected the foot clearance ability, so our study showed that the foot clearance ability of patients in the HFR group increased asymmetrically and increased the risk of fall.

Gait variability refers to the stability of gait during walking, which reflects the ability of the motion control system to maintain a stable and consistent walking rhythm (23). However, some studies have shown that the heterogeneity of gait time-space parameters is large, and gait variability is more effective in evaluating fall risk (24). In our study, we found that the stride length CV, single-limb support CV, terminal double support CV, swing CV, foot strike angle CV, and toe-off angle CV of patients with CSVD in the HFR group were significantly higher than those in the LFR group, suggesting that patients in the HFR group had decreased gait stability during walking. In addition, increased gait variability leads to increased energy expenditure, resulting in difficulty in maintaining postural balance and a higher risk of falls (25). We further included the indicators with statistical differences between the two groups for logistic regression analysis and found that toe-off angle, toe-off angle CV, stride length CV, and terminal double support CV were independent risk factors for falls in patients with CSVD. Terminal double support, which accounts for 10% of the gait cycle, is mainly responsible for weight release and weight transfer during walking (26). Its increased variability indicates that as the inconsistency of weight release and transfer of the lower limbs increases, the ability of the body to maintain stability decreases, and the risk of falling increases.

5. Conclusion

The high risk of falls in patients with CSVD is closely related to the time-space and kinematic parameters of gait, as well as the symmetry and variability of gait. In particular, toe-off angle, toe-off angle CV, stride length CV, and terminal double support CV were independent risk factors for falling in patients with CSVD. Our study could promote a better understanding of the risk factors for falling caused by gait disturbance in patients with CSVD. Our findings provide evidence for clinical work, which is helpful in administering targeted drugs or early rehabilitation intervention. However, this study has some room for improvement. First, some kinematic parameters, such as knee joint and hip joint, could be included while selecting some kinematic parameters which have the greatest impact on gait. In this way, it would be more sufficient

in reflecting the comprehensive effect of cerebral microvascular disease on gait. Second, we could conduct a multicenter study and carry out rehabilitation interventions on gait disorders in patients so as to provide a more effective basis for guiding clinical treatment.

Data availability statement

The datasets presented in this study can be found in online repositories. The name of the repository and accession number can be found below: Figshare, https://figshare.com/, doi: 10.6084/m9.figshare.22096259.

Ethics statement

The studies involving human participants were reviewed and approved by Ethics Committee member: Xinping Wang, Yanming Zhang, Jinling Zhang, Tong Han, Yi Li, Yangui Xu, and Mingyu Li. Chairman: Xinping Wang. The patients/participants provided their written informed consent to participate in this study.

Author contributions

YW conceived the study and was responsible for all research aspects. YL collected the data. SL and PL completed all statistical analyses and wrote the manuscript. ZZ assessed the gait function of patients. JW reviewed and commented on the data analysis and drafts. All the authors critically reviewed and approved the final version of the manuscript.

Funding

This study was funded by the Tianjin Key Medical Discipline (Specialty) Construction Project (No. TJYXZDXK-052B) and Tianjin Health Research Project (No. TJWJ2022MS031 and No. TJWJ2022MS030).

Acknowledgments

We are grateful to the patients and their families. We would also like to thank our colleagues for their assistance. Finally, we wish to thank Editage (www.editage.cn) for English language editing.

Conflict of interest

The authors declare that the research was conducted in the absence of any commercial or financial relationships that could be construed as a potential conflict of interest.

Publisher's note

All claims expressed in this article are solely those of the authors and do not necessarily represent those of their affiliated organizations, or those of the publisher, the editors and the reviewers. Any product that may be evaluated in this article, or claim that may be made by its manufacturer, is not guaranteed or endorsed by the publisher.

References

1. van der Holst HM, van Uden IW, Tuladhar AM, de Laat KF, van Norden AG, Norris DG, et al. Factors associated with 8-year mortality in older patients with cerebral small vessel disease: the Radboud University Nijmegen diffusion tensor and magnetic resonance cohort (RUN DMC) study. *JAMA Neurol*. (2016) 73:402–9. doi: 10.1001/jamaneurol.2015.4560

2. Bower K, Thilarajah S, Pua YH, Williams G, Tan D, Mentiplay B, et al. Dynamic balance and instrumented gait variables are independent predictors of falls following stroke. *J Neuroeng Rehabil*. (2019) 16:3. doi: 10.1186/s12984-018-0478-4

3. Kim YJ, Kwon HK, Lee JM, Cho H, Kim HJ, Park HK, et al. Gray and white matter changes linking cerebral small vessel disease to gait disturbances. *Neurology*. (2016) 86:1199–207. doi: 10.1212/WNL.0000000000002516

4. Ichihashi N, Ikezoe T, Sato S, Ibuki S. Gait asymmetry assessment for older adults by measuring circular gait speed. *Geriatr Gerontol Int*. (2019) 19:736–9. doi: 10.1111/ggi.13691

5. Galna B, Lord S, Rochester L. Is gait variability reliable in older adults and Parkinson's disease? Towards an optimal testing protocol. *Gait Posture*. (2013) 37:580–5. doi: 10.1016/j.gaitpost.2012.09.025

6. Son M, Han SH, Lyoo CH, Lim JA, Jeon J, Hong KB, et al. The effect of levodopa on bilateral coordination and gait asymmetry in Parkinson's disease using inertial sensor. *npj Parkinsons Dis*. (2021) 7:42. doi: 10.1038/s41531-021-00186-7

7. Zhang M, Artan NS, Gu H, Dong Z, Burina Ganatra L, Shermon S, et al. Gait study of Parkinson's disease subjects using haptic cues with A motorized walker. *Sensors*.(2018) 18:3549. doi: 10.20944/preprints201809.0211.v1

8. Serrao M, Chini G, Caramanico G, Bartolo M, Castiglia SF, Ranavolo A, et al. Prediction of responsiveness of gait variables to rehabilitation training in Parkinson's disease. *Front Neurol*. (2019) 10:826. doi: 10.3389/fneur.2019.00826

9. Tinetti ME, Powell L. Fear of falling and low self-efficacy: a case of dependence in elderly persons. *J Gerontol*. (1993) 48:35–8. doi: 10.1093/geronj/48.Special_Issue.35

10. Friedman SM, Munoz B, West SK, Rubin GS, Fried LP. Falls and fear of falling: which comes first? A longitudinal prediction model suggests strategies for primary and secondary prevention. *J Am Geriatr Soc*. (2002) 50:1329–35. doi: 10.1046/j.1532-5415.2002.50352.x

11. Liu TW, Ng GYF, Ng SSM. Effectiveness of a combination of cognitive behavioral therapy and task-oriented balance training in reducing the fear of falling in patients with chronic stroke: study protocol for a randomized controlled trial. *Trials*. (2018) 19:168. doi: 10.1186/s13063-018-2549-z

12. Li P, Wang Y, Jiang Y, Zhang K, Yang Q, Yuan Z, et al. Cerebral small vessel disease is associated with gait disturbance among community-dwelling elderly individuals: the Taizhou imaging study. *Aging*. (2020) 12:2814–24. doi: 10.18632/aging.102779

13. Studenski S, Perera S, Patel K, Rosano C, Faulkner K, Inzitari M, et al. Gait speed and survival in older adults. *JAMA*. (2011) 305:50–8. doi: 10.1001/jama.2010.1923

14. Cha HG, Kim TH, Kim MK. Therapeutic efficacy of walking backward and forward on a slope in normal adults. *J Phys Ther Sci*. (2016) 28:1901–3. doi: 10.1589/jpts.28.1901

15. Prateek GV, Mazzoni P, Earhart GM, Nehorai A. Gait cycle validation and segmentation using inertial sensors. *IEEE Trans Bio Med Eng*. (2020) 67:2132–44. doi: 10.1109/TBME.2019.2955423

16. Lindemann U. Spatiotemporal gait analysis of older persons in clinical practice and research: which parameters are relevant? *Z Gerontol Geriatr*. (2020) 53:171–8. doi: 10.1007/s00391-019-01520-8

17. Sakuma K, Tateuchi H, Nishishita S, Okita Y, Kitatani R, Koyama Y, et al. Immediate effects of stance and swing phase training on gait in patients with stroke. *Int J Rehabil Res*. (2021) 44:152–8. doi: 10.1097/MRR.0000000000000464

18. Moore SR, Martinez A, Kröll J, Strutzenberger G, Schwameder H. Simple foot strike angle calculation from three-dimensional kinematics: a methodological comparison. *J Sports Sci*. (2022) 40:1343–50. doi: 10.1080/02640414.2022.2080162

19. Anderson FC, Goldberg SR, Pandy MG, Delp SL. Contributions of muscle forces and toe-off kinematics to peak knee flexion during the swing phase of normal gait: an induced position analysis. *J Biomech*. (2004) 37:731–7. doi: 10.1016/j.jbiomech.2003.09.018

20. Auvinet E, Multon F, Manning V, Meunier J, Cobb JP. Validity and sensitivity of the longitudinal asymmetry index to detect gait asymmetry using Microsoft Kinect data. *Gait Posture*. (2017) 51:162–8. doi: 10.1016/j.gaitpost.2016.08.022

21. Cabral S, Fernandes R, Selbie WS, Moniz-Pereira V, Veloso AP. Inter-session agreement and reliability of the Global Gait Asymmetry index in healthy adults. *Gait Posture*. (2017) 51:20–4. doi: 10.1016/j.gaitpost.2016.09.014

22. Cabral S, Resende RA, Clansey AC, Deluzio KJ, Selbie WS, Veloso AP. A global gait asymmetry index. *J Appl Biomech*. (2016) 32:171–7. doi: 10.1123/jab.2015-0114

23. Jabbar KA, Tan DGH, Seah WT, Lau LK, Pang BW, Ng DH, et al. Enhanced gait variability index and cognitive performance in Asian adults: results from the Yishun Study. *Gait Posture*. (2022) 97:216–21. doi: 10.1016/j.gaitpost.2022.07.156

24. Nohelova D, Bizovska L, Vuillerme N, Svoboda Z. Gait variability and complexity during single and dual-task walking on different surfaces in outdoor environment. *Sensors*. (2021) 21. doi: 10.3390/s21144792

25. Schlachetzki JCM, Barth J, Marxreiter F, Gossler J, Kohl Z, Reinfelder S, et al. Wearable sensors objectively measure gait parameters in Parkinson's disease. *PLoS ONE*. (2017) 12:e0183989. doi: 10.1371/journal.pone.0183989

26. Michnik R, Nowakowska K, Jurkojć J, Jochymczyk-Wozniak K, Kopyta I. Motor functions assessment method based on energy changes in gait cycle. *Acta Bioeng Biomech*. (2017) 19:63–75. doi: 10.1007/978-3-319-39904-1_7

frontiers | Frontiers in Bioengineering and Biotechnology

TYPE Original Research
PUBLISHED 19 March 2024
DOI 10.3389/fbioe.2024.1240339

Check for updates

OPEN ACCESS

EDITED BY
Yih-Kuen Jan,
University of Illinois at Urbana-Champaign,
United States

REVIEWED BY
Ishraq Alim,
Cornell University, United States
Fu-Lien Wu,
University of Nevada, Las Vegas, United States

*CORRESPONDENCE
Yusuke Sekiguchi,
yusuke.sekiguchi.b2@tohoku.ac.jp

RECEIVED 14 June 2023
ACCEPTED 06 March 2024
PUBLISHED 19 March 2024

CITATION
Sekiguchi Y, Owaki D, Honda K, Izumi S-I and Ebihara S (2024), Differences in kinetic factors affecting gait speed between lesion sides in patients with stroke.
Front. Bioeng. Biotechnol. 12:1240339.
doi: 10.3389/fbioe.2024.1240339

COPYRIGHT
© 2024 Sekiguchi, Owaki, Honda, Izumi and Ebihara. This is an open-access article distributed under the terms of the Creative Commons Attribution License (CC BY). The use, distribution or reproduction in other forums is permitted, provided the original author(s) and the copyright owner(s) are credited and that the original publication in this journal is cited, in accordance with accepted academic practice. No use, distribution or reproduction is permitted which does not comply with these terms.

Differences in kinetic factors affecting gait speed between lesion sides in patients with stroke

Yusuke Sekiguchi[1]*, Dai Owaki[2], Keita Honda[1], Shin-Ichi Izumi[1,3] and Satoru Ebihara[4]

[1]Department of Physical Medicine and Rehabilitation, Graduate School of Medicine, Tohoku University, Sendai, Japan, [2]Department of Robotics, Graduate School of Engineering, Tohoku University, Sendai, Japan, [3]Department of Physical Medicine and Rehabilitation, Graduate School of Biomedical Engineering, Tohoku University, Sendai, Japan, [4]Department of Internal Medicine & Rehabilitation Science, Disability Sciences, Tohoku University Graduate School of Medicine, Sendai, Japan

The differences in kinetic mechanisms of decreased gait speed across brain lesion sides have not been elucidated, including the arrangement of motor modules reflected by kinetic interjoint coordination. The purpose of this study was to elucidate the differences in the kinetic factors of slow gait speed in patients with stroke on the lesion sides. A three-dimensional motion analysis system was employed to assess joint moment in the lower limb and representative gait parameters in 32 patients with right hemisphere brain damage (RHD) and 38 patients with left hemisphere brain damage (LHD) following stroke as well as 20 healthy controls. Motor module composition and timing were determined using principal component analysis based on the three joint moments in the lower limb in the stance phase, which were the variances accounted for principal components (PCs) and the peak timing in the time series of PCs. A stepwise multiple linear regression analysis was performed to identify the most significant joint moment and PC-associated parameter in explaining gait speed. A negligible difference was observed in age, weight, height, and gait speed among patients with RHD and LHD and controls. The following factors contributed to gait speed: in patients with RHD, larger ankle plantarflexion moment on the paretic (p = 0.001) and nonparetic (p = 0.002) sides and ankle dorsiflexion moment on the nonparetic side (p = 0.004); in patients with LHD, larger ankle plantarflexion moment (p < 0.001) and delayed peak timing of the first PC (p = 0.012) on the paretic side as well as ankle dorsiflexion moment on the nonparetic side (p < 0.001); in the controls, delayed peak timing of the first PC (p = 0.002) on the right side and larger ankle dorsiflexion moment (p = 0.001) as well as larger hip flexion moment on the left side (p = 0.023). The findings suggest that the kinetic mechanisms of gait speed may differ among patients with RHD following patients with stroke with LHD, and controls.

KEYWORDS

stroke, gait, kinetics, lesion side, laterality, kinetic coordination

1 Introduction

Patients with stroke have reduced gait speed, which impairs their mobility within the community (Fulk et al., 2017), limits their living space (Tashiro et al., 2019), compromises their independence in daily life (Compagnat et al., 2021), and hinders their ability to resume to work (Jarvis et al., 2019). This can ultimately affect their overall quality of life (Sprigg

et al., 2013). Gait speed is a crucial indicator of functional mobility and is associated with various aspects of daily life for patients with stroke.

Current interventions, such as electromechanical-assisted gait training and treadmill training with physiotherapy, have shown a modest increase in walking velocity for patients with stroke (Mehrholz et al., 2017; Mehrholz et al., 2020). However, these improvements may not reach the minimal clinically significant changes for gait speed, which range from 0.10 to 0.18 m/s (Fulk et al., 2011; Bohannon and Glenney, 2014). This suggests that current interventions may be insufficient. Various factors, such as ankle moment and trail limb angle, contribute to reduced propulsion force in patients with stroke (Hsiao et al., 2016b), indicating different mechanisms at play when it comes to increasing gait speed. Trail limb angle is defined as the angle between the laboratory's vertical axis and the vector connecting the greater trochanter and the fifth metatarsal head. Therefore, understanding individual-specific factors contributing to reduced gait speed is crucial for developing personalized training strategies.

Various studies have examined the relationship between gait speed and the side of the brain lesion in patients with stroke, but findings have been inconsistent (Chen et al., 2014; Kim et al., 2019; Ursin et al., 2019; Frenkel-Toledo et al., 2021; Vismara et al., 2022). Some studies found that patients with right hemisphere brain damage (RHD) have slower gait speed than those with left hemisphere brain damage (LHD), while others found no significant difference. Patients with RHD often exhibit decreased capacity to shift body weight and unstable body movement and posture control, which can lead to slower start and reduced muscle activation in the paretic leg (Fernandes et al., 2018; Coelho et al., 2019). These patients also show higher center of pressure (CoP) sway velocity during static standing (Fernandes et al., 2018). Hsiao et al. (2017) suggested that difficulties in transferring weight from side to side and maintaining stability while walking could decrease walking speed (Hsiao et al., 2017). This process leads to the generation of vertical ground reaction force, resulting in an increase in walking speed and control of whole body angular momentum (WBAM) in the frontal plane during gait (Silverman and Neptune, 2011; Hsiao et al., 2017). Patient with strokes often exhibit increased WBAM during their gait (Nott et al., 2014; Brough et al., 2019). The ankle plantar flexion moment in late stance, which begins when the foot contacts the ground and ends when the foot leaves the floor, was related to the vertical ground reaction force and WBAM during gait (Silverman and Neptune, 2011; Elhafez et al., 2019). These observations suggest that the reduction in walking speed and increase in WBAM observed in patients with RHD may be due to a significant decrease in ankle plantar flexion moment in late stance on the paretic side during gait. However, this is only a tentative explanation and further research is needed to confirm or refute this hypothesis.

Previous researches have shown that in patient with strokes, walking speed is linked to kinetic parameters in the paretic lower limb, particularly at the ankle and hip joints (Olney et al., 1994; Kim and Eng, 2004; Jonkers et al., 2009; Sekiguchi et al., 2012; Mentiplay et al., 2019). From the results of our previous study using principal component analysis (PCA) in healthy controls, we found that as gait speed increases, the later peak timing of the first principal component (PC) demonstrates that the timing of propulsion control, exhibited by kinetic coordination, plays an important role in generating propulsion (Sekiguchi et al., 2019). In patients with stroke, we have observed a decrease in ankle joint moment and disrupted kinetic coordination, which impacts their forward movement, using PCA (Sekiguchi et al., 2022). Additionally, the first PC during gait, which involves moments at the ankle and hip joints, occurs earlier in time and includes knee joint flexion or extension (Sekiguchi et al., 2022). However, it remains unclear whether there is a relationship between the timing of the first PC and gait speed in patients with stroke.

The purpose of this study was to elucidate the differences in the kinetic factors of slow gait speed between the lesion sides in patients with stroke. We conducted a stepwise multiple linear regression analysis to determine which joint moment and parameter associated with kinetic coordination are most explanatory for gait speed. In patients with right hemisphere damage (RHD), we hypothesize that the observed reduction in walking speed and increase in whole body angular momentum (WBAM) may be due to a significant decrease in the ankle plantar flexion moment in the late stance on the paretic (left) side during gait. Furthermore, in patients with left hemiplegia, difficulties in dynamic control may result in a lack of correlation between walking speed and kinetic coordination on the paretic (right) side.

This study provides valuable insights into the kinetic mechanisms underlying decreased gait speed in patients with stroke and may inform future rehabilitation strategies. By identifying specific joint moments and parameters associated with decreased gait speed, rehabilitation professionals may be able to develop more targeted interventions to improve walking speed and functional mobility in patients with stroke.

2 Materials and methods

2.1 Subject

The present study included 32 patients with right-sided (8 females, 58 ± 10 years old, Table 1) and 38 patients with left-sided (9 females, 54 ± 13 years old, Table 1) brain lesions following stroke as well as 20 healthy controls (8 females, 57 ± 16 years old, Table 1). All patients underwent post-stroke rehabilitation, which was tailored to each patient's needs and recovery phase. To be included, patient with strokes had to meet the following criteria. (1) being able to walk without a cane over a distance of at least 7 m, (2) experiencing paresis ranging from mild to severe, with a Brunnstrom recovery stage of VI or lower in the lower limb on the paretic side, and (3) having an ischemic or hemorrhagic supratentorial lesion. To be included as a control, healthy controls must not have had any neurological lesions. Healthy controls were not eligible if they had any of the following: (1) medical conditions that were not stable, (2) a history of major orthopedic surgery or current orthopedic conditions that could affect their ability to walk, or (3) higher brain dysfunction that could affect the accuracy of the measurements. Before participating in this study, the participants gave their written and informed consent. Our institutional review board approved this study (2016-1-354).

TABLE 1 Subjects' demographic characteristics.

	Right-sided brain lesion	Left-sided brain lesion	Controls
N	32	38	20
Gender (Male/Female)	24/8	29/9	12/8
Age (years)	58.6 ± 9.9	53.9 ± 13.0	57.4 ± 16.3
Height (cm)	165.3 ± 9.0	165.2 ± 7.5	165.9 ± 8.7
Weight (kg)	62.3 ± 9.1	64.8 ± 11.4	61.6 ± 11.1
Diagnosis (Hemorrhage/Infarction)	22/10	21/17	
Location of lesion (M/S)	3/29[d]	8/29	
Time since stroke (months)	26.8 ± 39.3	31.4 ± 40.5	

[a]Values are expressed as means ± standard deviations.
[b]No significant difference was observed in the physical characteristics, diagnosis, location of lesion and time since stroke among the groups.
[c]M/C represents mixed cortical & subcortical and cortical lesions.
[d]One patient with left hemisphere damage did not have CT or MRI images available as they were hospitalized in another facility.

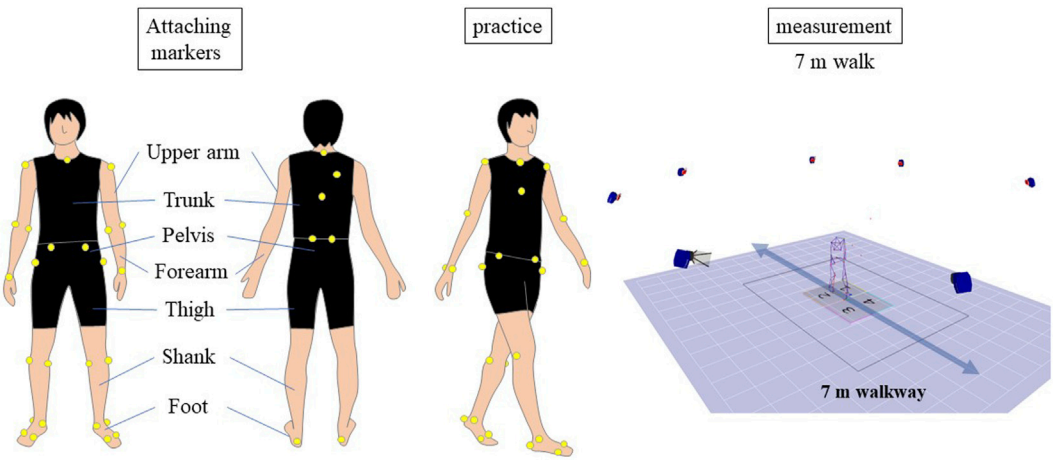

FIGURE 1
Gait Analysis Procedure. The diagram illustrates the experimental setup for the gait analysis study. Participants walked a 7-meter distance multiple times, with data from an average of more than five strides used for analysis. Reflective markers were placed on 12 body segments, and motion data were collected using an 8-camera motion analysis system. Ground reaction force data were collected using four force plates embedded in the walkway.

2.2 Gait analysis

The participants were asked to walk 7 m, repeating the task 2 to 10 times until data for five strides were collected. The patients walked barefoot at a comfortable pace without assistive devices and could rest between trials if needed. The walking speed of the healthy subjects over a distance of 7 m was determined using the patient's previously recorded walking speed as a reference, and they were instructed to walk the distance within that time. Participants had the opportunity to practice walking before the measurement (Figure 1). We calculated the duration required for the healthy individuals to traverse a distance of 7 m, aligning it with their previously recorded walking pace. The healthy subjects were guided to cover the 7-meter distance within the predetermined time frame. Prior to the actual gait measurement, the healthy controls rehearsed the 7-meter walk multiple times. Data from an average of more than five strides from successful trials were used for analysis. Whole-body motion data were collected using an 8-camera motion analysis system at a rate of 120 Hz (MAC 3D, Motion Analysis Corporation, Santa Rosa, CA, USA) with 33 reflective markers placed on 12 body segments (As shown in Supplementary Table). The three-dimensional coordinates were smoothed with a bidirectional fourth-order Butterworth low-pass filter with a cutoff frequency of 6 Hz. Ground reaction force data were collected at a rate of 1,200 Hz using four force plates (Anima Corporation, Chofu, Tokyo, Japan) embedded in the walkway and smoothed with a bidirectional fourth-order Butterworth low-pass filter with a cutoff frequency of 200 Hz.

A model consisting of 12 body segments, based on anthropometric data and following the work of (Dumas et al., 2007), included the feet, shanks, thighs, pelvis, thorax, upper arms, and forearms. A joint coordinate system was used to calculate the kinematic data for each joint in the lower extremities, as described by Winter (2009).

Additionally, inverse dynamics was employed to estimate the kinetics of the joints in the lower extremities (Selbie et al., 2013). All kinematic and kinetic data were normalized to 100% of a single gait cycle. The representative method was used to calculate spatiotemporal

parameters (Butler et al., 2006). The kinematic and kinetic data were used to obtain the representative gait parameters, following the methods outlined in a previous study by Kinsella and Moran (2008). The kinetic data was normalized to the patient's body weight.

A spatiotemporal decomposition using principal component analysis (PCA) was performed on the joint moments in the lower limb (ankle, knee, and hip) to calculate the coordination of the lower limb joints and the loading on each joint. This is the same method used in our previous study (Sekiguchi et al., 2022). The kinetic data in the stance phase during gait was used in this study unlike one gait cycle used in the previous study (Sekiguchi et al., 2022). The parameters of interest included the percentage of variance explained by each principal component (PC), the timing of the peak of the first PC, and the factor loadings of each joint in each PC. The percentage of variance explained by each PC and the peak timings represented the spatial and temporal aspects of the motor module.

The evaluation of balance control was conducted using the range of whole-body angular momentum ($WBAM_R$) in the frontal plane (Brough et al., 2019). The calculation of whole-body angular momentum (WBAM) was performed using a 12-segment inverse dynamics model. This involved aggregating the angular momentum of each body segment around the center of mass for the entire body in the frontal plane. The whole-body angular momentum was then normalized based on the subject's mass, walking speed, and leg length. $WBAM_R$ was characterized as the difference between the maximum positive and minimum negative peaks of WBAM, with an average taken across all strides.

All gait-related parameters were calculated using a custom software program created with MATLAB (MathWorks Inc., Natick, MA, USA).

2.3 Clinical characteristics

A physical therapist, Y.S., assessed the neurological impairment of patients using the Stroke Impairment Assessment Set (SIAS) (Tsuji et al., 2000). Information about the patients' demographic and clinical characteristics was gathered through interviews and medical records.

2.4 Statistical analysis

The number of gait cycles used for statistical analysis varied from 5 to 9 for each participant. The determination of the number of gait cycles was based on each patient's walking ability. In instances where a slower walking speed and high variability were expected, we incorporated a larger number of steps into our analysis. Gait speed, cycle time, stride length, step width, and $WBAM_R$ were compared between the three groups (RHD and LHD patients and controls) using one-way analysis of variance (ANOVA). Stance, swing, double stance, single-support phase times, step length, joint angle, joint moment, and PCA-related parameters were analyzed using a two-way ANOVA. Although we evaluated the normality of the gait dataset using the Shapiro-Wilk test, we did not conduct non-parametric tests for the two-way ANOVA, as these tests do not compute interactions between factors. The within-subject factor was side (paretic/nonparetic for hemiparesis patients and right/left for controls) and the independent factor was group (hemiparesis patients/controls). The two-way ANOVA was performed separately for left-sided and right-sided brain lesions. If a significant difference was found, a Bonferroni *post hoc* test was conducted. In addition, we compared all parameters between patients with RHD and LHD using unpaired t-test. A chi-square test of independence was conducted to investigate the relationship between the side of the lesion and the location of the lesion and the diagnosis. Stepwise multiple linear regression was used to determine which joint moments and PCA-related parameters best explained gait speed. Forward and backward selection methods were used. In each forward step, the independent variable with the smallest probability of F not in the regression equation and ≤0.05 was included. In each backward step, the independent variable with a probability of F ≥0.10 was removed. The analysis ended if no variables met the criteria for inclusion or exclusion. A *post hoc* statistical power was conducted using G*Power software (ver. 3.1.9.2; Heinrich-Heine-Universität Düsseldorf) and MATLAB (MathWorks Inc., Natick, MA, USA). The significance level was set at $p = 0.05$ and we estimated effect sizes using partial eta squared (η_p^2), eta squared (η^2), r, and Cohen's d. Statistical analyses were performed using SPSS ver. 24 (IBM-SPSS Inc., Chicago, IL, USA).

In our study, we initially conducted a sample size calculation using G*Power 3.1.9.2. We assumed a multiple regression model with 22 predictors and aimed to estimate the partial regression coefficients. With an effect size of $f^2 = 0.18$, corresponding to an adjusted coefficient of determination $R^2 \approx 0.15$, we performed our tests at a 5% significance level and aimed for 80% power. This led us to a required sample size of 140 participants in total.

3 Results

The common and differing results of the parameters related to gait for patients with LHD and RHD are compiled in the Supplementary Material Data Sheet, which also includes a summary due to the extensive amount of results for ease of reference.

The *post hoc* power analysis demonstrates that despite our sample size being less than the initially estimated 140 participants, the actual power achieved with our sample of 32 patients with right-sided brain lesions, 38 patients with left-sided brain lesions, and 20 healthy controls was 0.99. This high power indicates that our study was adequately powered to detect significant effects, despite the smaller sample size.

3.1 Subject characteristics

We did not find significant differences in gender, age, height, weight, diagnosis, and time since stroke among the groups. The speech ($p < 0.001$, $r = 3.15$) and finger function ($p = 0.030$, $r = 0.56$) item scores in patients with LHD were lower than those with RHD. No significant difference in the other items of SIAS was also found between patients with RHD and LHD.

3.2 Differences in gait parameters

Tables 2–4 present the representative gait, kinetic and kinematic, and PCA-related parameters, respectively, of patients with RHD, LHD, and also healthy controls. We presented the results of the

TABLE 2 Mean and standard deviation of spatiotemporal and $WBAM_R$ data in patients following stroke and healthy controls.

	Right-sided brain lesion		Left-sided brain lesion		Healthy controls		Two-way ANOVA					
							Right-sided brain lesion vs. controls			Left-sided brain lesion vs. controls		
							p-value			*p*-value		
	Paretic side	Nonparetic side	Paretic side	Nonparetic side	Right	Left	Subjects	Laterality	Interaction	Subjects	Laterality	Interaction
Gait speed (m/s)	0.52 ± 0.26		0.46 ± 0.27		0.48 ± 0.18							
Gait cycle time (s)	1.52 ± 0.47		1.67 ± 0.62		1.82 ± 0.52							
Stride length (m)	0.70 ± 0.27[a]		0.65 ± 0.27[a]		0.88 ± 0.17[a]							
Step width (m)	0.16 ± 0.05		0.16 ± 0.04		0.14 ± 0.03							
$WBAM_R$	**0.13 ± 0.10**		**0.16 ± 0.13**[b]		**0.08 ± 0.04**[b]							
Stance time (s)	0.96 ± 0.43[c,d]	1.17 ± 0.51[c]	1.14 ± 0.61[c]	1.35 ± 0.68[c]	1.25 ± 0.45	1.23 ± 0.43[d]	0.186	<0.000	<0.000	0.998	<0.000	<0.000
Swing time (s)	0.55 ± 0.10	0.37 ± 0.09	0.54 ± 0.10	0.38 ± 0.14	0.58 ± 0.10	0.59 ± 0.10	<0.000	<0.000	<0.000	<0.000	0.002	0.001
Step length (m)	0.36 ± 0.12[c,d]	0.32 ± 0.15[c,e]	0.33 ± 0.13[c,f]	0.31 ± 0.15[b,c]	0.43 ± 0.09[e,f]	0.43 ± 0.08[b,d]	0.008	0.030	0.146	0.001	0.500	0.140

[a]Significantly different between patients and healthy controls at $p < 0.05$.
[b]Significantly different between the left sides in patients with left-sided brain lesion and healthy controls at $p < 0.05$.
[c]Significantly different between the paretic and nonparetic sides in patients at $p < 0.05$.
[d]Significantly different between the left sides in patients with right-sided brain lesion and healthy controls at $p < 0.05$.
[e]Significantly different between the right sides in patients with right-sided brain lesion and healthy controls at $p < 0.05$.
[f]Significantly different between the right sides in patients with left-sided brain lesion and healthy controls at $p < 0.05$.

10.3389/fbioe.2024.1240339

TABLE 3 Mean and standard deviation of kinematic and kinetic data in patients following stroke and healthy controls.

	Right-sided brain lesion		Left-sided brain lesion		Healthy controls		Two-way ANOVA					
							Right-sided brain lesion vs. controls			Left-sided brain lesion vs. controls		
							p-value			*p*-value		
	Left side	Right side	Right side	Left side	Right side	Left side	Subjects	Laterality	Interaction	Subjects	Laterality	Interaction
	Paretic side	Nonparetic side	Paretic side	Nonparetic side								
Peak hip extension moment in early stance (Nm/kg)	0.42 ± 0.30[a]	0.61 ± 0.34[a,b]	0.34 ± 0.26[a,c]	0.46 ± 0.21[a,c,d]	0.29 ± 0.10[b]	0.31 ± 0.15[d]	0.004	0.010	0.002	0.066	0.004	0.031
Peak hip flexion moment in the stance phase (Nm/kg)	0.57 ± 0.33	0.62 ± 0.28	0.64 ± 0.32[a]	0.54 ± 0.26[a]	0.68 ± 0.28	0.61 ± 0.17	0.498	0.140	0.835	0.412	0.038	0.687
First peak knee extension moment in the stance phase (Nm/kg)	0.16 ± 0.14[a,e]	0.33 ± 0.20[a,b]	0.31 ± 0.21[e]	0.34 ± 0.26[d]	0.22 ± 0.17[b]	0.18 ± 0.15[d]	0.199	0.003	0.051	0.019	0.887	0.240
Peak knee flexion moment in the stance phase (Nm/kg)	0.37 ± 0.32[a,e,f]	−0.04 ± 0.17[a,b]	0.12 ± 0.27[a,e]	−0.01 ± 0.20[a,d]	0.15 ± 0.13[b]	0.18 ± 0.11[d,f]	0.968	<0.000	<0.000	0.011	0.226	0.047
Second peak knee extension moment in the stance phase (Nm/kg)	0.19 ± 0.16[a,e]	0.44 ± 0.25[a,b]	0.34 ± 0.23[a,e]	0.47 ± 0.30[a,d]	0.32 ± 0.14[b]	0.25 ± 0.08[d]	0.383	<0.000	0.013	0.025	0.479	0.004
Peak ankle dorsiflexion moment in early stance (Nm/kg)	0.03 ± 0.07[a,f]	0.09 ± 0.09[a]	0.03 ± 0.06[a,c,g]	0.07 ± 0.05[a,c]	0.07 ± 0.05[g]	0.07 ± 0.06[f]	0.626	0.016	0.012	0.093	0.175	0.221
Peak ankle plantarflexion moment in the stance phase (Nm/kg)	0.72 ± 0.27[a,f]	0.95 ± 0.20[a]	0.68 ± 0.30[a,g]	0.89 ± 0.24[a]	0.96 ± 0.17[g]	1.00 ± 0.16[f]	0.008	0.001	<0.000	0.002	<0.000	0.002
Peak hip extension in stance (°)	−6.1 ± 7.9[a,f]	−12.8 ± 17.1[a,b]	−8.9 ± 8.9[a,g]	−12.7 ± 14.2[a,d]	1.6 ± 6.5[b,g]	1.7 ± 6.5[f,d]	<0.000	0.035	0.043	<0.000	0.290	0.255
Peak hip flexion in early stance (°)	26.1 ± 7.1	23.5 ± 15.5	28.9 ± 8.0	27.7 ± 14.8	27.6 ± 4.3	27.4 ± 4.3	0.233	0.456	0.418	0.709	0.705	0.753
Peak knee flexion in early stance (°)	11.1 ± 9.9[a,e]	19.2 ± 5.8[a,b,e]	17.7 ± 9.3[a,g]	20.7 ± 8.5[a,d]	12.9 ± 5.7[b,g]	12.1 ± 5.0[d]	0.068	0.004	0.017	<0.000	0.362	0.109
Peak knee extension in stance (°)	−0.9 ± 9.0[a,e]	−8.1 ± 5.3[a,b,e]	−7.1 ± 8.2[a]	−9.5 ± 7.5[a,d]	−4.2 ± 5.3[b]	−2.2 ± 5.3[d]	0.346	0.001	0.050	0.003	0.877	0.051
Peak knee flexion in late stance (°)	22.5 ± 12.7[a,f]	44.4 ± 4.9[a,b]	27.7 ± 11.1[a,g]	43.7 ± 6.7[a,d]	35.3 ± 5.1[b,g]	34.9 ± 6.8[f,d]	0.345	<0.000	<0.000	0.718	<0.000	<0.000

(Continued on following page)

10.3389/fbioe.2024.1240339

TABLE 3 (*Continued*) Mean and standard deviation of kinematic and kinetic data in patients following stroke and healthy controls.

	Right-sided brain lesion		Left-sided brain lesion		Healthy controls		Two-way ANOVA					
							Right-sided brain lesion vs. controls			Left-sided brain lesion vs. controls		
							p-value			*p*-value		
	Left side	Right side	Right side	Left side	Right side	Left side	Subjects	Laterality	Interaction	Subjects	Laterality	Interaction
	Paretic side	Nonparetic side	Paretic side	Nonparetic side								
Ankle plantarflexion in early stance (°)	5.4 ± 8.7[a]	−1.4 ± 4.6[a,b]	3.3 ± 5.3[a]	0.4 ± 6.3[a]	3.4 ± 3.7[b]	2.9 ± 3.1	0.342	0.010	0.003	0.189	0.096	0.254
Ankle dorsiflexion in stance (°)	11.0 ± 9.6[a,e,f]	21.2 ± 3.4[a,b]	15.1 ± 6.5[a,f,g]	20.0 ± 5.7[a]	18.9 ± 3.8[b,g]	19.2 ± 2.8[f]	0.019	<0.000	<0.000	0.168	0.012	0.024

[a]Significantly different between the paretic and nonparetic sides in patients at $p < 0.05$.
[b]Significantly different between the right sides in patients with right-sided brain lesion and healthy controls at $p < 0.05$.
[c]Significantly different between the nonparetic sides in patients with left-sided and right-sided brain lesion.
[d]Significantly different between the left sides in patients with left-sided brain lesion and healthy controls at $p < 0.05$.
[e]Significantly different between the paretic sides in patients with left-sided and right-sided brain lesion.
[f]Significantly different between the left sides in patients with right-sided brain lesion and healthy controls at $p < 0.05$.
[g]Significantly different between the right sides in patients with left-sided brain lesion and healthy controls at $p < 0.05$.

10.3389/fbioe.2024.1240339

TABLE 4 Mean and standard deviation results for the PCA-related data.

	Right-sided brain lesion		Left-sided brain lesion		Healthy controls		Two-way ANOVA					
							Right-sided brain lesion vs. controls			Left-sided brain lesion vs. controls		
							p-Value			*p*-Value		
	Left side	Right side	Right side	Left side	Right side	Left side	Subjects	Laterality	Interaction	Subjects	Laterality	Interaction
	Paretic side	Nonparetic side	Paretic side	Nonparetic side								
Timing of peak PC1 (% stance phase)	67.22 ± 16.45[a,b]	75.28 ± 14.67[a]	68.74 ± 15.92[c]	54.40 ± 34.15[d]	79.15 ± 6.75[c]	81.35 ± 6.86[b,d]	0.170	0.227	0.037	< 0.000	0.163	0.059
Variance explained by PC1 (%)	0.78 ± 0.12	0.77 ± 0.12	0.81 ± 0.10[a]	0.74 ± 0.13[a]	0.79 ± 0.10	0.78 ± 0.08	0.631	0.766	0.663	0.550	0.063	0.086
Variance explained by PC2 (%)	0.20 ± 0.10	0.18 ± 0.10	0.17 ± 0.10	0.22 ± 0.11	0.20 ± 0.09	0.19 ± 0.08	0.879	0.712	0.616	0.950	0.224	0.192
Variance explained by PC1 + PC2 (%)	0.98 ± 0.03[a]	0.95 ± 0.04[a,e]	0.98 ± 0.02[a]	0.95 ± 0.04[a,d]	0.98 ± 0.02[c]	0.98 ± 0.02[d]	0.027	0.035	0.005	0.046	0.006	0.055
Loadings of ankle joint moment in PC1	0.66 ± 0.15	0.62 ± 0.09	0.66 ± 0.11[a,c]	0.61 ± 0.16[a]	0.60 ± 0.07[c]	0.63 ± 0.07	0.125	0.163	0.763	0.376	0.421	0.037
Loadings of knee joint moment in PC1	−0.23 ± 0.51[a,b,f]	0.37 ± 0.45[a]	0.27 ± 0.49[f]	0.38 ± 0.45	0.28 ± 0.53	0.23 ± 0.51[b]	0.122	< 0.000	0.001	0.541	0.720	0.307
Loadings of hip joint moment in PC1	−0.22 ± 0.44[a,b]	−0.39 ± 0.34[a]	−0.38 ± 0.32[c]	−0.32 ± 0.41[d]	−0.52 ± 0.15[c]	−0.54 ± 0.10[b,d]	0.005	0.127	0.058	0.012	0.638	0.379
Loadings of ankle joint moment in PC2	0.15 ± 0.38[a,b,f]	−0.25 ± 0.42[a]	−0.16 ± 0.41[f]	−0.12 ± 0.47	−0.19 ± 0.41	−0.19 ± 0.41[b]	0.137	0.005	0.005	0.616	0.779	0.765
Loadings of knee joint moment in PC2	0.57 ± 0.28[b]	0.50 ± 0.31[e]	0.60 ± 0.23[a]	0.47 ± 0.30[a]	0.68 ± 0.24[c,g]	0.73 ± 0.20[b,g]	0.005	0.253	0.860	0.004	0.253	0.017
Loadings of hip joint moment in PC2	−0.38 ± 0.56[a,b]	0.11 ± 0.65[a]	−0.10 ± 0.63	0.04 ± 0.69	0.10 ± 0.54	0.05 ± 0.49[b]	0.107	0.010	0.038	0.419	0.677	0.357

[a]Significantly different between the paretic and nonparetic sides in patients at $p < 0.05$.
[b]Significantly different between the left sides in patients with right-sided brain lesion and healthy controls at $p < 0.05$.
[c]Significantly different between the right sides in patients with left-sided brain lesion and healthy controls at $p < 0.05$.
[d]Significantly different between the left sides in patients with left-sided brain lesion and healthy controls at $p < 0.05$.
[e]Significantly different between the right sides in patients with right-sided brain lesion and healthy controls at $p < 0.05$.
[f]Significantly different between the paretic sides in patients with left-sided and right-sided brain lesion.
[g]Significantly different between the right and left sides in healthy controls at $p < 0.05$.

10.3389/fbioe.2024.1240339

statistical power in Supplementary Tables S6–S9 as Supplementary Material.

3.2.1 Gait speed, step length, gait cycle time, step width, and WBAM

No significant differences were observed in gait cycle time, gait speed, location of lesion, and step width among the three groups. However, significant differences were found in stride length ($F_{(2,87)}$ = 5.611, p = 0.005, η^2 = 0.11) and $WBAM_R$ ($F_{(2,87)}$ = 3.288, p = 0.042, η^2 = 0.07). The stride lengths of patients with RHD (p = 0.004, d = 0.95) and LHD (p = 0.034, d = 0.77) were shorter than those of healthy controls. There was no significant difference in $WBAM_R$ between patients with RHD and LHD. However, the $WBAM_R$ in patients with LHD was larger than that of healthy controls (p = 0.032, d = 0.68) (Table 2).

3.2.2 Spatiotemporal parameters in patients with RHD

Significant main effects of group ($F_{(1,50)}$ = 7.654, p = 0.008, η_p^2 = 0.13) and side ($F_{(1,50)}$ = 4.981, p = 0.030, η_p^2 = 0.09) on step length were found. Patients with RHD had shorter step lengths than controls, and the step length on the left side was longer than on the right side (Table 2).

Significant main effects of group ($F_{(1,50)}$ = 33.112, p < 0.001, η_p^2 = 0.40), side ($F_{(1,50)}$ = 29.223, p < 0.001, η_p^2 = 0.37), and interactions between group and side ($F_{(1,50)}$ = 28.013, p < 0.001, η_p^2 = 0.36) were also found on swing time. The swing time on the paretic (left) side was longer than on the nonparetic (right) side in patients with RHD (p < 0.001, d = 1.94). The swing time on the nonparetic (right) side in patients with RHD was shorter than that on the right side in healthy controls (p < 0.001, d = 2.33).

In addition, there were significant main effects of side ($F_{(1,50)}$ = 33.626, p < 0.001, η_p^2 = 0.40) and interaction between group and side ($F_{(1,50)}$ = 25.687, p < 0.001, η_p^2 = 0.34) on stance time. The *post hoc* test showed that the stance time was shorter on the paretic (left) side than on the nonparetic (right) side in patients with RHD (p < 0.001, d = 0.44). The stance time was shorter on the paretic (left) side in patients with RHD than on the left side in healthy controls (p = 0.031, d = 0.63).

3.2.3 Spatiotemporal parameters in patients with LHD

Significant main effects of group ($F_{(1,50)}$ = 11.766, p = 0.001, η_p^2 = 0.17) on step length, with patients with LHD having shorter step lengths than the controls, were found (Table 2).

There were also significant main effects of group ($F_{(1,50)}$ = 32.147, p < 0.001, η_p^2 = 0.37), side ($F_{(1,50)}$ = 11.030, p = 0.002, η_p^2 = 0.17), and interactions between group and side ($F_{(1,50)}$ = 12.974, p = 0.001, η_p^2 = 0.19) on swing time. The swing time on the paretic (right) side was longer than that on the nonparetic (left) side in patients with LHD (p < 0.001, d = 1.29). The swing time on the nonparetic (left) side was shorter than that on the left side in healthy controls (p < 0.001, d = 1.60).

Furthermore, there were significant main effects of side ($F_{(1,50)}$ = 15.989, p < 0.001, η_p^2 = 0.22) and interaction between group and side ($F_{(1,50)}$ = 20.884, p < 0.001, η_p^2 = 0.27) on stance time. The *post hoc* test found that the stance time was shorter on the paretic (right) side than on the nonparetic (left) side in patients with LHD (p < 0.001, d = 0.32).

3.2.4 Kinetic and kinematic parameters of patients with RHD

Significant main effects of side and interaction between group and side were observed on all kinetic parameters, except the peak hip flexion moment in the stance phase, as presented in Table 3. Moreover, the results showed significant main effects of group on the peak hip extension moment in early stance ($F_{(1,50)}$ = 9.307, p = 0.004, η_p^2 = 0.16) and peak ankle plantarflexion moment in the stance phase ($F_{(1,50)}$ = 7.599, p = 0.008, η_p^2 = 0.13). In patients with RHD, both the first (p < 0.001, d = 0.81) and second peak knee extension moments (p < 0.001, d = 0.76) on the paretic side during the stance phase were smaller than those in patients with LHD. The peak knee flexion moment during the stance phase on the paretic side was larger in patients with RHD than in those with LHD (p < 0.001, d = 0.86). Furthermore, the peak hip extension moment (p = 0.033, d = 0.52) and ankle dorsiflexion (p = 0.048, d = 0.48) in early stance on the nonparetic side were larger in patients with RHD than in those with LHD (Table 3).

The results of the *post hoc* test for kinetic parameters were as follows. The peak hip extension moment and first and second peak knee extension moments in stance on the nonparetic (right) side in patients with RHD were larger than those on the right side in healthy controls (p < 0.001, d = 1.13; p = 0.041, d = 0.60; p = 0.049, d = 0.58) and those on the paretic (left) side in patients with RHD (p < 0.001, d = 0.53; p < 0.001, d = 0.98; p < 0.001, d = 1.23). Although the peak knee flexion moment in the stance phase on the nonparetic (right) side was smaller than that on the paretic (left) side (p < 0.001, d = 1.59) and that on the right side in healthy controls (p < 0.001, d = 1.24), the peak knee flexion moment in the stance phase on the paretic (left) side in patients was larger than that on the left side in healthy controls (p = 0.015, d = 0.72). The peak ankle dorsiflexion moment in early stance and ankle plantarflexion moment in the stance phase on the paretic (left) side were smaller than those on the nonparetic (right) side in patients (p < 0.001, d = 0.76 and p < 0.001, d = 0.98) and those on the left side in healthy controls (p = 0.043, d = 0.59 and p < 0.001, d = 1.22).

There were significant main effects of group, side, and interaction between group, and side on kinematics such as the peak hip extension in stance, peak knee flexion in early stance, and peak ankle dorsiflexion in stance, as presented in Table 3. In addition, there were significant main effects of side and interaction between group and side on the peak knee extension in stance, peak knee flexion in late stance, and peak ankle plantarflexion in early stance. The peak knee flexion (p = 0.005, d = 0.69) and peak ankle dorsiflexion (p = 0.037, d = 0.51) in early stance on the paretic side in patients with RHD were smaller than those with LHD. On the other hand, the peak knee extension in stance on the paretic side with RHD was larger than those with LHD (p = 0.004, d = 0.72).

The results of the *post hoc* test for kinematic parameters were as follows. The peak hip extension in the stance phase, peak knee extension in the stance phase, and peak ankle plantarflexion in early stance on the nonparetic (right) side were lower than those on the paretic (left) side (p = 0.001, d = 0.59; p < 0.001, d = 0.97; p < 0.001, d = 0.98) and those on the right side (p = 0.001, d = 1.06; p = 0.013, d = 0.74; p < 0.001, d = 1.12) in healthy controls. The peak knee

flexion in early and late stance and peak ankle dorsiflexion in the stance phase on the nonparetic side (right) were higher than those on the paretic (left) side in patients ($p < 0.001$, $d = 1.01$; $p < 0.001$, $d = 2.27$; $p < 0.001$, $d = 1.41$) and those on the right side in healthy controls ($p < 0.001$, $d = 1.09$; $p < 0.001$, $d = 1.82$; $p = 0.030$, $d = 0.64$). The peak hip extension in stance, peak knee flexion in late stance, and peak ankle dorsiflexion in stance on the paretic (left) side were also smaller than those on the left side in healthy controls ($p = 0.001$, $d = 1.02$; $p < 0.001$, $d = 1.14$; $p = 0.001$, $d = 1.05$).

3.2.5 Kinetic and kinematic parameters of patients with LHD

A significant main effect of side on kinetics such as the peak hip flexion moment in the stance phase was observed, which was larger on the right side than on the left side. Significant main effects of group on the first peak knee extension moment in the stance phase and peak ankle dorsiflexion moment in early stance were also observed, which were larger in patients than in healthy controls. There were significant main effects of group and interaction between group and side on the peak knee flexion in the stance phase and second peak knee extension moment in the stance phase. Moreover, significant main effects of group, side, and interaction between group, and side on the peak ankle plantarflexion moment in the stance phase were found (Table 3).

The results of the *post hoc* test for kinetic parameters were as follows. The peak hip extension moment and second peak knee extension moment in stance on the nonparetic (left) side in patients with RHD were larger than those on the left side in healthy controls ($p = 0.006$, $d = 0.79$ and $p = 0.003$, $d = 0.48$) and those on the paretic (right) side in patients ($p < 0.001$, $d = 0.53$ and $p = 0.002$, $d = 0.90$). The peak knee flexion moment in the stance phase on the nonparetic (left) side in patients with RHD was smaller than that on the left side in healthy controls ($p < 0.001$, $d = 1.16$) and that on the paretic (right) side in patients ($p = 0.007$, $d = 0.52$). The peak ankle plantarflexion moment in the stance phase on the paretic (right) side was smaller than that on the nonparetic (left) side in patients ($p < 0.001$, $d = 0.78$) and that on the left side in healthy controls ($p < 0.001$, $d = 1.08$).

Significant main effects of side and interaction between group and side were observed on kinematics such as the peak knee flexion in the late stance phase and peak ankle dorsiflexion in the stance phase, as presented in Table 3. In addition, there were significant main effects of group and interaction between group and side on the peak knee extension in stance. Significant main effects of side on the peak ankle plantarflexion in early stance were found, which was larger on the right side than on the left side. Significant main effects of group on the peak hip extension and peak knee flexion in early stance were also observed, which were smaller, and larger, respectively, in patients than in healthy controls.

The results of the *post hoc* test for kinematic parameters were as follows. The peak knee extension in the stance phase on the nonparetic (left) side in patients was smaller than that on the left side in healthy controls ($p < 0.001$, $d = 1.07$). The peak knee flexion in the late stance phase on the paretic (right) side in patients was smaller than those on the nonparetic (left) side ($p < 0.001$, $d = 1.74$) and on the right side in healthy controls ($p = 0.005$, $d = 0.80$). The peak knee flexion in late stance on the nonparetic side (right) was higher than that on the right side in healthy controls ($p < 0.001$, $d = 1.31$).

3.2.6 PCA-related parameters of patients with RHD

There were significant main effects of group on the peak timing of the first PC ($F_{(1,50)} = 10.234$, $p = 0.002$, $\eta_p^2 = 0.17$) and the percent variance of the first two PCs ($F_{(1,50)} = 5.183$, $p = 0.027$, $\eta_p^2 = 0.09$) as well as of interaction between group and side on the peak timing of the first PC ($F_{(1,50)} = 4.581$, $p = 0.037$, $\eta_p^2 = 0.08$) and the percent variance of the first two PCs ($F_{(1,50)} = 8.837$, $p = 0.005$, $\eta_p^2 = 0.15$). A significant main effect of side was observed on the percent variance of the first two PCs ($F_{(1,50)} = 4.678$, $p = 0.035$, $\eta_p^2 = 0.09$). The *post hoc* test indicated earlier peak timing of the first PC on the paretic (left) side than on the nonparetic (right) side ($p = 0.009$, $d = 0.52$) and the left side in healthy controls ($p = 0.001$, $d = 1.04$). The percent variance of the first two PCs on the nonparetic (right) side was lower than those on the paretic (left) side ($p < 0.001$, $d = 0.85$) and on the right side in healthy controls ($p = 0.002$, $d = 0.94$) (Table 4).

There were significant main effects of side on the loading of knee joint moment for the first PC ($F_{(1,50)} = 17.572$, $p < 0.001$, $\eta_p^2 = 0.26$), of group on the loading of hip joint moment for the first PC ($F_{(1,50)} = 8.636$, $p = 0.005$, $\eta_p^2 = 0.15$), and of interaction between group and side on the loading of knee joint moment for the first PC ($F_{(1,50)} = 12.488$, $p = 0.001$, $\eta_p^2 = 0.20$). The *post hoc* test showed that the loading of hip joint moment for the first PC was a negative value and larger in patients than in healthy controls. On the paretic (left) side, the loading of knee joint moment for the first PC was a negative value and lower than those on the nonparetic (right) side ($p < 0.001$, $d = 1.26$) and on the left side in healthy controls ($p = 0.003$, $d = 0.90$). The loading of knee joint moment for the first PC on the paretic side in patients with RHD was smaller than those with LHD ($p < 0.001$, $d = 1.01$).

3.2.7 PCA-related parameters of patients with LHD

There were significant main effects of group on the peak timing of the first PC ($F_{(1,50)} = 18.800$, $p < 0.001$, $\eta_p^2 = 0.25$) and the percent variance of the first two PCs ($F_{(1,50)} = 4.169$, $p = 0.046$, $\eta_p^2 = 0.07$) as well as of side on the percent variance of the first two PCs ($F_{(1,50)} = 8.097$, $p = 0.006$, $\eta_p^2 = 0.13$). There seemed to be an interaction between group and side in the percent variance of the first two PCs ($F_{(1,50)} = 3.828$, $p = 0.055$, $\eta_p^2 = 0.06$). The *post hoc* test indicated earlier peak timing of the first PC on the paretic (right) and nonparetic (left) sides in patients than on the right ($p = 0.007$, $d = 0.77$) and left ($p = 0.008$, $d = 0.76$) sides in healthy controls. The percent variance of the first two PCs on the nonparetic (left) side was lower than those on the paretic (right) side ($p < 0.001$, $d = 0.78$) and the left side of healthy controls ($p = 0.023$, $d = 0.64$) (Table 4).

There were significant main effects of the group on the loading of hip joint moment for the first PC ($F_{(1,50)} = 6.723$, $p = 0.012$, $\eta_p^2 = 0.11$) as well as of interaction between group and side on the loading of ankle joint moment for the first PC ($F_{(1,50)} = 4.571$, $p = 0.037$, $\eta_p^2 = 0.08$). The *post hoc* test indicated that the loading of hip joint moment for the first PC was a negative value and larger in patients than in healthy controls. The loading of ankle joint moment for the first PC was higher on the paretic (right) side than on the nonparetic (left) side ($p = 0.015$, $d = 0.42$) and right side in healthy controls ($p = 0.016$, $d = 0.69$).

TABLE 5 Multiple regression analysis with gait speed in patients with hemiparesis and healthy controls.

Variable	Partial regression coefficient	Standardized partial regression coefficient	Variance, R^2	*p*-value	VIF
Healthy controls					
Peak ankle dorsiflexion moment in early stance on the left side	−1.640	−0.528	0.565	0.001	1.391
Timing of peak PC1 on the right side	0.011	0.402	0.735	0.002	1.051
Peak hip flexion moment in the stance phase on the right side	−0.091	−0.304	0.798	0.023	1.380
Patients with right-sided brain lesion					
Peak ankle plantarflexion moment in the stance phase on the paretic side	0.414	0.428	0.559	0.001	1.596
Peak ankle plantarflexion moment in the stance phase on the nonparetic side	0.495	0.380	0.662	0.002	1.475
Peak ankle dorsiflexion moment in early stance on the nonparetic side	−0.904	−0.310	0.741	0.004	1.165
Patients with left-sided brain lesion					
Peak ankle plantarflexion moment in the stance phase on the paretic side	0.506	0.548	0.517	0.000	1.147
Peak ankle dorsiflexion moment in early stance on the nonparetic side	−2.040	10.423	0.682	0.000	1.101
Timing of peak PC1 on the paretic side	0.004	0.233	0.728	0.012	1.054

[a]PC, principal component.

3.3 Influence of kinetic and PCA-Related parameters on walking speed

The results obtained from the multiple regression analysis of gait speed for patients with RHD and LHD lesions and healthy controls are presented in Table 5. In patients with LHD and healthy controls, the peak ankle dorsiflexion moment in early stance on the left side (nonparetic side) and timing of peak PC1 on the right side (paretic side) were found to be significant gait speed predictors. Furthermore, only in patients with LHD, the peak ankle plantarflexion moment in the stance phase on the right side (paretic side) found to be a significant gait speed predictor. In healthy controls, the peak hip flexion moment in the stance phase on the left side was found to contribute to gait speed. In patients with RHD, the peak ankle dorsiflexion moment in early stance and ankle plantarflexion moment in the stance phase on the right side (nonparetic side), as well as ankle plantarflexion moment in the stance phase on the left side (paretic side), were identified as contributors to gait speed. The statistical power in the multiple regression analysis across all groups was 0.99, indicating that the findings are likely reflecting actual effects rather than being products of chance (Table 5).

4 Discussion

The factors that contributed to gait speed varied among patients with RHD, patients with LHD, and controls. Consistent with hypothesis, in patients with RHD, larger ankle plantarflexion moments on both the paretic (left) and nonparetic (right) sides as well as ankle dorsiflexion moment on the nonparetic (right) side were contributing factors. However, contrary to hypothesis, WBAM in RHD did not differ from that in patient with LHD and healthy controls. The results may reflect the cautious gait in patients with RHD, who have instability while standing. In patients with LHD, larger ankle plantarflexion moment and delayed peak timing of the first PC on the paretic (right) side as well as ankle dorsiflexion moment on the nonparetic (left) side were contributing factors. In controls, larger ankle dorsiflexion moment as well as larger hip flexion moment on the left side and delayed peak timing of the first PC on the right side were contributing factors. Contrary to hypothesis, our results indicated that patients with LHD controlled walking speed by the timing of kinetic coordination on the paretic (right) side, similar to control groups. No study has investigated the factors contributing to gait speed in patients with stroke by simultaneously including kinetic parameters of both the paretic and nonparetic sides. To the best of our knowledge, this is the first study that included bilateral kinetic factors in a multiple regression analysis and demonstrated that the kinetic factors contributing to gait speed differ between patients with LHD and RHD.

Our findings suggested that, much like the control groups, patients with LHD managed their walking speed by coordinating the timing of kinetic movements on their paretic (right) side. Previous research has shown that left hemisphere dominance for skilled movement is attributed to anatomical and functional hemispheric asymmetries of the primary motor cortex, descending pathways, and somatosensory association and premotor cortices (Serrien et al., 2006). Indeed, patients with a left hemisphere lesion performing an upper-limb task demonstrated a deficit in intersegmental coordination (Schaefer et al., 2012). Additionally, our study observed a more pronounced impairment of motor function and language abilities in the paretic (right) hand of patients with left hemisphere damage (LHD) compared to those

with right hemisphere damage (RHD). This observation may be attributed to the lateralization of brain function, where the left hemisphere, typically dominant in right-handed individuals, is primarily responsible for tasks involving language and fine motor skills. These findings suggest that the significant relationship between gait speed and the timing of kinetic coordination on the right side in controls and patients with LHD may be due to left hemisphere dominance. Furthermore, previous studies have demonstrated that the processing of sensory-motor data is carried out by a more extensive and densely connected network in the dominant left hemisphere (Guye et al., 2003). Therefore, damage to one network component is more easily compensated for by other network components, indicating that patients with LHD could control gait speed by timing kinetic coordination despite a left hemisphere lesion.

In healthy controls, gait speed was associated with the timing of peak PC1 on the right side and hip flexion moment and ankle dorsiflexion moment on the left side. Healthy controls with delayed timing of peak PC1 on the right side had faster gait speed, consistent with a previous study (Sekiguchi et al., 2019). Furthermore, hip flexion moment was involved in gait speed, consistent with another previous study (Fukuchi et al., 2019). Hip flexion moment may also be involved in the propulsion of the lower limb during the swing phase. The involvement of the ankle dorsiflexion moment on the left side may be due to the influence of the heel rocker function during gait. The period when the peak ankle dorsiflexion moment on the left side was observed is the early stance phase on the left side and the late stance phase on the right side, respectively. During this period, as walking speed increases due to increased propulsion of the lower limb on the right side, the left lower limb may be possibly stabilized by an appropriate ankle dorsiflexion moment on the left side to break the ankle plantarflexion movement. Patients with lesion in the right hemisphere had decreased ability to shift body weight as well as poorer body sway and stance control, indicating that the right hemisphere may be associated with stability (Fernandes et al., 2018; Coelho et al., 2019). These facts support the idea that as walking speed increases, the ankle dorsiflexion moment is controlled by the right hemisphere to stabilize the left lower limb, whereas the left hemisphere is involved in skilled movements such as intersegmental coordination.

In patients with LHD, gait speed was associated with left ankle dorsiflexion moment and right PC1 timing. In these patients, the factors involved in gait speed were similar to those in healthy controls, except for the plantarflexion moment of the paretic (right) ankle. Contrary to patients with RHD, the right hemisphere involved in stability was not damaged and was able to maintain balance control in the paretic lower limb, such as increased knee flexion and decreased hip extension angle in early stance and increased knee extension moment which is support moment in patients with LHD. This may be a factor in performing similar kinetic control as healthy individuals with similar gait speed. Consistent with the previous study, the timing of peak PC1 was earlier on the paretic side (Sekiguchi et al., 2022). Like in other studies on muscle synergy, the timing of the impaired motor module involved in paretic propulsion may be involved in gait speed (Routson et al., 2013). The hip flexion moment was greater in the paretic (right) than in the nonparetic (left) side in patients with LHD, similar to healthy subjects. However, the plantarflexion moment was reduced on the paretic (right) side. Thus, it is possible that the impaired plantarflexion moment on the paretic side had a greater effect on gait speed, similar to the result of a previous study (Olney et al., 1994).

The absolute values of the loadings of ankle and hip joint moments for the first PC were high in both patients and healthy controls. The first motor module, which comprised of ankle, and hip joint moments, plays a role in inducing propulsion and supporting weight (Sadeghi et al., 2001). In patients with RHD, the loading of knee joint moment for the first PC on the paretic (left) side was a negative value, representing flexion moment, which is unlike the patients with LHD. A previous study showed excessive cocontraction of ankle plantar flexors and knee flexors in the stance phase during gait in patients with stroke (Fujita et al., 2018). In addition, patients with RHD had larger knee flexion moments in the stance phase on the paretic (left) side than those with LHD and in healthy controls. These facts indicate that the first motor module of kinetic variables merged with the knee flexion moment due to excessive cocontraction of knee flexor and ankle plantar flexor on the paretic (left) side in patients with RHD. As the knee flexion moment decreases the support moment, patients with RHD have controls that reduce both the quantity and quality of the support moments in the stance phase on the paretic side during gait. Kinetic control by kinetic coordination on the paretic side in patients with RHD may cause lower-limb instability on the paretic side and larger knee extension and smaller ankle dorsiflexion in the stance phase on the paretic side to increase stability. Hip extension on the nonparetic side was decreased to prevent instability in the stance phase on the paretic (left) side by taking shorter steps like caution gait (Eils et al., 2004). Additionally, the stance time on the paretic (left) side in patients with RHD was shorter than that in controls. However, this was not observed on the paretic (right) side in patients with LHD. The impulse, calculated by multiplying the stance time by the ground reaction force, influences angular momentum. The reduced stance time could explain why the $WBAM_R$ in patients with RHD did not differ from that in healthy controls. This may also be indicative of a cautious gait pattern. A decrease in hip extension on the nonparetic side, a component of trail limb angle that contributes to propulsion, relatively increases the contribution of ankle plantarflexion moment on the nonparetic side to gait speed (Hsiao et al., 2015; Hsiao et al., 2016a).

Patients with RHD had different results in kinetic factors contributing to gait speed from healthy subjects and patients with LHD. In patients with RHD, the kinetic factors included dorsiflexion moment in the early stance on the nonparetic (right) side and plantarflexion moment in the late stance on the paretic (left) side, consistent with those in patients with LHD. The results of this study indicate that kinetic control by ankle plantarflexion moment on the paretic side, which induces propulsion (Hsiao et al., 2015; Hsiao et al., 2016a), and ankle dorsiflexion moment on the nonparetic side, which controls ankle plantarflexion and braking, in the late stance in patients with stroke is important for increasing gait speed. However, from a left–right perspective, the kinetic factors in patients with left-sided brain lesions differed from those in patients with right-sided brain lesions. Contrary to normal subjects and patients with left-sided lesions, in patients with right-sided brain lesions, the left lower limb is responsible for propulsion, whereas the right lower limb is responsible for braking and stability. In fact, in patients with right-sided brain lesions, the timing of peak

PC1 was not related to gait speed as the right limb is responsible for stability. This suggests that after stroke onset, patients with right-sided brain lesions may alternate kinetic roles of the lower limbs in gait speed between the left and right limbs.

This study has several limitations. First, there were differences in finger motor dysfunction and language dysfunction between the left and right lesion sides. These differences may reflect dominant and nondominant hemispheric effects due to the lesion side. Finger motor dysfunction may affect the lower-limb kinetic variables and gait speed, consistent with the result of a previous study indicating that changes in finger spasticity following botulinum toxin treatment were associated with changes in stride (Lee et al., 2023). In this study, the differences in multiple regression analysis results due to the variance between the left and right brain lesion sides may be influenced by differences caused by finger motor dysfunction rather than differences between the left and right brain lesion sides. However, because healthy controls and patients with left brain damage had similar results in multiple regression analysis, the influence of finger motor dysfunction is thought to be small. The second limitation is that this study measured barefoot walking and walked without using a cane. Therefore, it is possible that the kinetic factors of walking speed examined were different from those of daily walking. Third limitation is that we did not investigate the dominant foot. According to a previous study, about 61.6% of the general population with a broad age range is right-footed, while 8.2% is left-footed and 30.2% is mixed-footed (Tran, U. S., & Voracek, M., 2016). Since the majority of people are right-footed, it is possible that the majority of the subjects in this study were also right-footed. The fourth limitation is that due to the lack of MRI images for all cases, we were unable to perform a detailed analysis of the size and severity of the lesions in the subjects. Therefore, it is unclear whether there is difference in the size and severity of the lesions between the patients with RHD and LHD.

In conclusion, this study has provided valuable insights into the kinetic mechanisms of decreased gait speed in patient with strokes, with a specific focus on differences across brain lesion sides. For patients with right hemisphere brain damage, larger ankle plantarflexion moments on both the paretic and nonparetic sides, as well as ankle dorsiflexion moment on the nonparetic side, were significant contributors to gait speed. In contrast, for patients with left hemisphere brain damage, larger ankle plantarflexion moment and delayed peak timing of the first principal component on the paretic side, along with ankle dorsiflexion moment on the nonparetic side, were the key factors. These findings highlight the necessity of taking into account the side of the brain lesion when devising rehabilitation strategies aimed at improving gait speed in patients with stroke.

Data availability statement

The raw data supporting the conclusion of this article will be made available by the authors, with their permission, without undue reservation.

Ethics statement

The studies involving humans were approved by Ethics Committee Tohoku University Graduate School of Medicine. The studies were conducted in accordance with the local legislation and institutional requirements. The participants provided their written informed consent to participate in this study.

Author contributions

Conceptualization, YS; methodology, YS and KH; software, YS and KH; validation, YS, KH, and DO; formal analysis, YS, KH, and DO; investigation, YS and KH; re-sources, YS, KH, DO, S-II, and SE; data curation, YS; writing-original draft preparation, YS; writing-review and editing, YS, KH, DO, S-II, and SE; visualization, YS; supervision, S-II and SE; project administration, S-II; funding acquisition, DO, YS, and S-II. All authors have read and agreed to the published version of the manuscript.

Funding

This work was supported by JSPS KAKENHI Grant Number JP18K17665 and JP22K11443.

Acknowledgments

We are grateful to the staff at the Department of Physical Medicine and Rehabilitation at Tohoku University for their valuable advice and assistance.

Conflict of interest

The authors declare that the research was conducted in the absence of any commercial or financial relationships that could be construed as a potential conflict of interest.

Publisher's note

All claims expressed in this article are solely those of the authors and do not necessarily represent those of their affiliated organizations, or those of the publisher, the editors and the reviewers. Any product that may be evaluated in this article, or claim that may be made by its manufacturer, is not guaranteed or endorsed by the publisher.

Supplementary material

The Supplementary Material for this article can be found online at: https://www.frontiersin.org/articles/10.3389/fbioe.2024.1240339/full#supplementary-material

References

Bohannon, R. W., and Glenney, S. S. (2014). Minimal clinically important difference for change in comfortable gait speed of adults with pathology: a systematic review. *J. Eval. Clin. Pract.* 20 (4), 295–300. doi:10.1111/jep.12158

Brough, L. G., Kautz, S. A., Bowden, M. G., Gregory, C. M., and Neptune, R. R. (2019). Merged plantarflexor muscle activity is predictive of poor walking performance in post-stroke hemiparetic subjects. *J. Biomechanics* 82, 361–367. doi:10.1016/j.jbiomech.2018.11.011

Butler, E., Druizin, M., Sullivan, E., Rose, J., and Gamble, J. (2006). *Human walking*. 3. Philadelphia, MD: Lippincott, Williams and Wilkins, 131–147.

Chen, I. H., Novak, V., and Manor, B. (2014). Infarct hemisphere and noninfarcted brain volumes affect locomotor performance following stroke. *Neurology* 82 (10), 828–834. doi:10.1212/wnl.0000000000000186

Coelho, D. B., Fernandes, C. A., Martinelli, A. R., and Teixeira, L. A. (2019). Right in comparison to left cerebral hemisphere damage by stroke induces poorer muscular responses to stance perturbation regardless of visual information. *J. Stroke Cerebrovasc. Dis.* 28 (4), 954–962. doi:10.1016/j.jstrokecerebrovasdis.2018.12.021

Compagnat, M., Mandigout, S., Perrochon, A., Lacroix, J., Vuillerme, N., Salle, J. Y., et al. (2021). The functional independence of patients with stroke sequelae: how important is the speed, oxygen consumption, and energy cost of walking? *Archives Phys. Med. Rehabilitation* 102 (8), 1499–1506. doi:10.1016/j.apmr.2021.01.085

Dumas, R., Cheze, L., and Verriest, J. P. (2007). Adjustments to McConville et al and Young et al body segment inertial parameters. *J. Biomech.* 40 (3), 543–553. doi:10.1016/j.jbiomech.2006.02.013

Eils, E., Behrens, S., Mers, O., Thorwesten, L., Volker, K., and Rosenbaum, D. (2004). Reduced plantar sensation causes a cautious walking pattern. *Gait Posture* 20 (1), 54–60. doi:10.1016/S0966-6362(03)00095-X

Elhafez, S. M., Ashour, A. A., Elhafez, N. M., Elhafez, G. M., and Abdelmohsen, A. M. (2019). Percentage contribution of lower limb moments to vertical ground reaction force in normal gait. *J. Chiropr. Med.* 18 (2), 90–96. doi:10.1016/j.jcm.2018.11.003

Fernandes, C. A., Coelho, D. B., Martinelli, A. R., and Teixeira, L. A. (2018). Right cerebral hemisphere specialization for quiet and perturbed body balance control: evidence from unilateral stroke. *Hum. Mov. Sci.* 57, 374–387. doi:10.1016/j.humov.2017.09.015

Frenkel-Toledo, S., Ofir-Geva, S., Mansano, L., Granot, O., and Soroker, N. (2021). Stroke lesion impact on lower limb function. *Front. Hum. Neurosci.* 15, 592975. doi:10.3389/fnhum.2021.592975

Fujita, K., Miaki, H., Fujimoto, A., Hori, H., Fujimoto, H., and Kobayashi, Y. (2018). Factors affecting premature plantarflexor muscle activity during hemiparetic gait. *J. Electromyogr. Kinesiol* 39, 99–103. doi:10.1016/j.jelekin.2018.02.006

Fukuchi, C. A., Fukuchi, R. K., and Duarte, M. (2019). Effects of walking speed on gait biomechanics in healthy participants: a systematic review and meta-analysis. *Syst. Rev.* 8 (1), 153. doi:10.1186/s13643-019-1063-z

Fulk, G. D., He, Y., Boyne, P., and Dunning, K. (2017). Predicting home and community walking activity poststroke. *Stroke* 48 (2), 406–411. doi:10.1161/STROKEAHA.116.015309

Fulk, G. D., Ludwig, M., Dunning, K., Golden, S., Boyne, P., and West, T. (2011). Estimating clinically important change in gait speed in people with stroke undergoing outpatient rehabilitation. *J. Neurologic Phys. Ther.* 35 (2), 82–89. doi:10.1097/npt.0b013e318218e2f2

Guye, M., Parker, G. J., Symms, M., Boulby, P., Wheeler-Kingshott, C. A., Salek-Haddadi, A., et al. (2003). Combined functional MRI and tractography to demonstrate the connectivity of the human primary motor cortex *in vivo*. *Neuroimage* 19 (4), 1349–1360. doi:10.1016/s1053-8119(03)00165-4

Hsiao, H., Awad, L. N., Palmer, J. A., Higginson, J. S., and Binder-Macleod, S. A. (2016a). Contribution of paretic and nonparetic limb peak propulsive forces to changes in walking speed in individuals poststroke. *Neurorehabil Neural Repair* 30 (8), 743–752. doi:10.1177/1545968315624780

Hsiao, H., Gray, V. L., Creath, R. A., Binder-Macleod, S. A., and Rogers, M. W. (2017). Control of lateral weight transfer is associated with walking speed in individuals post-stroke. *J. Biomech.* 60, 72–78. doi:10.1016/j.jbiomech.2017.06.021

Hsiao, H., Knarr, B. A., Higginson, J. S., and Binder-Macleod, S. A. (2015). The relative contribution of ankle moment and trailing limb angle to propulsive force during gait. *Hum. Mov. Sci.* 39, 212–221. doi:10.1016/j.humov.2014.11.008

Hsiao, H., Knarr, B. A., Pohlig, R. T., Higginson, J. S., and Binder-Macleod, S. A. (2016b). Mechanisms used to increase peak propulsive force following 12-weeks of gait training in individuals poststroke. *J. Biomech.* 49 (3), 388–395. doi:10.1016/j.jbiomech.2015.12.040

Jarvis, H. L., Brown, S. J., Price, M., Butterworth, C., Groenevelt, R., Jackson, K., et al. (2019). Return to employment after stroke in young adults: how important is the speed and energy cost of walking? *Stroke* 50 (11), 3198–3204. doi:10.1161/strokeaha.119.025614

Jonkers, I., Delp, S., and Patten, C. (2009). Capacity to increase walking speed is limited by impaired hip and ankle power generation in lower functioning persons post-stroke. *Gait Posture* 29 (1), 129–137. doi:10.1016/j.gaitpost.2008.07.010

Kim, C. H., Chu, H., Kang, G. H., Sung, K. K., Kang, D. G., Lee, H. S., et al. (2019). Difference in gait recovery rate of hemiparetic stroke patients according to paralyzed side: a cross-sectional study based on a retrospective chart review. *Med. Baltim.* 98 (46), e18023. doi:10.1097/md.0000000000018023

Kim, C. M., and Eng, J. J. (2004). Magnitude and pattern of 3D kinematic and kinetic gait profiles in persons with stroke: relationship to walking speed. *Gait Posture* 20 (2), 140–146. doi:10.1016/j.gaitpost.2003.07.002

Kinsella, S., and Moran, K. (2008). Gait pattern categorization of stroke participants with equinus deformity of the foot. *Gait Posture* 27 (1), 144–151. doi:10.1016/j.gaitpost.2007.03.008

Lee, J., Park, J. E., Kang, B. H., and Yang, S. N. (2023). Efficiency of botulinum toxin injection into the arm on postural balance and gait after stroke. *Sci. Rep.* 13 (1), 8426. doi:10.1038/s41598-023-35562-1

Mehrholz, J., Thomas, S., and Elsner, B. (2017). Treadmill training and body weight support for walking after stroke. *Cochrane Database Syst. Rev.* 8, Cd002840. doi:10.1002/14651858.CD002840.pub4

Mehrholz, J., Thomas, S., Kugler, J., Pohl, M., and Elsner, B. (2020). Electromechanical-assisted training for walking after stroke. *Cochrane Database Syst. Rev.* 10 (10), Cd006185. doi:10.1002/14651858.CD006185.pub5

Mentiplay, B. F., Williams, G., Tan, D., Adair, B., Pua, Y. H., Bok, C. W., et al. (2019). Gait velocity and joint power generation after stroke: contribution of strength and balance. *Am. J. Phys. Med. Rehabil.* 98 (10), 841–849. doi:10.1097/phm.0000000000001122

Nott, C. R., Neptune, R. R., and Kautz, S. A. (2014). Relationships between frontal-plane angular momentum and clinical balance measures during post-stroke hemiparetic walking. *Gait Posture* 39 (1), 129–134. doi:10.1016/j.gaitpost.2013.06.008

Olney, S. J., Griffin, M. P., and McBride, I. D. (1994). Temporal, kinematic, and kinetic variables related to gait speed in subjects with hemiplegia: a regression approach. *Phys. Ther.* 74 (9), 872–885. doi:10.1093/ptj/74.9.872

Routson, R. L., Clark, D. J., Bowden, M. G., Kautz, S. A., and Neptune, R. R. (2013). The influence of locomotor rehabilitation on module quality and post-stroke hemiparetic walking performance. *Gait Posture* 38 (3), 511–517. doi:10.1016/j.gaitpost.2013.01.020

Sadeghi, H., Sadeghi, S., Prince, F., Allard, P., Labelle, H., and Vaughan, C. L. (2001). Functional roles of ankle and hip sagittal muscle moments in able-bodied gait. *Clin. Biomech. (Bristol, Avon)* 16 (8), 688–695. doi:10.1016/s0268-0033(01)00058-4

Schaefer, S. Y., Mutha, P. K., Haaland, K. Y., and Sainburg, R. L. (2012). Hemispheric specialization for movement control produces dissociable differences in online corrections after stroke. *Cereb. Cortex* 22 (6), 1407–1419. doi:10.1093/cercor/bhr237

Sekiguchi, Y., Muraki, T., Kuramatsu, Y., Furusawa, Y., and Izumi, S. (2012). The contribution of quasi-joint stiffness of the ankle joint to gait in patients with hemiparesis. *Clin. Biomech. (Bristol, Avon)* 27 (5), 495–499. doi:10.1016/j.clinbiomech.2011.12.005

Sekiguchi, Y., Owaki, D., Honda, K., and Izumi, S. (2019). "The contribution of intralimb kinetic coordination in lower limb to control of propulsion and weight support at a wide range of gait speed in young and elderly people," in *ISPGR world congress*, 305–306.

Sekiguchi, Y., Owaki, D., Honda, K., and Izumi, S.-I. (2022). Kinetic interjoint coordination in lower limbs during gait in patients with hemiparesis. *Biomechanics* 2 (3), 466–477. doi:10.3390/biomechanics2030036

Selbie, W. S., Hamill, J., and Kepple, T. M. (2013). "Three-dimensional kinetics," in *Human kinetics champaign* (Champaign, Illinois: Human Kinetics).

Serrien, D. J., Ivry, R. B., and Swinnen, S. P. (2006). Dynamics of hemispheric specialization and integration in the context of motor control. *Nat. Rev. Neurosci.* 7 (2), 160–166. doi:10.1038/nrn1849

Silverman, A. K., and Neptune, R. R. (2011). Differences in whole-body angular momentum between below-knee amputees and non-amputees across walking speeds. *J. Biomech.* 44 (3), 379–385. doi:10.1016/j.jbiomech.2010.10.027

Sprigg, N., Selby, J., Fox, L., Berge, E., Whynes, D., and Bath, P. M. (2013). Very low quality of life after acute stroke: data from the Efficacy of Nitric Oxide in Stroke trial. *Stroke* 44 (12), 3458–3462. doi:10.1161/strokeaha.113.002201

Tashiro, H., Isho, T., Takeda, T., Nakamura, T., Kozuka, N., and Hoshi, F. (2019). Life-space mobility and relevant factors in community-dwelling individuals with stroke in Japan: a cross-sectional study. *Prog. Rehabil. Med.* 4, 20190014. doi:10.2490/prm.20190014

Tsuji, T., Liu, M., Sonoda, S., Domen, K., and Chino, N. (2000). The stroke impairment assessment set: its internal consistency and predictive validity. *Arch. Phys. Med. Rehabil.* 81 (7), 863–868. doi:10.1053/apmr.2000.6275

Ursin, M. H., Bergland, A., Fure, B., Thommessen, B., Hagberg, G., Øksengård, A. R., et al. (2019). Gait and balance one year after stroke; relationships with lesion side, subtypes of cognitive impairment and neuroimaging findings-a longitudinal, cohort study. *Physiotherapy* 105 (2), 254–261. doi:10.1016/j.physio.2018.07.007

Vismara, L., Cimolin, V., Buffone, F., Bigoni, M., Clerici, D., Cerfoglio, S., et al. (2022). Brain asymmetry and its effects on gait strategies in hemiplegic patients: new rehabilitative conceptions. *Brain Sci.* 12 (6), 798. doi:10.3390/brainsci12060798

Winter, D. A. (2009). *Biomechanics and motor control of human movement*. Hoboken, New Jersey: John Wiley & Sons, Inc.

Frontiers in
Bioengineering and Biotechnology

Accelerates the development of therapies, devices, and technologies to improve our lives

A multidisciplinary journal that accelerates the development of biological therapies, devices, processes and technologies to improve our lives by bridging the gap between discoveries and their application.

Discover the latest Research Topics

See more →

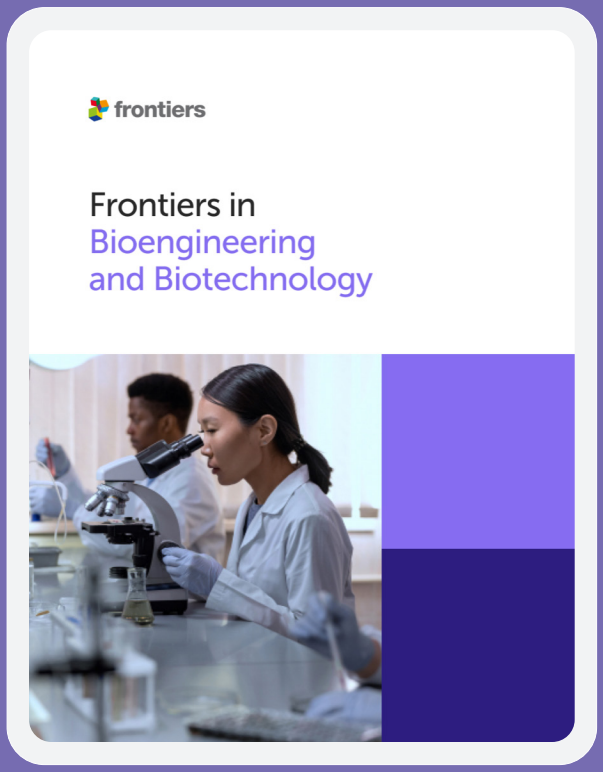

Frontiers

Avenue du Tribunal-Fédéral 34
1005 Lausanne, Switzerland
frontiersin.org

Contact us

+41 (0)21 510 17 00
frontiersin.org/about/contact